STUDIES ON BIOAVAILABILITY ENHANCEMENT AND SITE-SPECIFIC DELIVERY OF POORLY WATER SOLUBLE DRUG: EFAVIRENZ

Thesis submitted to

The Maharaja Sayajirao University of Baroda

for the degree of

DOCTOR OF PHILOSOPHY
IN
PHARMACY

Guide:
Prof. Sadhana J. Rajput, Ph.D.

Submitted by:
Greeshma V. Patel

PHARMACY DEPARTMENT
FACULTY OF TECHNOLOGY AND ENGINEERING
THE M. S. UNIVERSITY OF BARODA
VADODARA– 390001, GUJARAT.

JAN- 2013

STUDIES ON BIOAVAILABILITY ENHANCEMENT AND SITE-SPECIFIC DELIVERY OF POORLY WATER SOLUBLE DRUG: EFAVIRENZ

Thesis submitted to

The Maharaja Sayajirao University of Baroda

for the degree of

Doctor of Philosophy

in

Pharmacy

Guide:
Prof. Sadhana J. Rajput, Ph.D.

Submitted by:
Greeshma V. Patel

PHARMACY DEPARTMENT
FACULTY OF TECHNOLOGY AND ENGINEERING
THE M. S. UNIVERSITY OF BARODA
VADODARA– 390001, GUJARAT.

JAN- 2013

CERTIFICATE

This is to certify that, thesis entitled,

STUDIES ON BIOAVAILABILITY ENHANCEMENT AND SITE-SPECIFIC DELIVERY OF POORLY WATER SOLUBLE DRUG: EFAVIRENZ

Submitted by

Mrs. GREESHMA V. PATEL

for the degree of

Doctor of Philosophy

in

Pharmacy

to Pharmacy Department, The Maharaja Sayajirao University of Baroda, Vadodara has been carried out under my supervision and guidance. The matter compiled in this thesis has not been submitted earlier for the award of any other degree or fellowship.

GUIDE
Prof. Sadhana J. Rajput, Ph.D.
Pharmacy Department,
Faculty of Tech. & Engg.,
The M.S. University of Baroda,
Vadodara-390001

HEAD
Pharmacy Department,
Faculty of Tech. & Engg.,
The M.S. University of Baroda,
VADODARA-390001

DEAN
Faculty of Tech. & Engg.,
The M.S. University of Baroda,
VADODARA-390001

PLACE: Vadodara
DATE:

DECLARATION

I hereby declare that the topic entitled **"Studies on bioavailability enhancement and site-specific delivery of poorly water soluble drug: efavirenz"** which is submitted herewith to The Maharaja Sayalirao University of Baroda, Vadodara for the degree of **Doctor of Philosophy** in Pharmacy is the result of work done by me in Pharmacy Department, Faculty of Technology and Engineering, The Maharaja Sayajirao University of Baroda, under the guidance of **Dr. Sadhana J. Rajput**, Professor, Pharmacy Department, Faculty of Technology and Engineering, The M. S. University of Baroda, Vadodara.

I further declare that the result of this work have not been previously been submitted for any degree or fellowship.

GREESHMA V. PATEL

PLACE: Vadodara
DATE:

DEDICATED
WITH
RESPECT AND LOVE
TO MY
PARENTS
AND
MY BELOVED HUSBAND

ACKNOWLEDGEMENT

Research is a never ending acquisition of knowledge or data, which can not be done solely by any single person without the help of others. At this point of time, I feel that the present work would not have been completed by thus far without the blessing of my parents, the able guidance of my teachers, co-operation offered by my friends and the encouragement and support of my well wishers. I am indebted to all those who have contributed directly and indirectly towards the completion of this project work.

With a deep sense of respect and gratitude, I express my indebtedness to my guide, Dr. Sadhana J. Rajput, Professor of Pharmaceutical Analysis, Pharmacy Department, Faculty of Technology and Engineering, The M S University of Baroda for her invaluable guidance, boundless enthusiasm and constant inspiration through out the course of the study. It is with affection and reverence that I dedicate often beyond the call of duty; it was pleasure working under her guidance.

I express my sincere thanks to Dr. M. R. Yadav, Head, Pharmacy department, Faculty of technology & Engineering, The M. S. University of Baroda and entire staff of Pharmacy department for their co-operation and support during my course of work.

Special thanks to Abhinesh Kumar, Kiran Chaudhari and Vaibhav Patel also for their valuable suggestion, constructive criticism and the unending inspiration that has given the shape to this work.

I acknowledge the support of my colleagues and my friends Abhishek, Hardik, Reshma, Diti, Dipti and others for their wonderful company and support during the whole study.

I would like to bid special thanks to Hasumati Madam, Heenaben and other office staff who have indirectly contributed to this work.

I acknowledge Dr. Ravi Jadeja and Dr. Menka Thounaojam, Department of Zoology for allowing me to access the facilities at Department of Zoology, The M. S. University of Baroda.

Finally I would like to appreciate the endless love, care, patience and faith shown on me by my parents and sisters and the whole family who have stood behind me in every endeavor and have provided constant encouragement whatever be the situation.

I am very grateful to my husband Vaibhav, for his love and patience during the Ph. D. period.

I am thankful to The M.S. University of Baroda for providing the financial support to the study in the form of Research Scholarship.

I am thankful to all those who have helped me in whatsoever manner during this work whom I might have missed inadvertently.

Greeshma V. Patel

INDEX

LIST OF ABBREVIATIONS

%EE -	% Entrapment efficiency
%RSD -	% relative standard deviation
ACN -	Acetonitrile
AFM -	Atomic force microscopy
AIDS -	Acquired immunodeficiency syndrome
ANOVA -	Analysis of variance
API -	Active pharmaceutical ingredient
ARV -	Antiretroviral
AUC -	Area under curve
DE -	Dissolution efficiency
DHSS -	US Department of Health and Human Services
DNA -	Deoxyribonucleic acid
DOSS -	Docusate sodium
DSC -	Differential scanning calorimetry
DTA -	Differential thermal analysis
EFV -	Efavirenz
FBS -	Fetal bovine serum
FCS -	Fetal calf serum
FDA -	Food and drug administration
FTIR -	Fourier transform infrared spectroscopy
GIT -	Gastrointestinal tract
HAART -	Highly active anti-retroviral therapy
HIV -	Human immunodeficiency virus
HLB -	Hydrophilic lipophilic balance
HPC -	Hydroxypropyl cellulose

HPH - High-pressure homogenization

HPLC - High performance liquid chromatography

HPMC - Hydroxypropyl methyl cellulose

IAS - International AIDS society

ISTD - Internal standard

LC - Liquid crystalline

LCT - Long chain triglycerides

LNS - Lyophilized nanosuspension

LOD - Limit of detection

LOQ - Limit of quantification

L-SMEDDS - Liquid self- microemulsifying drug delivery system

MCT - Medium chain triglycerides

MDS - Mean droplet size

MDT - Mean dissolution time

MF - Marketed formulation

MN - Mannose

MPS - Mean particle size

MRT - Mean residence time

MTT - 3-(4,5-dimethylthiazole-2-yl)-2,5-diphenyltetrazolium bromide

NMR - Nuclear magnetic resonance

NNRTI - Non-nucleoside reverse transcriptase inhibitor

NPs - Nanoparticles

NRTIs - Nucleoside reverse transcriptase inhibitor

NS - Nanosuspension

PAMPA - Parallel artificial membrane permeability assay

PBS - Phosphate buffered saline

PCL - Poly (ε-caprolactone)

PCS - Photon correlation spectroscopy

PDI - Poly dispersity index

PI - Protease inhibitor

PLA - Polylactic acid

PLGA - Poly(lactic-co-glycolic) acid

PRESS - Predicted residual sum of square

PVA - Polyvinyl alcohol

PVP K30 - Povidone K30

QC - Quality control

RI - Refractive index

RNA - Ribonucleic acid

SD - Standard deviation

SEDDS - Self-emulsifying drug delivery system

SEM - Scanning electron microscopy

SLS - Sodium lauryl sulfate

SMEDDS - Self- microemulsifying drug delivery system

S-SMEDDS - Solid self- microemulsifying drug delivery system

TEM - Transmission electron microscopy

THF - Tetrahydrofuran

WHO - World health organization

XPS - X-ray photoelectron spectroscopy

XRD - X-ray diffraction

ZP - Zeta potential

LIST OF FIGURES

LIST OF TABLES

CHAPTER 1:

INTRODUCTION

Advances in combinatorial chemistry, biology and genetics in the recent years have led to a steady increase in the number of drug candidates under development. Due to the phospholipidic nature of cell membranes, a certain degree of lipophilicity is often a requirement for the drug compound, not only to be absorbed through the intestinal wall following oral administration but possibly also to exert its pharmacological action in the target tissue. While high lipophilicity is advantageous in terms of compound permeability, it intrinsically translates into poor aqueous solubility. **Since the first step in the oral absorption process is dissolution of the drug compound in the gastrointestinal lumen contents, poor aqueous solubility is rapidly becoming the leading hurdle for formulation scientists working on oral delivery of drug compounds.**[1,2]

Majority of new drug candidates have poor aqueous solubility. Poorly soluble drugs are a general problem in pharmaceutical drug formulation.[3] Typical problems associated with poorly soluble drugs are a too low bioavailability and/or erratic absorption. In case of a too low bioavailability after oral administration, parenteral administration cannot solve this problem in many cases. Due to the poor solubility, intravenous injection as a solution is not possible. Parenteral administration as a micronized product (e.g. i.m. or i.p.) does not lead necessarily to sufficiently high drug levels because the solute volume at the injection site is too low.

Given the increasing number of compounds emerging from discovery programs having poor aqueous solubility and/or dissolution, pharmaceutical scientists are constantly seeking new formulation approaches in order to obtain an adequate oral bioavailability. Currently, novel possibilities are offered by the rapidly emerging field of nanoscience.

"Nanoscience and Nanotechnology: Opportunities and Uncertainties", reads "Nanoscience is the study of phenomena and manipulation of materials at atomic, molecular and macromolecular scales, where properties differ significantly from those at a larger scale."[3]

British Standards Institution defines a nanoparticle/nanoparticulate as a "particle with one or more dimensions at the nanoscale", "nanoscale" being defined as "having one or more dimensions of the order of 100 nm or less"[4]

Several strategies to improve the solubility and dissolution of poorly water soluble drugs have been developed and described in literature, which were at start primarily based on modifying the drug's physicochemical properties. Many approaches have been used in an effort to increase the solubility, wetting and dissolution rate of poorly water soluble drugs including chemical modification (salt formation and prodrug), complexation with cyclodextrins, formation of solid dispersions and solubilization in surfactant systems, liposomes, nanosuspension (NS), lipid based delivery system, polymeric nanoparticles.[5-11] Complexation is a known solubility enhancing strategy, though its use is restricted to a considerably small group of molecules. Liposomes often have poor shelf stability and insufficient (for lipophilic drugs) loading. Although these approaches have shown some success to improve bioavailability, since last decade, NS and self- microemulsifying drug delivery system (SMEDDS) have gained a great interest as a commercially feasible novel drug delivery system.

Methods to improve drug bioavailability may involve the alteration of various key factors that determine drug dissolution, as described by the Noyes-Whitney equation[12]

$$dM/dt = DA/h\ (C_s - C_t)$$

in which dM/dt represents the dissolution rate, A the specific surface area of the drug particle, D the diffusion coefficient, h the diffusion layer thickness, Cs the saturation solubility and Ct the drug concentration at time t. That is, dissolution rate can be increased by increasing the surface area from where dissolution can take place, by decreasing the diffusional layer thickness and by altering the solubility of the drug. NS and SMEDDS can induce a considerable increase in dissolution rate as these strategies can simultaneously alter various of these factors.[13-15]

1.1 Nanosuspension

Nanosizing refers to the reduction of the active pharmaceutical ingredient (API) particle size down to the sub-micron range. These particles have a size below 1 μm, typically a few hundred nanometers.[16] The sub-micron particles are stabilized with surfactants or polymers in NSs, which can be further processed into standard dosage forms, such as capsules or tablets, suitable for oral administration. [1] These nano-

formulations offer increased dissolution rates and enhance bioavailability of insoluble compounds (BCS Class II and IV).

Several production techniques like precipitation[17], jet milling, pearl milling[18,19] and high-pressure homogenization (HPH)[20,21] have been applied to produce NSs. Currently, media milling is preferred over HPH technique because it is easy to scale up to industrial pharmaceutical unit operations.[22-26] Also, crystalline nature of the drug remains largely intact during the media milling processing, thus relieving any stability concerns. Furthermore, no organic solvent or harsh environment is needed. Recently, APIs have been successfully processed into NSs through media milling method by the pharmaceutical industry and some commercial products currently in the market include Emend® (Aprepitant, Merck & Co.), Rapamune® (Sirolimus, Wyeth), Tricor® (Fenofibrate, Abott) and Megace® ES (Megestrol acetate, Par Pharmaceuticals).[24,27,28]

NSs efficiently improve oral absorption of poorly soluble drugs and achieve a higher bioavailability compared to traditional formulation.[15] Major advantages of NS technology are increased dissolution velocity, increased saturation solubility, versatility in surface modification and ease of post-production processing. NSs show adhesion to the gastrointestinal mucosa, prolonging contact time of the drug and thereby enhancing its uptake via the gastrointestinal tract (GIT).[29-31]

Formulation of NS requires a careful selection of stabilizers. Stabilizers are needed to stabilize the nanoparticles against inter-particle forces and prevent them from aggregating. At the nanometer domain, attractive forces between particles, due to dispersion or van der Waals forces, come into play. This attractive force increases dramatically as the particles approach each other, ultimately resulting in an irreversible aggregation.

To overcome the attractive interaction, repulsive forces are needed. There are two modes of imparting repulsive forces or energetic barriers to a colloidal system-steric stabilization and electrostatic stabilization. Steric stabilization is achieved by adsorbing polymers onto the particle surface. As the particles approach each other, the osmotic stress created by the encroaching steric layers acts to keep the particles separate. Electrostatic stabilization is obtained by adsorbing charged molecules,

which can be ionic surfactants or charged polymers, onto the particle surface. Charge repulsion provides an electrostatic potential barrier to particle aggregation. Steric stabilization is often combined with electrostatic stabilization for additional repulsive contribution.

Common pharmaceutical excipients that are suitable for use as polymeric stabilizers include the cellulosics, such as hydroxypropylcellulose (HPC) and hydroxypropylmethylcellulose (HPMC), povidone (PVP K30), and pluronics (F68 and F127). The surfactant stabilizers can be non-ionic, such as polysorbate (Tween 80), or anionic, such as sodium lauryl sulfate (SLS) and docusate sodium (DOSS).

1.2. SMEDDS

SMEDDS is isotropic mixtures of an oil, surfactant, co-surfactant (or solubilizer), and drug. The basic principle of this system is its ability to form fine oil-in-water (o/w) microemulsions under gentle agitation following dilution by aqueous phases.[32,33]

The spontaneous formation of an emulsion upon drug release in the GIT advantageously presents the drug in a dissolved form and the small droplet size provides a large interfacial surface area for drug absorption. Specific components of SMEDDS promote the intestinal lymphatic transport of drugs. Main mechanisms include increasing membrane fluidity to facilitate transcellular absorption, opening tight junction to allow paracellular transport, inhibiting P-gp and/or CYP450 to increase intracellular concentration and residence time by surfactants, and stimulating lipoprotein/chylomicron production by lipid.[34,35]

Because of their unique solubilization properties, SMEDDS offer the following advantages[36]

1. Bioavailability enhancement of poorly aqueous soluble drugs: SMEDDS offer the opportunity to present lipophilic drugs to the gastrointestinal tract in a dissolved state, avoiding the dissolution step (which can limit absorption rate of BCS Class II and IV drugs).
2. Reduction in inter-subject and intra-subject variability.
3. Reduction of food effect.

4. Ease of manufacturing and scale up.
5. Ability to deliver peptides that are prone to enzymatic hydrolysis in GIT.
6. No influence of lipid digestion process.

At present, there are four drug products, Sandimmune® and Sandimmun Neoral® (cyclosporin A), Norvir® (ritonavir), and Fortovase® (saquinavir) on the pharmaceutical market, the active compounds of which have been formulated into specific self-emulsifying formulations, triggers much more attention on SMEDDS.[37] SMEDDS formulations are normally prepared as liquids and dispensed in form of soft or hard gelatin capsule filled which give rise to some drawbacks such as interaction of the fill with the capsule shell, risks of leakage from into hard gelatin filled capsules, limited shelf-life.[38,39] In recent years, there is a growing trend to formulate solid SMEDDS (S-SMEDDS) by adsorbing liquid SMEDDS (L-SMEDDS) onto suitable solid carriers.[40] Such S-SMEDDS can be easily filled in capsules and overcome the disadvantages of liquid formulations. On oral administration, they readily form microemulsion *in vivo*; presenting the drug in nano-sized and 'ready to absorb' form.[41] There are a limited number of publications reporting the oral bioavailability of solid SEDDS or SMEDDS.[38,41-45] Formulation of L-SMEDDS requires a careful selection of oil, surfactant and cosurfactant. Selection of excipients should be optimized considering solubility, phase diagram and self-emulsification property.

1.3. Nanoparticles

Another focus of research is the development of nanoparticle technologies to improve and enable drug targeting. Most drugs currently on the market are delivered in a non-specific manner throughout the whole body, rather than directly to the site of action where they are needed. This may result in unintentional side effects or toxicity in other tissues. Site specific targeting (both passive and active targeting) can reduce systemic toxicity by enabling drugs to accumulate selectively in the target tissue. As a result, the local concentration of the drug at the site of action will be high, while its concentration in non-target tissue will be below a certain minimum level to prevent side effects. In addition, targeting ability may allow for lower dosing requirements which also potentially decrease side effects of the drug while maintaining the same

therapeutic results. The need to achieve selective delivery of drugs to specific areas of the body has been recognized for many years.

Polymeric nanoparticles can be identified as submicron size (<1 μm) colloidal carriers. Compared with other colloidal carriers, polymeric nanoparticles hold significant promise for the advancement of treating diseases and disorders. They have attractive physicochemical properties such as size, surface potential, and hydrophilic-hydrophobic balance, and for this reason they have been recognized as potential drug carriers for bioactive ingredients such as anticancer drugs, vaccines, oligonucleotides, and peptides. Their widespread use for oral delivery also aims at improving the bioavailability of drugs with poor absorption characteristics, reducing GI irritation caused by drugs, and assuring stability of drugs in the GIT. Thus, these characteristics of nanoparticles qualify them as a promising candidate in drug delivery technology.[46]

Out of a large array of particulate carriers, polymeric nanoparticles are well-established for drug delivery, specifically poly(lactic-co-glycolic acid (PLGA)-based nanoparticles due to their well-known inherent advantages. PLGA is a food and drug administration (FDA) approved biodegradable and biocompatible polymer that had been widely used in the manufacturing of surgical sutures and in several controlled release drug products for human use.[47,48] PLGA nanoparticles represent an interesting carrier system for the transport of antiviral drugs to monocytes/macrophage in an attempt to reduce the required dose, minimize toxicity and side effects, and improve the delivery of substances, which have insufficient intracellular uptake.[48]

1.4 Rationale of project

Worldwide, over 60 million people are reported to be infected with the Human Immunodeficiency Virus **(**HIV).[49] The High Activity Antiretroviral Therapy (HAART) introduced in 1996 combines at least three antiretroviral (ARV) drugs [50-52] and, for over a decade, has been used to extend the lifespan of the HIV-infected patients. In this context, the formerly fatal HIV-associated disease, acquired immunodeficiency syndrome (AIDS), has become a manageable chronic infection in most developed countries.[53] Chronic intake of HAART is mandatory to control HIV infection[54]; without it, viral replication resumes several weeks after withdrawal.

Epidemiology reveals that optimal therapeutic results are attained when treatment adherence levels are greater than 95% (no more than two doses missed monthly in a twice-a-day regime); adherence levels below 95% could diminish therapeutic effectiveness by 50%.[51,52] **The frequent administration of several drugs in relatively high doses is a main cause of patient incompliance and a hurdle toward the fulfillment of the pharmacotherapy.[55]**

Regardless of the remarkable progress made in ARV pharmacotherapy, HIV is able to conserve its replication machinery in anatomical and intracellular sites where the ARV drugs have restricted access. HAART does not eliminate these reservoirs, nor prevent their generation and hence, a rebound in viral plasma levels occurs upon HAART withdrawal.[56] CD4+ T lymphocytes are the best investigated reservoir. Others reservoirs are the cells of the mononuclear phagocyte system (e.g., monocytes/macrophages, dendritic cells and Langerhans cells), the brain, hepatocytes and the gastrointestinal tract. In this framework, the use of nanoparticles has arguably become the most attractive research avenue for targeting monocytes/macrophages.[57] Macrophages possess various receptors such as fucose receptors, mannosyl, galactosyl, and many others. Mannose receptors are present at the surface of monocyte macrophages, alveolar macrophages, astrocytes in brain, hepatocytes in liver, and so on. **Therefore, targeting of ARV drugs to HIV infected macrophages could be an attractive approach for improving the therapeutic efficacy and reducing the toxicity of ARV bioactives.[46]**

1.4.1. Selection of drug

Non-Nucleoside Reverse Transcriptase Inhibitor (NNRTI) drugs were first introduced in 1998. The mechanism of action involves the non-competitive binding of the drug to the reverse transcriptase enzyme. According to the guidelines, HAART usually includes at least one NNRTI as a first-choice drug, The British HIV Association, the US Department of Health and Human Services (DHSS) and the International AIDS Society (IAS) guidelines indicate Efavirenz (EFV) as the preferred NNRTI. EFV is also the NNRTI of election recommended by the WHO for the initial treatment of

children above the age of 3. Molecular structure of EFV [(S)-6-chloro-4-(cyclopropylethynyl)-1,4-dihydro-4-(trifluoromethyl)-2(H)-3,1-bensoxazin-2-one].

According to the biopharmaceutical classification system guidance by FDA, EFV comes under a class II category drug, i.e. it has low solubility and high intestinal permeability.[58,59] It is a crystalline lipophilic solid with an aqueous solubility of 3-9 μg/ml and with a low intrinsic dissolution rate of 0.037 mg/cm^2/min. Hence, it has very low bioavailability.[60,61] To achieve effective therapy against viral diseases for orally administered drugs, it is essential that the drug should be adequately and consistently absorbed. Therefore, the recommended dose of EFV in adults is 600 mg q.d. The frequent administration of several drugs in relatively high doses is a main cause of patient incompliance.[62] The reason for this is very low solubility of EFV hinders its administration, absorption and biodistribution. Thus, there is need to have some innovative formulation approach to enhance the bioavailability.

1.5. Hypothesis

It was hypothesized that NS and SMEDDS formulations of EFV might lead to improved oral bioavailability due to enhanced solubility, dissolution and, thus absorption.

Another hypothesis was that PLGA nanoparticles of EFV coupled with mannose can be utilized to target mannosyl receptor on macrophages for site-specific delivery.

These formulations would help to improve clinical utility, decrease the dose and frequency of dosing, reduce side effects and improve therapeutic efficacy of EFV.

1.6. Aims and objectives

The first aim of study was to develop stable formulations of EFV for improvement of oral bioavailability by improving its solubility, dissolution and absorption properties. The detail objectives of this study were as below:

- To develop formulations of NS and SMEDDS loaded with EFV.
- Optimization of the various formulation and process parameters by factorial design study.
- To characterize the prepared formulations for particle size, zeta potential and its morphological properties by Scanning Electron Microscopy and Transmission Electron Microscopy.
- To study the Differential Scanning Calorimeter thermograms and X-ray diffraction patterns of excipients and optimized formulations.
- To carryout stability studies at various temperature conditions.
- To carryout *in vitro* dissolution study of optimized formulations and compared with standard EFV and marketed formulation.
- To carryout *in situ* intestinal perfusion study in rats for absorption of EFV from optimized formulations and compare with marketed formulation.
- To carryout parallel artificial membrane permeability assay (PAMPA) for permeability of EFV from optimized formulations and compared with standard EFV and marketed formulation.
- To carryout *in vivo* pharmacokinetic (bioavailability) study from optimized formulations to compare with standard EFV and marketed formulation.

The second aim of study was to develop EFV loaded mannose (MN) incorporated PLGA nanoparticles (MN-PLGA NPs) for site-specific delivery to macrophages. The detailed objectives were as follows:

- To carryout MN incorporation in PLGA polymer.
- To formulate MN-PLGA NPs loaded with ARV drug EFV.
- Optimization of the various formulation and process parameters by factorial design.
- To characterize the prepared formulations for entrapment efficiency (%), particle size, zeta potential and its morphological properties by transmission electron microscopy.
- To carryout *in vitro* diffusion study from optimized formulation.
- To carryout stability studies at various temperature conditions.
- To carryout drug uptake study in peritoneal macrophages.
- *In vivo* biodistribution study of optimized formulation in rats.

REFERENCES

1 Kesisoglou, F., Panmai, S. & Wu, Y. Nanosizing--oral formulation development and biopharmaceutical evaluation. *Advanced drug delivery reviews* **59**, 631-644, (2007).

2 Lipinski, C. Poor aqueous solubility— an industry wide problem in drug discovery. . *Am. Pharm. Rev.* **5**, 82-85, (2002).

3 Royal Society and Royal Academy of Engineering. Nanoscience and Nanotechnology: Opportunities and Uncertainties. *http://www.nanotec.org.-uk/finalReport.htm.*, (2004).

4 British Standards Institution. http://www.bsiglobal.com/upload/-Standards%20&%20Publications/Nanotechnologies/PAS71.pdf., (2005).

5 Shown, I., Banerjee, S., Ramchandran, A. V., Geckeler, K. E. & Murthy, C. N. Synthesis of Cyclodextrin and Sugar-Based Oligomers for the Efavirenz Drug Delivery. *Macromol Symp* **287**, 51-59, (2010).

6 Serajuddin, A. T. M. Solid dispersion of poorly water-soluble drugs: Early promises, subsequent problems, and recent breakthroughs. *Journal of pharmaceutical sciences* **88**, 1058-1066, (1999).

7 Sathigari, S. *et al.* Physicochemical Characterization of Efavirenz-Cyclodextrin Inclusion Complexes. *Aaps Pharmscitech* **10**, 81-87, (2009).

8 Pollock, S., Dwek, R. A., Burton, D. R. & Zitzmann, N. N-Butyldeoxynojirimycin is a broadly effective anti-HIV therapy significantly enhanced by targeted liposome delivery. *AIDS* **22**, 1961-1969, (2008).

9 Patravale, V. B., Date, A. A. & Kulkarni, R. M. Nanosuspensions: a promising drug delivery strategy. *Journal of Pharmacy and Pharmacology* **56**, 827-840, (2004).

10 Chiappetta, D. A., Hocht, C. & Sosnik, A. A Highly Concentrated and Taste-Improved Aqueous Formulation of Efavirenz for a More Appropriate Pediatric Management of the Anti-HIV Therapy. *Curr Hiv Res* **8**, 223-231, (2010).

11 Chiappetta, D. A., Hocht, C., Taira, C. & Sosnik, A. Oral pharmacokinetics of the anti-HIV efavirenz encapsulated within polymeric micelles. *Biomaterials* **32**, 2379-2387, (2011).

12 Dokoumetzidis, A. & Macheras, P. A century of dissolution research: from Noyes and Whitney to the biopharmaceutics classification system. *International journal of pharmaceutics* **321**, 1-11, (2006).

13 Woo, J. S., Song, Y. K., Hong, J. Y., Lim, S. J. & Kim, C. K. Reduced food-effect and enhanced bioavailability of a self-microemulsifying formulation of itraconazole in healthy volunteers. *European journal of pharmaceutical sciences : official journal of the European Federation for Pharmaceutical Sciences* **33**, 159-165, (2008).

14 Grove, M., Mullertz, A., Nielsen, J. L. & Pedersen, G. P. Bioavailability of seocalcitol II: development and characterisation of self-microemulsifying drug delivery systems (SMEDDS) for oral administration containing medium and long chain triglycerides. *European journal of pharmaceutical sciences :*

official journal of the European Federation for Pharmaceutical Sciences **28**, 233-242, (2006).

15 Gao, L. *et al.* Studies on pharmacokinetics and tissue distribution of oridonin nanosuspensions. *Int J Pharm* **355**, 321-327, (2008).

16 Müller, R. H., Möschwitzer, J. & Bushrab, F. N. *Nanoparticle Technology for Drug Delivery, Drugs and the pharmaceutical sciences.*, Vol. 159 21-51 (Taylor & Francis Group, 2006).

17 Trotta, M., Gallarate, M., Pattarino, F. & Morel, S. Emulsions containing partially water-miscible solvents for the preparation of drug nanosuspensions. *J Control Release* **76**, 119-128, (2001).

18 Liversidge, G. G. & Conzentino, P. Drug Particle-Size Reduction for Decreasing Gastric Irritancy and Enhancing Absorption of Naproxen in Rats. *Int J Pharm* **125**, 309-313, (1995).

19 Niwa, T., Miura, S. & Danjo, K. Design of Dry Nanosuspension with Highly Spontaneous Dispersible Characteristics to Develop Solubilized Formulation for Poorly Water-Soluble Drugs. *Pharm Res* **28**, 2339-2349, (2011).

20 Teeranachaideekul, V., Junyaprasert, V. B., Souto, E. B. & Muller, R. H. Development of ascorbyl palmitate nanocrystals applying the nanosuspension technology. *Int J Pharm* **354**, 227-234, (2008).

21 Muller RH, J. C., Kayser O. *Nanosuspensions for the formulation of poorly soluble drugs. Pharmaceutical Emulsions and Suspensions.*, Vol. 105 (Marcel Dekker Inc, 2000).

22 Detroja, C., Chavhan, S. & Sawant, K. Enhanced antihypertensive activity of candesartan cilexetil nanosuspension: formulation, characterization and pharmacodynamic study. *Scientia pharmaceutica* **79**, 635-651, (2011).

23 Van Eerdenbrugh, B. *et al.* Microcrystalline cellulose, a useful alternative for sucrose as a matrix former during freeze-drying of drug nanosuspensions - A case study with itraconazole. *Eur J Pharm Biopharm* **70**, 590-596, (2008).

24 Singh, S. K. *et al.* Investigation of preparation parameters of nanosuspension by top-down media milling to improve the dissolution of poorly water-soluble glyburide. *Eur J Pharm Biopharm* **78**, 441-446, (2011).

25 Cerdeira, A. M., Mazzotti, M. & Gander, B. Miconazole nanosuspensions: Influence of formulation variables on particle size reduction and physical stability. *Int J Pharm* **396**, 210-218, (2010).

26 Van Eerdenbrugh, B. *et al.* Drying of crystalline drug nanosuspensions-the importance of surface hydrophobicity on dissolution behavior upon redispersion. *Eur J Pharm Sci* **35**, 127-135, (2008).

27 Lee, J., Choi, J. Y. & Park, C. H. Characteristics of polymers enabling nano-comminution of water-insoluble drugs. *Int J Pharm* **355**, 328-336, (2008).

28 Van Eerdenbrugh, B. *et al.* Characterization of physico-chemical properties and pharmaceutical performance of sucrose co-freeze-dried solid nanoparticulate powders of the anti-HIV agent loviride prepared by media milling. *Int J Pharm* **338**, 198-206, (2007).

29 Kayser, O. A new approach for targeting to Cryptosporidium parvum using mucoadhesive nanosuspensions: research and applications. *Int J Pharm* **214**, 83-85, (2001).

30 Muller, R. H. & Peters, K. Nanosuspensions for the formulation of poorly soluble drugs - I. Preparation by a size-reduction technique. *Int J Pharm* **160**, 229-237, (1998).

31 Hanafy, A. *et al.* Pharmacokinetic evaluation of oral fenofibrate nanosuspensions and SLN in comparison to conventional suspensions of micronized drug. *Adv Drug Deliver Rev* **59**, 419-426, (2007).

32 Lawrence, M. J. & Rees, G. D. Microemulsion-based media as novel drug delivery systems. *Advanced drug delivery reviews* **45**, 89-121, (2000).

33 Humberstone, A. J. & Charman, W. N. Lipid-based vehicles for the oral delivery of poorly water soluble drugs. *Advanced drug delivery reviews* **25**, 103-128, (1997).

34 Wu, W., Wang, Y. & Que, L. Enhanced bioavailability of silymarin by self-microemulsifying drug delivery system. *European journal of pharmaceutics and biopharmaceutics : official journal of Arbeitsgemeinschaft fur Pharmazeutische Verfahrenstechnik e.V* **63**, 288-294, (2006).

35 Kommuru, T. R., Gurley, B., Khan, M. A. & Reddy, I. K. Self-emulsifying drug delivery systems (SEDDS) of coenzyme Q10: formulation development and bioavailability assessment. *International journal of pharmaceutics* **212**, 233-246, (2001).

36 Singh, A. K. *et al.* Exemestane loaded self-microemulsifying drug delivery system (SMEDDS): development and optimization. *AAPS PharmSciTech* **9**, 628-634, (2008).

37 Elnaggar, Y. S. R., El-Massik, M. A. & Abdallah, O. Y. Self-nanoemulsifying drug delivery systems of tamoxifen citrate: Design and optimization. *International journal of pharmaceutics* **380**, 133-141, (2009).

38 Balakrishnan, P. *et al.* Enhanced oral bioavailability of dexibuprofen by a novel solid self-emulsifying drug delivery system (SEDDS). *Eur J Pharm Biopharm* **72**, 539-545, (2009).

39 Mura, P., Valleri, M., Cirri, M. & Mennini, N. New solid self-microemulsifying systems to enhance dissolution rate of poorly water soluble drugs. *Pharmaceutical development and technology*, (2010).

40 Ito, Y. *et al.* Oral solid gentamicin preparation using emulsifier and adsorbent. *Journal of Controlled Release* **105**, 23-31, (2005).

41 Joshi, M., Pathak, S., Sharma, S. & Patravale, V. Solid microemulsion preconcentrate (NanOsorb) of artemether for effective treatment of malaria. *International journal of pharmaceutics* **362**, 172-178, (2008).

42 Yi, T., Wan, J. L., Xu, H. B. & Yang, X. L. A new solid self-microemulsifying formulation prepared by spray-drying to improve the oral bioavailability of poorly water soluble drugs. *Eur J Pharm Biopharm* **70**, 439-444, (2008).

43 Yan, Y. D. *et al.* Enhanced Oral Bioavailability of Curcumin via a Solid Lipid-Based Self-Emulsifying Drug Delivery System Using a Spray-Drying Technique. *Biol Pharm Bull* **34**, 1179-1186, (2011).

44 Chen, Y. *et al.* Development of a Solid Supersaturatable Self-Emulsifying Drug Delivery System of Docetaxel with Improved Dissolution and Bioavailability. *Biol Pharm Bull* **34**, 278-286, (2011).

45 Wang, Z. Y. *et al.* Solid self-emulsifying nitrendipine pellets: Preparation and in vitro/in vivo evaluation. *International journal of pharmaceutics* **383**, 1-6, (2010).

46 Jain, S. K., Gupta, Y., Jain, A., Saxena, A. R. & Khare, P. Mannosylated gelatin nanoparticles bearing an anti-HIV drug didanosine for site-specific delivery. *Nanomedicine : nanotechnology, biology, and medicine* **4**, 41-48, (2008).

47 Jain, R. A., Rhodes, C. T., Railkar, A. M., Malick, A. W. & Shah, N. H. Controlled release of drugs from injectable in situ formed biodegradable PLGA microspheres: effect of various formulation variables. *European journal of pharmaceutics and biopharmaceutics : official journal of Arbeitsgemeinschaft fur Pharmazeutische Verfahrenstechnik e.V* **50**, 257-262, (2000).

48 Bala, I., Hariharan, S. & Kumar, M. N. PLGA nanoparticles in drug delivery: the state of the art. *Critical reviews in therapeutic drug carrier systems* **21**, 387-422, (2004).

49 AIDS Epidemic Update, World Health Organization. http://www.who.int/hiv/epiupdates/en/index.html., (2007).

50 Lin, J. H. Role of pharmacokinetics in the discovery and development of indinavir. *Advanced drug delivery reviews* **39**, 33-49, (1999).

51 Panel of Clinical Practices for Treatment of HIV Infection, Guidelines for the use of antiretroviral agents to treat HIV infection in pediatric patients. *Pan. Am. J. Public Health* **10**, 426-435, (2001).

52 Shah, C. A. Adherence to high activity antiretrovial therapy (HAART) in pediatric patients infected with HIV: issues and interventions. *Indian journal of pediatrics* **74**, 55-60, (2007).

53 Delaney, M. History of HAART - the true story of how effective multi-drug therapy was developed for treatment of HIV disease. *Retrovirology* **3**, (2006).

54 Smith, K. A. To cure chronic HIV infection, a new therapeutic strategy is needed. *Current opinion in immunology* **13**, 617-624, (2001).

55 Baert, L. *et al.* Development of an implantable infusion pump for sustained anti-HIV drug administration. *International journal of pharmaceutics* **355**, 38-44, (2008).

56 Saksena, N. K. & Haddad, D. N. Viral reservoirs an impediment to HAART: new strategies to eliminate HIV-1. *Current drug targets. Infectious disorders* **3**, 179-206, (2003).

57 von Briesen, H., Peter Ramge, Jörg Kreuter. Controlled Release of Antiretroviral Drugs. *AIDS Reviews* **2**, 31-38, (2000).

58 Kasim, N. A. *et al.* Molecular properties of WHO essential drugs and provisional biopharmaceutical classification. *Mol Pharmaceut* **1**, 85-96, (2004).

59 Takano, R. *et al.* Oral absorption of poorly water-soluble drugs: Computer simulation of fraction absorbed in humans from a miniscale dissolution test. *Pharm Res* **23**, 1144-1156, (2006).

60 Zakeri-Milani, P., Barzegar-Jalali, M., Azimi, M. & Valizadeh, H. Biopharmaceutical classification of drugs using intrinsic dissolution rate (IDR) and rat intestinal permeability. *Eur J Pharm Biopharm* **73**, 102-106, (2009).

61 Bindu Madhavi B, K. B., Krishna Chatanya CH, Naga Madhu M, Sri Harsha V , David Banji. Dissolution enhancement of efavirenz by solid dispersion and PEGylation techniques. *Int J Pharm Invest* **1**, 29-34, (2011).

62 Baert, L. *et al.* Development of an implantable infusion pump for sustained anti-HIV drug administration. *Int J Pharm* **355**, 38-44, (2008).

CHAPTER 2:

LITERATURE REVIEW

2.1. Human Immunodeficiency Virus (HIV)

HIV is a lentivirus, and like all viruses of this type, it attacks the immune system. Lentiviruses are in turn part of a larger group of viruses known as retroviruses. Retroviruses are the exception because their genes are composed of Ribonucleic Acid (RNA). The name 'lentivirus' literally means 'slow virus' because they take such a long time to produce any adverse effects in the body. There are two types of HIV: HIV-1 and HIV-2. HIV-2 is less easily transmitted, and the period between initial infection and illness is longer in the case of HIV-2. Worldwide, the predominant virus is HIV-1, and generally when people refer to HIV without specifying the type of virus they will be referring to HIV-1. The relatively uncommon HIV-2 type is concentrated in West Africa and is rarely found elsewhere.[1]

2.1.1. HIV life cycle

2.1.1.1. Entry

Outside of a human cell, HIV exists as roughly spherical particles (sometimes called virions). The surface of each particle is studded with lots of little spikes. HIV can only replicate inside human cells. The process typically begins when a virus particle bumps into a cell that carries on its surface a special protein called CD4. The spikes on the surface of the virus particle stick to the CD4 and allow the viral envelope to fuse with the cell membrane. The contents of the HIV particle are then released into the cell, leaving the envelope behind.

2.1.1.2. Reverse transcription and integration

Once inside the cell, the HIV enzyme reverse transcriptase converts the viral RNA into DNA, which is compatible with human genetic material. This DNA is transported to the cell's nucleus, where it is spliced into the human DNA by the HIV enzyme integrase. Once integrated, the HIV DNA is known as provirus

2.1.1.3. Transcription and Translation

HIV provirus may lie dormant within a cell for a long time. But when the cell becomes activated, it treats HIV genes in much the same way as human genes. First it converts them into messenger RNA (using human enzymes). Then the messenger RNA is transported outside the nucleus, and is used as a blueprint for producing new HIV proteins and enzymes.

2.1.1.4. Assembly, budding and maturation

Among the strands of messenger RNA produced by the cell are complete copies of HIV genetic material. These gather together with newly made HIV proteins and enzymes to form new viral particles. The HIV particles are then released or 'bud' from the cell. The enzyme protease plays a vital role at this stage of the HIV life cycle by chopping up long strands of protein into smaller pieces, which are used to construct mature viral cores. The newly matured HIV particles are ready to infect another cell and begin the replication process all over again. In this way the virus quickly spreads through the human body.

2.2. Acquired Immune Deficiency Syndrome (AIDS)

AIDS is a disease of the human immune system caused by the HIV.[2] The illness interferes with the immune system, making people with AIDS much more likely to get infections, including opportunistic infections and tumors that do not affect people with working immune systems. This susceptibility gets worse as the disease continues. HIV is transmitted in many ways, such as: sexual intercourse; contaminated blood transfusions and hypodermic needles; and exchange between mother and baby during pregnancy, childbirth, and breastfeeding. It can be transmitted by any contact of a mucous membrane or the bloodstream with a bodily fluid that has the virus in it, such as the blood, semen, vaginal fluid, preseminal fluid, or breast milk from an infected person.[3]

AIDS is the ultimate clinical consequence of infection with HIV. HIV primarily infects vital organs of the human immune system such as CD4+ T cells (a subset of T

cells), macrophages and dendritic cells. It directly and indirectly destroys CD4+ T cells.[4] Once the number of CD4+ T cells per microliter of blood drops below 200, cellular immunity is lost. Acute HIV infection usually progresses over time to clinical latent HIV infection and then to early symptomatic HIV infection and later to AIDS, which is identified either on the basis of the amount of CD4+ T cells remaining in the blood, and/or the presence of infections.[5]

The virus and disease are often referred to together as HIV/AIDS. The disease is a major health problem in many parts of the world, and is considered a pandemic, a disease outbreak that is not only present over a large area but is actively spreading.[6] In 2009, the World Health Organization (WHO) estimated that there are 33.4 million people worldwide living with HIV/AIDS, with 2.7 million new HIV infections per year and 2.0 million annual deaths due to AIDS.[7] In 2007, UNAIDS estimated: 33.2 million people worldwide were HIV positive; AIDS killed 2.1 million people in the course of that year, including 330,000 children, and 76% of those deaths occurred in sub-Saharan Africa.[8] According to UNAIDS 2009 report, worldwide some 60 million people have been infected since the start of the pandemic, with some 25 million deaths, and 14 million orphaned children in southern Africa alone.[8] However, with the adherence to HAART the efficacy rate of the available treatment has increased upto 85% against the AIDS as well as secondary diseases such as Kaposi's sarcoma.[9,10]

2.3. Antiretroviral (ARV) drug treatment

Antiretroviral drugs are medications for the treatment of infection by retroviruses, primarily HIV. The aim of antiretroviral treatment is to keep the amount of HIV in the body at a low level. This stops any weakening of the immune system and allows it to recover from any damage that HIV might have caused already. The treatment consists of drugs that have to be taken every day for the rest of a person's life. If only one drug was taken, HIV would quickly become resistant to it and the drug would stop working. There are different classes of ARV drugs that act on different stages of the HIV life-cycle. (Table 2.1) HIV can easily develop resistance to individual ARV therapies, but it is harder for HIV to become drug-resistant when multiple ARV drugs with varied mechanisms of action are combined into a single HIV treatment. Taking

two or more ARV at the same time vastly reduces the rate at which resistance would develop, making treatment more effective in the long term.

Table 2.1. Classification of ARV drugs.

Antiretroviral drug class	**Mechanism of action**	**Generic name of drugs**
Fusion or Entry Inhibitors	Prevent HIV from binding to or entering human immune cells	Enfuvirtide, Maraviroc
Nucleoside/Nucleotide Reverse Transcriptase Inhibitors (NRTIs)	NRTIs inhibit reverse transcription by being incorporated into the newly synthesized viral DNA strand as faulty nucleotides	Zidovudine, Didanosine, Zalcitabine, Stavudine, Lamivudine, Abcavir, Emtricitabine, Tenofovir
Non-Nucleoside Reverse Transcriptase Inhibitors (NNRTIs)	NNRTIs inhibit reverse transcriptase by binding to an allosteric site of the enzyme	Efavirenz, Nevirapine, Loviride, Delavirdine, Etravirine, Rilpivirine, Lersivirine
Protease Inhibitors (PIs)	PIs target viral assembly by inhibiting the activity of protease, an enzyme used by HIV to cleave nascent proteins for the final assembly of new virions.	Saquinavir, Ritonavir, Indinavir, Nelfinavir, Amprenavir, Tipranavir, Lopinavir, Darunavir, Atazanavir, Nelfinavir
Integrase Inhibitors	Inhibit the enzyme integrase, which is responsible for integration of viral DNA into the DNA of the infected cell.	Raltegravir

Taking a combination of three or more anti-HIV drugs is referred to as Highly Active Antiretroviral Therapy (HAART). The usual HAART regimen combines three or more different drugs such as two nucleoside reverse transcriptase inhibitors (NRTIs) and a protease inhibitor (PI), two NRTIs and a non-nucleoside reverse transcriptase inhibitor (NNRTI) or other such combinations.[11]

2.4. Current limitations in ARV drug therapy

ARV drug therapy has contributed significantly to improved patient/disease management, its current use is associated with several disadvantages and inconveniences to the HIV/AIDS patient.[12] Many ARV drugs undergo extensive first pass metabolism and gastrointestinal degradation leading to low and erratic bioavailability. The half-life for several ARV drugs is short, which then requires frequent administration of doses leading to decreased patient compliance.[13] A major limitation is that HIV is localised in certain inaccessible compartments of the body such as the CNS, the lymphatic system and within the macrophages. These sites cannot be accessed by the majority of drugs in the therapeutic concentrations required; and the drugs also cannot be maintained for the necessary duration at the site of HIV localisation.[14] These sub-therapeutic drug concentrations and short residence time at the required sites of action contribute significantly to both the failure of eliminating HIV from these reservoirs, and the development of multidrug-resistance against the ARV drugs.[15] The severe side effects associated with ARV therapy can therefore be attributed to the subsequent large doses essential for achieving a therapeutic effect, due to the inadequate drug concentrations at the site of action, and/or the poor bioavailability of several ARV drugs. These drugs also suffer from physico-chemical problems such as poor solubility that may lead to formulation difficulties.[16,17] Strategies currently being investigated to overcome these limitations include the identification of new and chemical modification of existing chemical entities, the examination of various dosing regimens, as well as the design and development of novel drug delivery systems (NDDS) that can improve the efficacy of both existing and new ARV drugs. More specifically, in the past decade there has been an explosion of interest in the development of NDDS for the incorporation of ARV drugs as a way of circumventing the problems described above and optimising the treatment of HIV/AIDS patients. NDDS present an opportunity for formulation scientists to overcome the many challenges associated with ARV drug therapy. The nanometer size and high surface area to volume ratio which affect the pharmacokinetics and biodistribution of the associated drug molecule are main features of NDDS.

2.5. Nanotechnology in drug delivery system

Nanotechnology received a lot of attention with the never-seen-before enthusiasm because of its future potential that can literally revolutionize each field in which it is being exploited. In drug delivery, nanotechnology is just beginning to make an impact. Many of the current "nano" drug delivery systems, however, are remnants of conventional drug delivery systems that happen to be in the nanometer range, such as liposomes, polymeric micelles, nanoparticles, dendrimers, and nanocrystals. The importance of nanotechnology in drug delivery is in the concept and ability to manipulate molecules and supramolecular structures for producing devices with programmed functions.

Successful delivery of drugs often requires processing in order to create more desirable physicochemical properties for effective drug delivery. Due to rapid advancements in nanotechnology, significant effort has been devoted to developing nanoparticle processes in order to address issues associated with the current pharmaceutical challenges. These challenges include delivering drugs with poor water solubility, target-specific drug therapy, cost-reduction and product lifecycle extension. In addition, these technologies offer a suitable means of delivering a wide range of drugs including small molecular weight drugs, as well as macromolecules such as proteins, peptides or genes by either localized or targeted delivery to the tissue of interest. Nanoparticle technologies have already had a significant impact on drug delivery systems in terms of improving the performance of existing drugs and enabling the use of new drug candidates.

2.6. Drug delivery systems selected for the study

2.6.1. Nanosuspension (NS)

NSs consist of an internal phase and an external phase in which the internal phase is dispersed uniformly throughout the external phase. The dispersed phase can be pharmaceutical solid or semi-solid colloidal particles with the particle size ranging from 10 to 1000 nm.[18] NSs demonstrate special physical and chemical properties being different to the bulk materials. The main properties of drug NSs are increased

saturation solubility and increased surface area, both leading to an increase in the rate of dissolution. Nanocrystals are therefore useful in increasing the oral bioavailability where drug dissolution is the rate limiting step (Biopharmaceutics Classification System (BCS) class II drugs).

NS can be defined as colloidal dispersions of nano-sized drug particles produced by nanonization methods and stabilized by GRAS (Generally regarded as safe) listed stabilizers.[19,20] The dispersion can be in water, aqueous solutions or non-aqueous solutions. The stabilizer character and concentration play an important role in creating a stable formulation. Too little stabilizer induces agglomeration or aggregation and too much stabilizer promotes Ostwald ripening.

In order to obtain a stable suspension, stabilizers are usually necessary to stabilize the nanoparticles against attractive forces between particles. These attractive forces, caused by dispersion or van der Waals forces, can increase significantly when the particles approach each other, eventually resulting in an irreversible agglomeration. This process can be slowed down by either enhancing the repulsive forces or reducing the attractive forces between the particles.[21] There are two stabilization mechanisms imparting repulsive forces or energy barriers to a dispersion system—steric stabilization and electrostatic stabilization.

Steric stabilization is obtained by adsorbing polymers onto the particle surface which provides effective steric barriers to aggregation. Steric stabilizers commonly used in pharmaceutical systems include non-ionic polymers such as hydroxypropyl cellulose (HPC), hydroxypropylmethyl cellulose (HPMC), povidone (PVP), polyvinyl alcohol (PVA), and poloxamer. Stabilizing polymers should have a strong surface affinity to the solid-liquid interface, and their polymer chains should be long enough to provide enough steric barriers at the interface, but not too large to impede dissolution. Non-ionic nonpolymeric surfactants such as polysorbate 80 (Tween 80) have also been used as stabilizers. In addition to stabilizing the system, these can also help as wetting and dispersant agents for very hydrophobic drugs.[21-23]

However, smaller surfactants alone do not effectively provide enough barriers at the interface, and are more prone to a shift in size distribution to larger particles (Oswald ripening) and particle growth.[21] Oswald ripening is a process that occurs due to differences in the dissolution rates of particles of different sizes. Since smaller

particles dissolve faster as described by the Prandtl equation, their contribution to the drug in solution phase is higher. Due to the dynamic nature of equilibrium of drug in solid and solution phase, larger particles begin to receive more drug from the solution phase and grow in size.

Electrostatic stabilization is obtained by adsorbing charged molecules onto the particle surface to provide effective electrostatic barriers to aggregation. Electrostatic stabilizers commonly used in pharmaceutical system include anionic surfactants or polymers such as sodium lauryl sulfate (SLS), and sodium di(2-ethylhexyl) sulfosuccinate (DOSS).[21,23] The negatively charged ions or molecules on the particle surface provide an electrical barrier to the particles. The combination of steric and electrostatic stabilization is often used to obtain long-term stabilization. For example, an increase in the stability of nanoformulations containing glycol copolymers was caused by the addition of SLS, an anionic surfactant. At high temperatures, the solubility of glycol copolymers in water is reduced, which leads to visible polymer aggregates (cloud point). Therefore, the ability to autoclave such formulations are limited. SLS in this case also acts as a cloud point modifier by raising the cloud point of the polymer, thus enhancing stability at higher temperature.[22] Another example is in the case of viscosity increase in NSs due to flocculation. This problem could be minimized by the addition of anionic surfactants, such as SLS or DOSS, which would improve surface wetting and may also provide electrostatic stabilization.[21] However, adding excessive surfactants should be avoided as this can cause increased solubility and Ostwald ripening, which is a phenomenon caused by the diffusion of smaller particles to form larger particles.

This technology can meet the drug development industry requirements, such as increasing solubility of poorly water soluble drugs; easily transferable to the production scale; cost effective and with little or no regulatory hurdles.[24]

2.6.1.1. Properties of nanosuspension and formulation theory

NS can be formed by building drug particles up from the molecular dimensions as in precipitation, or by nanonizing the micron sized particles down as in milling.[19] In either case, a new surface area ΔA, is created, and also is free energy (ΔG). $\Delta G = \gamma s/l$

.ΔA, in which γs/l is the interfacial tension. The system prefers to reduce this increase in surface area by either dissolving incipient crystalline nuclei, in the case of precipitation, or by agglomerating nanosized particles.

This tendency is resisted by addition of surface-active agents, which reduce the γs/l and therefore the free energy of the system. Surface active agents are more effective when present at the time of creation of the new, fresh surface than if added afterwards. Nanocrystals are stabilized by two classes of surface-active agents; charged or ionic surfactants, which affect the electrostatic repulsion among the particles; and non-inonic polymers, which confer a steric repulsion i.e., they resist aggregation.[19]

Nano-sizing of drugs results in increased dissolution velocity and saturation solubility. Dissolution velocity is an important parameter affecting the oral bioavailability of drugs. Poor water solubility correlates with slow dissolution rate (dc/dt), and inherently lower bioavailability. According to the Noyes Whitney equation: dc/dt = D.A (Cs-C)/h, where, dc/dt is the dissolution velocity and it is proportional to the surface area (A) of the particle and saturation solubility (Cs). Saturation solubility is a compound specific constant and depends on the temperature and properties of dissolution medium. However, for a particle below 1-2 μm, the saturation solubility is also a function of particle size.[25] Nano-sizing increases the saturation solubility because the dissolution pressure (dissolving molecules) increases due to the strong curvature of the particles. [20] Both enlarging the surface area (A) and increasing the saturation solubility (Cs) can improve the drug dissolution rate. Oral NSs have been specifically used to increase the rate and extent of drug absorption.[26]

In such an example, a comparison between a danazol NS (average particle size 169 nm) and a conventional danazol suspension (particle size 10 μm) was made. The NS showed higher Cmax and AUC values in a pharmacokinetic study conducted in dogs. The bioavailability of the NS was equivalent to that of a cyclodextrin solution formulation indicating that the dissolution rate limited bioavailability observed with the 10 μm suspension had been overcome.[27]

2.6.1.2. Preparation of nanosuspension

There are several production techniques to manufacture NS. Typically, NSs can be produced by precipitation or disintegrating process and are stabilized by surfactant (s) or polymer (s). Owing to their small particle size, the NS can be given by different routes of administration. In addition NS can be converted into solid dosage forms intended for oral delivery (tablets, pellets or granules containing capsules) for increased patient convenience.

Precipitation and disintegration are so called bottom up and top down technologies in NS production. In a precipitation method the drug is dissolved in one solvent, which is subsequently poured into a non-solvent. There are two phases involved in precipitation process, the initial creation of nuclei and their subsequent growth into nanocrystals.[19] Examples of this technique are hydrosols developed by Sucker (Novartis, previously Sandoz).

The basic advantage of the precipitation technique is that they use relatively simple, low cost equipment. Scale-up is relatively easy using static blenders or micromixers. Disadvantages are the use of organic solvents and difficulty in avoiding growth from nanocrystal to microcrystal dimensions during precipitation. In addition, drugs should be soluble in all organic solvents to produce nanocrystals.[28] As a result of the disadvantages addressed, this method hasn't been widely used by the pharmaceutical industry.

Commonly used methods for NS formation are disintegration processes, which are top down techniques. Drugs are disintegrated using two basic disintegration technologies; wet milling or high pressure homogenization principles.

2.6.1.2.1. Wet milling

Wet milling is a particle size reduction technology whereby drug crystals are comminuted using high-shear media mills in the presence of surface stabilizer(s) and grinding media.[29,30] The grinding media consist of rigid media with an average size ranging from 0.4 to 3 mm. The grinding materials may be composed of glass, zirconium oxide, ceramics and plastics (e.g., cross-linked polystyrene resin). The

typical process temperature during is less than 40°C to prevent thermal degradation. In general, the technology involves pre-dispersing drug in aqueous solution containing hydrophilic stabilizers and then the slurry is wet milled with a grinding media over a specified time period. High energy shear forces and the forces generated during impaction mechanically break down drug crystals into nanometer-sized particles which are suspended in a polymer solution.

Wet milling often requires grinding for hours to days in order to achieve a desired size range of nanocrystalline particles. The level and type of stabilizer are important parameters to achieve nanoparticle size using this technology and should be investigated for each situation. It was found that higher molecular weight polymeric stabilizers were optimal for effective particle size reduction and shelf stability. Additionally, the size of the grinding media, flow rate and speed of the mill rotor can also be adjusted to achieve optimum results.

NanoSystems™ has commercialized its technology resulting in two products. The first product approved by the United States Food and Drug Administration (FDA) is the reformulation of Rapamune®, a lipophilic macrolide immunosuppressant (marketed by Wyeth Pharmaceuticals). Previously, Rapamune® (sirolimus) was only available as an oral solution which contains solubilizing agents such as tween 80, phosphatidylcholine, mono- or diglycerides and propylene glycol. The current oral formulation requires storage under refrigerated conditions and additional preparation steps prior to use. A new formulation is now available as a tablet dosage form in which the particle size of the drug substance is reduced to less than 200nm in order to improve drug's water solubility. The new tablet formulation also enables more convenient administration and storage than the Rapamune oral solution. The second product is Emend® (aprepitant) developed as a new drug in a NanoCrystal® formulation. It is an antiemetic therapeutic agent used to prevent and control nausea and vomiting caused by chemotherapy treatment.

2.6.1.2.2. High pressure homogenization

The second most frequently used disintegration method is high pressure homogenization. The two existing homogenization methods applied are

microfluidisation and piston-gap homogenization. In microfluidisation, the suspension is sprayed with high velocity into specially designed homogenization chamber. Where, the flow of the suspension stream changes its direction a few times leading to particle collision and shear forces. A disadvantage of the technique is a relatively large fraction of microparticles in the final product thus losing the benefits of a homogenous suspension.

An alternative to wet milling and the microfluidisation is the piston-gap type high pressure homogenizers (e.g. Avestin, APV Gaulin, Stansted). DissoCubes® technology (trade name currently owned by Skye Pharma) was developed by Muller *et al.*[31] using a piston-gap homogenizer.

The initial drug suspension contained in a cylinder of diameter about 3 mm, passes suddenly through a very narrow homogenization gap of 25 μm. During homogenization, the fracture of drug particles is brought about by cavitations, high shear forces and the collision of the particles against each other, breaking the microcrystals into nanocrystals.[32] The implosion forces are sufficiently high to break down the drug microparticles into nanoparticles. Additionally, the collision of the particles at high speed helps to achieve nano-sizing of the drug.

Low temperature manufacturing is preferred. The addition of viscosity enhancers is advantageous in certain cases as increasing the viscosity increases the powder density within the dispersion zone (homogenization gap).[32] The high pressure homogenizer can be operated at pressures varying from 100 to 2000 bars. A number of homogenization cycles usually 3, 5 or 10 cycles can be carried out to obtain the nanosized drug. However, the drug should be pre-milled to get the particle size below 25 μm in order to prevent blocking of the homogenization gap.

Characteristics of the particles (particle size distribution) are influenced by homogenizer type, applied pressure, number of homogenization cycles and hardness of the drug particles. Changes in drug crystallinity have been reported for high pressure homogenization technology.[33] The use of high pressures can cause changes in the crystal structure and may also produce uncontrollable variations of amorphous structure.

2.6.1.3. Characterization tests

A prerequisite for the development of optimized NS is its characterization. A NS must have a minimal tendency for the agglomeration of particles. A suspension with slow sedimentation rate is preferable, provided the product is re-suspendable and homogeneous. In addition, NS products must be free from toxicity or irritation. A NS given by parenteral route must also be isotonic and non-pyrogenic.

2.6.1.3.1. Particle size distribution and charge

Particle size growth is mainly responsible for agglomeration. Precise sizing techniques can give useful information about the particle size distribution in NS. The frequently used techniques are laser diffraction and photon correlation spectroscopy (PCS), which are based on different operating principles to measure the particles size. Laser diffraction is fast and suitable for screening large numbers of samples, acquiring data in the useful range of 0.02-2,000 μm. However, input of the refractive index (RI) of the samples is required. PCS is also rapid, but only covers the range of 0.02-3 μm.[24]

The zeta potential is the potential at the surface of the hydrodynamic shear plane and can be obtained from electrophoretic mobility. Zeta potential is one of the methods to predict stability of suspensions since it measures the potential difference between the electrical double layer and the bulk liquid. Both the stabilizer and the drug govern the zeta potential of a NS.[34] For electrostatically stabilized NS, minimum zeta potential should be ±30 mV, and for combined steric and electrostatic stabilization, it should be a minimum of ±20 mV.[21,35]

2.6.1.3.2. Particle morphology and crystalline state

The particle morphology assessment helps in understanding the morphological changes that a drug might undergo when subjected to nanosizing. In order to get an actual idea of particle morphology, scanning electron microscopy (SEM) can be applied.[32]

It is essential to investigate the extent of amorphous drug nanoparticles generated during the production of NS. The change in the physical state of the drug particle as well as the extent of the amorphous fraction can be determined by X-ray diffraction (XRD) analysis and can be supplemented by differential scanning calorimetry (DSC).[36]

DSC can detect the presence of crystallinity phase. Compared to the sharp melting peak of the drug crystal, the NS present a broader peak with a markedly lower maximum of temperature. Moreover, a decrease of the temperature maximum related to the NS melting peak is observed when the NS size decreases. The amorphous phase does not show any thermal event.

2.6.1.3.3. *In Vitro* dissolution to assess the *in vivo* performance

The bioavailability of a NS given by any route of administration depends on the dissolution of the drug. *In vitro* dissolution testing in a bio-relevant medium is very important to predict the drug *in vivo* performance (bioavailability and pharmacokinetics) of the drug (96, 97).[37,38] Dissolution velocity of the nanocrystal can be affected by pH and the nature of the polymorph, which can inturn affect pharmacokinetics.[19]

Poor solubility is generally associated with poor dissolution rate and thus poor oral bioavailability. Nanosized drug can undergo faster dissolution than the un-milled drug because of enhanced surface area, thus increasing a drugs bioavailability. Hecq *et al.* showed the enhanced dissolution rate through the nanosizing of nifedipine, 95% of the nanosized nifedipine was dissolved in 60 min compared to 5% for the un-milled nifedipine.[29] The absolute bioavailability in fasted male beagle dogs of nanocrystalline danazol was found to be about 82.3%. However, the bioavailability of an aqueous suspension of conventional danazol particles was found to be just 5.1%. [27] The increased dissolution and oral bioavailability resulting from nanosizing a drug can enhance the pharmacological activity of the drug. Kaysers *et al.* reported better efficacy with a NS compared to a liposomal formulation of amphotericin B.[30] About 23% reduction in *Leishmania donovani* was achieved after oral administration of amphotericin B NS, but a 0% reduction was observed after oral administration of the

lipsomal dosage form. It has been demonstrated in rats that reducing drug particle size decreased the gastric irritation and increased the rate of absorption by about four-fold following oral administration of naproxen.[39]

2.6.1.4. Benefits of nanosuspension

NS provide a convenient remedy for administering high doses of drug without the risks routinely associated with conventional formulations containing co-solvents.[40] Table 2.2 shows benefits of NSs.[19] Some products produced by NS technology in clinical development or available commercially are shown in Table 2.3.[19,24]

Table 2.2. Benefits of nanosuspensions

Physicochemical characteristic	**Potential benefits**
Increased drug amount in dosage form without harsh vehicles (extreme pH, co-solvents)	Intravenous: reduced toxicity, increased efficacy
Reduced particle size: increased drug dissolution rate	Oral: increased rate and extent of absorption, increased bioavailability of drug: area under plasma versus time curve, onset time, peak drug level, reduced variability, reduced fed/fasted effects. Pulmonary: increased delivery to deep lung
Solid state: increased drug loading	Reduced administration volumes; essential for intramuscular, subcutaneous, ophthalmic use
Solid state: increased stability	Increased resistance to hydrolysis and oxidation, increased physical stability to settling
Particulate dosage form	Intravenous: potential for intravenous sustained release via monocyte phagocytic system targeting, reduced toxicity, increased efficacy. Oral: potential for reduced first-pass hepatic metabolism

Table 2.3. Overview of nanosuspension based formulations (until 2009) of drugs in the market and in different clinical phases

Drug	Indication	Drug Delivery Company	Route	Status
Paclitaxel	Anti-cancer	American BioScience	Intravenous	Phase III
Undisclosed multiple	Anti-infective	Baxter NANOEDGE	Oral, intravenous	Preclinical to Phase II
Undisclosed	Anticancer	Baxter NANOEDGE	Intravenous, oral	Preclinical to Phase II
Rapamune (sirolimus)	Immuno-suppressant	Elan Nanosystems	Oral	Marketed
Emend (aprepitant)	Anti-emetic	Elan Nanosystems	Oral	Marketed
Cytokine inhibitor	Crohn's disease	Elan Nanosystems	Oral	Phase II
Diagnostic agent	Imaging agent	Elan Nanosystems	Intravenous	Phase I/II
Thymectacin	Anticancer agent	Elan Nanosystems	Intravenous	Phase I/II
Budesonide	Asthma	Elan Nanosystems	Pulmonary	Phase I
Tricor (fenofibrate)	Lipid lowering	Abbott Laboratories	Oral	Marketed
Fenofibrate	Lipid lowering	SkyePharma	Oral	Phase I
Busulfan	Anticancer	SkyePharma	Intrathecal	Phase I
Megace ES (megestrol)	Weight gain	Elan Nanosystems	Oral	Marketed
Insulin	Diabetes	BioSante	Oral	Phase I
Calcium phosphate	Mucosal vaccine adjuvant for herpes	BioSante	Oral	Phase I

2.6.2. Self-microemulsifying drug delivery system (SMEDDS)

For drug substances that exhibit poor water solubility but sufficient lipophilic properties, it will be beneficial to dose them in a predissolved state, e.g. in a lipid formulation,[41-43] thereby reducing the energy associated with a solid-liquid phase transition and overcoming the slow dissolution process after oral intake. Lipid formulations include lipid solutions, emulsions, microemulsions, self-emulsifying drug delivery systems (SEDDS) or SMEDDS.[44,45] A simple classification system of lipid formulations, based on the polarity of the blend, has been proposed by Pouton (Table 2.4).[46,47] The most straightforward lipid-based formulation is a lipid solution, classified as a Type I formulation. The obvious advantage of this formulation is its relative simplicity. Nonetheless these formulations are highly dependent on the digestion process and suffer from low solvent capacity. Unless the drug is sufficiently lipophilic (log P>4), formulation as an oil solution is limited to highly potent compounds. Solvent capacity can be increased by adding surface active agents as is the case in type II and III formulations. In addition, the most polar formulations, comprising hydrophilic surfactants and represented by class III, often exhibit self-emulsifying properties.

The application of self-emulsifying systems has gained considerable interest after the commercial success of lipid-based formulations of cyclosporine A ('Neoral Sandimmune^{TM}' previously known as 'Sandimmune^{TM}') and HIV protease inhibitors, saquinavir ('Fortovase^{TM}') and ritonavir ('Norvir^{TM}'), which are commercially available as SMEDDS formulations.[48-50]

SMEDDS are isotropic mixtures made up of oil, surfactant and sometimes cosurfactant or cosolvent. In an aqueous environment a homogeneous, transparent (or at least translucent), isotropic and thermodynamically stable dispersion will result, the formation of which is improved by gentle agitation, *in vivo* provided by gastrointestinal motility.[51,52] The drug will be solubilised in the GI tract in oil droplets, the large amount and small size (submicron size) of which lead to a considerable increase of surface area from where drug dissolution can take place. Furthermore, these formulations are known to reduce inter- and intra-individual variations in bioavailability, which is believed to be caused by a decreased sensitivity of formulation performance to pre-absorptive solubilisation and dietary status.

SMEDDS can enhance drug absorption by a number of ancillary mechanisms, including reduction of gastric motility and alteration of the physical and biochemical barrier function of the gastro-intestinal mucosa. Considering the classification system as determined by Pouton, SMEDDS are generally categorized as Type III (B) formulations, although literature is not clear on this subject nor is the sub-classification well defined.[53]

2.6.2.1. Role of SEDDS/SMEDDS in improvement of oral absorption

SEDDS/SMEDDS partially avoids the additional drug dissolution step prior to absorption in the GI tract. They increase the amount of solubilized drug in the intestinal fluids resulting in good drug absorption. Apart from this, absorption of the drug may also be enhanced by using lipid based excipients in the formulation. There are several mechanisms through which increased absorption can be achieved such as: Retardation of gastric emptying time; Increase in effective drug solubility in lumen; Lymphatic transport of the drug; Enterocyte based drug transport; Increasing membrane permeability.[54]

Medium-chain glycerides induce structural and fluidity changes in the mucosal membrane thus resulting in significant permeability changes. Supporting to this, several in vitro studies have shown that medium-chain glycerides markedly affect the permeability of paracellular markers. Several physical and physiological factors, that may affect the drug absorption from this systems include: 1) whether drug is formulated in an oil or emulsified form and in the later form how it is distributed between the two phases, 2) the absorption pathway of the drug, 3) the nature and particle size of the *in vivo* emulsion, 4) the role of surfactants/enhancers 5) the metabolic pathway of oil and 6) the tendency of the formulation to slow gastric motility and to promote emptying of the gall bladder. The literature reports that the absorption of drugs from oral dosage forms containing oil(s)/lipid(s) is sometimes increased by the presence of a lipophilic solvent and sometimes remains unaffected or reduced if oil is non-digestible. So it can be predicted that effect of lipid(s) on drug absorption is dependent on the specific combination of drug and lipid involved. The nature of drug and that of lipid, as well as aqueous and lipid solubility of drug are

crucial factors that control drug release/absorption from lipid-based dosage formulation.

Table 2.4. Typical properties of type I, II, III and IV lipid formulations

Formulation type	**Materials**	**Characteristics**	**Advantages**	**Disadvantages**
Type I	Oils without surfactants (e.g. tri-, di-and monoglycerides)	Non-dispersing, requires digestion	GRAS status; simple; excellent capsule compatibility	Formulation has poor solvent capacity unless drug is highly lipophilic
Type II	Oils and water insoluble surfactants	SEDDS formed without water-soluble components	Unlikely to lose solvent capacity on dispersion	Turbid o/w dispersion (particle size 0.25–2 μm)
Type IIIA	Oils, surfactants, cosolvents (both water insoluble and water soluble excipients)	SEDDS/SMEDDS formed with water soluble components	Clear or almost clear dispersion; drug absorption without digestion	Possible loss of solvent capacity on dispersion; less easily digested
Type IIIB	Oils, surfactants, cosolvents	SMEDDS with water-soluble components and low oil content	Clear dispersion, drug absorption without digestion	Likely loss of solvent capacity on dispersion
Type IV	Water-soluble surfactants and colsolvents (no oils)	Formulation disperses typically to form micellar solution	Formulation has good solvent capacity for many drugs	Likely loss of solvent capacity on dispersion; may not be digestible

For SMEDDS, it has been shown that the oil/water partition coefficient of the drug and droplet size can modulate drug release. The droplet size upon dilution with aqueous media is primarily controlled by the nature and concentration of the emulsifier, and phase diagrams of the oil/nonionic surfactant/ drug can be constructed to identify regions where maximum self-microemulsification occurs. The higher the concentration of emulsifier, the smaller the droplet sizes of the resulting emulsion and the faster is the drug release. The combination of small droplets along with a low oil/water partition coefficient will allow for an optimum drug release from SMEDDS. Similarly, drug release from microemulsion (o/w and w/o), depends on a number of process parameters, such as oil/aqueous phase ratio, the droplet size, the distribution of drug in the phases of microemulsion system and its diffusion rate in both phases. It is observed that the higher water/oil partition coefficient favors the higher bioavailability. It is therefore not surprising that not all water soluble or insoluble drugs can be formulated in water-in-oil microemulsion with a concomitant improvement of their intestinal absorption. Though direct determination of drug distribution between the aqueous and oil phases of microemulsion is difficult water/oil partitioning studies using the aqueous and oil phases of the corresponding microemulsion should be conducted and correlated to the observed oral bioavailability and/or *in vitro* permeability.[52]

2.6.2.2. Mechanism of self-emulsification

Conventional emulsions are formed by mixing two immiscible liquids namely water and oil stabilized by an emulsifying agent. When an emulsion is formed surface area expansion is created between the two phases. The emulsion is stabilized by the surfactant molecules that form a film around the internal phase droplet. In conventional emulsion formation, the excess surface free energy is dependent on the droplet size and the interfacial tension. If the emulsion is not stabilized using surfactants, the two phases will separate reducing the interfacial tension and the free energy.[55] In case of SMEDDS, the free energy of formation is very low and positive or even negative which results in thermodynamic spontaneous emulsification. It has been suggested that self-emulsification occurs due to penetration of water into the Liquid Crystalline (LC) phase that is formed at the oil/surfactant-water interface into

which water can penetrate assisted by gentle agitation during self-emulsification. After water penetrates to a certain extent, there is disruption of the interface and a droplet formation. This LC phase is considered to be responsible for the high stability of the resulting nanoemulsion against coalescence.[56]

2.6.2.3. SMEDDS components

SMEDDS are easily manufactured and physically stable isotropic mixture of oil, surfactant, cosurfactant and drug substances that are suitable for oral delivery in soft and hard gelatin capsules. Self-emulsifying formulations are easily dispersed in the GI tract, where the motility of stomach and small intestine provides the agitation necessary for emulsification. SMEDDS forms transparent microemulsion with a size of less than 100 nm.[51] Small lipid droplet size and associated greater lipid surface are produced by SMEDDS formulation facilitating lipid digestion resulting in more rapid incorporation of the drug into the bile salt mixed micelles. The ultimate result is an increase in the degree and uniformity of drug absorption relative to that associated with simple lipid solution of drug.[42] The improved drug absorption provided by SMEDDS depends upon maintenance of drug in solubilized state until it is absorbed from GIT.[46] In intestine where lipid vehicle hydrolysis rate exceeds that of drug absorption, luminal drug precipitation can occur resulting in suboptimal and more variable drug absorption.[57]

Self-emulsification has been shown to be specific to the nature of the oil/surfactant pair; the surfactant concentration and oil/surfactant ratio; and the temperature at which self-emulsification occurs. In support of these facts, it has also been demonstrated that only very specific pharmaceutical excipient combinations could lead to efficient self-emulsifying systems.[58]

2.6.2.3.1. Oils

The oil represents one of the most important excipients in the SMEDDS formulation not only because it can solubilize marked amounts of the lipophilic drug or facilitate self-emulsification but also and mainly because it can increase the fraction of

lipophilic drug transported via the intestinal lymphatic system, thereby increasing absorption from the GI tract depending on the molecular nature of the triglyceride.[59] Both long and medium chain triglyceride oils with different degrees of saturation have been used for the design of self-emulsifying formulations. Furthermore, edible oils which could represent the logical and preferred lipid excipient choice for the development of SMEDDS are not frequently selected due to their poor ability to dissolve large amounts of lipophilic drugs. Modified or hydrolyzed vegetable oils have been widely used since these excipients form good emulsification systems with a large number of surfactants approved for oral administration and exhibit better drug solubility properties.[52] They offer formulative and physiological advantages and their degradation products resemble the natural end products of intestinal digestion. Novel semi synthetic medium chain derivatives, which can be defined as amphiphilic compounds with surfactant properties, are progressively and effectively replacing the regular medium chain triglyceride oils in the SEOFs.

2.6.2.3.2. Surfactants

Several compounds exhibiting surfactant properties may be employed for the design of self-emulsifying systems, the most widely recommended ones being the non-ionic surfactants with a relatively high hydrophilic−lipophilic balance (HLB). The commonly used emulsifiers are various solid or liquid ethoxylated polyglycolyzed glycerides and polyoxyethylene 20 oleate (Tween 80). Safety is a major determining factor in choosing a surfactant.[52,60] Usually the surfactant concentration ranges between 30 and 60% w/w in order to form stable SMEDDS. It is very important to determine the surfactant concentration properly as large amounts of surfactants may cause GI irritation. The surfactant involved in the formulation of SMEDDS should have a relatively high HLB and hydrophilicity so that immediate formation of o/w droplets and/or rapid spreading of the formulation in the aqueous media (good self-emulsifying performance) can be achieved.[51] Surfactants are amphiphilic in nature and they can dissolve or solubilize relatively high amounts of hydrophobic drug compounds. The lipid mixtures with higher surfactant and co-surfactant/oil ratios lead to the formation of SMEDDS.[52] The formulation of w/o microemulsions for use as SEDDS or SMEDDS has been investigated using blends of low and high HLB

surfactants, which are commercially available and pharmaceutically acceptable, typically sorbitan esters and Tween 80. The oil phase comprised long or medium chain length glycerides.[61]

2.6.2.3.3. Co-solvents

The production of an optimum SMEDDS requires relatively high concentrations (generally more than 30% w/w) of surfactants. Organic solvents such as, ethanol, propylene glycol (PG), and polyethylene glycol (PEG) are suitable for oral delivery, and they enable the dissolution of large quantities of either the hydrophilic surfactant or the drug in the lipid base. These solvents can even act as co-surfactants in microemulsion systems. On the other hand, alcohols and other volatile co-solvents have the disadvantage of evaporating into the shells of the soft gelatin, or hard, sealed gelatin capsules in conventional SEDDS leading to drug precipitation. Thus, alcohol−free formulations have been designed[52], but their lipophilic drug dissolution ability may be limited.

2.6.2.4. Formulation of SMEDDS

SMEDDS are composed of oil, hydrophilic surfactant, and a cosurfactant. The process of self-emulsification is only specific to certain combinations of pharmaceutical excipients. The primary step during formulation of a SMEDDS is the identification of specific combinations of excipients and constructing a phase diagram which shows various concentrations of excipients necessary for self-emulsification. Mutual miscibility of these excipients is also important for producing a stable liquid formulation. Selection of excipients for SMEDDS lies in identifying excipients combination which will solubilize the entire dose of drug in volume acceptable for unit oral administration. Excipients combinations yielding SMEDDS formulations are identified by construction of pseudo-ternary phase diagram. Pseudo-ternary phase diagram can be represented in a triangular format (triangle) which has three coordinates. Each coordinate represents one component of microemulsion system.

2.6.2.4.1. Drug incorporation

Poorly water soluble drugs are often a choice for SMEDDS based dosage form. It is essential that the therapeutic dose of the drug be soluble in an acceptable volume of self-emulsifying mixture. The uses of newer synthetic oils that are amphiphilic in nature can dissolve large quantities of the drug when compared to conventionally used pure vegetable oils or its derivatives. Surfactants also provide good solvency for the drug. Although, the cosolvent is capable of dissolving a large quantity of the drug, they may cause drug precipitation on aqueous dilution due to loss of solvent capacity. This necessitates performing equilibrium solubility measurements of the drug in the excipients under use. The drug may affect the self-emulsification efficiency by changing optimal oil/surfactant ratio. It may interact with the LC phase of some of the mixture components causing blockage of charge movement through the system or may penetrate the surfactant monolayer.[62] The incorporated drug may increase or decrease the self-emulsifying efficiency or may not affect it at all.[41] Hence SMEDDS should also be evaluated for its self-emuslification efficiency in the presence of the drug. SMEDDS are known to be more sensitive towards any changes in the ratio of excipients. Because of these reasons, pre-formulation solubility and phase diagrams should be thoroughly evaluated when choosing the optimized formulation.

2.6.2.4.2. Capsule compatibility

Liquid SMEDDS (L-SMEDDS) filled in hard and soft gelatin capsules are more acceptable as dosage forms. Presence of hygroscopic material in the liquid formulation may cause dehydration of capsule shell or polar molecules such as polyethylene glycol or alcohol may penetrate into the capsule shell. Thus it is necessary to investigate such effects at an early stage of development.[63] Solid SMEDDS possess an advantage in this regard due to lack of contact of liquid material with the capsule shell.

2.6.2.5. Conversion of L-SMEDDS to Solid SMEDDS

L-SMEDDS can be filled in soft or hard gelatin capsule. Recently, there have been efforts by research groups working on SEDDS/SMEDDS to convert L-SEDDS/SMEDDS to S-SEDDS/SMEDDS.[54] These Solid SEDDS/SMEDDS can be made into tablets or be encapsulated. The primary reason to formulate SEDDS/SMEDDS in a solid form is to consolidate the advantages of L-SMEDDS with convenience of solid oral dosage forms. Oral solid dosage forms have the following advantages[64]: (a) low production cost (b) convenience of process control (c) high stability and reproducibility and (d) better patient compliance. Generally, the formulated SMEDDS are liquid in state, but sometimes it could be in a semisolid state depending on the physical state of excipients used. Researchers have adopted various techniques to obtain this conversion. S-SMEDDS also offers added versatility in terms of possible dosage forms. The following description elaborates various Liquid to Solid SMEDDS conversion techniques.

Spray drying: Spray drying is the most widely used technique to convert Liquid SEDDS/SMEDDS into solid state. In this method the Liquid SEDDS/SMEDDS is mixed with a solid carrier in a suitable solvent. The solvent is then atomized into a spray of fine droplets. These droplets are introduced into a drying chamber, where the solvent gets evaporated forming dry particles under a controlled temperature and airflow conditions.[64] The process parameters required to be controlled are inlet and outlet temperature, feed rate of solvent, and aspiration and drying air flow rate. The dry particles can then be either filled into capsules or made into tablets after addition of suitable excipients. Various solid carriers that have been used for this purpose are: Aerosil 200 suspended in ethanol[65] and aqueous solution of Dextran 40.[66]

Adsorption to solid carriers: The L-SEDDS/SMEDDS can be made to adsorb onto free flowing powders that possess very large surface area and are capable of adsorbing high quantities of oil material. The adsorption can be done either by mixing L-SEDDS/SMEDDS and the adsorbent in a blender or by simple physical mixing. The resulting powders can be either filled into capsules or can be made into tablets after addition of appropriate excipients. The adsorbents are capable of adsorbing Liquid SEDDS up to 70 %w/w of its own weight. Solid carriers used for this purpose can be microporous inorganic substances, high surface area colloidal inorganic

substances or cross-linked polymers.[64] Categories of solid adsorbents used are: silicates, magnesium trisilicate, talcum, crospovidone, cross-linked sodium carboxymethyl cellulose and cross-linked polymethyl methacrylate. Oral solid heparin and gentamicin SMEDDS were prepared using three kinds of adsorbents: microporous calcium silicate (Florite RE), magnesium aluminometa silicate (Neusilin US2) and silicon dioxide (Sylysia 320).[67,68]

Encapsulation of Liquid and Semisolid SEDDS: It is one of the simplest techniques for conversion of Liquid SEDDS to solid oral dosage form. Liquid SEDDS can be simply filled in capsules, sealed using a microspray or a banding process. For a semisolid SEDDS, it is a four step process: (1) heating the semisolid excipients to at least 20°C above its melting point; (2) adding the drug in the molten mixture while stirring; (3) filling the drug loaded molten mixture into the capsule shell and (4) cooling the product to room temperature. The compatibility of the excipients used with the capsule shell should be well investigated. Lipid excipients compatible with the capsule shell are described by Cole et al.[69] Capsule filling of SEDDS is suitable for low dose highly potent drugs and allows high drug incorporation.[64]

Extrusion Spheronization: This is a solvent free technique that converts Liquid SEDDS into pellets using extrusion and spheronization processes. In this method the Liquid SEDDS is first mixed with a binder, followed by addition of water until the mass is suitable for extrusion. The extruded mass is then spheronized to form uniform sized pellets. The pellets are then dried and size separated. The relative quantity of water and Liquid SEDDS used in the process has an effect on size distribution, extrusion force, surface roughness of pellets, and disintegration time. High drug incorporation can be achieved by using this technique. Abdalla et al. used microcrystalline cellulose (MCC) as a binder in preparation of progesterone self-emulsifying pellets.[70] A mixture of silicon dioxide, glyceryl behenate, pregelatinized starch, sodium croscarmellose, and MCC were used by Setthacheewakul et al. in the preparation of curcumin loaded SMEDDS pellets.[71]

Melt Granulation: Melt Granulation is another solvent free technique for converting liquid SEDDS into solid form. In this method, Liquid SEDDS is mixed with a binder that melts or softens at relatively low temperature. This melted mixture can be granulated. This technique is advantageous since it does not require addition of a

liquid binder and subsequent drying unlike conventional wet granulation. The variables to be controlled in this process are impeller speed, mixing time, binder particle size, and the viscosity of the binder.[64] A mixture of mono-, di- and triglycerides and esters of polyethylene glycol (PEG) called as Gelucire are used as binders to prepare immediate release pellets by melt granulation and as a self-emulsifying drug delivery system by capsule moulding or as powder obtained by cryogenic grinding.[72]

2.6.2.6. Benefits of SMEDDS

Several benefits of SMEDDS over conventional formulations have been reported:

- Enhanced oral bioavailability enabling reduction in dose.
- More consistent temporal profiles of drug absorption.
- Selective targeting of drug(s) towards specific absorption window in GIT.
- Protection of drug(s) from the hostile environment in gut.
- Reduced variability including food effects.
- Protection of sensitive drug substances.
- Liquid or solid dosage forms.
- In SMEDDS, the lipid matrix interacts readily with water, forming a fine particulate oil-in-water (o/w) emulsion. The emulsion droplets will deliver the drug to the gastrointestinal mucosa in the dissolved state readily accessible for absorption. Therefore increase in AUC i.e. bioavailability and C max is observed with many drugs when presented in SMEDDS.
- Fine oil droplets empty rapidly from the stomach and promote wide distribution of drug throughout the intestinal tract and thereby minimizing irritation frequently encountered with extended contact of drugs and gut wall.
- Ease of manufacture and scale up is one of the most important advantage that make SMEDDS unique when compared to other drug delivery systems like solid dispersion, liposomes, nanoparticles etc.
- SMEDDS has potential to deliver peptides that are processed to enzymatic hydrolysis in GIT.

- When polymer is incorporated in composition of SMEDDS it gives prolonged release of medicament.
- SMEDDS formulation is composed of lipids, surfactants and co-solvents. The system has the ability to form an oil-on-water emulsion when dispersed by an aqueous phase under gentle agitation. SMEDDS present drugs in a small droplet size and well-proportioned distribution and increase the dissolution and permeability. Furthermore, because drugs can be loaded in the inner phase and delivered to the lymphatic system, can bypass first pass metabolism. Thus SMEDDS protect drugs against hydrolysis by enzymes in the GI tract and reduce the presystemic clearance in the GI mucosa and hepatic first-pass metabolism.[73]

2.6.3. Nanoparticles

The term 'nanoparticle' may be defined as a submicron drug carrier system which is generally (but not necessarily) composed of polymer. The polymer used may or may not be biodegradable even if the polymer biodegradability appears a main characteristic for drug delivery carriers. As a function of the morphological and structural organization of the polymer, we distinguish the 'nanosphere' which is a nanoparticle system with a matrix character and constituted by a solid core with a dense polymeric network, and the 'nanocapsule' which is formed by a thin polymeric envelope surrounding an oil or water filled cavity. Nanocapsules may, thus, be considered as a 'reservoir' system. Practically, the nanoparticles have a size around 200 nm and the drugs or other molecules may be dissolved into the nanoparticles, entrapped, encapsulated and/or adsorbed or attached. Figure 2.1 depicts various nanocarrier based drug delivery carrier systems used for effective drug delivery research.

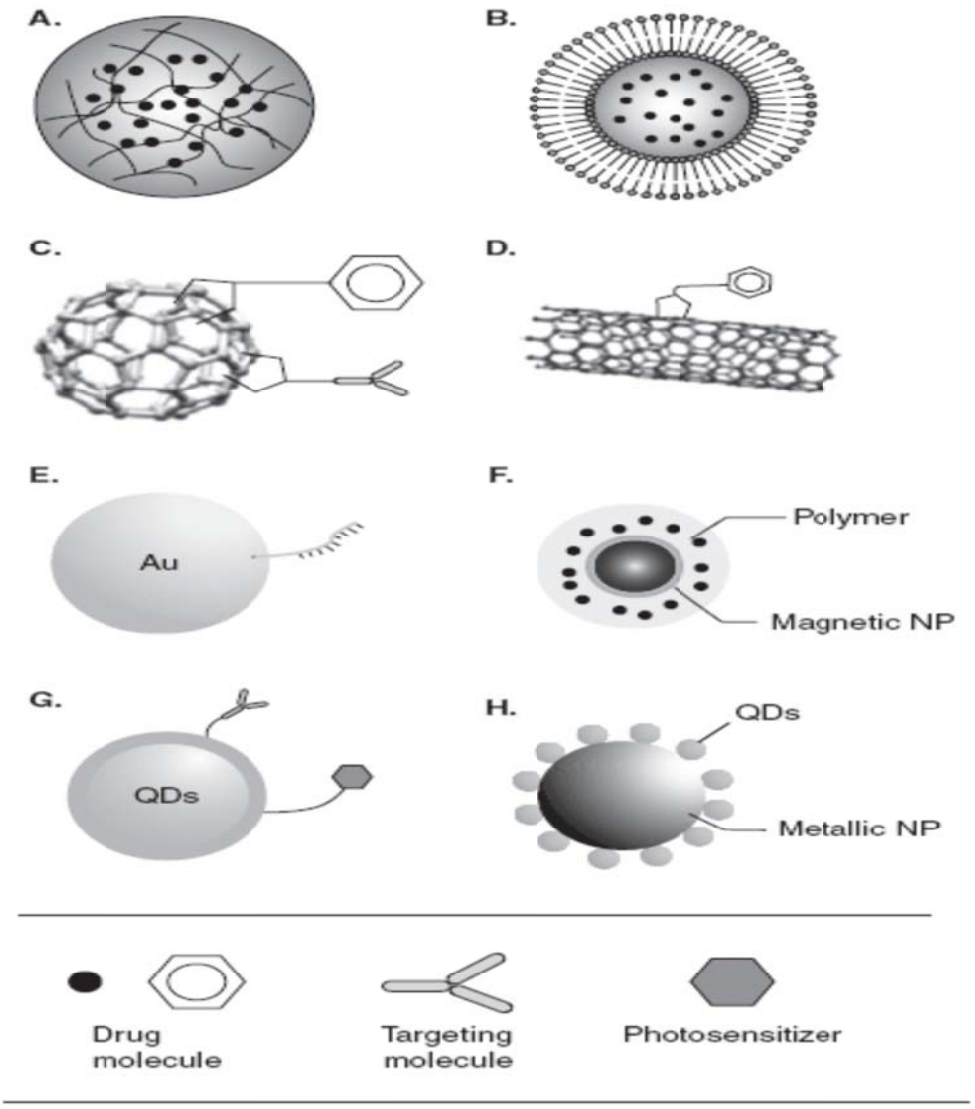

Figure 2.1. Various nanomaterial-based drug delivery platforms: A. Polymeric nanoparticles/micelles B. Liposome C. Buckyball D. Carbon nanotube E. Colloidal gold nanoparticle F. Magnetic nanoparticle G. Quantum dots H. Multifunctional nanoparticle with metallic nanoparticle core (metallic nanoparticle) and semiconductor quantum dots surrounding the shell. Drug molecules can be attached to these carrier systems through encapsulation, mixing, covalent conjugation or electrostatic and affinity interactions.

2.6.3.1. PLGA Nanoparticles

Recently, nano-sized drug delivery systems especially biocompatible and biodegradable polymer nanoparticles have attracted considerable interest since they can offer a suitable means of delivering small molecular weight drugs, proteins or genes to a targeted tissue or organ.[74,75] Nanoparticles are colloidal systems that have size typically in the range of 10-1000 nm in diameter, and drug can be entrapped in, adsorbed or chemically coupled onto the polymer nanoparticle matrix. On the other hand, a number of polymers have been investigated for formulating biodegradable nanoparticles, such as polylactide (PLA), poly(3-caprolactone) (PCL) and poly(lactide-co-glycolide) (PLGA) (Figure 2.2). They are biocompatible and biodegradable polymers approved by FDA and have been studied extensively.[76,77]

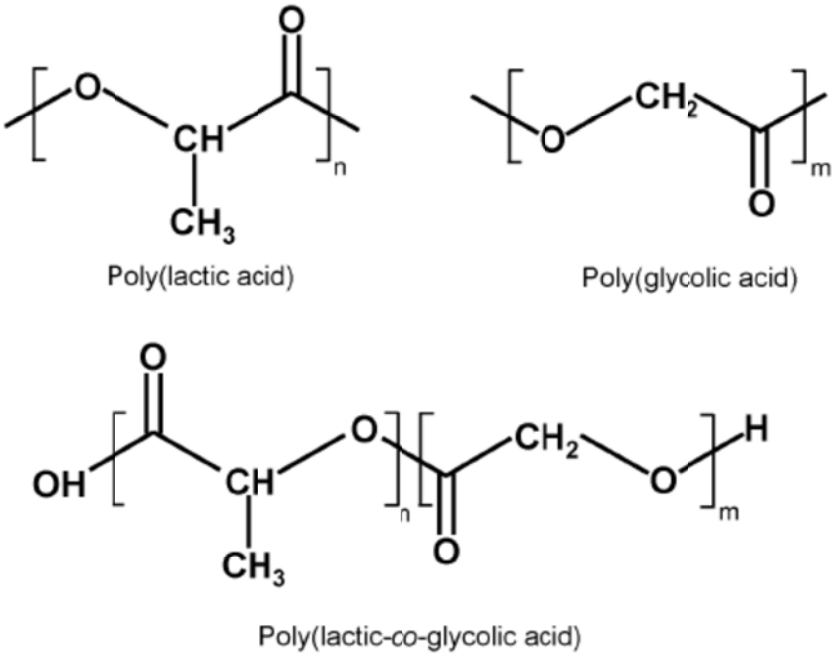

Figure 2.2. Molecular structure of lactide and glycolide based biodegradable polymers

PLGA is one of the most successfully used biodegradable nanosystem for the development of nanomedicines because it undergoes hydrolysis in the body to produce the biodegradable metabolite monomers, lactic acid and glycolic acid. Since

the body effectively deals with these two monomers, there is very minimal systemic toxicity associated by using PLGA for drug delivery or biomaterial applications. PLGA nanoparticles have been mostly prepared by emulsification–diffusion[78], solvent emulsion–evaporation[79], interfacial deposition[80] and nanoprecipitation method[81] (Figure 2.3). Briefly, in emulsification–diffusion method, the PLGA polymers are dissolved in organic solvent, poured and separated in aqueous phase having stabilizer and subsequently emulsified by homogenizer. In solvent evaporation method, the polymers are dissolved in volatile organic solvent and poured into continuously stirring aqueous phase with or without emulsifier/stabilizer and sonicated. Interfacial deposition methods have been used for the formation of both nanocapsule and nanospheres. The nanoparticles are synthesized in the interfacial layer of water and organic solvent (water miscible) and finally the nanoparticles are separated by centrifugations.[80] Most commonly used method for the preparation of PLGA nanoparticles is nanoprecipitation. Polymer dissolved in acetone is added drop-wise into continuously stirring aqueous phase with or without emulsifier/stabilizer and consequently organic phase is evaporated under reduced pressure (Figure 2.3).

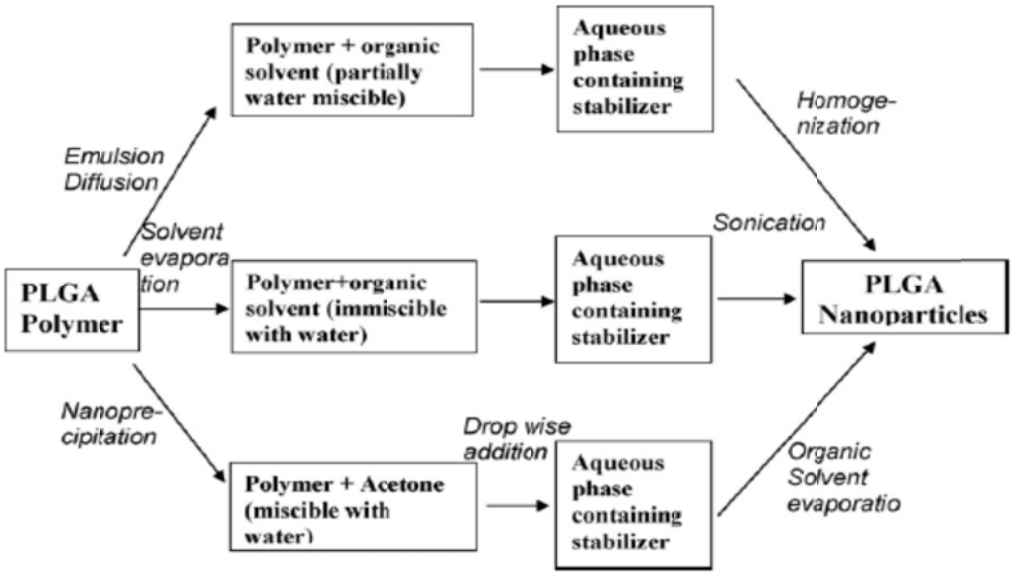

Figure 2.3. Different method for preparation of PLGA nanoparticles: PLGA nanoparticles were synthesized by emulsion diffusion, solvent evaporation and nanoprecipitation methods.

PLGA nanoparticles have been used to develop the proteins and peptides nanomedicine, nano-vaccines, nanoparticles based gene delivery system, nano-antigen and growth factor, etc.[82,83] Surface modification of PLGA, drug encapsulation methods and particle size, additives added during formulation, molecular weight of drug, ratio of lactide to glycolide moieties has strong influence on the release and effective response of formulated nanomedicines.[84] The acidic nature of PLGA monomers is not suitable for some sensitive drugs or bioactive molecules.[85] However, the approaches to overcome these problems have been developed. PLGA nanomedicine formulations are blended with alginate, chitosan, pectin[86], poly(propylenefumarate)[87], polyvinylacohol[88], poly(orthoester)[89] etc. The approval of PLGA has been granted by US Food and Drug Administration (USFDA) for human use and nanomedicines.[90]

PLGA is approved by FDA for therapeutic use in humans. Various preparation methods have been optimized for PLGA nanoparticles synthesis and numerous cancer related drugs have been incorporated in PLGA. These loaded nanoparticles protect poorly soluble and unstable payloads from the biological milieu and are small enough for capillary penetrations, cellular internalization and endosomal escape.[82] Furthermore, their surface is modified for targeted delivery of molecules to tumor or other tissues.[91] The larger size of PLGA nanoparticles is advantageous as multifunctional imaging and probes which incorporate encapsulated cancer drug, release, imaging, and targeting in a single nanoparticles platform.[92]

The performance of these nanoparticles is not completely satisfactory and great effort is needed to improve its physiochemical properties and synthesis process. The properties of nanoparticles as precursor of good nanomedicine are particle size, size distribution, surface morphology, surface chemistry, surface charge, surface adhesion, surface erosion, interior porosity, drug diffusivity, drug encapsulation efficiency, drug stability, drug release kinetics and hemodynamic. The surface charge of the nanoparticles is important for the cellular internalization of the NPs, clustering in blood flow, adherence, and interaction with oppositely charged cells membrane.[93] PLGA nanoparticles are frequently used for the encapsulation of various drugs and their successful delivery in vivo. PLGA nanoparticles loaded with hydrophobic poorly soluble drugs aremost commonly formulated by nanoprecipitation. Drug release and effective response of PLGA nanoparticles are influenced by (i) the surface

modification, (ii) the method of preparation, (iii) the particle size, (iv) the molecular weight of the encapsulated drug and (v) the ratio of lactide to glycolide moieties.[94] The cancer related drug paclitaxel, doxorubicin, 5-fluorouracil, 9-nitrocamptothecin, cisplatin, triptorelin, dexamethasone, xanthone, etc., have been successfully encapsulated on PLGA nanoparticles.[94]

The CD4+ T lymphocyte is the major target for infection by HIV-1. Cells of the mononuclear phagocyte system also serve as a reservoir for HIV. Macrophages are mature, non-proliferating and immunologically active cells that can be productively infected with HIV-1 and HIV-2.[95-97] Altered cellular functions in the macrophage population may contribute to the development and clinical progression of AIDS. Evidence has accumulated that cells of the macrophage lineage are vectors for the transmission of HIV-1. The placental macrophage is likely to be the primary cell type responsible for vertical transmission of HIV-1.[98] An important property of HIV-1 for mucosal transmission is the ability to infect macrophages.[99] Because of the important role of cells of the monocytes/macrophage lineage in the pathogenesis of HIV-1, fully effective ARV must react with monocytes/macrophage in addition to other targets.

Macrophages possess various receptors such as fucose receptors, mannosyl, galactosyl, and many others. Mannose receptors are present at the surface of monocyte macrophages, alveolar macrophages, astrocytes in brain, hepatocytes in liver and so on.[100-102] Therefore, targeting of ARV drugs to HIV infected macrophages could be an attractive approach in improving the therapeutic efficacy and reducing the toxicity of ARV bioactives.[103]

Polymeric nanoparticles have been used to target ARVs to (i) macrophages/monocytes[104-106] and (ii) CNS[107] which act as viral reservoir sites during HIV infection.[108] Macrophages have been reported to be a major cause of dissemination of the infection in the body in the later stages of the disease during which there is a continuous depletion of CD4+ T lymphocytes.[109] During this period, virus production from these mature non-proliferating macrophages/ monocytes is dramatically enhanced without being affected by the lethal effect of the replicating virus. Nanoparticulate mediated targeting of macrophages is well known and has been reported by several authors.[105,110,111] Following i.v. administration, nanoparticles are removed from the blood circulation by macrophages.[74] The recognition of particles by

macrophages is mediated by a process called opsonization.[112] When the distance between the particles and the opsonins is sufficiently small, they can bind to the surface of particles by any of the interactions such as van der Waals, electrostatic, ionic etc. After binding to the surface, particles become recognizable by macrophages and phagocytosis takes place.[112]

PLGA-nanoparticles are internalized in cells partly through fluid phase pinocytosis and also through clathrin-mediated endocytosis. PLGA-nanoparticles rapidly escape the endo-lysosomes and enter the cytoplasm within 10 min of incubation. This facilitates interactions of nanoparticles with the vesicular membranes leading to transient and localized destabilization of the membrane resulting in the escape of nanoparticles into the cytosol.[113] The body recognizes hydrophobic particles as foreign. The reticulo-endothelial system (RES) eliminates these from the blood stream and takes them up in the liver or the spleen. This process is one of the most important biological barriers to nanoparticles-based controlled drug delivery.[94] The binding of opsonin proteins present in the blood serum to injected nanoparticles leads to attachment of opsonized particles to macrophages and subsequently to their internalization by phagocytosis.[112]

PLGA nanoparticles can act as potential drug carriers to improve the delivery of ARV agents to the mononuclear phagocyte system in vivo, overcoming pharmacokinetic problems and enhancing the activity of drugs for treatment of HIV infection and AIDS. PLGA nanoparticles are worth investigating in this area of research.

2.6.3.2. Characterization of nanoparticles

Characterization of the nanoparticle carrier systems to thoroughly understand the properties is essential before putting them to pharmaceutical application. After preparation, nanoparticles are characterized at two levels. The physicochemical characterization consists of the evaluation of the particle size, size distribution, and surface properties (composition, charge, hydrophobicity) of the nanoparticles. The biopharmaceutical characterization includes measurements of drug encapsulation, in vitro drug release rates, and in vivo studies revealing biodistribution, bioavailability, and efficacy of the drug.

There are many sensitive techniques for characterizing nanoparticles, depending upon the parameter being looked at; laser light scattering (LLS) or photon correlation spectroscopy (PCS) for particle size and size distribution; scanning electron microscopy (SEM), transmission electron microscopy (TEM), and atomic force microscopy (AFM) for morphological properties; X-ray photoelectron spectroscopy (XPS), Fourier transform infrared spectroscopy (FTIR) and nuclear magnetic resonance spectroscopy (NMR) for surface chemistry; and differential scanning calorimetry (DSC) for thermal properties. Parameters such as density, molecular weight, and crystallinity affect release and degradation properties, whereas surface charge, hydrophilicity, and hydrophobicity significantly influence interaction with the biological environment.

2.6.3.2.1. Particle size and morphology

Nanoparticle size is critical not only in determining its release and degradation behaviour but also in determining the efficacy of the therapeutic agent by affecting tissue penetration or even intracellular uptake. [114] Particle size can be determined by PCS, SEM, TEM, AFM.

PCS is a technique employed to determine the mean particle size (PCS diameter) and size distribution (polydispersity index, PI) in Malvern Zetasizer Nanoseries-ZS. It is a light scattering experiment in which the statistical intensity fluctuations in light scattered from the particles are measured. These fluctuations are due to the random brownian motion of the particles. Brownian motion is the random movement of particles due to the bombardment by the solvent molecules that surround them. The parameter calculated is defined as the translational diffusion coefficient (usually given as D). The particle size is then calculated from the translational diffusion coefficient by the Stokes-Einstein equation.

PCS diameter gives information about the average particle size. The measured PCS diameter is based on the intensity of scattered light and therefore is not identical to the numeric diameter except in case of monodisperse particle suspensions. For polydisperse samples, PCS diameter is larger because it is based on the scattering intensity of the particles.

2.6.3.2.2. Crystallinity

The physical state of both the drug and the polymer are determined because this will have an influence on the *in vitro* and *in vivo* release characteristics of the drug. The crystalline behaviour of polymeric nanoparticles is studied using XRD and thermo-analytical methods such as DSC and differential thermal analysis (DTA).[115,116] DSC and XRD techniques are often combined to get useful information on the structural characteristics of both drugs and polymers.

2.6.3.2.3. Surface charge

Zeta potential is measure of the surface charge of the nanoparticles. The zeta potential value can influence particle stability and mucoadhesion as well as intracellular trafficking of nanoparticles as a function of pH. High zeta potential values, either positive or negative, should be achieved to ensure stability and to avoid aggregation of the particles. The extent of surface hydrophilicity can then be predicted from the values of zeta potential.[82] Surface charge is generally determined by well-known electrophoresis method with the help of Zetasizer.[117]

2.6.3.3. Commercial product based on Poly(lactic acid) (PLA), Poly(glycolic acid) (PGA), and PLGA

The first FDA-cleared PLGA product was the Lupron Depot drug-delivery system (TAP Pharmaceutical Products, Lake Forest, Illinois), a controlled release device for the treatment of advanced prostate cancer that used biodegradable microspheres of 75:25 lactide/glycolide to administer leuprolide acetate over a period of 4 months (replacing daily injections).[118] A list of commercial products is presented in Table 2.5.

Table 2.5. FDA-approved and under development (until 2009) drug delivery products using PLGA.

Product	Polymer	Active ingredient	Indication	Route of administration	Status
Nutropin Depot®	PLGA	Human growth hormone	Growth defi ciencies	SC/IM	Marketed
Sandostatin LAR®	PLGA-glucose	Octreotide acetate	Acromegaly	SC/IM	Marketed
Trelstar™ Depot	PLGA	Triptorelin pamoate	Prostate cancer	IM	Marketed
Decapeptyl®	PLGA	Triptorelin pamoate	Prostate cancer	IM	Marketed
Pamorelin	PLGA	Leuprolide acetate	Prostate cancer	SC	Marketed
Oncogel®	PEG-PLGA-PEG	Paclitaxel	Solid tumors	Intratumoral injection	Clinical trial; Phase II
Atridox®	PLGA	Doxycycline hyclate 10%	Chronic adult periodontitis	Topical	Marketed
Sanvar® SR	PLGA	Vapreotide	Esophageal bleeding varices (EVB)	SC/IM	Clinical trial; Phase III
Lupron depot	PLA	Leuprolide acetate	Prostate cancer, endometriosis	SC/IM	Marketed
Zoladex	PLA	Goserelin acetate	Prostate cancer, endometriosis	SC	Marketed

2.7. Model Drug – Efavirenz

Efavirenz (EFV) is an HIV-1 specific, NNRTI. EFV is chemically described as (S)-6-chloro-4-(cyclopropylethynyl)-l,4-dihydro-4-(trifluoromethyl)-2H-3,l-benzoxazin-2-one. Its empirical formula is $C_{14}H_9ClF_3NO_2$ and its structural formula is shown in Figure 2.4. EFV is a white to slightly pink crystalline powder with a molecular mass of 315.68. It is practically insoluble in water (< 10 μg/ml).[119]

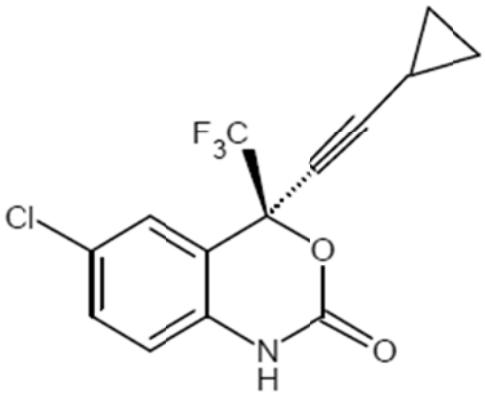

Figure 2.4. Molecular structure of EFV.

2.7.1. Physicochemical properties

State: solid[120]

Melting Point: 139-141°C

Predicted water solubility: 8.55e-03 g/l

Log P: 4.6

pK_a: 10.2

2.7.2. Mechanism of action

EFV inhibits the activity of viral RNA-directed DNA polymerase (i.e., reverse transcriptase).[119] Antiviral activity of EFV is dependent on intracellular conversion to the active triphosphorylated form. The rate of EFV phosphorylation varies, depending on cell type. It is believed that inhibition of reverse transcriptase interferes with the generation of DNA copies of viral RNA, which, in turn, are necessary for synthesis of new virions. Intracellular enzymes subsequently eliminate the HIV particle that previously had been uncoated, and left unprotected, during entry into the host cell. Thus, reverse transcriptase inhibitors are virustatic and do not eliminate HIV from the body. Even though human DNA polymerase is less susceptible to the pharmacologic effects of triphosphorylated EFV, this action may nevertheless account for some of the drug's toxicity.

2.7.3. Pharmacokinetics

2.7.3.1. Absorption and distribution

Peak EFV plasma concentrations of 1.6-9.1 μM were attained by 5 hours following single oral doses of 100 mg to 1600 mg administered to uninfected volunteers.[119] Dose-related increases in C_{max} and AUC were seen for doses up to 1600 mg; the increases were less than proportional suggesting diminished absorption at higher doses. In HIV-l-infected patients at steady state, mean C_{max}, mean C_{min}, and mean AUC were dose proportional following 200-mg, 400-mg, and 600-mg daily doses. Time-to-peak plasma concentrations were approximately 3-5 hours and steady-state plasma concentrations were reached in 6-10 days. EFV is highly bound (approximately 99.5-99.75%) to human plasma proteins, predominantly albumin. In HIV-1 infected patients who received 200 to 600 mg once daily for at least one month, cerebrospinal fluid concentrations ranged from 0.26 to 1.19% (mean 0.69%) of the corresponding plasma concentration. This proportion is approximately 3-fold higher than the non-protein-bound (free) fraction of EFV in plasma.

2.7.3.2. Metabolism

Studies in humans and in vitro studies using human liver microsomes have demonstrated that EFV is principally metabolized by the cytochrome P450 system to hydroxylated metabolites with subsequent glucuronidation of these hydroxylated metabolites. These metabolites are essentially inactive against HIV-1. The in vitro studies suggest that CYP3A and CYP2B6 are the major isozymes responsible for EFV metabolism. EFV has been shown to induce CYP enzymes, resulting in the induction of its own metabolism.

2.7.3.3. Elimination

The elimination pathway for EFV was mainly through the faeces. Approximately 14-34% of the radiolabel was recovered in the urine and 16-61% was recovered in the feces. Nearly all of the urinary excretion of the drug was in the form of metabolites.

The majority of the compound was recovered in faeces as the 8-hydroxy glucuronide. Less than 1 % was excreted in urine as unchanged EFV.

2.7.4. Adverse effect

Psychiatric symptoms, including insomnia, nightmares, confusion, memory loss, and depression, are common, [121] and more serious symptoms such as psychosis may occur in patients with compromised liver or kidney function. [122,123] The most common adverse effects are rash, dizziness, nausea, headache, fatigue, insomnia, and vomiting. A general guideline about EFV and pregnancy states that EFV can cause birth defects and should not be used in women who might become pregnant. A later study, however, found no increased risk of overall birth defects among women exposed to EFV during the first trimester of pregnancy compared with exposure to other antiretroviral drugs. [124]

2.7.5. Literature review

Some of the research articles on EFV are as follow:

- King J. et al has carried out a randomized crossover study to determine relative bioequivalence of tenofovir, emtricitabine, and efavirenz (Atripla) fixed-dose combination tablet compared with a compounded oral liquid formulation derived from the tablet. [125]
- Chiappetta D. A. et al investigated the synergistic performance of mixed polymeric micelles made of linear and branched poly(ethylene oxide)-poly(propylene oxide) for the more effective encapsulation of the anti-HIV drug efavirenz.[126] Chiappetta D. A. et al also investigated oral pharmacokinetics of the anti-HIV efavirenz encapsulated within polymeric micelles.[127]
- Rajesh Y.V. et al. investigated the impact of superdisintegrants on efavirenz release from tablet formulations. Efavirenz tablets of different doses were prepared by a wet granulation process using different superdisintegrants such as crosscarmellose sodium (CCS), sodium starch glycollate (SSG) and

crosspovidone (CP) to evaluate the role of different disintegrants on the in vitro release of EFV.[128]

- Chiappetta D. A. et al investigated a highly concentrated and taste-improved aqueous formulation of efavirenz for a more appropriate pediatric management of the anti-HIV therapy. [129]
- Balkundi S. et al studied nano-formulations of crystalline indinavir, ritonavir, atazanavir, and efavirenz by wet milling, homogenization or sonication with a variety of excipients.[130]
- Sathigari S. et al investigated the physicochemical characterization of efavirenz-cyclodextrin inclusion complexes. This study was to characterize the inclusion complexes of EFV with beta-cyclodextrin (beta-CD), hydroxypropyl beta-CD, and randomly methylated beta-CD to improve the solubility and dissolution of EFV.[131]
- Dutta T. et al has studied poly (propyleneimine) dendrimer based nanocontainers for targeting of efavirenz to human monocytes/macrophages in vitro.[132] Dutta T. et al also investigated the targeting of efavirenz loaded tuftsin conjugated poly(propyleneimine) dendrimers to HIV infected macrophages in vitro.[133]
- Destache C. J. et al has developed PLGA nanoparticle of three ARV drugs. Poly-(lactic-co-glycolic acid) nanoparticles containing ritonavir, lopinavir, and efavirenz were fabricated using multiple emulsion-solvent evaporation procedure.[134]

The present study was carried out to develop NS, SMEDDS to improve oral bioavailability of EFV. Mannose incorporated PLGA nanoparticles of EFV were developed for site-specific drug delivery.

REFERENCES

1 http://www.avert.org/hiv-virus.htm.

2 Sepkowitz, K. A. AIDS--the first 20 years. *The New England journal of medicine* **344**, 1764-1772, (2001).

3 http://web.archive.org/web/20050204141148/ http://www.cdc.gov/HIV/pubs/facts/transmission.htm.

4 Alimonti, J. B., Ball, T. B. & Fowke, K. R. Mechanisms of CD4+ T lymphocyte cell death in human immunodeficiency virus infection and AIDS. *The Journal of general virology* **84**, 1649-1661, (2003).

5 Lipman, M. C. I., Gluck, T. A. & Johnson, M. A. *An atlas of differential diagnosis in HIV disease*. Second edn, (Parthenon Pub. Group, 2003).

6 Kallings, L. O. The first postmodern pandemic: 25 years of HIV/ AIDS. *Journal of internal medicine* **263**, 218-243, (2008).

7 *http://www.unaids.org/en/media/unaids/contentassets/dataimport/pub/report/-2009/jc1700_epi_update_2009_en.pdf*.

8 *http://en.wikipedia.org/wiki/AIDS*.

9 Bower, M. *et al.* The effect of HAART in 254 consecutive patients with AIDS-related Kaposi's sarcoma. *AIDS* **23**, 1701-1706, (2009).

10 Katlama, C. *et al.* Efficacy of darunavir/ritonavir maintenance monotherapy in patients with HIV-1 viral suppression: a randomized open-label, noninferiority trial, MONOI-ANRS 136. *AIDS* **24**, 2365-2374, (2010).

11 *http://en.wikipedia.org/wiki/Antiretroviral_drug*.

12 Ojewole, E., Mackraj, I., Naidoo, P. & Govender, T. Exploring the use of novel drug delivery systems for antiretroviral drugs. *Eur J Pharm Biopharm* **70**, 697-710, (2008).

13 Li, X. & Chan, W. K. Transport, metabolism and elimination mechanisms of anti-HIV agents. *Advanced drug delivery reviews* **39**, 81-103, (1999).

14 Vyas, S. P., Subhedar, R. & Jain, S. Development and characterization of emulsomes for sustained and targeted delivery of an antiviral agent to liver. *The Journal of pharmacy and pharmacology* **58**, 321-326, (2006).

15 Amiji, M. M., Vyas, T. K. & Shah, L. K. Role of nanotechnology in HIV/AIDS treatment: potential to overcome the viral reservoir challenge. *Discovery medicine* **6**, 157-162, (2006).

16 Xiang, J., Fang, X. & Li, X. Transbuccal delivery of 2',3'-dideoxycytidine: in vitro permeation study and histological investigation. *International journal of pharmaceutics* **231**, 57-66, (2002).

17 Mirchandani, H. & Chien, Y. W. Drug-Delivery Approaches for Anti-Hiv Drugs. *International journal of pharmaceutics* **95**, 1-21, (1993).

18 Kreuter, J. *In Nanoparticles. Colloidal Drug Delivery Systems.*, 245-250 (Marcel Dekker Inc., New York. , 1994).

19 Rabinow, B. E. Nanosuspensions in drug delivery. *Nature reviews. Drug discovery* **3**, 785-796, (2004).

20 Muller, R. H. & Keck, C. M. Challenges and solutions for the delivery of biotech drugs--a review of drug nanocrystal technology and lipid nanoparticles. *Journal of biotechnology* **113**, 151-170, (2004).

21 Kesisoglou, F., Panmai, S. & Wu, Y. H. Nanosizing - Oral formulation development and biopharmaceutical evaluation. *Advanced drug delivery reviews* **59**, 631-644, (2007).

22 Kipp, J. E. The role of solid nanoparticle technology in the parenteral delivery of poorly water-soluble drugs. *International journal of pharmaceutics* **284**, 109-122, (2004).

23 Kocbek, P., Baumgartner, S. & Kristl, J. Preparation and evaluation of nanosuspensions for enhancing the dissolution of poorly soluble drugs. *International journal of pharmaceutics* **312**, 179-186, (2006).

24 Ganta, S. *Development and Evaluation of Nanoparticulate Drug Delivery Systems for Anticancer Drugs* Doctor of Philosophy thesis, The University of Auckland, (2008).

25 Müller, R. H., Böhm, B. H. L. & Grau, M. J. *Nanosuspensions - a formulation approach for poorly soluble and poorly bioavailable drugs. Handbook of pharmaceutical controlled release.*, (Marcel Dekker, New York, 2000).

26 Jia, L., Wong, H., Cerna, C. & Weitman, S. D. Effect of nanonization on absorption of 301029: ex vivo and in vivo pharmacokinetic correlations determined by liquid chromatography/mass spectrometry. *Pharmaceutical research* **19**, 1091-1096, (2002).

27 Liversidge, G. G. & Cundy, K. C. Particle-Size Reduction for Improvement of Oral Bioavailability of Hydrophobic Drugs .1. Absolute Oral Bioavailability of Nanocrystalline Danazol in Beagle Dogs. *International journal of pharmaceutics* **125**, 91-97, (1995).

28 Rasenack, N. & Muller, B. W. Dissolution rate enhancement by in situ micronization of poorly water-soluble drugs. *Pharmaceutical research* **19**, 1894-1900, (2002).

29 Hecq, J., Deleers, M., Fanara, D., Vranckx, H. & Amighi, K. Preparation and characterization of nanocrystals for solubility and dissolution rate enhancement of nifedipine. *International journal of pharmaceutics* **299**, 167-177, (2005).

30 Kayser, O., Olbrich, C., Yardley, V., Kiderlen, A. F. & Croft, S. L. Formulation of amphotericin B as nanosuspension for oral administration. *International journal of pharmaceutics* **254**, 73-75, (2003).

31 Muller, R. H., Becker, R., Kruss, B. & Peters, K. Pharmaceutical nanosuspensions for medicament administration as systems with increased saturation solubility and rate of solution. US patent 5,858,410. (1999).

32 Patravale, V. B., Date, A. A. & Kulkarni, R. M. Nanosuspensions: a promising drug delivery strategy. *The Journal of pharmacy and pharmacology* **56**, 827-840, (2004).

33 Allen, T. M. & Everest, J. M. Effect of liposome size and drug release properties on pharmacokinetics of encapsulated drug in rats. *The Journal of pharmacology and experimental therapeutics* **226**, 539-544, (1983).

34 Jacobs, C. & Muller, R. H. Production and characterization of a budesonide nanosuspension for pulmonary administration. *Pharmaceutical research* **19**, 189-194, (2002).

35 Muller, R. H., Jacobs, C. & Kayser, O. Nanosuspensions as particulate drug formulations in therapy Rationale for development and what we can expect for the future. *Advanced drug delivery reviews* **47**, 3-19, (2001).

36 Giron, D. Thermal-Analysis and Calorimetric Methods in the Characterization of Polymorphs and Solvates. *Thermochim Acta* **248**, 1-59, (1995).

37 Nicolaides, E., Symillides, M., Dressman, J. B. & Reppas, C. Biorelevant dissolution testing to predict the plasma profile of lipophilic drugs after oral administration. *Pharmaceutical research* **18**, 380-388, (2001).

38 Dressman, J. B. & Reppas, C. In vitro-in vivo correlations for lipophilic, poorly water-soluble drugs. *Eur J Pharm Sci* **11 Suppl 2**, S73-80, (2000).

39 Liversidge, G. G. & Conzentino, P. Drug Particle-Size Reduction for Decreasing Gastric Irritancy and Enhancing Absorption of Naproxen in Rats. *International journal of pharmaceutics* **125**, 309-313, (1995).

40 Merisko-Liversidge, E. *et al.* Formulation and antitumor activity evaluation of nanocrystalline suspensions of poorly soluble anticancer drugs. *Pharmaceutical research* **13**, 272-278, (1996).

41 Charman, S. A. *et al.* Self-Emulsifying Drug Delivery Systems - Formulation and Biopharmaceutic Evaluation of an Investigational Lipophilic Compound. *Pharmaceutical research* **9**, 87-93, (1992).

42 Humberstone, A. J. & Charman, W. N. Lipid-based vehicles for the oral delivery of poorly water soluble drugs. *Advanced drug delivery reviews* **25**, 103-128, (1997).

43 Porter, C. J. H., Kaukonen, A. M., Boyd, B. J., Edwards, G. A. & Charman, W. N. Susceptibility to lipase-mediated digestion reduces the oral bioavailability of danazol after administration as a medium-chain lipid-based microemulsion formulation. *Pharmaceutical research* **21**, 1405-1412, (2004).

44 Kang, B. K. *et al.* Development of self-microemulsifying drug delivery systems (SMEDDS) for oral bioavailability enhancement of simvastatin in beagle dogs. *International journal of pharmaceutics* **274**, 65-73, (2004).

45 Pouton, C. W. & Porter, C. J. H. Formulation of lipid-based delivery systems for oral administration: Materials, methods and strategies. *Advanced drug delivery reviews* **60**, 625-637, (2008).

46 Pouton, C. W. Lipid formulations for oral administration of drugs: non-emulsifying, self-emulsifying and 'self-microemulsifying' drug delivery systems. *Eur J Pharm Sci* **11**, S93-S98, (2000).

47 Pouton, C. W. Formulation of poorly water-soluble drugs for oral administration: physicochemical and physiological issues and the lipid formulation classification system. *Eur J Pharm Sci* **29**, 278-287, (2006).

48 Tarr, B. D. & Yalkowsky, S. H. Enhanced intestinal absorption of cyclosporine in rats through the reduction of emulsion droplet size. *Pharmaceutical research* **6**, 40-43, (1989).

49 Grevel, J., Nuesch, E., Abisch, E. & Kutz, K. Pharmacokinetics of oral cyclosporin A (Sandimmun) in healthy subjects. *European journal of clinical pharmacology* **31**, 211-216, (1986).

50 Vonderscher, J. & Meinzer, A. Rationale for the development of Sandimmune Neoral. *Transplantation proceedings* **26**, 2925-2927, (1994).

51 Shah, N. H., Carvajal, M. T., Patel, C. I., Infeld, M. H. & Malick, A. W. Self-Emulsifying Drug-Delivery Systems (Sedds) with Polyglycolyzed Glycerides for Improving in-Vitro Dissolution and Oral Absorption of Lipophilic Drugs. *International journal of pharmaceutics* **106**, 15-23, (1994).

52 Constantinides, P. P. Lipid microemulsions for improving drug dissolution and oral absorption: physical and biopharmaceutical aspects. *Pharmaceutical research* **12**, 1561-1572, (1995).

53 Goddeeris, C. *Study of the physicochemical properties of Self-Micro Emulifying Drug Delivery Systems and solid dispersions containing the water soluble drug UC 781* PhD thesis, Katholieke Universiteit Leuven, (2008).

54 Shah, I. *Development and Characterization of Oil-in-Water Nanoemulsions from Self-Microemulsifying Mixtures*, The University of Toledo, (2011).

55 Craig, D. Q. M., Barker, S. A., Banning, D. & Booth, S. W. An Investigation into the Mechanisms of Self-Emulsification Using Particle-Size Analysis and Low-Frequency Dielectric-Spectroscopy. *International journal of pharmaceutics* **114**, 103-110, (1995).

56 Groves, M. J. & de Galindez, D. A. The self-emulsifying action of mixed surfactants in oil. *Acta pharmaceutica Suecica* **13**, 361-372, (1976).

57 Myers, R. A. & Stella, V. J. Systemic Bioavailability of Penclomedine (Nsc-338720) from Oil-in-Water Emulsions Administered Intraduodenally to Rats. *International journal of pharmaceutics* **78**, 217-226, (1992).

58 Wakerly, M. G., Pouton, C. W., Meakin, B. J. & Morton, F. S. Self-Emulsification of Vegetable Oil-Nonionic Surfactant Mixtures - a Proposed Mechanism of Action. *Acs Sym Ser* **311**, 242-255, (1986).

59 Charman, W. N. & Stella, V. J. Transport of Lipophilic Molecules by the Intestinal Lymphatic-System. *Advanced drug delivery reviews* **7**, 1-14, (1991).

60 Yuasa, H., Sekiya, M., Ozeki, S. & Watanabe, J. Evaluation of milk fat-globule membrane (MFGM) emulsion for oral administration: absorption of alpha-linolenic acid in rats and the effect of emulsion droplet size. *Biological & pharmaceutical bulletin* **17**, 756-758, (1994).

61 Serajuddin, A. T., Sheen, P. C., Mufson, D., Bernstein, D. F. & Augustine, M. A. Effect of vehicle amphiphilicity on the dissolution and bioavailability of a poorly water-soluble drug from solid dispersions. *Journal of pharmaceutical sciences* **77**, 414-417, (1988).

62 Malcolmson, C. & Lawrence, M. J. A Comparison of the Incorporation of Model Steroids into Nonionic Micellar and Microemulsion Systems. *Journal of Pharmacy and Pharmacology* **45**, 141-143, (1993).

63 Singh, B., Bandopadhyay, S., Kapil, R., Singh, R. & Katare, O. Self-emulsifying drug delivery systems (SEDDS): formulation development, characterization, and applications. *Critical reviews in therapeutic drug carrier systems* **26**, 427-521, (2009).

64 Tang, B., Cheng, G., Gu, J. C. & Xu, C. H. Development of solid self-emulsifying drug delivery systems: preparation techniques and dosage forms. *Drug discovery today* **13**, 606-612, (2008).

65 Balakrishnan, P. *et al.* Enhanced oral bioavailability of dexibuprofen by a novel solid self-emulsifying drug delivery system (SEDDS). *Eur J Pharm Biopharm* **72**, 539-545, (2009).

66 Yi, T., Wan, J., Xu, H. & Yang, X. A new solid self-microemulsifying formulation prepared by spray-drying to improve the oral bioavailability of poorly water soluble drugs. *Eur J Pharm Biopharm* **70**, 439-444, (2008).

67 Ito, Y. *et al.* Preparation and evaluation of oral solid heparin using emulsifier and adsorbent for in vitro and in vivo studies. *International journal of pharmaceutics* **317**, 114-119, (2006).

68 Ito, Y. *et al.* Oral solid gentamicin preparation using emulsifier and adsorbent. *Journal of controlled release : official journal of the Controlled Release Society* **105**, 23-31, (2005).

69 Cole, E. T., Cade, D. & Benameur, H. Challenges and opportunities in the encapsulation of liquid and semi-solid formulations into capsules for oral administration. *Advanced drug delivery reviews* **60**, 747-756, (2008).

70 Abdalla, A., Klein, S. & Mader, K. A new self-emulsifying drug delivery system (SEDDS) for poorly soluble drugs: characterization, dissolution, in vitro digestion and incorporation into solid pellets. *Eur J Pharm Sci* **35**, 457-464, (2008).

71 Setthacheewakul, S., Mahattanadul, S., Phadoongsombut, N., Pichayakorn, W. & Wiwattanapatapee, R. Development and evaluation of self-microemulsifying liquid and pellet formulations of curcumin, and absorption studies in rats. *Eur J Pharm Biopharm* **76**, 475-485, (2010).

72 Chambin, O. *et al.* Influence of cryogenic grinding on properties of a self-emulsifying formulation. *International journal of pharmaceutics* **278**, 79-89, (2004).

73 Vishvajit, A. K., Deepali, M. J. & Vilasrao, J. K. Self micro emulsifying drug delivery system. *International Journal of Pharma and Bio Sciences* **1**, 1-9, (2010).

74 Moghimi, S. M., Hunter, A. C. & Murray, J. C. Long-circulating and target-specific nanoparticles: theory to practice. *Pharmacological reviews* **53**, 283-318, (2001).

75 Zweers, M. L., Grijpma, D. W., Engbers, G. H. & Feijen, J. The preparation of monodisperse biodegradable polyester nanoparticles with a controlled size.

Journal of biomedical materials research. Part B, Applied biomaterials **66**, 559-566, (2003).

76 Rouzes, C., Gref, R., Leonard, M., De Sousa Delgado, A. & Dellacherie, E. Surface modification of poly(lactic acid) nanospheres using hydrophobically modified dextrans as stabilizers in an o/w emulsion/evaporation technique. *Journal of biomedical materials research* **50**, 557-565, (2000).

77 Berton, M., Allemann, E., Stein, C. A. & Gurny, R. Highly loaded nanoparticulate carrier using an hydrophobic antisense oligonucleotide complex. *Eur J Pharm Sci* **9**, 163-170, (1999).

78 Sahana, D. K., Mittal, G., Bhardwaj, V. & Kumar, M. N. PLGA nanoparticles for oral delivery of hydrophobic drugs: influence of organic solvent on nanoparticle formation and release behavior in vitro and in vivo using estradiol as a model drug. *Journal of pharmaceutical sciences* **97**, 1530-1542, (2008).

79 Zambaux, M. F., Bonneaux, F., Gref, R., Dellacherie, E. & Vigneron, C. Preparation and characterization of protein C-loaded PLA nanoparticles. *Journal of controlled release : official journal of the Controlled Release Society* **60**, 179-188, (1999).

80 Pinto Reis, C., Neufeld, R. J., Ribeiro, A. J. & Veiga, F. Nanoencapsulation I. Methods for preparation of drug-loaded polymeric nanoparticles. *Nanomedicine : nanotechnology, biology, and medicine* **2**, 8-21, (2006).

81 Barichello, J. M., Morishita, M., Takayama, K. & Nagai, T. Encapsulation of hydrophilic and lipophilic drugs in PLGA nanoparticles by the nanoprecipitation method. *Drug development and industrial pharmacy* **25**, 471-476, (1999).

82 Soppimath, K. S., Aminabhavi, T. M., Kulkarni, A. R. & Rudzinski, W. E. Biodegradable polymeric nanoparticles as drug delivery devices. *Journal of controlled release : official journal of the Controlled Release Society* **70**, 1-20, (2001).

83 Carrasquillo, K. G. *et al.* Non-aqueous encapsulation of excipient-stabilized spray-freeze dried BSA into poly(lactide-co-glycolide) microspheres results in release of native protein. *Journal of controlled release : official journal of the Controlled Release Society* **76**, 199-208, (2001).

84 Mittal, G., Sahana, D. K., Bhardwaj, V. & Ravi Kumar, M. N. Estradiol loaded PLGA nanoparticles for oral administration: effect of polymer molecular weight and copolymer composition on release behavior in vitro and in vivo. *Journal of controlled release : official journal of the Controlled Release Society* **119**, 77-85, (2007).

85 Kumar, M. N. *et al.* Cationic poly(lactide-co-glycolide) nanoparticles as efficient in vivo gene transfection agents. *Journal of nanoscience and nanotechnology* **4**, 990-994, (2004).

86 Liu, L. *et al.* Pectin/poly(lactide-co-glycolide) composite matrices for biomedical applications. *Biomaterials* **25**, 3201-3210, (2004).

87 Hedberg, E. L. *et al.* In vivo degradation of porous poly(propylene fumarate)/poly(DL-lactic-co-glycolic acid) composite scaffolds. *Biomaterials* **26**, 4616-4623, (2005).

88 Patil, S. D., Papadimitrakopoulos, F. & Burgess, D. J. Dexamethasone-loaded poly(lactic-co-glycolic) acid microspheres/poly(vinyl alcohol) hydrogel composite coatings for inflammation control. *Diabetes technology & therapeutics* **6**, 887-897, (2004).

89 Wang, L. *et al.* Preparation, characterization, and in vitro evaluation of physostigmine-loaded poly(ortho ester) and poly(ortho ester)/poly(D,L-lactide-co-glycolide) blend microspheres fabricated by spray drying. *Biomaterials* **25**, 3275-3282, (2004).

90 Di Toro, R., Betti, V. & Spampinato, S. Biocompatibility and integrin-mediated adhesion of human osteoblasts to poly(DL-lactide-co-glycolide) copolymers. *Eur J Pharm Sci* **21**, 161-169, (2004).

91 Nobs, L., Buchegger, F., Gurny, R. & Allemann, E. Poly(lactic acid) nanoparticles labeled with biologically active Neutravidin for active targeting. *Eur J Pharm Biopharm* **58**, 483-490, (2004).

92 Torchilin, V. P. Multifunctional nanocarriers. *Advanced drug delivery reviews* **58**, 1532-1555, (2006).

93 Feng, S. S. Nanoparticles of biodegradable polymers for new-concept chemotherapy. *Expert review of medical devices* **1**, 115-125, (2004).

94 Kumari, A., Yadav, S. K. & Yadav, S. C. Biodegradable polymeric nanoparticles based drug delivery systems. *Colloids and surfaces. B, Biointerfaces* **75**, 1-18, (2010).

95 Gartner, S. *et al.* The role of mononuclear phagocytes in HTLV-III/LAV infection. *Science* **233**, 215-219, (1986).

96 Nicholson, J. K., Cross, G. D., Callaway, C. S. & McDougal, J. S. In vitro infection of human monocytes with human T lymphotropic virus type III/lymphadenopathy-associated virus (HTLV-III/LAV). *J Immunol* **137**, 323-329, (1986).

97 von Briesen, H. *et al.* Infection of monocytes/macrophages by HIV in vitro. *Research in virology* **141**, 225-231, (1990).

98 McGann, K. A. *et al.* Human immunodeficiency virus type 1 causes productive infection of macrophages in primary placental cell cultures. *The Journal of infectious diseases* **169**, 746-753, (1994).

99 Milman, G. & Sharma, O. Mechanisms of HIV/SIV mucosal transmission. *AIDS research and human retroviruses* **10**, 1305-1312, (1994).

100 Levy, J. A. Pathogenesis of human immunodeficiency virus infection. *Microbiological reviews* **57**, 183-289, (1993).

101 Weiss, R. A. How does HIV cause AIDS? *Science* **260**, 1273-1279, (1993).

102 Largent, B. L., Walton, K. M., Hoppe, C. A., Lee, Y. C. & Schnaar, R. L. Carbohydrate-specific adhesion of alveolar macrophages to mannose-derivatized surfaces. *The Journal of biological chemistry* **259**, 1764-1769, (1984).

103 Jain, S. K., Gupta, Y., Jain, A., Saxena, A. R. & Khare, P. Mannosylated gelatin nanoparticles bearing an anti-HIV drug didanosine for site-specific delivery. *Nanomedicine : nanotechnology, biology, and medicine* **4**, 41-48, (2008).

104 Lobenberg, R., Araujo, L., von Briesen, H., Rodgers, E. & Kreuter, J. Body distribution of azidothymidine bound to hexyl-cyanoacrylate nanoparticles after i.v. injection to rats. *Journal of controlled release : official journal of the Controlled Release Society* **50**, 21-30, (1998).

105 Schafer, V. *et al.* Phagocytosis of nanoparticles by human immunodeficiency virus (HIV)-infected macrophages: a possibility for antiviral drug targeting. *Pharmaceutical research* **9**, 541-546, (1992).

106 Shah, L. K. & Amiji, M. M. Intracellular delivery of saquinavir in biodegradable polymeric nanoparticles for HIV/AIDS. *Pharmaceutical research* **23**, 2638-2645, (2006).

107 Zensi, A. *et al.* Albumin nanoparticles targeted with Apo E enter the CNS by transcytosis and are delivered to neurones. *Journal of controlled release : official journal of the Controlled Release Society* **137**, 78-86, (2009).

108 Giri, M. S. *et al.* Circulating monocytes in HIV-1-infected viremic subjects exhibit an antiapoptosis gene signature and virus- and host-mediated apoptosis resistance. *J Immunol* **182**, 4459-4470, (2009).

109 Orenstein, J. M., Fox, C. & Wahl, S. M. Macrophages as a source of HIV during opportunistic infections. *Science* **276**, 1857-1861, (1997).

110 Chellat, F., Merhi, Y., Moreau, A. & Yahia, L. Therapeutic potential of nanoparticulate systems for macrophage targeting. *Biomaterials* **26**, 7260-7275, (2005).

111 Pierige, F., Serafini, S., Rossi, L. & Magnani, M. Cell-based drug delivery. *Advanced drug delivery reviews* **60**, 286-295, (2008).

112 Owens, D. E., 3rd & Peppas, N. A. Opsonization, biodistribution, and pharmacokinetics of polymeric nanoparticles. *International journal of pharmaceutics* **307**, 93-102, (2006).

113 Vasir, J. K. & Labhasetwar, V. Biodegradable nanoparticles for cytosolic delivery of therapeutics. *Advanced drug delivery reviews* **59**, 718-728, (2007).

114 Dunne, M., Corrigan, I. & Ramtoola, Z. Influence of particle size and dissolution conditions on the degradation properties of polylactide-co-glycolide particles. *Biomaterials* **21**, 1659-1668, (2000).

115 Oh, I. *et al.* Release of adriamycin from poly(gamma-benzyl-L-glutamate)/poly(ethylene oxide) nanoparticles. *International journal of pharmaceutics* **181**, 107-115, (1999).

116 Ubrich, N., Bouillot, P., Pellerin, C., Hoffman, M. & Maincent, P. Preparation and characterization of propranolol hydrochloride nanoparticles: a comparative study. *Journal of controlled release : official journal of the Controlled Release Society* **97**, 291-300, (2004).

117 Panagi, Z. *et al.* Effect of dose on the biodistribution and pharmacokinetics of PLGA and PLGA-mPEG nanoparticles. *International journal of pharmaceutics* **221**, 143-152, (2001).

118 Bala, I., Hariharan, S. & Kumar, M. N. PLGA nanoparticles in drug delivery: the state of the art. *Critical reviews in therapeutic drug carrier systems* **21**, 387-422, (2004).

119 *http://www.rxlist.com/sustiva-drug/clinical-pharmacology.htm*.

120 *http://www.drugbank.ca/drugs/DB00625*.

121 Cespedes, M. S. & Aberg, J. A. Neuropsychiatric complications of antiretroviral therapy. *Drug safety : an international journal of medical toxicology and drug experience* **29**, 865-874, (2006).

122 Hasse, B., Gunthard, H. F., Bleiber, G. & Krause, M. Efavirenz intoxication due to slow hepatic metabolism. *Clinical Infectious Diseases* **40**, E22-E23, (2005).

123 Lowenhaupt, E. A., Matson, K., Qureishi, B., Saitoh, A. & Pugatch, D. Psychosis in a 12-year-old HIV-positive girl with an increased serum concentration of efavirenz. *Clinical Infectious Diseases* **45**, E128-E130, (2007).

124 Ford, N. *et al.* Safety of efavirenz in first-trimester of pregnancy: a systematic review and meta-analysis of outcomes from observational cohorts. *AIDS* **24**, 1461-1470, (2010).

125 King, J. *et al.* A randomized crossover study to determine relative bioequivalence of tenofovir, emtricitabine, and efavirenz (Atripla) fixed-dose combination tablet compared with a compounded oral liquid formulation derived from the tablet. *J Acquir Immune Defic Syndr* **56**, e130-132, (2011).

126 Chiappetta, D. A., Facorro, G., de Celis, E. R. & Sosnik, A. Synergistic encapsulation of the anti-HIV agent efavirenz within mixed poloxamine/poloxamer polymeric micelles. *Nanomed-Nanotechnol* **7**, 624-637, (2011).

127 Chiappetta, D. A., Hocht, C., Taira, C. & Sosnik, A. Oral pharmacokinetics of the anti-HIV efavirenz encapsulated within polymeric micelles. *Biomaterials* **32**, 2379-2387, (2011).

128 Rajesh, Y. V. *et al.* Impact of superdisintegrants on efavirenz release from tablet formulations. *Acta Pharmaceut* **60**, 185-195, (2010).

129 Chiappetta, D. A., Hocht, C. & Sosnik, A. A Highly Concentrated and Taste-Improved Aqueous Formulation of Efavirenz for a More Appropriate Pediatric Management of the Anti-HIV Therapy. *Curr Hiv Res* **8**, 223-231, (2010).

130 Balkundi, S. *et al.* Comparative manufacture and cell-based delivery of antiretroviral nanoformulations. *International journal of nanomedicine* **6**, 3393-3404, (2011).

131 Sathigari, S. *et al.* Physicochemical Characterization of Efavirenz-Cyclodextrin Inclusion Complexes. *Aaps Pharmscitech* **10**, 81-87, (2009).

132 Dutta, T. *et al.* Poly (propyleneimine) dendrimer based nanocontainers for targeting of efavirenz to human monocytes/macrophages in vitro. *J Drug Target* **15**, 89-98, (2007).

133 Dutta, T., Garg, M. & Jain, N. K. Targeting of efavirenz loaded tuftsin conjugated poly(propyleneimine) dendrimers to HIV infected macrophages in vitro. *Eur J Pharm Sci* **34**, 181-189, (2008).

134 Destache, C. J. *et al.* Combination antiretroviral drugs in PLGA nanoparticle for HIV-1. *Bmc Infect Dis* **9**, (2009).

CHAPTER 3:

ANALYTICAL METHOD DEVELOPMENT AND VALIDATION

HPLC analytical methods were developed and validated to estimate efavirenz (EFV) in various developed formulations (NS, SMEDDS, PLGA nanoparticles) and for *in vitro* and *in vivo* studies. Various HPLC methods have been reported for analysis of EFV in biological fluids[1-7], but none of those could be used in laboratory.

3.1. Materials

EFV was kindly gifted by Merck Ltd. (Mumbai, India). Capsules (Efavir 200, Cipla Ltd.) were purchased from local pharmacy. Chemicals and reagents used for the preparation of buffers, analytical solutions, and other general experimental purposes are shown in Table 3.1. Purified HPLC grade water was obtained by filtering double distilled water through nylon filter paper 0.45 μm pore size and 47 mm diameter (Pall Life sciences, Mumbai, India).

Table 3.1. List of chemicals and reagents

Chemicals/Reagents	**Manufacturer/Supplier**
Acetonitrile, HPLC grade	Spectrochem Labs Ltd, Vadodara, India
Ammonium acetate buffer, AR grade	S.D. Fine Chemicals, Mumbai, India
Disodium hydrogen phosphate, AR grade	S.D. Fine Chemicals, Mumbai, India
Glacial Acetic acid, HPLC grade	Spectrochem Labs Ltd, Vadodara, India
Hydrochloric acid, AR grade	Spectrochem Labs Ltd, Vadodara, India
Lucifer Yellow	Sigma
Methanol, HPLC grade	Spectrochem Labs Ltd, Vadodara, India
Orthophosphoric acid, HPLC grade	Spectrochem Labs Ltd, Vadodara, India
Potassium dihydrogen phosphate, AR grade	S.D. Fine Chemicals, Mumbai, India
Sodium dihydrogen phosphate, AR grade	S.D. Fine Chemicals, Mumbai, India
Sodium hydroxide, AR grade	Spectrochem Labs Ltd, Vadodara, India
Tert- butyl methyl ether, HPLC grade	Spectrochem Labs Ltd, Vadodara, India

3.2. HPLC instrumentation and conditions

Chromatography was performed on Shimadzu (Shimadzu Corporation, Kyoto, Japan) chromatographic system equipped with Shimadzu LC-20AT pump and Shimadzu SPD-20AV absorbance detector. Samples were injected through a Rheodyne 7725 injector valve with fixed loop at 20 µL.

The chromatographic separation was performed using a Phenomenex Hypersil C4 (100 mm × 4.6 mm i.d., 5 µm particle size) column. Separation was achieved using a mobile phase consisting of acetonitrile and 100 mM ammonium acetate buffer pH 7.0 in the ratio of 45:55 (v/v), pumped at a flow rate of 1 ml/min. The eluent was monitored using UV detector at a wavelength of 247 nm. The column was maintained at 40°C and an injection volume of 20 µL was used. The mobile phase was vacuum filtered through 0.45 µm nylon membrane filter followed by degassing in an ultrasonic bath prior to use. Data acquisition and integration was performed using Spinchrome software (Spincho Biotech, Vadodara).

Table 3.2. Optimized HPLC parameters for EFV

Column	Phenomenex Hypersil C4 (100mm X 4.6 mm i.d., 5 µm particle size)
Mobile phase	Ammonium acetate buffer (pH 7.0) : ACN (55:45) (Mobile phase was filtered with nylon filter paper 0.45µ pore size and 47 mm diameter)
Flow rate	1.0 ml/min
Retention time	4.650 min
Detector	UV detector – 247nm
Needle wash	Water : Methanol (50:50)
Temperature	40°C

3.3. HPLC method

3.3.1. Standard stock solution

25 mg of EFV was accurately weighed in to 25 mL volumetric flask. Approximately 20 mL of methanol was added and vortex mixed to dissolve drug into methanol. The final volume was adjusted up to the mark with methanol to prepare stock solution of concentration 1 mg/ml.

3.3.2. Working stock solution

5 ml of EFV stock solution was added to 50 ml volumetric flask and diluted to 50 ml with mobile phase to produce a working stock solution of 100 µg/ml.

3.3.3. Calibration curve of EFV

Aliquots ranging from 0.5 ml to 6 ml were taken, from working stock solution, in 10 ml volumetric flask and diluted to 10 ml with mobile phase to give final concentration of 5, 10, 20, 30, 40, 50, 60 µg/ml. Injections of 20 µl were made for each concentration and chromatographed under the condition described in Table 3.2. (Figure 3.1) Calibration graph was constructed by plotting peak area versus concentration of EFV and the regression equation was calculated.

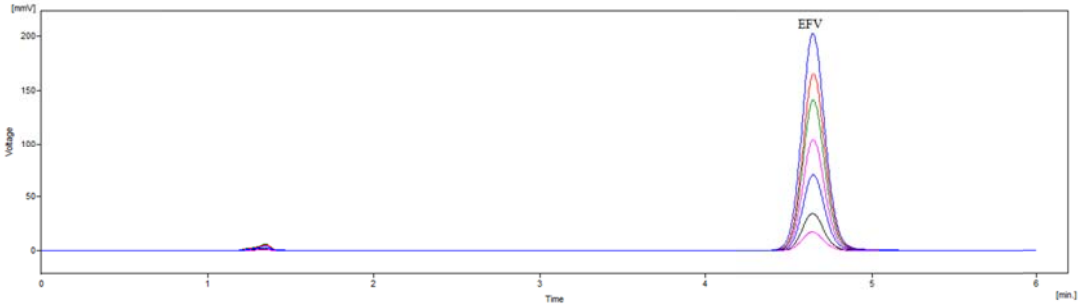

Figure 3.1. Overlay chromatograms of EFV standards: 5, 10, 20, 30, 40, 50, 60 µg/ml.

3.3.4. Validation of HPLC method

The method was validated with respect to parameters including linearity, limit of quantification (LOQ), limit of detection (LOD), precision, accuracy, selectivity and recovery. Validation of developed HPLC method was carried out as per ICH guidelines Q2 (R1).[8,9]

3.3.4.1. System suitability

System suitability experiment was performed by injecting six consecutive injections of solution having concentration of 30 µg/ml during the start of method validation and the start of each day. Different peak parameters were observed like retention time, tailing factor, theoretical plates and % relative standard deviation (% RSD) of area. These are summarized in Table 3.3.

Table 3.3. System suitability parameters.

Parameters	**Mean ± SD**
Retention time (min)	4.650 ± 0.008
Asymmetry	1.08 ± 0.07
Theoretical plates	4826 ± 24.27
% RSD of area	1.05

3.3.4.2. Linearity

The calibration curves (n=3) constructed for EFV were linear over the concentration range of 5-60 µg/ml. Peak areas of EFV were plotted versus EFV concentration and linear regression analysis was performed on the resultant curves. Three correlation co-efficient of (1) $r^2 = 0.9998$ (2) $r^2 = 0.9997$ (3) $r^2 = 0.9997$ with % RSD values less than 2 across the concentration range studied were obtained following linear regression analysis (Table 3.4). Typically, the regression equation for the calibration curve was found to be $y = 33.179x – 6.2747$, where x is the concentration in µg/ml (Figure 3.2).

Table 3.4. Area of EFV for calibration curve.

Conc. (µg/ml)	[a] Area (mv)	% RSD
5	162.243	0.188
10	321.827	0.092
20	662.619	0.029
30	992.19	0.011
40	1317.514	0.012
50	1632.864	0.025
60	2000.287	0.029

[a] Average of three determinants.

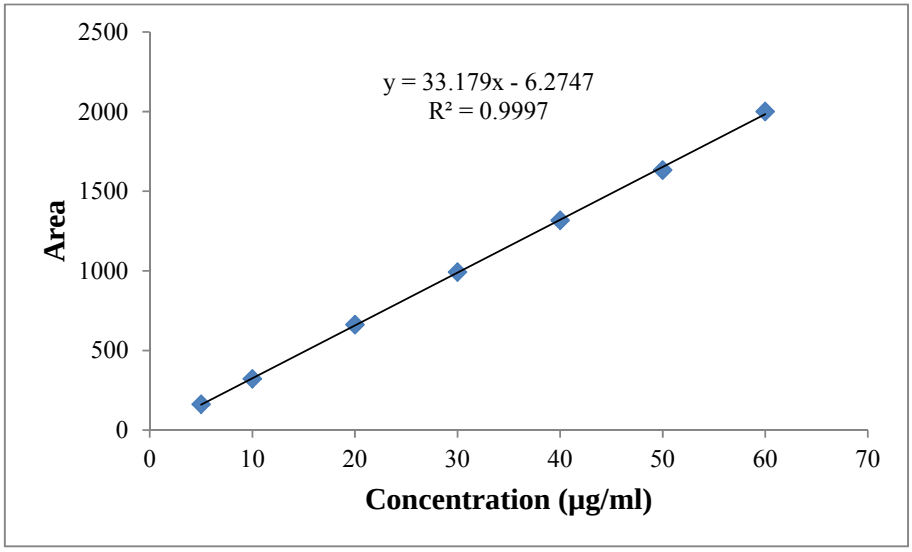

Figure 3.2. Calibration curve of EFV.

3.3.4.3. Limit of quantification (LOQ) and limit of detection (LOD)

The LOQ and LOD were determined based on a signal –to- noise ratios and were based on analytical responses of 10 and 3 times the background noise respectively. LOD and LOQ were experimentally verified by diluting known concentration of EFV until the average responses were approximately 3 or 10 times the standard deviation of the responses for six replicate determinations. The LOQ was found to be 0.1 µg/ml with resultant % RSD of 1.2 % (n=5). The LOD was found to be 0.03 µg/ml.

3.3.4.4. Precision

Six injections of three different concentrations (5, 30, 60 µg/ml) were given on the same day and the values of the % RSD were calculated to determine intra-day precision. Three injections of three different concentrations (5, 30, 60 µg/ml) were given on three different days to determine inter-day precision. Table 3.5 shows that for both the cases, % RSD was less than 2% which complies with specified limit.

Table 3.5. Intra-day Precision

Actual Conc. (µg/ml)	Intra-day Precision		Inter-day Precision	
	[a] Mean (µg/ml)	% RSD	[b] Mean (µg/ml)	% RSD
5	5.10	1.44	5.13	1.65
30	30.12	1.08	30.17	0.83
60	60.08	1.05	60.23	0.94

[a] mean concentration of six determinants.
[b] mean concentration of nine determinants.

3.3.4.5. Recovery

The preanalyzed marketed formulation samples were spiked with 80, 100,120 % of standard EFV and the mixture were analyzed by the proposed method. At each level of the amounts six determinations were performed. This was done to check the recovery of the drug at different levels in the formulations (Table 3.6).

3.3.4.6. Stability in sample solutions

Three different concentrations of EFV (5, 30, 60 µg/ml) were prepared from sample solution and stored at room temperature for 2 days. They were then injected in to HPLC system. No additional peak was found in chromatogram indicating the stability of EFV in the sample solution (Table 3.7).

Table 3.6. Recovery Study

Excess drug added to analyte (%)	Theoretical Content (µg/ml)	[a] Amount Found (µg/ml)	[b] Recovery (%)	% RSD
0	25	24.99	99.99	0.005
80	45	46.098	102.4	0.879
100	50	50.18	100.37	1.254
120	55	55.49	100.90	1.050

[a] mean concentration of six determinants.

[b] % Recovery = mean measured concentration / nominal concentration X 100.

Table 3.7. Stability of EFV in sample solution.

Actual conc. (µg/ml)	[a] Measured conc. (µg/ml)	% RSD
5	5.05	1.232
30	30.25	1.282
60	59.82	0.247

[a] mean concentration of three determinants.

3.3.4.7. Robustness

To evaluate LC method robustness, a few parameters were deliberately varied. The parameters included variation of flow rate, percentage of acetonitrile in the mobile phase and acetonitrile of different lots. Robustness of the method was done at three different concentration levels 5, 30, 60 µg/ml, respectively.

Each factor selected (except solvents of different lots) to examine were changed at three levels (-1, 0, 1). One factor at the time was changed to estimate the effect. Thus replicate injections (n=3) of standard solution at three concentration levels were performed under small changes of three chromatographic parameters (factors). Results, presented in Table 3.8 indicate that the selected factors remained unaffected by small variation of these parameters. It was also found that acetonitrile of different lots from the same manufacture has no significant influence on the determination. Insignificant difference in asymmetric factor and less variability in retention time were observed.

Table 3.8. [a] Robustness evaluation

[b] Factor	Level	Retention time (t_R) of EFV (min.)	Asymmetric factor of EFV peak
A: flow rate (ml/min)			
0.95	-1	4.660	1.110
1.0	0	4.650	1.118
1.05	1	4.648	1.115
Mean ± S.D.		4.653 ± 0.006	1.114 ± 0.004
B: percentage of acetonitrile in mobile phase			
43	-1	4.657	1.112
45	0	4.65	1.118
47	1	4.643	1.109
Mean ± S.D.		4.650 ± 0.007	1.113 ± 0.004
C: solvents of different Lots			
First lot		4.650	1.118
Second lot		4.654	1.120
Mean ± S.D.		4.652 ± 0.003	1.119 ± 0.001

[a] Average of three concentration (0.1, 45, 100 µg/ml), three replicates each.
[b] Factors were slightly changed at three levels (1, 0, -1); each time a factor was changed from level (0), the other factors remained at level (0)

3.3.4.8. Analysis of marketed and developed formulations of EFV

To determine the content of EFV in formulations (Efavir 200, NS, SMEDDS) An accurately weighed amount equivalent to 50 mg of EFV was transferred in to 50 ml volumetric flask, dissolved in 25 ml of methanol and volume was made up to the mark with the same solvent. The volumetric flask was sonicated for 2 min for complete dissolution and then filtered. The concentration of EFV in sample stock solution was 1 mg/ml. Suitable aliquot of the filtered solution was added to the volumetric flask and made up to the mark with mobile phase to yield the final concentration of 25 µg/ml. Then 20 µl of this solution was injected in to column & chromatogram was recorded. The analysis was repeated in triplicate.

The validated LC method was successfully applied for the assay of EFV in marketed and developed formulations. Assay results are represented in Table 3.9.

Table 3.9. Assay of different formulations

Formulations	Actual amount	[a]Amount found ± S.D	% Assay
Efavir 200	200 mg	200.07 ± 1.33	100.01 %
NS	200 mg	195.20 ± 0.54	97.60 %
SMEDDS	50 mg	48.83 ± 0.01	97.60 %

[a] mean concentration of three determinants

Table 3.10. Summary of validation parameters

Validation parameters	Results
Linearity and range	
r^2	0.9997
Slope	33.179
Intercept	-6.2747
Range	5-60 (µg/ml)
LOD	0.03 µg/ml
LOQ	0.1 µg/ml
Precision (% RSD)	
Intra-day precision	1.05 – 1.44
Intra-day precision	0.83 – 1.65
Accuracy	99.99 – 102.4 %

3.4. Estimation of EFV in plasma

3.4.1. Preparation of EFV working stock solutions

20 mg EFV was accurately weighed and dissolved in 10 ml methanol to make stock solution of final concentration of EFV equivalent to 2 mg/ml. Aliquots ranging from 37.5 ml to 1.5 ml were taken, from stock solution, in 5 ml volumetric flask and diluted to 5 ml with methanol to give final concentration of 15, 30, 60, 150, 300, 600 µg/ml.

3.4.2. Preparation of ezetimibe (internal standard) working stock solution

20 mg ezetimibe internal standard (ISTD) was accurately weighed and dissolved in 10 ml methanol to make stock solution of ezetimibe equivalent to 2 mg/ml. 0.4 ml of

ezetimibe stock solution was taken and diluted up 10 ml with methanol to produce a working stock solution of 80 µg/ml.

Use of internal standard is common in bioanalytical methods especially with chromatographic procedures. The assumption for the use of internal standard is that the partition coefficient of analyte and the ISTD are very similar. Ezetimibe has similar physicochemical properties as EFV (Table 3.11)[10,11], therefore ezetimibe was selected as ISTD.

Table 3.11. Physicochemical properties

Parameters	EFV	Ezetimibe
Log P	4.6	4.5
water solubility (g/l)	0.00855	0.00846
Log S	-4.6	-4.7
PKa	10.0	14.44

3.4.3. Preparation of calibration curve standard solution

0.1 ml aliquot was taken from each working stock solution of EFV and 4.9 ml of plasma was added to yield concentrations of 0.3, 0.6, 1.2, 3.0, 6.0, 12.0 µg/ml.
The procedure for extraction of drug from plasma was as follows[12]:

- 0.5 ml of plasma or tissue homogenate sample was transferred in to prelabelled ria vial.
- 50 µl of ISTD Solution (Ezetimibe- 80 µg/ml) was added to all samples except STD Blank and vortexed for about 20 seconds.
- Then 100 µl of Extraction buffer (1% NaOH Solution) was added to all samples and vortexed for 20 seconds.
- 2.5 ml TBME was added to all samples and vortexed for 30 min.
- The samples were centrifuged at 4000 rpm at 10 °C for 5 min.
- About 2 ml of supernatant was transferred to prelabelled ria vials and the samples were evaporated to dryness in vacuum oven at 40 °C.
- The dried samples were reconstituted with 100 µl of mobile phase and vortexed for 30 seconds.

Injections of 20 µl were made for each concentration and chromatographed under the condition described above. Figure 3.3 shows overlay chromatograms of different concentration of EFV recovered from plasma.

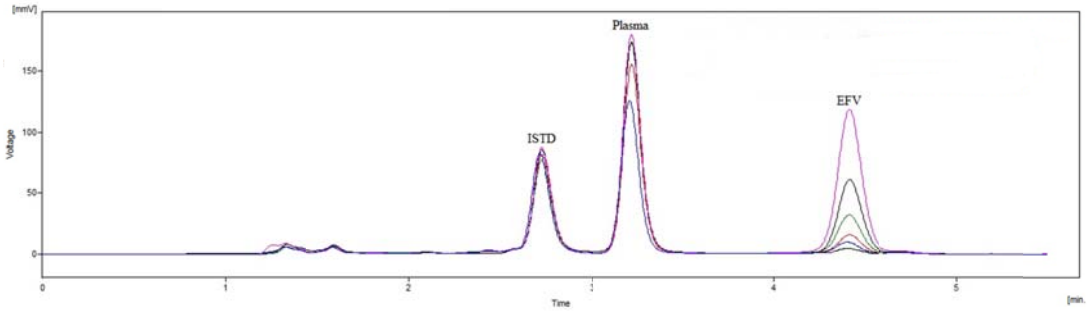

Figure 3.3. Overlay chromatograms of EFV standards in plasma: 0.3, 0.6, 1.2, 3.0, 6.0, 12 µg/ml.

3.4.4. Procedure for un-extracted sample preparation

- 100 µl of respective spiking solutions were added into pre-labeled ria vials.
- 500 µl of ISTD dilution (80 µg/ml) was added in the respective vials and vortex to mix.
- 400 µl of mobile phase was added and the vials were vortexed for about 10 seconds.

3.4.5. Validation of bioanalytical HPLC method

3.4.5.1. System suitability

System suitability experiments were performed by injecting six consecutive injections using aqueous standard equivalent to middle quality control for mixture of drug and ISTD during the start of method validation and the start of each day. Different peak parameters were observed like retention time, tailing factor, theoretical plates and % RSD of area. These are summarized in Table 3.12.

Table 3.12. System suitability parameters.

Parameters	**Mean ± SD**
Retention time (min)	4.410 ± 0.01
Asymmetry	1.12 ± 0.07
Theoretical plates	4718 ± 37.11
% RSD of area	2.14

3.4.5.2. Linearity

The calibration curves (n=3) were constructed for linearity of EFV in plasma. Linearity was determined by measuring correlation co-efficient, accuracy was evaluated by measuring % mean accuracy at each concentration level of calibration curve standard and precision was measured by measuring % RSD at each concentration level of calibration curve standard.

The concentrations of standards were calculated by plotting EFV concentration on X-axis and area ratio (Drug/ISTD) on Y-axis. The calibration curves (n=3) constructed for EFV were linear over the concentration range of 0.3 to 12 µg/ml. (Figure 3.4) The correlation co-efficient observed more than 0.999 during the course of validation. The mean accuracy and precision observed for calibration curve standards of EFV were ranged from 99.05 to 106.67 % and 1.28 to 2.42 %, respectively, which are within the acceptance limits of 85.00 to 115.00 % for all calibration curve standards. (Table 3.13)

Table 3.13. Back calculated concentration of calibration curve standards

Actual conc. (µg/ml)	**[a] Back calculated conc. (µg/ml)**	**% RSD**	**% Mean Accuracy**
0.3	0.32	2.18	106.67
0.6	0.62	2.42	103.91
1.2	1.20	2.23	100.19
3.0	3.19	1.86	106.40
6.0	5.94	1.28	99.05
12.0	11.98	2.01	99.85

[a] Average of three determinants.

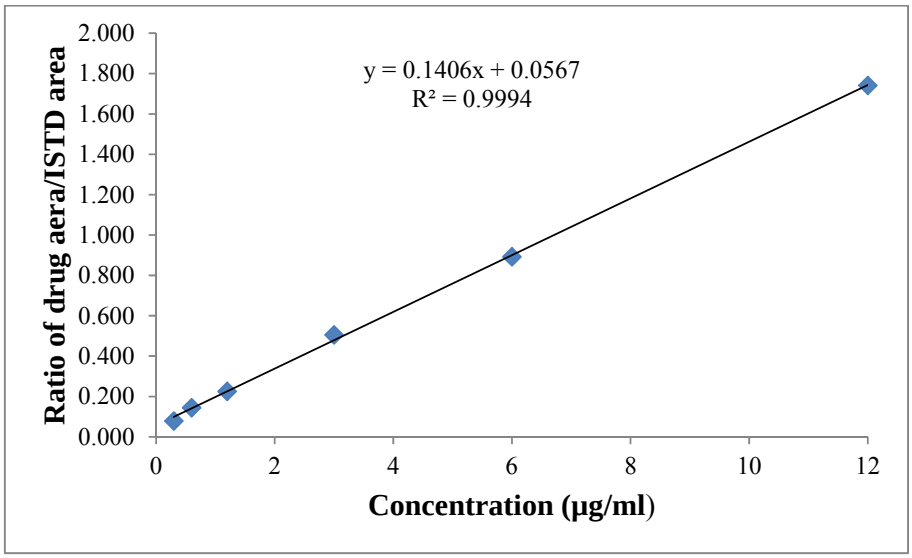

Figure 3.4. Calibration curve of EFV in plasma.

3.4.5.3. Precision

Six injections of three different quality control (QC) concentrations (0.3, 3, 12 µg/ml) were given on the same day and the values of the % RSD were calculated to determine intra-day precision. Three injections of three different QC concentrations (0.3, 3, 12 µg/ml) were given on three different days to determine inter-day precision. Table 3.14 shows that for both the cases, % RSD was found to be in the range of 3.45 to 7.23 % which is within the acceptance limit of 15 %.

Table 3.14. Precision

Actual Conc. (µg/ml)	Intra-day Precision		Inter-day Precision	
	[a] Mean (µg/ml)	% RSD	[b] Mean (µg/ml)	% RSD
0.3	0.33	3.45	0.35	4.39
3	3.41	5.05	3.24	7.23
12	12.52	6.54	11.46	6.01

[a] mean concentration of six determinants.
[b] mean concentration of nine determinants.

3.4.5.4. Specificity

The specificity of the intended method was established by screening the standard blank without spiking with EFV of plasma. Overlay chromatograms of standard blank and 0.3 µg/ml standard are shown in Figure 3.5. Area of the peak at retention time of EFV in standard blank samples was <20.0 % of the area of EFV in extracted 0.3 µg/ml standard sample. Area of the peak at retention time of ISTD in standard blank samples was <5.0 % of the area of ISTD in extracted 0.3 µg/ml standard sample.

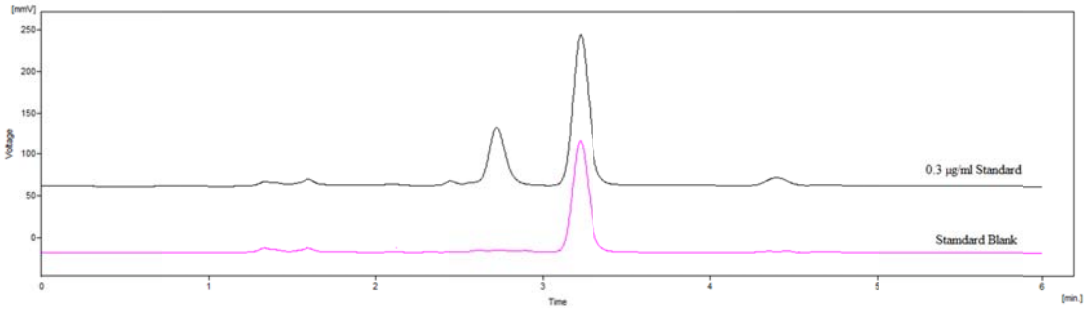

Figure 3.5. Overlay chromatogram of standard blank and 0.3 µg/ml standard.

3.4.5.5. Recovery

Six replicates of QC concentrations 0.3, 3 and 12 µg/ml were analyzed by following the procedure for unextracted sample preparation and compared with same concentration level samples processed by following the procedure for extracted sample preparation. The % mean recovery for drug in 0.3. 3 and 12 µg/ml was 89.34, 90.68 and 95.33 %, respectively. The % mean recovery for ISTD in 0.3. 3 and 12 µg/ml was 84.42, 84.24 and 82.34 %, respectively. (Table 3.15)

Table 3.15. Recovery study

Actual Conc. (µg/ml)	EFV		ISTD	
	[a] % Recovery	% RSD	[a] % Recovery	% RSD
0.3	89.34	3.32	84.42	2.07
3	90.68	2.94	84.24	1.67
12	95.33	2.01	82.34	2.68

[a] mean concentration of six determinants.

3.4.5.6. Stability

The stability of EFV in plasma was determined using two QC samples (0.3 and 12 µg/ml). The freeze and thawed stability of 0.3 and 12 µg/ml quality control samples were tested after third freeze-thawed cycle, where the first storage of 24 h at below -20ºC was followed by two additional periods of 12 h. The stability was determined by comparing the mean of calculated concentration of drug from the three freeze-thawed samples with that of freshly thawed quality control samples.

The bench top stability at room temperature of 0.3 and 12 µg/ml QC samples were determined by comparing the mean of calculated concentrations from the freshly thawed QC samples of those were kept on bench top for about 6 hours.

The results of stability of EFV in plasma are shown in Table 3.16. The % mean stability of EFV was found within the acceptance limit of 85.00 to 115.00%.

Table 3.16. Stability of EFV in plasma

	Freeze-thaw stability		**Bench-top stability**	
Actual conc. (µg/ml)	**[a] % Mean**	**% RSD**	**[a] % Mean**	**% RSD**
0.25	98.72	3.29	101.40	1.18
5	100.3	0.02	98.68	0.63

[a] mean percentage of three determinants.

3.5. Application of HPLC method for estimation of EFV in different tissues of rat (Brain, Kidney, Liver, Lung and Spleen)

3.5.1. Preparation of EFV working stock solutions

Same as described in section 3.5.1.

3.5.2. Preparation of ezetimibe (internal standard) working stock solution

Same as described in section 3.5.2.

3.5.3. Preparation of tissue homogenate

Tissues of interest (Brain, Kidney, Liver, Lung and Spleen) were collected immediately after sacrificing the animals and rinsed with normal saline and dried with tissue paper. Tissue samples were frozen at -20°C until analysis. Tissue samples were thawed to room temperature and weighed accurately and homogenized using a glass tissue homogenizer after addition of Tris-sucrose buffer. In all tissues, the calibration curves were linear in the concentration range of 0.3 to 12 µg/ml of EFV.

3.5.4. Preparation of calibration curve standard solution

0.1 ml aliquot was taken from each working stock solutions of EFV, add 4.9 ml of tissue homogenate to yield concentrations of 0.3, 0.6, 1.2, 3.0, 6.0, 12.0 µg/ml. Tissue homogenates were processed similarly as 500µl plasma samples and analyzed by HPLC. Figure 3.6 - 3.10 shows overlay chromatograms of different concentration of EFV recovered from different tissue homogenate. Figure 3.11 shows calibration curves of EFV in different tissue homogenates.

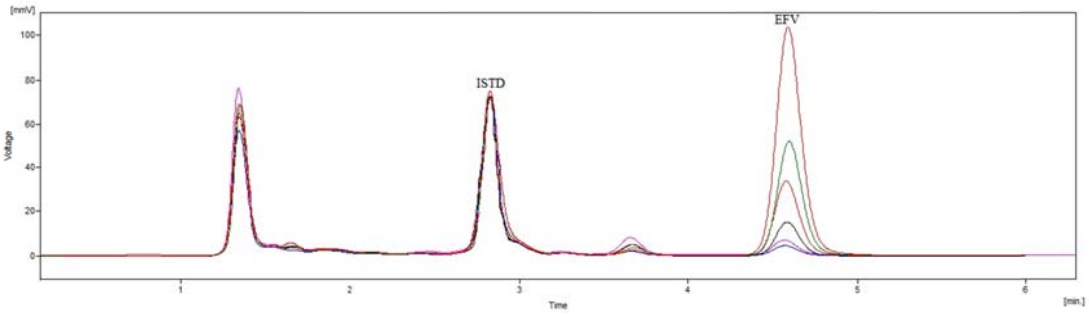

Figure 3.6. Overlay chromatograms of EFV standards in brain homogenate: 0.3, 0.6, 1.2, 3.0, 6.0, 12 µg/ml.

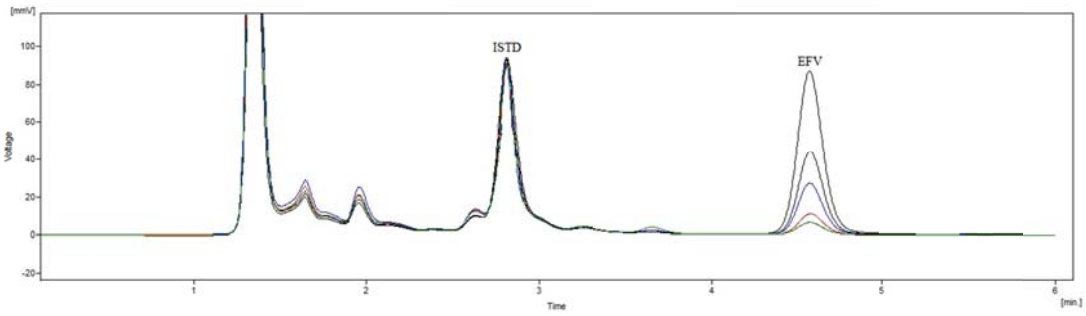

Figure 3.7. Overlay chromatograms of EFV standards in Kidney homogenate: 0.3, 0.6, 1.2, 3.0, 6.0, 12 µg/ml.

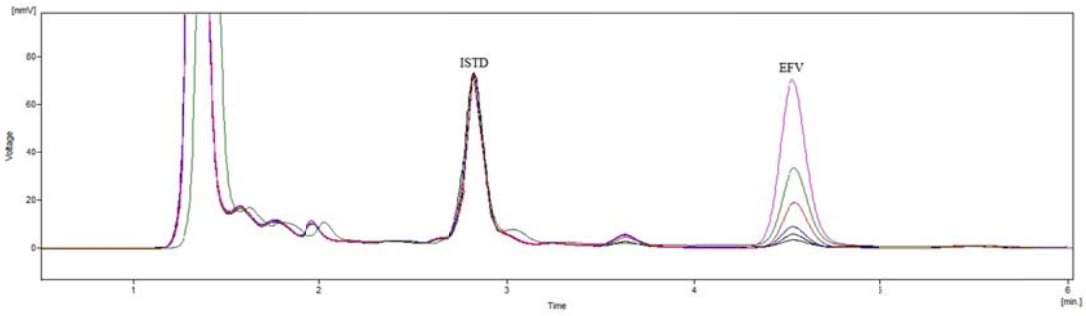

Figure 3.8. Overlay chromatograms of EFV standards in liver homogenate: 0.3, 0.6, 1.2, 3.0, 6.0, 12 µg/ml.

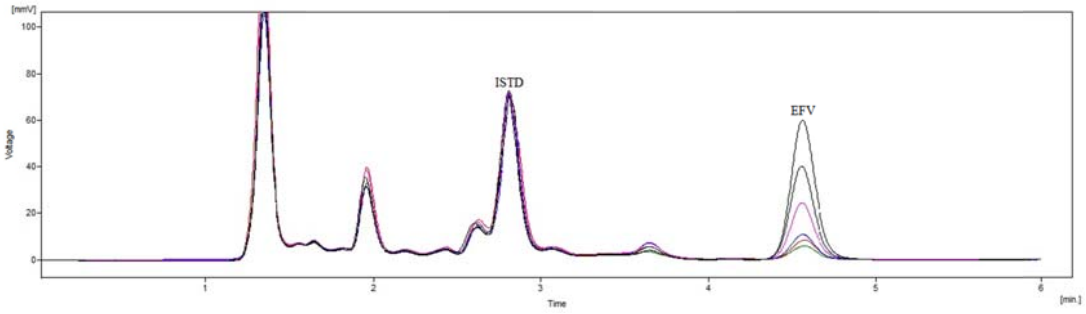

Figure 3.9. Overlay chromatograms of EFV standards in lung homogenate: 0.3, 0.6, 1.2, 3.0, 6.0, 12 µg/ml.

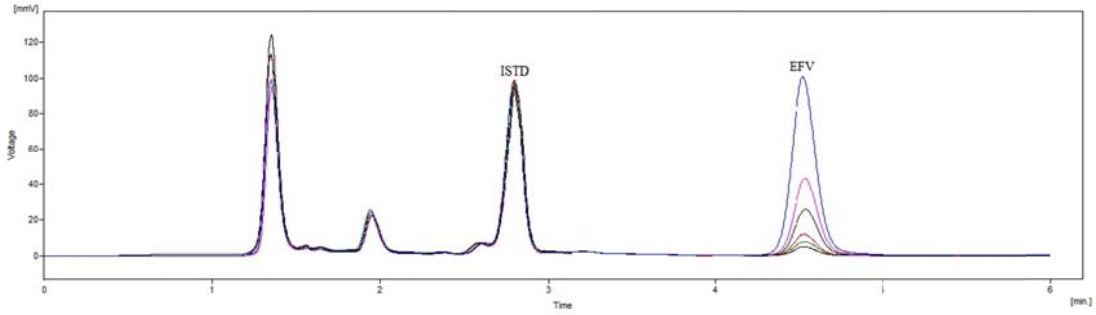

Figure 3.10. Overlay chromatograms of EFV standards in spleen homogenate: 0.3, 0.6, 1.2, 3.0, 6.0, 12 µg/ml.

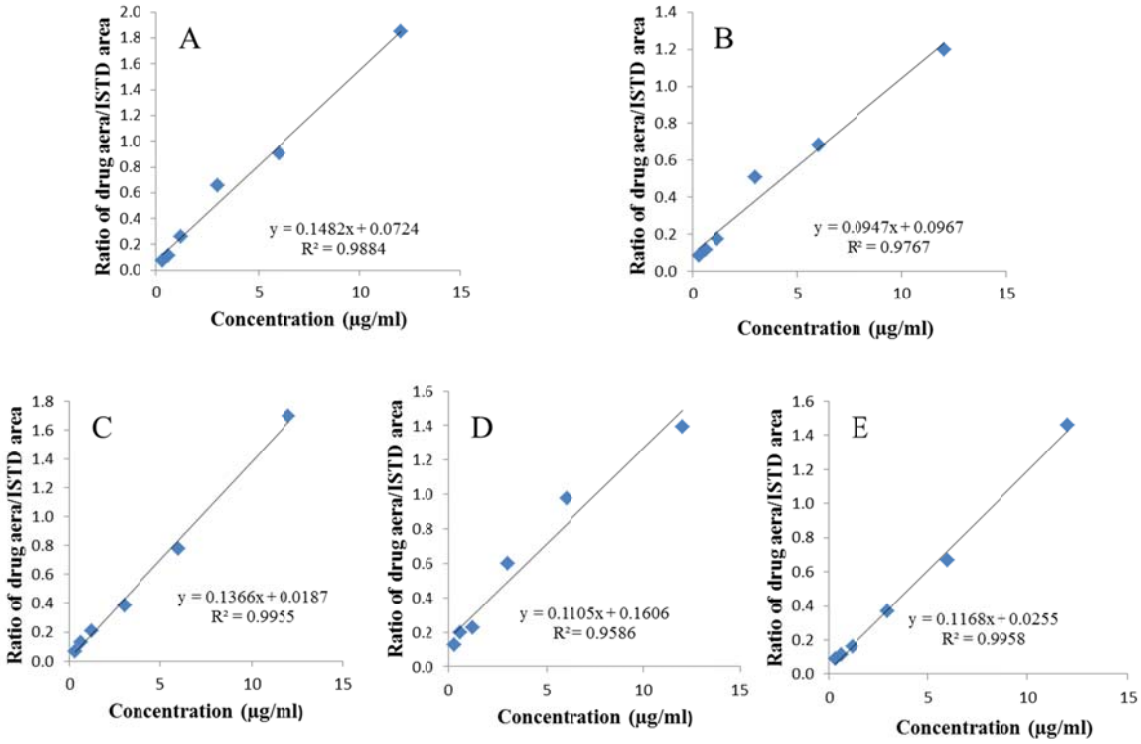

Figure 3.11. Calibration curve of EFV in different tissue homogenate. (A) Brain (B) Kidney (C) Liver (D) Lung (E) Spleen

REFERENCES

1 Langmann, P., Schirmer, D., Vath, T., Zilly, M. & Klinker, H. High-performance liquid chromatographic method for the determination of HIV-1 non-nucleoside reverse transcriptase inhibitor efavirenz in plasma of patients during highly active antiretroviral therapy. *Journal of chromatography. B, Biomedical sciences and applications* **755**, 151-156 (2001).

2 Fox, D., O'Connor, R., Mallon, P. & McMahon, G. Simultaneous determination of efavirenz, rifampicin and its metabolite desacetyl rifampicin levels in human plasma. *Journal of pharmaceutical and biomedical analysis* **56**, 785-791, doi:10.1016/j.jpba.2011.07.041 (2011).

3 Kappelhoff, B. S., Rosing, H., Huitema, A. D. & Beijnen, J. H. Simple and rapid method for the simultaneous determination of the non-nucleoside reverse transcriptase inhibitors efavirenz and nevirapine in human plasma using liquid chromatography. *Journal of chromatography. B, Analytical technologies in the biomedical and life sciences* **792**, 353-362 (2003).

4 Mogatle, S. & Kanfer, I. Rapid method for the quantitative determination of efavirenz in human plasma. *Journal of pharmaceutical and biomedical analysis* **49**, 1308-1312, doi:10.1016/j.jpba.2009.03.008 (2009).

5 Ramachandran, G. *et al.* Simple and rapid liquid chromatography method for determination of efavirenz in plasma. *Journal of chromatography. B, Analytical technologies in the biomedical and life sciences* **835**, 131-135, doi:10.1016/j.jchromb.2006.03.014 (2006).

6 Saras-Nacenta, M. *et al.* Determination of efavirenz in human plasma by high-performance liquid chromatography with ultraviolet detection. *Journal of chromatography. B, Biomedical sciences and applications* **763**, 53-59 (2001).

7 Veldkamp, A. I. *et al.* Quantitative determination of efavirenz (DMP 266), a novel non-nucleoside reverse transcriptase inhibitor, in human plasma using isocratic reversed-phase high-performance liquid chromatography with ultraviolet detection. *Journal of chromatography. B, Biomedical sciences and applications* **734**, 55-61 (1999).

8 ICH. Text on Validation of Analytical Procedures. International Conference on Harmonisation, IFPMA, Geneva, 1994.

9 ICH. Validation of Analytical Procedures: Methodology. International Conference on Harmonisation, IFPMA, Geneva, 1996.

10 Drug bank, Dpen Data Drug and Drug Target Database. http://www.drugbank.ca/drugs/DB00973.

11 Drug bank, dpen data drug and drug target database. http://www.drugbank.ca/drugs/DB00625.

12 Lakshmi Sailaja, A. *et al.* Development and Validation of a Liquid Chromatographic Method for Determination of Efavirenz in Human Plasma. *Chromatographia* **65**, 359–361, doi:DOI: 10.1365/s10337-006-0170-x (2007).

CHAPTER 4:

DEVELOPMENT OF EFAVIRENZ NANOSUSPENSION

4.1. Introduction

The very low solubility of efavirenz (EFV) hinders its administration, absorption and biodistribution. Thus, there is need to have some innovative formulation approach to enhance the bioavailability. It was hypothesized that this problem can be overcome by increasing the solubility of the drug. Reduction of the particle size to nanometer range is suitable approach to improve the solubility of drugs. Over a decade, nanosuspensions (NSs) are considered to be the best alternative and universal approach for poorly water soluble drugs to enhance oral bioavailability.[1,2] Several production techniques like precipitation[3], jet milling, pearl milling[4,5] and high-pressure homogenization (HPH)[6,7] have been applied to produce NSs.

Currently, media milling is preferred over HPH technique because it is easy to scale up to industrial pharmaceutical unit operations.[8-12] Also, crystalline nature of the drug remains largely intact during the media milling processing, thus relieving any stability concerns. Furthermore, no organic solvent or harsh environment is needed. NSs efficiently improve oral absorption of poorly soluble drugs and achieve a higher bioavailability compared to traditional formulation.[13] Major advantages of NS technology are increased dissolution velocity, increased saturation solubility, versatility in surface modification and ease of post-production processing. NSs show adhesion to the gastrointestinal mucosa, prolonging contact time of the drug and thereby enhancing its uptake via the gastrointestinal tract (GIT).[14-16]

Present study has been undertaken to develop NS of EFV, by media milling method, with improved oral bioavailability. Formulation of NS requires a careful selection of stabilizers. Steric and electrostatic stabilizers are needed to stabilize the nanoparticles against inter-particle forces and prevent them from aggregating. Steric stabilization is often combined with electrostatic stabilization for additional repulsive contribution. Different pharmaceutical excipients including povidone (PVP K30), and poloxamers (188 and 407) as steric stabilizer and sodium lauryl sulphate (SLS) as anionic electroststic stabilizer were used in an effort to develop stable EFV loaded NS. In order to obtain best formulation of NS, the relationship between dependent variable and independent variable must be understood. Design of experiment can serve as an efficient and economical method of obtaining the necessary information to understand

relationship between variables. Box-Behnken design, one of response surface method (RSM) design, was applied to optimize the NS formulation.[17] The independent variables for the present study were the following: concentration of drug (X_1), concentration of polymer (X_2), concentration of surfactant (X_3) and milling time (X_4). The dependent variables included mean particle size (MPS) and zeta potential (ZP).

NSs were subsequently transformed to dry powder by lyophilization, to enhance the stability of EFV. The physicochemical properties of NSs in terms of MPS, polydispersity index (PDI), and ZP before and after lyophilisation were investigated. Dissolution velocity and saturation solubility are generally performed using official pharmacopoeia methods. Corresponding physical properties of the prepared EFV NS were characterized by differential scanning calorimetry (DSC), X-ray diffraction (XRD), scanning electronic microscopy (SEM) and transmission electron microscopy (TEM). The chemical stability of NS was assessed by determining percentage of EFV present in the formulations stored at different temperatures (4-8°C and 25°C) during a period of 6 months. *In situ* intestinal permeability and *in vitro* parallel artificial membrane permeability assay (PAMPA) study were carried out to assess permeability of EFV in NS. Finally, oral bioavailability of NS was evaluated in rabbits and compared with standard EFV and marketed EFV formulation (MF). We hypothesized that NS formulation of EFV might lead to improved oral bioavailability due to enhanced solubility, dissolution and, thus absorption.

4.2. Materials and instruments

EFV was kindly gifted by Merck Ltd. (Mumbai, India). Capsules (Efavir 200, Cipla Ltd.) were purchased from local pharmacy. Zirconium oxide beads were received as gift sample from SPARC, India. Excipients used for formulation development are shown in Table 4.1 and were used as received. Chemicals and reagents used for the preparation of buffers, analytical solutions, and other general experimental purposes are shown in Table 4.2. Equipments used at various stages are listed in Table 4.3. Purified HPLC grade water was obtained by filtering double distilled water through nylon filter paper 0.45 μm pore size and 47 mm diameter (Pall Life sciences, Mumbai, India).

Table 4.1. List of excipients

Excipients	**Manufacturer/Supplier**
Mannitol	S.D. Fine Chemicals, Mumbai, India
Poloxamer 188	BASF, Germany
Poloxamer 407	BASF, Germany
PVP K30	S.D. Fine Chemicals, Mumbai, India
SLS	S.D. Fine Chemicals, Mumbai, India
Trehalose	S.D. Fine Chemicals, Mumbai, India

Table 4.2. List of chemicals and reagents

Chemicals/Reagents	**Manufacturer/Supplier**
Acetonitrile, HPLC grade	Spectrochem Labs Ltd, Vadodara, India
Ammonium acetate buffer, AR grade	S.D. Fine Chemicals, Mumbai, India
Disodium hydrogen phosphate, AR grade	S.D. Fine Chemicals, Mumbai, India
Glacial Acetic acid, HPLC grade	Spectrochem Labs Ltd, Vadodara, India
Glucose, AR grade	S.D. Fine Chemicals, Mumbai, India
Hydrochloric acid, AR grade	Spectrochem Labs Ltd, Vadodara, India
Lucifer Yellow	Sigma Aldrich, India
Magnesium chloride, AR grade	S.D. Fine Chemicals, Mumbai, India
Methanol, HPLC grade	Spectrochem Labs Ltd, Vadodara, India
Orthophosphoric acid, HPLC grade	Spectrochem Labs Ltd, Vadodara, India
Potassium chloride, AR grade	S.D. Fine Chemicals, Mumbai, India
Potassium dihydrogen phosphate, AR grade	S.D. Fine Chemicals, Mumbai, India
Sodium acetate, AR grade	Spectrochem Labs Ltd, Vadodara, India
Sodium bicarbonate, AR grade	S.D. Fine Chemicals, Mumbai, India
Sodium chloride, AR grade	S.D. Fine Chemicals, Mumbai, India
Sodium dihydrogen phosphate, AR grade	S.D. Fine Chemicals, Mumbai, India
Sodium hydroxide, AR grade	Spectrochem Labs Ltd, Vadodara, India
Tert- butyl methyl ether, HPLC grade	Spectrochem Labs Ltd, Vadodara, India

Table 4.3. List of instruments

Equipment	Manufacturer/Supplier
Bath sonicator	B. N. Scientific Enterprise, India
Centrifuge	Remi Instrument
Column oven	PCI Analytics, India
Differential scanning calorimeter (DSC 60)	Shimadzu, Japan
Dissolution apparatus	Veevo, India
High performance liquid chromatography	Shimadzu, Japan
Lyophilizer	Heto Dry Winner, Germany
Magnetic stirrer	Remi equipments Pvt Ltd., India
Particle size analyzer (Malvern Zetasizer Nano ZS)	Malvern Instrument, UK
Peristaltic pump	Electrolab, Mumbai, India
pH meter	LabIndia, India
Scanning electron microscopy	JSM 6380 LV, JEOL, Japan
Transmission electron microscopy	Tecnai 20 Philips
UV-visible spectrophotometer (UV-1700)	Shimadzu, Japan
Ventilator	Ugo-Basile, Germany
Vortex mixer	Spinix, Japan
Weighing Balance	Shimadzu, Japan
X-ray diffractometer	Bruker AXS D8, Germany

4.3. Development of EFV NS formulation

NS are composed of the pure drug particles plus stabilizing agents in an aqueous medium. NS was prepared by media milling technique. Zirconium oxide beads were used as milling media. In glass vial, weighed quantity of zirconium oxide beads was taken and 5 ml distilled water was added in this vial. Surfactant and drug were incorporated and comminution process was carried out for a specific time period. The optimization of parameters in the development of NS formulation is discussed in the following sections.

4.3.1. Formulation optimization

The optimized formulation was selected on the basis mean particle size (MPS), particle dispersity index (PDI) and zeta potential (ZP) and stability.

4.3.1.1. Preliminary experiments for NS formulation

Preliminary parameters were optimized by varying one parameter at a time, while keeping other constant, so that effect of various parameters could be evaluated. For optimization of NS, various parameters affecting the NS like concentration of drug, concentration of zirconium beads, concentration of excipients (different stabilizers were used) and stirring time were studied. The parameters were optimized to obtain nano-ranged particles with narrow size distribution.

Polymeric stabilizers such as poloxamer 188, poloxamer 407, PVP K30 were taken for study. In order to select the appropriate stabilizer, preliminary experiments with 0.5 %, 1 % and 2.0 % (w/v) of various stabilizers were performed. Also, effect of combination of polymeric and surfactant stabilizer (SLS) on MPS and ZP were investigated. Effect of different concentrations of drug (0.5 %, 1 % and 2.0 % w/v) on particle size was investigated. Three concentration level of zirconium beads were considered for optimization i.e. 80%, 100% and 120% w/v of batch size.

4.3.1.2. Optimization of NS using factorial design

Various formulation and process variables relating to effectiveness and usefulness should be optimized simultaneously when developing pharmaceutical formulations. In case of traditional method of optimization, combined effects of the independent variables are not considered. The difficulties in optimizing a pharmaceutical formulation are due to difficulty in understanding the real relationship between dependent and independent responses. Factorial design has often been applied to optimize the formulation variables with basic need of understanding of interaction of independent variables.[18]

Preliminary experiments were carried out for evaluating the formulation and processing aspects of NS. These experiments suggested that concentration of drug, concentration of polymer, concentration of surfactant and milling time are the main factors which affect the MPS and ZP of the NS.

The response surface methods like Central composite designs or Box-Behnken designs can be used to determine relationship between different response variables and set of quantitative parameters.[17,19] However, central composite designs usually have axial points outside the cube unless alpha, the axial spacing for ensuring orthogonality, is specified as less than or equal to one. Box–Behnken designs do not have axial points and they ensure that all factors are never simultaneously set at their high levels. Therefore, all the design points fall within the safe operating zone. Box–Behnken experimental designs have fewer design points and fewer experiments to be performed. Furthermore, each factor requires only three levels instead of five, required for central composite designs (unless alpha is equal to one), which is experimentally more convenient and less expensive to perform than central composite designs with the same number of factors.[19-22]

Based on this information, we decided to apply the four-factorial three-level Box–Behnken experimental design for optimization of EFV NS formulation. Four independent factors selected for this study included concentration of drug, concentration of polymer, concentration of surfactant and milling time. All these factors were operated at three levels i.e., +1, 0 and −1. Type of polymer (PVP K30), type of surfactant (SLS), milling media (zirconium oxide beads), concentration of milling media (120% w/v), batch size (5 ml) and solvent (double distilled water) were kept same for all the experiments.

A four-factor, three-level Box-Behnken design was generated by Design-Expert® 8.0 software to conduct the study. A total of 26 experiments were designed by the software with 2 center points. Table 4.4 shows the independent factors and their design levels used in this study. Dependent variables were MPS (Y_1) and ZP (Y_2). After generating the polynomial equations relating dependent and independent variables, the process was optimized for responses Y_1 and Y_2 values. Optimization was performed to obtain the levels of independent variables, which minimize Y_1 while maximizing Y_2.

Table 4.4. Variables for Box-Behnken design

Independent variables		Design level		
Uncoded	**Coded**	**Low (-1)**	**Middle (0)**	**High (+1)**
Concentration of drug (%w/v)	X_1	2.0	4.0	6.0
Concentration of polymer (%w/v)	X_2	0.5	1.0	1.5
Concentration of surfactant (%w/v)	X_3	0.5	1.0	1.5
Milling Time (h)	X_4	16	20	24

4.3.1.3. Preparation of EFV NS

EFV NS was prepared by media milling technique A solution of PVP K30 (1% w/v) and SLS (0.5% w/v) in 5 ml double distilled water was prepared in a 20 ml glass vial. EFV (4.0 %w/v) was then dispersed in this stabilizers solution. Subsequently, 6.0 g of zirconium oxide beads (diameter ranging from 0.4 to 0.7 mm) used as milling media were added. Comminution was carried out on a magnetic stirrer (Remi equipment Pvt Ltd, India) using polygon magnetic stirring bar (Ø 8 mm × l 22 mm) at 800 rpm for 22 h at ambient temperature. Subsequently, NS was separated from milling media by decanting the suspension, followed by washing of the beads with double distilled filtered water.

4.3.1.4. Lyophilization of EFV NS

Mannitol and trehalose were used as cryoprotective agent in NS formulations to form a lyophilized product. It was added to NS after the media milling step but just before the freezing step. The freshly prepared EFV NSs were lyophilized with cryoprotective agent (i.e. trehalose or mannitol) at different concentrations (5%, 10%, 20%, 30% and 40% w/v). Briefly, EFV NSs were cooled down to −70°C for 12 h followed by freeze-dried in a freeze-drier (Heto DryWinner, Denmark) under vacuum for 24 h. The lyophilized product was re-dispersed with the double distilled filtered water.

4.4. Characterization of EFV NS formulation

4.4.1. Particle size measurement

The particle size analysis and PDI of EFV NSs were determined using a Malvern Zeta Sizer Nano ZS 90 (Malvern Instruments, Malvern, UK). The PDI indicates the width of a particle distribution (e.g. 0.0 for a narrow, 0.5 for a very broad distribution). Prior to the measurement, the samples were diluted with double distilled filtered water to a suitable scattering intensity and re-dispersed by shaking before the measurement. All measurements were performed in triplicate. The results are expressed as mean ± standard deviation (SD).

4.4.2. ZP measurement

The ZP is a measure of the electric charge at the surface of the particles indicating the physical stability of colloidal systems.[6] ZP was measured using a Zeta Sizer Nano ZS 90 (Malvern Instruments, Malvern, UK). Each sample was suitably diluted with double distilled filtered water and placed in a disposable zeta cell. The ZP values were assessed by determining the particle electrophoretic mobility. The electrophoretic mobility was converted to the ZP via the Helmholtz–Smoluchowski equation. All measurements were performed in triplicate. The results are expressed as mean ± SD.

4.4.3. Solid state evaluation

Changes in the crystalline state can affect the solubility, dissolution velocity, the oral bioavailability as well as the stability of a pharmaceutical formulation.[23,24] Therefore, the influence of media milling on the crystalline structure of EFV in nasuspension was investigated via DSC and XRD analysis.

4.4.3.1. DSC analysis

Thermal properties of the lyophilized NS (LNS) samples were investigated with a Shimadzu differential scanning calorimeter (Shimadz, Japan). Thermograms of

standard EFV powder, PVP K30, SLS, trehalose, their physical mixture (PM) and LNS were recorded in order to characterize the physical state of EFV in the NS. A heating rate of 10°C/min was employed in the range of 25-300°C with nitrogen atmosphere supplied at 40 ml/min. Each sample was taken (~4-8 mg) in an aluminium pan, crimped and sealed. An empty aluminum pan was used as reference.

4.4.3.2. XRD analysis

XRD diffractograms of standard EFV powder, PVP K30, SLS, trehalose, their PM and LNS were obtained using Bruker AXS D8 Advance X-ray diffractometer. Scans were performed between $5º < 2\theta < 80º$.

4.4.4. Morphology of NS by SEM and TEM

Morphological evaluation of LNS was conducted through the SEM (JSM 6380 LV, JEOL, Japan) and TEM (Tecnai 20 Philips). For SEM analysis, LNS and standard EFV were fixed on a brass stub using a carbon double sided tape. Samples were then subjected to conductive coating with Au-Pd (80% - 20%). SEM was operated at an acceleration voltage of 20 kV. For TEM analysis, LNS was diluted with double distilled water and a drop of it was placed on a carbon-coated copper grid (300 mesh, 3mm) and air dried.

4.4.5. Drug assay

The NS formulation was assayed for EFV by diluting with methanol and further dilution with mobile phase. A 20 µl aliquot was injected into the HPLC for EFV measurement. (See section 4.4.4.8.)

4.4.6. Saturation solubility

Saturation solubility of standard EFV, PM and LNS formulation was carried out in double distilled water. LNS, PM and standard EFV were dispersed in water, 10 ml each, to obtain suspension and placed on a mechanical shaker for 24 h. Samples were centrifuged and the resulting supernatant was analyzed using HPLC (Shimadzu Corporation, Kyoto, Japan) method after suitable dilution with methanol. The experiment was conducted in triplicate. The mean results of three experiments of each sample and SD were reported.

4.4.7. Dissolution study

In vitro dissolution studies were performed using gelatin capsules containing an amount of the formulation (LNS, PM or standard drug) equivalent to 50 mg of EFV and compared with MF dissolution profile. Tests were performed according to the United States Pharmacopeia (USP) and "Dissolution Methods for Drug Products" guide of FDA using dissolution apparatus II.[25] Experiments were performed using 900 ml media (1% SLS in water) at 37 ± 0.5°C at a rotation speed of 50 rpm. At preselected time intervals, 5 ml samples were withdrawn and replaced with 5 ml of pre-thermostated fresh dissolution medium. Samples were filtered through 0.1 µm syringe filter; filtrate was diluted with mobile phase and 20 µl was injected into HPLC for analysis. Dissolution tests were performed in triplicate. Graph of percent cumulative drug release *vs.* time was plotted. Dissolution profiles were evaluated on the basis of dissolution efficiency (DE) and percentage of drug dissolved (DP) at 5 min and 60 min, time needed to dissolve 50% of drug ($t_{50\%}$), area under curve (AUC) and mean dissolution time (MDT). An add-in program, DD solver, for comparison of drug dissolution profiles was used to calculate different dissolution parameters.[26]

4.4.8. Stability studies

Physical and chemical stability was evaluated by storing the LNS samples at 4-8°C (refrigerator) and 25°C for up to 6 months. Samples were withdrawn at predetermined time intervals after 1, 2, 3 and 6 months. MPS and ZP were measured for physical

stability of EFV NS. In addition, chemical stability of EFV in LNS was determined by HPLC assay and dissolution method.

4.4.9. PAMPA study

The BD Gentest™ pre-coated PAMPA plates were used to perform permeability assays for standard EFV, MF and LNS. The permeability assay was carried out as per protocol described in references.[27-29] The 96-well filter plate, pre-coated with lipids, was used as the permeation acceptor and a matching 96-well receiver plate was used as the permeation donor. Sample solutions were prepared by diluting 10 mM stock solutions in 20% methanolic PBS pH 7.4 (final concentration of 200 µM). Sample solutions were added to the wells (300 µl/well) of receiver plate and 20% methanolic PBS pH 7.4 was added to the wells (200 µl/well) of pre-coated filter plate. Filter plate was then coupled with receiver plate and the plate assembly was incubated at room temperature without agitation for 5 h. The assembled plate was placed into a sealed container with wet paper towels to avoid evaporation. At the end of incubation, samples from the donor and receiver plate were analyzed for EFV concentration by HPLC method described in chapter 3.

Permeability of the EFV was calculated using the following formula:

$$\text{Permeability } (P_e)\ (cm/s) = \{-\ln[1-C_A(t)/C_{equilibrium}]\}/\ [A*(1/V_D + 1/V_A)*t] \quad (1)$$

A = filter area (0.3 cm^2), V_D = donor well volume (0.3 ml), V_A = acceptor well volume (0.2 ml), t = incubation time (seconds), $C_A(t)$ = compound concentration in acceptor well at time t (mM), $C_D(t)$ = compound concentration in donor well at time t (mM), and $C_{eq} = [C_D(t)*V_D+C_A(t)*V_A]/(V_D+V_A)$.

4.4.9.1. Membrane integrity test

Lucifer Yellow, a fluorescence dye was selected to study membrane integrity in PAMPA with and without the addition of placebo which contains excipients of same concentrations used to prepare NS. Studies in the literature have shown that Lucifer Yellow CH does not cross the cell membrane as long as the cell lipid membrane

remains intact.[30] Thus, in order to measure the stability of the lipid bilayer, the amount of Lucifer Yellow found in the acceptor well was measured. Three hundred microliters of Lucifer yellow solution (concentration range- 0.03-1.0 μM) was added to selected wells in a donor plate. Three hundred microliters of Lucifer yellow solution (concentration - 0.3 μM) contain placebo (Mixture of excipients without drug used to prepare optimized EFV NS) was added to another selected wells in a donor plate. 20% methanolic PBS pH 7.4 was added to the wells (200 μl/well) of acceptor plate. The donor plate was then coupled with the acceptor plate and the plate assembly was incubated at room temperature without agitation for 5 h. The assembled plate was placed into a sealed container with wet paper towels to avoid evaporation. At the end of the incubation, fluorescence intensity of Lucifer Yellow in the wells of acceptor plate was measured by HPLC consisted fluorescence detector. Chromatographic separation was performed using a Phenomenex Hypersil C4 (100 mm × 4.6 mm i.d., 5 μm particle size) column. Separation was achieved using a mobile phase consisting of acetonitrile and 100 mM ammonium acetate buffer pH 7.0 in the ratio of 70:30 (v/v), pumped at a flow rate of 1 ml/min. Column was maintained at ambient temperature and an injection volume of 20 μl was used. The wavelength of the excitation filter was 430 nm. The wavelength of the emission filter was 530 nm.[31]

4.5. Evaluation of EFV NS formulation

4.5.1. Animals

Male Albino rats (200 ± 15 g) and New Zealand white male rabbits (2.0 ± 0.2 kg) were used for the *in situ* intestinal absorption study and *in vivo* pharmacokinetic study, respectively. Animals were maintained at a temperature of 25 ± 2°C and a relative humidity of 70 ± 5% under natural light/dark conditions and were fed with food and water *ad libitum*. Prior to experiment the animals were kept under overnight fasting. Animal experiments were approved by the Institute Animal Ethics Committee of Pharmacy Department (Protocol No. FTE/PHR/CPCSEA/2007/04) and were conducted as per the guidelines of the Committee for the Purpose of Control and Supervision of Experiments on Animals, India.

4.5.2. *In situ* rat intestinal perfusion study

The absorption property of EFV in LNS and MF was investigated with the established *in situ* intestinal perfusion methods in rats.[32-39] Briefly, rats were anaesthetized with ketamine (100 mg/kg, i.p.) and xylazine (7 mg/kg, i.m.) and were placed on a warming pad in a supine position under a surgical lamp to maintain body temperature at 37 ± 1°C. The abdomen was opened with a midline longitudinal incision of 3 - 4 cm. The small intestine segment approximately 10-12 cm was exposed and a semi-circular incision was made at both sides of the segment. The selected intestinal segment was gently rinsed with pre-warmed normal saline (37±1°C) so as to eliminate any residual fecal matter and debris. The remaining saline was expelled with air. Both ends were cannulated with silicon tubing (diameter 0.4 cm) and ligated using silk suture. The silicon tubes were attached to the perfusion assembly which consisted of a peristaltic pump (Electrolab, Mumbai, India) and a 100 ml volumetric cylinder as reservoir. The small intestine was returned to the abdominal cavity to maintain its viability without disrupting blood vessels. The exposed area was covered with sterilized absorbent gauze and saline (37°C) was applied to keep it warm and moist during the experiment. LNS equivalent to 35 mg EFV was dispersed in 100 ml perfusion solution (Krebs- Ringer's solution; 7.8 g NaCl, 0.35 g KCl, 1.37 g $NaHCO_3$, 0.02 g $MgCl_2$, 0.22 g NaH_2PO_4 and 1.48 g glucose in 1L purified water), maintained at 37°C in a volumetric cylinder. Perfusion was started by recirculation through the cannulated intestine segment at a flow rate of 5 ml/min for 10 min to achieve steady state. Flow rate of perfusion was then adjusted to 2.5 ml/min and the volume of perfusion solution in the circulation system as the 0 min volume was recorded. Perfusion experiment lasted for 6 h and samples were collected at predetermined time intervals. Sample solution (1 ml) was taken out at each time interval, volume of solution in the circulation system was recorded, and then 2 ml Krebs-Rings solution was added in. Samples were frozen immediately and stored at -20°C until analysis. Before analysis, samples were thawed at room temperature and diluted to 5 ml with mobile phase and the resulting solution was centrifuged at 10000 rpm for 10 min. A 20 µl of supernatant was injected into HPLC for determination of EFV using the HPLC method as described earlier. MF was dispersed in perfusion solution and processed with the above experimental method for comparison.

The absorption constant (K_a) is calculated using Fick's equation:

$$K_a = [-\ln(X/X_0)]/t \quad (2)$$

where X_0 is the amount of drug before absorption, X is the residue amount of drug after absorption. K_a can be obtained as the slope from the regression curve of $-\ln(X/X_0)$ *versus* time, and $t_{1/2}$ can be obtained when X is equal to $X_0/2$.[40]

Subsequently, the amount of drug absorbed into systemic circulation (mg) versus time (h) curve was constructed and AUC_{0-6h} *in situ* was calculated, in order to assess extent of drug absorption.

4.5.2.1. Stability of EFV in blank intestinal circulating solution

According to the rat's intestinal perfusion experiment *in situ* above, the blank intestinal circulating solution can be obtained after 6 h circulation. LNS and MF was diluted to 100 ml by blank perfusion solution, and then the resulting solution was treated with a water bath at 37°C for 6 h. The concentrations at 0 h and 6 h were determined and compared with each other.

4.5.3. *In vivo* pharmacokinetic study

Bioavailability of LNS was compared with MF and standard EFV. Rabbits were allocated at random to three treatment groups and administered standard EFV, MF and LNS. The standard EFV, MF and LNS equivalent to 10 mg/kg dose of EFV were filled in mini hard capsules and administrated orally. Blood samples (1.5 ml) were collected through the marginal ear vein into heparinized tubes at 0, 0.5, 1, 1.5, 2, 2.5, 3, 3.5, 4, 8, 12, 24 and 48 h after administration. Blood samples were centrifuged at 3000 rpm for 10 min using a high speed centrifuge machine and plasma samples were withdrawn and stored at -20°C until analysis.

4.5.3.1. Pharmacokinetic analysis

Plasma samples collected from the rabbits were analyzed using developed reverse phase HPLC method described in chapter 3. The drug plasma concentration values were determined from the calibration curve. Non-compartmental pharmacokinetic analysis was performed.[41] Trapezoidal method was employed to calculate the area under the curve (AUC) of plasma concentration as a function of time (t). Mean residence time (MRT) was calculated as area under the first moment curve (AUMC) divided by AUC. AUMC was determined from the plot of plasma concentration multiplied by time (C X t) versus time. All the pharmacokinetic parameters were calculated using MS-Excel software. The maximum plasma concentration (C_{max}) and the time to reach maximum plasma concentration (t_{max}) were determined by the plasma concentration curve using MS-Excel software. The elimination rate constant (K_{el}) was calculated by the regression analysis from the slope of the line and the half-life ($t_{1/2}$) of the drug was obtained by $0.693/K_{el}$. Other parameters, clearance (Cl) and volume of distribution at steady state (V_{ss}) were calculated using the following equations: Cl = Dose/AUC and V_{ss} = Dose X AUMC/$(AUC)^2$.

4.6. Statistical analysis

All data are reported as mean ± SD. The statistical significance of the differences between the groups was tested by one-way ANOVA followed by Bonferroni multiple comparison test using computer based program (Graphpad Prism 5.0).

4.7. Results and discussion

NSs are useful as oral dosage forms for poorly soluble drugs.[42,43] EFV is a very hydrophobic compound with low density, high flow resistance and practically insoluble in water. In this study, EFV was formulated into NS for oral administration using media milling method**.**

The NS of EFV prepared without any stabilizer showed rapid agglomeration of drug nanoparticles immediately after preparation. The agglomeration of EFV nanoparticles

is not only due to the attractive forces between the particles in the absence of significant energy barrier, but also it is a result of the so-called hydrophobic effect. The presence of hydrophobic particles or molecules in water causes distortion and re-arrangement of hydrogen bonding in the aqueous medium, therefore, greatly increasing the free energy of the system.[44] As a result, these hydrophobic particles tend to agglomerate to reduce the system free energy.

NS formulation of EFV requires a careful selection of stabilizers. Stabilizers are needed to stabilize the nanoparticles against inter-particle forces and prevent them from aggregating. At the nanometer domain, attractive forces between particles, due to dispersion or van der Waals forces, come into play. This attractive force increases dramatically as the particles approach each other, ultimately resulting in an irreversible aggregation.[43] In the media milling process, comminution continually fractures organic crystals while stabilizer adsorb onto fresh surface and stabilize each broken particle.[45]

4.7.1. Preliminary experiments for NS formulation

To select a suitable polymeric stabilizer, EFV (0.5%, 1.0% and 2.0% w/v) was milled using different types of polymers (0.5%, 1.0% and 2.0% w/v) (Table 4.5). The milling media (zirconium oxide beads), concentration of milling media (120% w/v), batch size (5 ml), stirring time (24 Hr) and solvent i.e. purified water were kept same for the experiments. Milling was carried out under ambient temperature. Results of preliminary experiments are shown in Table 4.5. The concentration of stabilizer employed to stabilize a NS has marked effect on the particle size and the PDI value of the NS. Three different polymeric stabilizers (poloxamer 188, poloxamer 407 and PVP K30) were tested.

The MPS in NSs stabilized with poloxamers was significantly higher than that stabilized with PVP K30. While comparing the different grades, poloxamer 407 produced smaller particles compared to poloxamer 188 after milling process.[46]

As can be seen from Figure 4.1 and 4.2, the MPS of NSs stabilized with poloxamers decreases significantly at low concentration of drug (0.5% w/v) as compared to high concentration of drug (2.0 %w/v). The MPS of NSs stabilized with poloxamer 188

was found to be ranged from 478.1 nm to 1793.9 nm with high PDI value ranged from 0.395 to 0.700. The MPS of NSs stabilized with poloxamer 407 was found to be ranged from 314.6 nm to 1016.3 nm with high PDI value ranged from 0.386 to 0.580.

While comparing the different grades, poloxamer 407 produced smaller particles compared to poloxamer 188 after milling process. The molecular weight of poloxamer 407 is more than poloxamer 188. The molecular weight of a polymer influences the thermodynamic driving force of physical adsorption.[47] Differences in adsorption strength and the thickness of adsorption layers can result from different molecular weights. In particular, polymers of higher molecular weights have less entropy loss related to their freedom of motion, which results in a higher affinity to the drug surface (stronger adsorption and slower desorption).[47] Therefore, according to the thermodynamic prediction, polymers of higher molecular weights should provide better stabilization.

The MPS was found to be less at lower drug and polymer concentration (0.5 %w/v). The probable reason for this may be that at lower polymer concentration collision of drug particles due to high impaction of milling media is increased, which in turn decreases the MPS of NS.[10] Although poloxamers have been shown to be successful in regard to particle size reduction at low concentration of drug, but often found to be inefficient at higher concentration of drug. Reason for inefficiency of poloxamers may be that due to less adsorption of poloxamers, the stability of NS was decreased and aggregation may occur. The amount of stabilizer should not be sufficient for full coverage of newly generated particle surfaces to provide enough steric repulsion between the particles. Insufficient surface coverage of stabilizer could result in rapid crystal growth and agglomeration.[48,49] Another reason may be, the viscosity of polymer increases at higher polymer concentration, and this alters or hinders the processing of NS on milling.[10]

Table 4.5. Various compositions evaluated for the development of EFV NS formulations.

Batch No.	Excipient Name	Concentration of Excipient (% w/v)	Concentration of Drug (%w/v)	MPS[a]	PDI[a]
1	Poloxamer 188	0.5 %	0.5 %	786.2 ± 5.43	0.500 ± 0.04
2		1.0 %		547.3 ± 5.22	0.437 ± 0.02
3		2.0%		478.1 ± 14.34	0.395 ± 0.02
4	Poloxamer 407	0.5 %	0.5 %	517.5 ± 6.90	0.666 ± 0.06
5		1.0 %		391.7 ± 13.21	0.502 ± 0.05
6		2.0%		314.6 ± 4.95	0.386 ± 0.06
7	PVP K30	0.5 %	0.5 %	377.9 ± 9.92	0.231 ± 0.03
8		1.0 %		340.2 ± 11.75	0.287 ± 0.02
9		2.0%		336.5 ± 5.98	0.312 ± 0.03
10	Poloxamer 188	0.5 %	1.0 %	1134.6 ± 12.21	0.639 ± 0.06
11		1.0 %		823.4 ± 14.31	0.538 ± 0.05
12		2.0%		584.2 ± 10.28	0.426 ± 0.04
13	Poloxamer 407	0.5 %	1.0 %	893.6 ± 12.14	0.492 ± 0.09
14		1.0 %		721.9 ± 21.00	0.339 ± 0.03
15		2.0%		382.9 ± 8.61	0.332 ± 0.03
16	PVP K30	0.5 %	1.0 %	494.2 ± 8.84	0.315 ± 0.01
17		1.0 %		399.4 ± 12.59	0.295 ± 0.02
18		2.0%		351.2 ± 9.23	0.300 ± 0.02
19	Poloxamer 188	0.5 %	2.0 %	1723.6 ± 13.20	0.584 ± 0.10
20		1.0 %		1574.9 ± 23.15	0.402 ± 0.09
21		2.0%		1793.9 ± 16.92	0.700 ± 0.07
22	Poloxamer 407	0.5 %	2.0 %	1016.3 ± 15.28	0.580 ± 0.08
23		1.0 %		562.4 ± 14.29	0.471 ± 0.07
24		2.0%		700.6 ± 15.14	0.466 ± 0.07
25	PVP K30	0.5 %	2.0 %	516.0 ± 10.28	0.251 ± 0.04
26		1.0 %		419.5 ± 7.27	0.283 ± 0.03
27		2.0%		400.1 ± 7.52	0.212 ± 0.02

[a]Data are shown as Mean ± SD, n=3.

The crystal growth/aggregation could be explained by the Ostwald ripening. Generally, Ostwald ripening is a result of the difference in solubility between small and large particles due to a higher degree of curvature of the smaller particles leading to a higher solubility compared with the larger ones.[50] As a result, the small particles dissolve and deposit at the surface of larger particles, which show lower solubility. Subsequently, the small particles disappear while the overall particle growth increases during storage.[6] It was found that PDI of EFV NS stabilized with poloxamers was very high. Generally, the more pronounced Ostwald ripening occurs at higher PDI value. A PDI value of 0.1–0.3 indicates a narrow size distribution whereas a PDI

value greater than 0.3 indicate a very broad size distribution.[51,52] In summary, poloxamers were not able to reduce the particle size to a nano-range and at those levels, were not sufficient to stabilize EFV suspensions.

A decrease in the MPS of EFV NS was observed when PVP K30 used as stabilizer. (Figure 4.3) The size of particles in NS stabilized with PVP K30 was ranged from 336.5 nm to 516.0 nm with narrow PDI value ranged from 0.212 to 0.315. PVP K30 was able to reduce the particle size in nano-range even though at higher concentration of drug. PVP K30 is efficient for full coverage of newly generated particles in NS.

The ZP of NSs stabilized with PVP K30 was found to be in range from -15.7 mV to -20.5 mV which is considered to be low value for long term stability of NS. Generally, a ZP of approximately ±30mV is required as minimum for stable NS.[6]

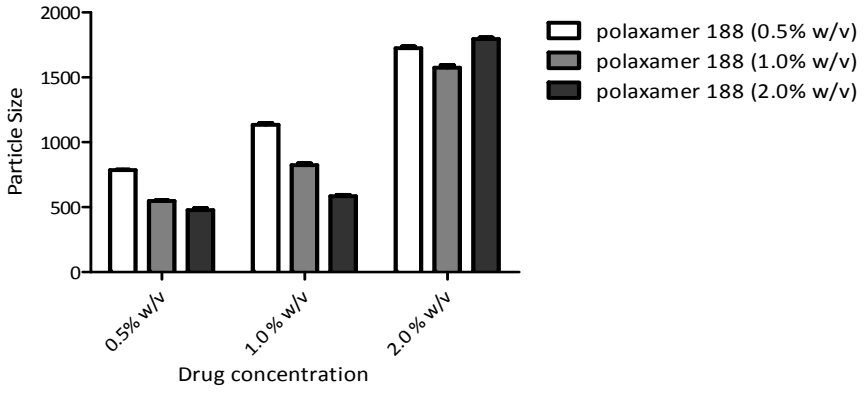

Figure 4.1. MPS and PDI of EFV NSs stabilized with poloxamer 188.

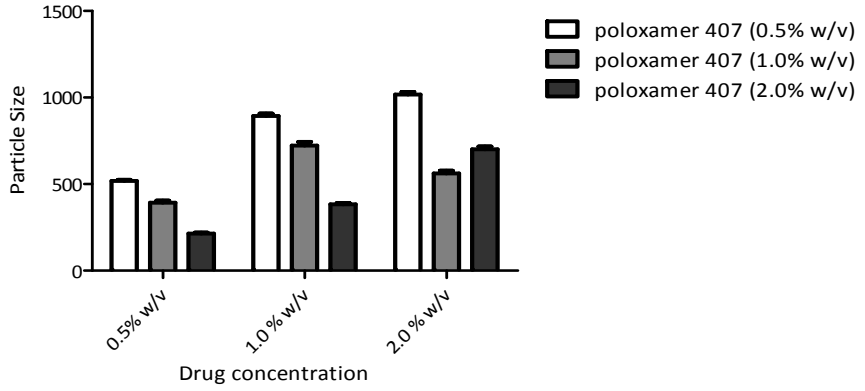

Figure 4.2. MPS and PDI of EFV NSs stabilized with poloxamer 407.

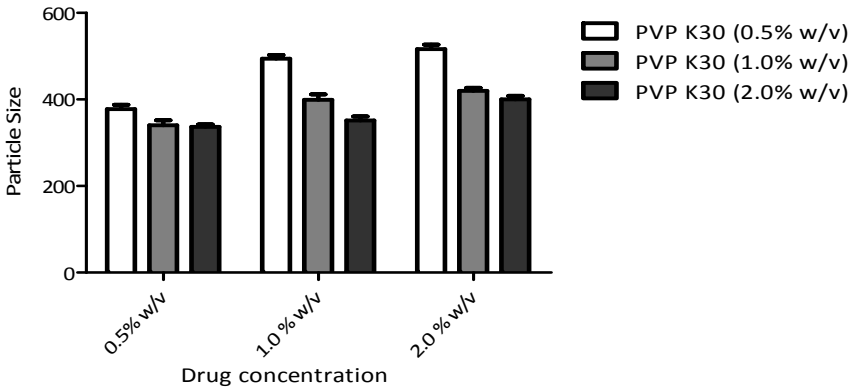

Figure 4.3. MPS and PDI of EFV NSs stabilized with PVP K30.

The physical stability of the NSs stabilized with PVP K30 was evaluated for 2 weeks of storage. The NSs were kept in a closed clear glass vial and stored at 25°C. Samples were subjected to particle size analysis after 2 weeks of storage. The two week stability studies of prepared NSs were carried out to evaluate whether the NSs were sufficiently stable for further processing into the lyophilized form or not. NSs containing PVP K30 as stabilizer show increase in MPS after two weeks of storage. The MPS was found to be in the range of 418.5 - 724.1 nm. (Table 4.6) This might be because of potential Ostwald ripening during storage.[53]

Combination of stabilizers is preferred for long-term stabilization as reported by Muller et al and Rabinow et al.[50,54] Combination of PVP K30 and SLS was tried as stabilizer for long term stability. The rationale for using combination of PVP K30 and SLS was based on combined effect of steric and electrostatic stabilization.[55] Sodium lauryl sulpahate is nonionic surfactant which offer an advantage over polymeric stabilizer in that it have a higher adsorption potential than an equal-chain-length polymer.[56] The PVP K 30 and SLS interactions accumulated at the surfaces around the drug particles thus leading to growth inhibition and additional prolonged stability. Maximum size reduction was achieved by 120% w/v zirconium beads concentration. Therefore, further experiments were carried out using 120% w/v zirconium beads concentration.

Table 4.6. Particle size as a measure of physical stability for NSs stored at 25°C for 2 weeks.

Batch No.	MPS[a]	
	Initial	After 2 Week
7	377.9 ± 9.92	450.6 ± 12.32
8	340.2 ± 11.75	435.2 ± 13.52
9	336.5 ± 5.98	418.5 ± 10.29
16	494.2 ± 8.84	581.9 ± 10.36
17	399.4 ± 12.59	592.4 ± 11.39
18	351.2 ± 9.23	561.4 ± 15.24
25	516.0 ± 10.28	724.1 ± 14.29
26	419.5 ± 7.27	649.1 ± 10.37
27	400.1 ± 7.52	623.0 ± 12.39

[a]Data are shown as Mean ± SD, n=3.

4.7.2. Optimization of NS by factorial design

The effect of combination of polymer (PVP K30) and surfactant (SLS) stabilizer on EFV particle size was assessed by using Design-Expert® 8.0 software. PVP K30 when used alone was found to be a highly effective polymeric excipient for nanosizing of EFV as show in Table 4.5. Box–Behnken experimental design is an orthogonal design. Therefore, the factor levels are evenly spaced and coded for low, medium and high settings, as −1, 0 and +1.[21,57,58] The experimental parameters and the observed and predicted responses for the 26 formulations are reported in Table 4.7. The values of response Y_1 (MPS) and Y_2 (ZP) ranges from 276.3 to 643.3 nm and −16.2 to −34.3 mV, respectively. The ratio of maximum to minimum for both the responses Y_1 and Y_2 is 2.33 and 2.12, respectively; therefore power transformation was not applied to the obtained values.

The selection of model for analyzing the response was done after comparing several statistical parameters including SD, R-squared values and predicted residual sum of square (PRESS). The model having low SD, higher R-square value and lower PRESS value was selected. The details of these significant parameters are mentioned in Table 4.8 and 4.9, which suggests linear model for analyzing the both the responses. The predicted R-Square of 0.8990 and 0.4414 are in reasonable agreement with the

adjusted R-Square of 0.9235 and 0.5764 for MPS and ZP, respectively. The higher value of correlation coefficients signifies an excellent correlation between the independent variables. All the above considerations indicate an excellent adequacy of the regression model.

For estimation of significance of the model, the analysis of variance (ANOVA) was applied. The ANOVA for Y1 and Y2 was summarized in Table 4.10. Using 5% significance level, a model is considered significant if the *p*-value (significance probability value) is less than 0.05. From the *p*-values presented in Table 4.10, it can be concluded that for responses Y1 and Y2, linear model was significant. As shown in Table 4.10, the Model F-values of 76.49 and 9.50 for MPS and ZP, respectively, implies the model is significant. Values of "Prob > F" less than 0.05 indicate model terms are significant. Therefore, X_1, X_2, X_3 and X_4 are significant model terms for MPS and X_2 and X_3 are significant model terms for ZP.

The mathematical relationship in the form of a polynomial equation generated by Design-Expert® 8.0 software for the measured responses, Y_1 and Y_2, are shown below as equation 3 and 4, respectively.

$$Y_1 = 240.86 + 52.52\ X_1 + 107.20\ X_2 + 161.62\ X_3 - 13.35\ X_4 \quad (3)$$

$$Y_2 = -18.25 + 0.95\ X_1 + 10.53\ X_2 - 4.92\ X_3 - 0.87\ X_4 \quad (4)$$

The above equations represent the quantitative effect of independent variables (X_1, X_2, X_3 and X_4) and their interactions on the responses (Y_1 and Y_2). A positive sign represents a synergistic effect, while a negative sign indicates an antagonistic effect. The theoretical values of Y_1 and Y_2 were obtained by substituting the values of X_1-X_4 into the above equation, which were in reasonably good agreement with the observed values as seen in Table 4.7.

Table 4.7. Box-Behnken design: Independent (X) and dependent variables (Y), Observed and predicted and residuals values for the responses Y_1 and Y_2.

	Independent Variables				Observed Values		Predicted Values		Residuals	
Standard order	**X_1**	**X_2**	**X_3**	**X_4**	**Y_1**	**Y_2**	**Y_1**	**Y_2**	**Y_1**	**Y_2**
1	2.0	0.5	1.0	20.0	316.3	-30.5	294.2	-33.4	22.10	2.92
2	6.0	0.5	1.0	20.0	551.1	-28.4	504.3	-29.6	46.84	1.22
3	2.0	1.5	1.0	20.0	403.2	-20.1	401.4	-22.9	1.80	2.78
4	6.0	1.5	1.0	20.0	643.3	-17.9	611.5	-19.1	31.84	1.18
5	4.0	1.0	0.5	18.0	342.5	-19.6	398.7	-22.1	-56.2	2.45
6	4.0	1.0	1.5	18.0	553.4	-29.2	560.3	-27.0	-6.93	-2.2
7	4.0	1.0	0.5	22.0	317.7	-32.4	345.3	-28.5	-27.6	-3.8
8	4.0	1.0	1.5	22.0	480.1	-33.4	506.9	-30.5	-26.8	-2.9
9	2.0	1.0	1.0	18.0	397.2	-25.9	374.5	-26.4	22.71	0.51
10	6.0	1.0	1.0	18.0	614.1	-20.4	584.6	-22.6	29.54	2.21
11	2.0	1.0	1.0	22.0	331.4	-29.2	321.1	-29.9	10.29	0.69
12	6.0	1.0	1.0	22.0	548.7	-22.6	531.2	-26.1	17.53	3.49
13	4.0	0.5	0.5	20.0	363.2	-24.8	318.4	-29.1	44.78	4.26
14	4.0	1.5	0.5	20.0	410.0	-16.2	425.6	-18.5	-15.6	2.33
15	4.0	0.5	1.5	20.0	462.9	-32.6	480.0	-34.0	-17.1	1.38
16	4.0	1.5	1.5	20.0	577.4	-21.1	587.2	-23.4	-9.84	2.34
17	2.0	1.0	0.5	20.0	276.3	-30.8	267.0	-25.7	9.31	-5.1
18	6.0	1.0	0.5	20.0	443.9	-28.0	477.1	-21.9	-33.2	-6.1
19	2.0	1.0	1.5	20.0	432.9	-34.3	428.6	-30.6	4.29	-3.7
20	6.0	1.0	1.5	20.0	616.6	-30.7	638.7	-26.8	-22.1	-3.9
21	4.0	0.5	1.0	18.0	411.6	-31.5	425.9	-29.8	-14.3	-1.7
22	4.0	1.5	1.0	18.0	539.7	-18.4	533.1	-19.2	6.58	0.84
23	4.0	0.5	1.0	22.0	342.8	-28.7	372.5	-33.3	-29.7	4.56
24	4.0	1.5	1.0	22.0	517.5	-19.6	479.7	-22.7	37.76	3.13
25	4.0	1.0	1.0	20.0	439.9	-28.1	452.8	-26.3	-12.9	-1.9
26	4.0	1.0	1.0	20.0	439.9	-28.1	452.8	-26.3	-12.9	-1.9

X_1: Drug concentration (% w/v); X_2: Polymer concentration (% w/v); X_3: Surfactant concentration (%w/v); X_4: Milling Time (h); Y_1: Mean particle size (nm); Y_2: zeta potential (mV).

Table 4.8. Fit summaries for responses Y_1 and Y_2

Source	Sum of Squares		df		Mean Square		F Value		p-value Prob > F	
	Y_1	Y_2	Y_1	Y_2	Y_1	Y_2	Y_1	Y_2	Y_1	Y_2
Linear	253768.7	485.1	4	4	63442.2	121.3	76.5	9.5	< 0.0001	0.0002
2FI	2348.6	25.1	6	6	391.4	4.2	0.4	0.3	0.8743	0.9482
Quadratic	7401.3	129.9	4	4	1850.3	32.5	2.7	3.2	0.0901	0.0585
Cubic	6607.7	58.3	8	8	826.0	7.3	2.3	0.4	0.2613	0.8668
Residual	1059.8	54.7	3	3	353.3	18.2				
Total	5602634.5	18668.7	26	26	215485.9	718.0				

Table 4.9. Regression analysis for responses Y_1 and Y_2

Source	R-Squared		Adjusted R-Squared		Predicted R-Squared		PRESS	
	Y_1	Y_2	Y_1	Y_2	Y_1	Y_2	Y_1	Y_2
Linear	0.9358	0.6442	0.9235	0.5764	0.8990	0.4414	27399.4	420.7
2FI	0.9444	0.6775	0.9074	0.4624	0.8157	-0.0657	49991.5	802.5
Quadratic	0.9717	0.8500	0.9357	0.6591	0.8371	0.1360	44164.8	650.6
Cubic	0.9961	0.9274	0.9674	0.3948	0.4372	-9.4582	152615.6	7875.5

Table 4.10. ANOVA for responses Y_1 and Y_2

Source	Sum of Squares		df		Mean Square		F Value		p-value Prob > F	
	Y_1	Y_2	Y_1	Y_2	Y_1	Y_2	Y_1	Y_2	Y_1	Y_2
Model	253768.7	485.1	4	4	63442.2	121.3	76.49	9.50	< 0.0001	0.0002
X_1	132384.0	43.3	1	1	132384.0	43.3	159.61	3.40	< 0.0001	0.0796
X_2	34475.5	332.9	1	1	34475.5	332.9	41.57	26.09	< 0.0001	< 0.0001
X_3	78359.8	72.5	1	1	78359.8	72.5	94.48	5.68	< 0.0001	0.0266
X_4	8549.3	36.4	1	1	8549.3	36.4	10.31	2.85	0.0042	0.1060
Residual	17417.4	268.0	21	21	829.4	12.8				
Lack of Fit	17417.4	268.0	20	20	870.9	13.4				
Cor Total	271186.1	753.0	25	25						

The relationship between the dependent and independent variables was further elucidated using perturbation and response surface plots. A perturbation graph was plotted to find those factors that affect the response most significantly. A steep slope or curvature in a factor shows that the response is sensitive to that factor. A relatively flat line shows insensitivity to change in that particular factor. In case of response Y_1, factors X_1, X_2 and X_3 shows a steep slope and factor X_4 exhibits a slight slope.

Whereas, in case of response Y_2, factor X_2 shows a steep slope and factors X_3 and X_4 exhibit slight slope. Figure 4.4 represent perturbation plots for response Y_1 and Y_2.

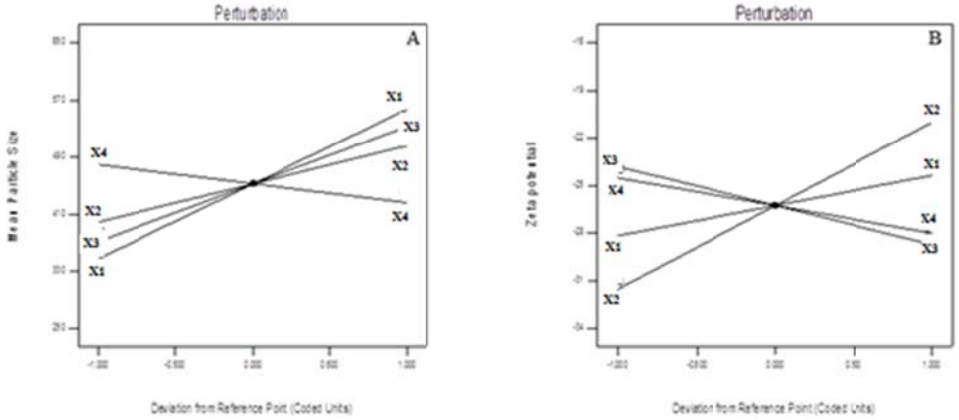

Figure 4.4. Perturbation graph for effect of individual factor on response (A) Y_1 (MPS) and (B) Y_2 (ZP)

Three-dimensional (3D) response surface plots for the measured responses were formed, based on the model polynomial functions to assess the change of the response surface. Also the relationship between the dependent and independent variables can be further understood by these plots. Since the model has four factors, two factors were held constant for each diagram. Figure 4.5 represents the effect of factors X_1, X_2, X_3 and X_4 on the response Y_1. The MPS shows linear pattern with factors X_1 and X_4 at middle level of factors X_2 and X_3 illustrated in Figure 4.5A, it increased as drug concentration increased whereas it decreased as milling time increased. As shown in Figure 4.5A, the MPS of NS decreases at the lower polymer concentration. Effect of polymer and surfactant concentrations on MPS can be discussed with the help of Figure 4.5B. As shown in this Figure 4.5B, NS containing PVP K30 as polymeric stabilizer and SLS as a surfactant stabilizer, gave a particle size in the range of 300.5 to 683.3 nm. A combination of PVP K30 and SLS yields NS with particle size not significantly different than PVP K30 alone. PVP K30 and SLS both are effective at lower concentration to reduce particle size of EFV. At higher concentration of

stabilizers, viscosity increased which might be affect particle size reduction process. Figure 4.5C exhibits that at higher concentration of SLS, MPS of NS increased, attributed to reduction in the adsorption of PVP K30 on EFV particles.[59-61] Displacement of the polymeric stabilizer from the drug surface likely lowers the steric stabilization provided by PVP K30. Steric stabilization by PVP K30 was found to be very efficient for particle size reduction.[62]

The effect of factors X_1, X_2, X_3 and X_4 on the response Y_2 is shown in Figure 4.6. Figure 4.6A shows the effect of factors X_2 and X_3 on response Y_2 at middle level of factors X_1 and X_4. As can be seen from Figure 4.6A the ZP values increases at low level of factor X2 where the level of factor X3 is high. SLS is non-ionic surfactant. At low level of factor X2 the particle surface of drug is not covered so densely with PVP K30, due to which SLS diffuses faster to the particle surfaces; since it has excellent dispersion properties.[63] Adsorption of SLS onto the particle surface leads to high ZP value. The ZP value of NS decreases at high level of factor X2, irrespective of factor level X3. At this stage due to increased concentration of PVP K30 in NS its adsorption on drug particles increases which leads to a reduction of the measured ZP. Figure 4.6B shows the effect of factors X_2 and X_4 on response Y_2. It was observed from the Figure 4.6B that ZP value increases at high milling time and lower polymer concentration. The probable reason for this may be that due to high milling time the adsorption of steric and electrostatic stabilizer is more which increases the particle mobility and ZP value. These results are in agreement with other researcher reports.[10,63] NSs containing PVP K30 and SLS as stabilizers shows stability in MPS after two weeks of storage at 25°C.

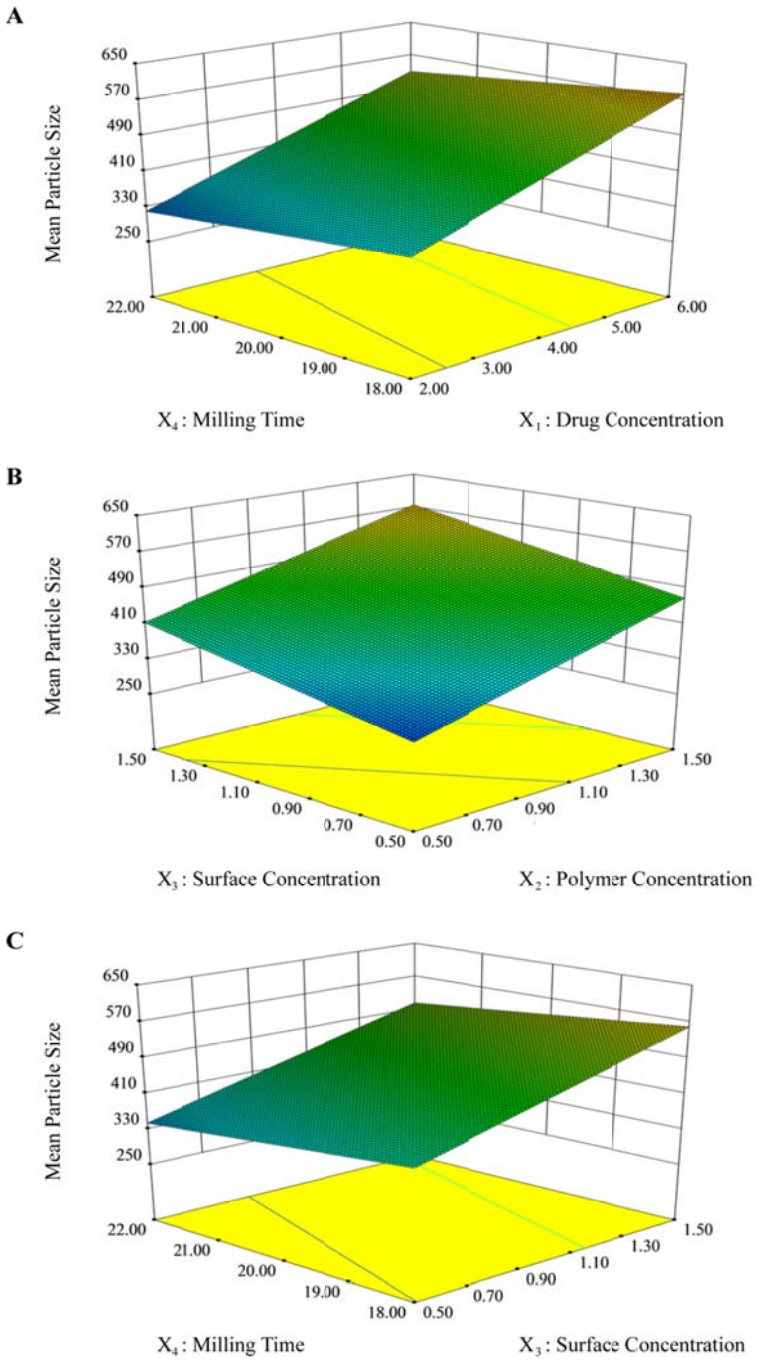

Figure 4.5. 3D Response surface plots: (A) Effect of drug concentration (X_1) and milling time (X_4) on the response Y_1, (B) effect of polymer concentration (X_2) and surfactant concentration (X_3) on the response Y_1, (C) effect of surfactant concentration (X_3) and milling time (X_4) on the response Y_1.

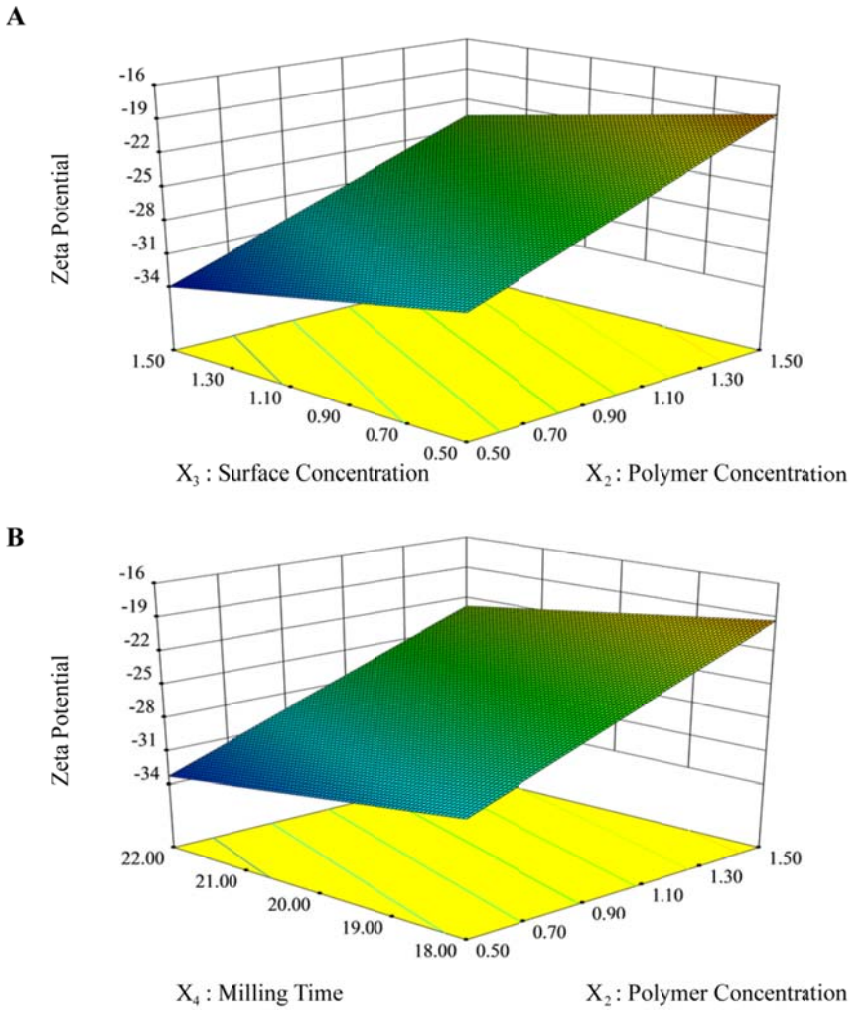

Figure 4.6. 3D Response surface plots: (A) Effect of polymer concentration (X_2) and surfactant concentration (X_3) on the response Y_2, (B) effect of polymer concentration (X_2) and milling time (X_4) on the response Y_2.

As discussed above, the steric and electrostatic repulsive forces between the nanoparticles provided by PVP K30 and SLS were able to reduce particle size and prevent aggregation of the nanoparticles, respectively. This could also prohibit the crystal growth caused by Ostwald ripening, and thus, no change in the particle size of the NS was observed.

4.7.3. Optimum Formula

After studying the effect of the independent variables on the responses, the levels of these variables that give the optimum response were determined. Optimization was performed to find out the level of independent variables (X_1, X_2, X_3 and X_4) that would yield a minimum value of MPS with maximum value of ZP. It is evident from the polynomial equation and 3D response surface plots that PVP K30 increases MPS while SLS improves ZP value of NS. The optimum formulation is one that gives a minimum MPS and high ZP value along with a high amount of drug and low amount of stabilizers in the resultant NS. Using a Design-Expert® 8.0 software optimization process, selected values of X_1, X_2, X_3 and X_4 were 4.0% w/v, 1.0% w/v, 0.5% w/v and 22 h, respectively, which gives theoretical values of 345.3 nm and -28.5 mV for MPS and ZP, respectively. For confirmation, a fresh formulation in triplicate was prepared at the optimum levels of the independent variables, and the resultant NS formulations were evaluated for the responses. The observed values of MPS and ZP were found to be 320.4 ± 3.62 nm and -32.8 ± 0.4 mV, respectively, which were in close agreement with the theoretical values. PDI of optimized NS formulation was found to be 0.216 which shows narrow size distribution. Figure 4.7 shows particle size distribution and ZP curve of optimized EFV NS formulation.

4.7.4. Lyophilization of EFV NS

Lyophilization technique is simplest way to obtain the powder from the milled suspension.[64-66] Lyophilization can be used to overcome stability problems of NS formulations. The NS formulation can be converted into dry form by lyophilization technique to increase stability during storage.[67] First, freezing of NS formulation, sublimation and then drying for elimination of adsorbed water are the main steps for the lyophilization process.[68] During the lyophilization process, nanocrystals are likely to agglomerate and are not able to return to their original size upon reconstitution. Therefore, materials such as mannitol, sucrose, trehalose, polyvinyl alcohol, low molecular weight polyvinyl pyrrolidone, and its derivatives are used as cryoprotectant to protect nanoparticles from undergoing changes during lyophilization.[68]

Lyophilization produces the porous and bulky powder, which is highly advantageous to be soaked up by and dispersed in water.

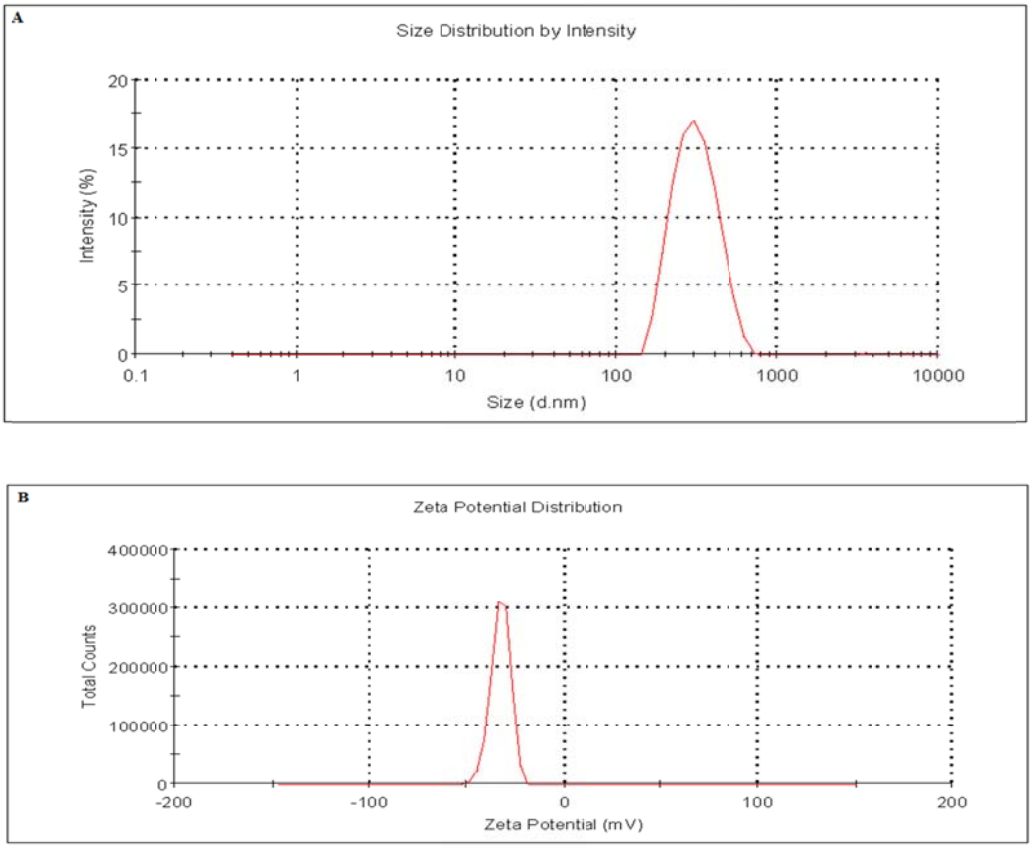

Figure 4.7. (A) Particle size distribution curve and (B) ZP curve of optimized EFV NS

Different concentrations (5%, 10%, 20%, 30% an 40% w/v) of mannitol and trehalose were screened to stabilize the EFV NS (Composition: 0.5% w/v PVP K30, 1.0% w/v SLS and 4.0%w/v EFV, EFV-NS-PVP K30/SLS) during the freeze-drying process to produce an effective solid dosage form. Table 4.11 depicts the effect of mannitol and trehalose concentrations on the MPS of EFV NS after reconstituting the lyophilized powder with double distilled water.

Mannitol and trehalose was used as cryoprotectant for batch A-E and F-J, respectively. The results showed that trehalose was effective cryoprotectant than mannitol in preventing nanoparticles from aggregation during lyophilization process. At higher concentration of mannitol (Batch E), NS formulation was not re-dispersing with water after lyophilization. Also, sonication required for re-dispersion of NS formulation (Batch C and D) with water after lyophilization. Formulations containing higher amounts of sucrose, larger agglomerates were observed, reported by Van Eerdenbrugh Bernard et al. (2008).[9] Similar results were obtained in our study with higher concentration of mannitol. As seen from the Table 4.11, MPS of Batch A-D after re-dispersion of the lyophilized product was higher than the MPS before lyophilization process.

LNS formulations with trehalose as cryoprotector could completely re-disperse by manual shaking for 1 min. The NS formulation stabilized with 5% and 10% trehalose had small particle size than the suspension before lyophilization. The MPS increased by about 18 nm, 25 nm and 32 nm after re-dispersion, respectively, with 20%, 30% and 40% concentration of trehalose. As seen from the Table 4.11, MPS of 312.3 nm after re-dispersion of the lyophilized product was close to the MPS of 320.4 nm before lyophilization process with 5% trehalose. Stabilization with trehalose at low concentration yielded optimal results.[6,69] In addition, trehalose did not show any significant effect on the recorded ZP values.

Table 4.11. Particle size of NS formulations before and after lyophilization

Batch	Preparation of EFV NS	MPS[a]
	Before lyophilization (EFV-NS-PVP K30/SLS)	320.4 ± 3.62
A	lyophilization with 5% mannitol	350.5 ± 5.34
B	lyophilization with 10% mannitol	347.2 ± 6.41
C[1]	lyophilization with 20% mannitol	378.4 ± 8.16
D[1]	lyophilization with 30% mannitol	409.4 ± 8.61
E[2]	lyophilization with 40% mannitol	Not Re-disperse
F	lyophilization with 5% trehalose	312.3 ± 2.93
G	lyophilization with 10% trehalose	317.2 ± 3.34
H	lyophilization with 20% trehalose	338.9 ± 4.41
I	lyophilization with 30% trehalose	345.2 ± 4.84
J	lyophilization with 40% trehalose	351.7 ± 5.51

[a]Data are shown as Mean ± SD, n=3. Re-dispersion was done by manual shaking for 1 min, the re-dispersion volume being equivalent to the original volume of the NS.

[1]Sonication required for re-dispersion. [2]Re-dispersion was not occurring even after sonication.

4.7.5. Characterization of EFV NS formulation

PM, used in characterization studies, was prepared using the same drug and stabilizers concentrations of the optimized LNS, as proper comparison to avoid introduction of any other variable that could affect results.

4.7.5.1. DSC analysis

DSC was performed to investigate the effect of excipients on the inner structure of EFV NS. DSC curve of pure EFV exhibited a single endothermic peak at a temperature of 139.80°C, corresponding to its fusion temperature (Figure 4.8A). DSC curve of SLS exhibited two endothermic peaks at 101.49°C and 191.03°C, respectively (Figure 4.8B). PVP K30 is an amorphous polymer; therefore it did not show a melting peak, however, it showed a broad endotherm ranging from 60°C to 120°C due to the presence of residual moisture (Figure 4.8C). Trehalose showed a single endothermic peak at 99.38°C (Figure 4.8D). Three endothermic peaks were observed in the LNS and PM. The first peak belonged to the melting of trehalose. Secondly, the EFV melting peak was observed. However, the temperature for the melting of EFV in NS shifted to a lower value (133°C) as compared with the PM (137.2°C) and pure EFV (139.80°C) (Figure 4.8E and 4.8F). Furthermore the peak becomes broader. This phenomenon is probably caused by the depression of the melting point of materials in form of small crystals as predicted by the Gibbs–Thomson equation.[70] A similar observation with other drugs was also reported by some researchers.[9,71-73] Both in the LNS and PM, a weak SLS melting signal could be distinguished. NS stabilized with PVP K30 and SLS was chosen for further studies because of this absence of drug–stabilizer interaction.

4.7.5.2. XRD analysis

XRD was performed with the same batch of NS that was measured by DSC. XRD can be used to get information on the crystalline characteristics of both the EFV and the excipients. The XRD patterns of LNS powder (Figure 4.9H) were compared to those of the standard materials (Figure 4.9A–F) and PM (Figure 4.9G) in order to investigate the crystalline form of EFV in the LNS powder. The preservation of the crystal structure of the drug in the formulation is crucial for the sustained stability of the drug during its shelf-life. On the other hand, the drug in the amorphous state has better dissolution properties compared to the crystal form. Thus, decreasing the drug particle size to nanorange while preserving the crystal morphology, leads to improved dissolution profile while keeping the drug intact (*i.e.* sustained chemical stability).[66] It was confirmed that no crystalline change was found in the nanosupension, because its X-ray diffraction pattern shows characteristics 2θ values of the standard EFV. However, the virtual elimination in the relative intensities of LNS peaks as compared to standard EFV peaks might be attributed to small particle size (nanometer range), high specific surface area and presence of excipients on the surface of EFV nanocrystals.[24,71] The results were in accordance with those of DSC studies, which also indicated decrease in crystallinity due to nanosizing.

4.7.5.3. Morphology of NS by SEM and TEM

Analysis by SEM has been used to evaluate the morphology of drug nanocrystals.[7] SEM images revealed distinct differences in the morphologies of standard EFV and LNS (Figure 4.10). Standard EFV showed irregular shape and crystalline nature (Figure 4.10A). Media milling of the standard EFV in presence of stabilizers (PVP K30 and SLS) led to a change in morphology of drug particles and a decrease in particle size to nanometer range with relatively narrow size distribution (Figure 4.10B). LNS could be re-dispersed into water without forming any large aggregates as demonstrated by TEM image (Figure 4.10C). TEM image exhibited that the particles were discrete, non-aggregated, homogenously dispersed and nearly spherical in shape.

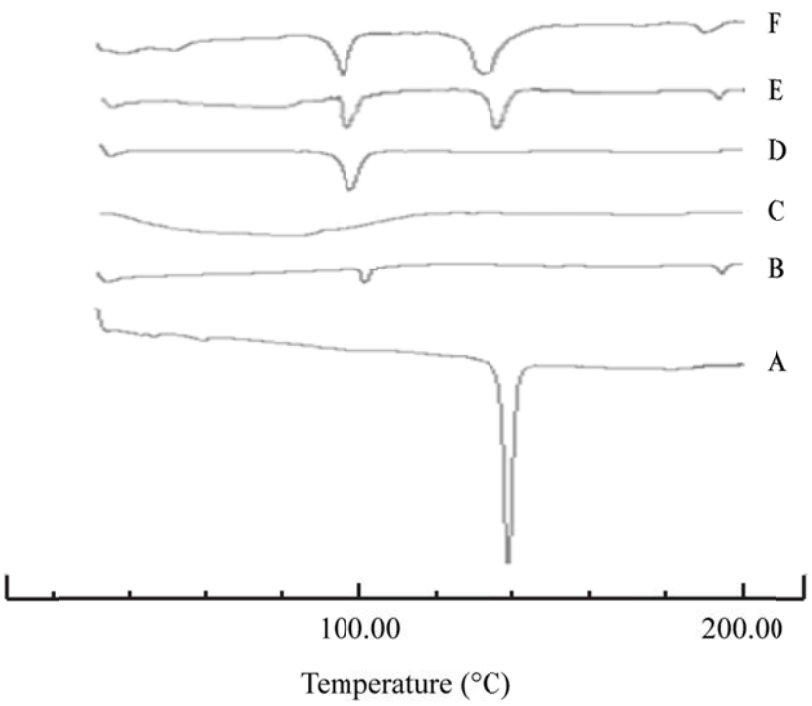

Figure 4.8. DSC thermograms of (A) standard EFV, (B) SLS, (C) PVP K30, (D) trehalose (E) PM (F) LNS showing the preservation of crystalline form of EFV in NS.

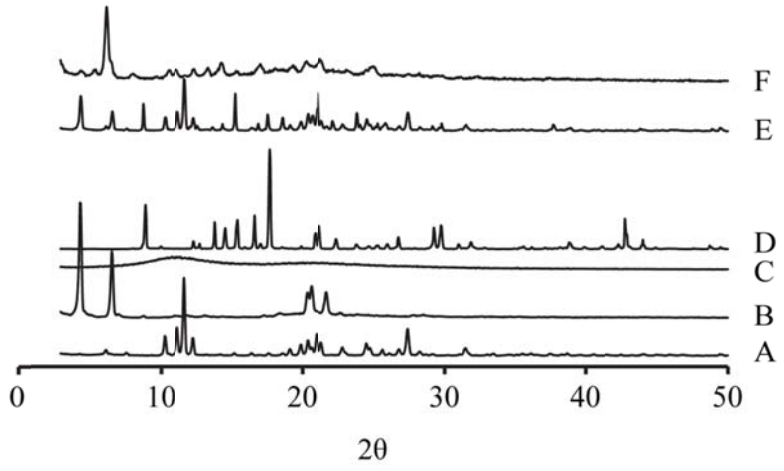

Figure 4.9. XRD spectra of (A) standard EFV, (B) SLS, (C) PVP K30, (D) trehalose (E) PM (F) LNS showing the preservation of crystalline form of EFV in NS.

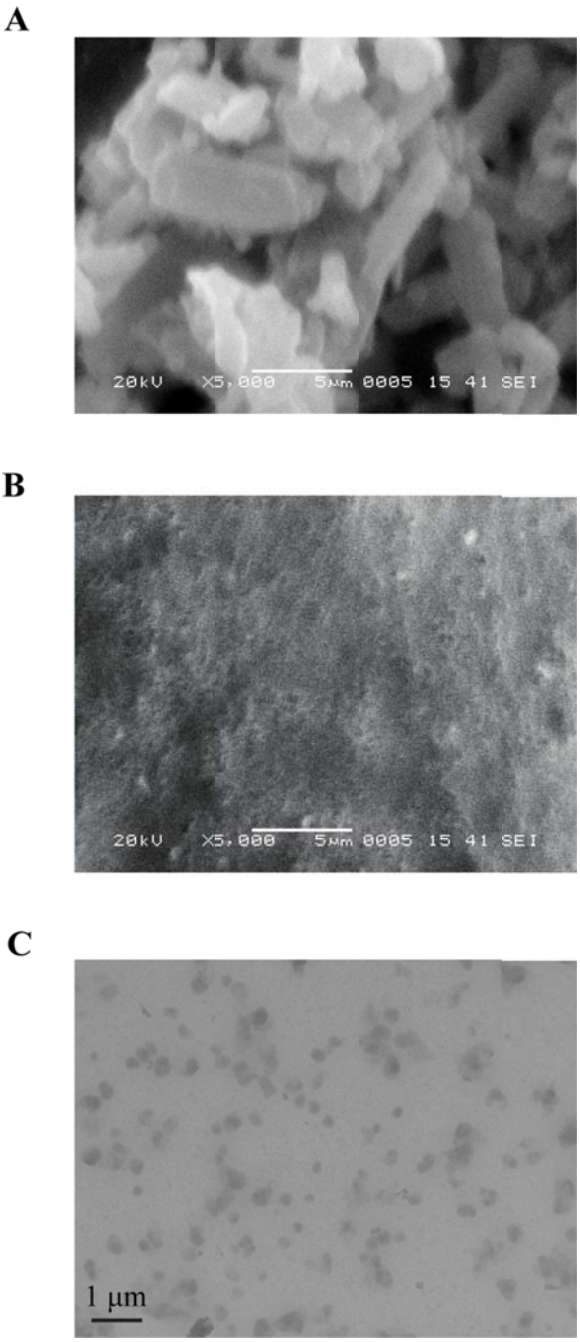

Figure 4.10. SEM images of (A) standard EFV and (B) LNS showing the particle size reduction with NS formulation. TEM image of (C) LNS showing spherical shape of EFV particles in NS.

4.7.5.4. Saturation solubility

Saturation solubility is defined as the maximum quantity of a compound (solute) that can be dissolved in a certain quantity of a specific solvent at a specified temperature.[74] The saturation solubility increases with decreasing particle size. However, this effect is only pronounced for particles below 1μm.[75] This increase in saturation solubility can be explained by the Freundlich–Ostwald equation:[15,43]

$$\text{Log } C_s/C_\infty = 2\sigma V / 2.303RT\rho r \quad (5)$$

Where C_s is the saturation solubility, C_∞ is the solubility of the solid consisting of large particles. σ, V, R and T means the interfacial tension of substance, molecular weight, gas constant and absolute temperature, respectively. ρ and r are the density of the solid and radius of particles, respectively. The saturation solubility of standard EFV was extremely low being only 5.84 ± 0.3 μg/ml. PM showed saturation solubility of 25.62 ± 1.6 μg/ml, which is almost 4.4 fold higher than standard EFV. In contrast, EFV in LNS showed enhanced saturation solubility 235.6 ± 6.1 μg/ml, which is almost 9-fold and 40-fold higher than standard EFV and PM, respectively, attributed to nano-sized EFV particles.

4.7.5.5. Dissolution study

The dissolution profiles of capsules containing standard EFV, PM of EFV with PVP K30, SLS and trehalose, MF and LNS are illustrated in Figure 4.11 and Table 4.12. The dissolution rate was markedly enhanced in the LNS, as 90.25% ± 1.11 of the drug dissolved in 5 min, as compared to only 4.72% ± 2.52, 8,89% ± 2.08 and 19.54% ± 0.75 from standard EFV, PM and MF, respectively. The standard EFV and PM did not achieve complete dissolution during the 60 min test period and only 49.05% ± 5.13 and 63.04% ± 5.02 of the drug dissolved over 60 min, respectively, owing to the large crystal size, while NS showed a significantly enhanced dissolution rate with 99.13% ± 0.21 of the drug dissolved over 60 min. This enhanced dissolution rate can be attributed to the higher surface area of nanoparticles available for dissolution.[76] Dissolution profile of PM show a slight increase of dissolution rate compared to the standard EFV attributed to the improved wettability of the drug due to surfactant.

Different dissolution parameters are reported in Table 4.13. The DE of a pharmaceutical form is defined as the area under the dissolution curve up to a certain time, *t*, expressed as a percentage of the area of the rectangle described by 100% dissolution in the same time.[77,78] It can be calculated by the following equation:

$$\mathrm{DE} = \frac{\int_0^t y \times \mathrm{d}t}{y100 \times t} \times 100\% \quad (6)$$

where *y* is the percentage of dissolved product.

Another dissolution parameter, MDT, which is a measure of the rate of the dissolution process, was calculated using equation 7,

$$\mathrm{MDT} = \frac{\sum_{i=1}^{i=n} \mathrm{tmid} \times \Delta \mathrm{M}}{\sum_{i=1}^{i=n} \Delta \mathrm{M}} \quad (7)$$

where *i* is the dissolution sample number, *n* is the number of observations, t_{mid} is the midpoint time between *i* and *i*−1, and Δ*M* is the additional amount of drug dissolved between *i* and *i*−1.[79]

As can be seen, dissolution efficiency and dissolution percentage values increased in the following order: standard EFV < PM < MF < NS; while the MDT and $t_{50\%}$ decreased in the same order. As the MDT and $t_{50\%}$ decreases, the drug release rate increases. The time to dissolve 50% of the drug was strongly reduced to 2.8 min for LNS as compared to 16.2 min required for MF. The LNS showed a 1.5-fold higher AUC than MF.

The obtained results are in line with the Noyes–Whitney equation describing the dissolution velocity dc/dt. The Noyes–Whitney equation:

$$dC/dt = D \cdot S \cdot C_s - C_t / h \quad (8)$$

where dC/dt represents the dissolution rate, D is the diffusion coefficient of the solute, h denotes the thickness of the dissolution boundary layer and S represents the surface area, C_s is the saturation solubility and C_t the bulk concentration. According to the Noyes–Whitney equation, dissolution velocity depends on the surface area of solid particles, diffusion transport of dissolved material and saturation solubility of the solute. An increase in dissolution velocity is proportional to an increase in surface

area which occurs when the particle size is reduced. The dissolution velocity also increased by the reduction of the diffusion layer thickness by particle size reduction to nanometer range.[80-84]

The model-independent simple method includes the difference factor (f_1) and the similarity factor (f_2). The f_1 factor measures the percent error between two curves over all time points. The percent error is zero when the test and drug reference profiles are identical and increase proportionally with the dissimilarity between the two dissolution profiles. The f_2 factor is a logarithmic transformation of the sum-squared error of differences between the test and the reference products over all time points. This factor is 100 when the test and reference profiles are identical and tends to 0 as the dissimilarity increases. Two dissolution profiles are declared similar if f_1 is between 0 and 15 and if f_2 is between 50 and 100.[85,86] The difference factor f_1 and similarity factors f_2 were calculated between LNS and MF. The results of f_1 and f_2, 64.82 and 17.56, respectively, showed that the profiles are not similar.

All these results confirm that particle size is an important parameter in enhancing drug dissolution rate and therefore drug bioavailability.

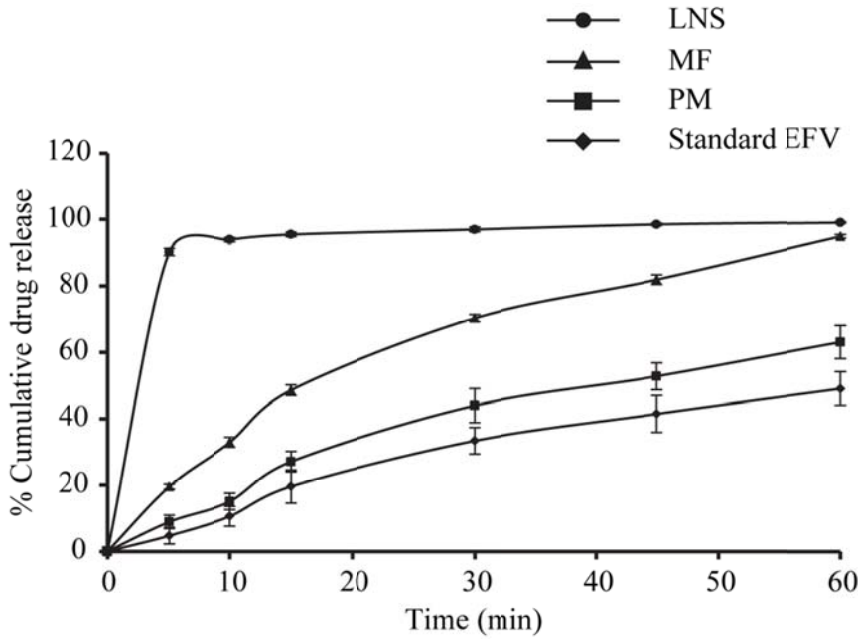

Figure 4.11. % Cumulative drug release of standard EFV (♦), PM (▪), MF (▲), and LNS (•) from capsule in 1% SLS in water dissolution media showing higher

dissolution rate of LNS compared to standard EFV and MF. Data are represented as Mean ± SD; n=3 for each group.

Table 4.12. Release profile of standard EFV, PM, MF and LNS from capsule in dissolution media (1% SLS in water).

	% Cumulative Drug Release[a]			
Time (min)	**Standard EFV**	**PM**	**MF**	**LNS**
5	4.72 ± 2.52	8.89 ± 2.08	19.54 ± 0.75	90.25 ± 1.11
10	10.59 ± 3.00	15.08 ± 2.52	32.93 ± 1.51	93.83 ± 0.63
15	19.58 ± 5.00	27.09 ± 3.07	48.58 ± 1.60	95.39 ± 0.69
30	33.36 ± 4.03	43.96 ± 5.13	70.27 ± 1.08	96.90 ± 0.77
45	41.47 ± 5.54	52.77 ± 4.03	81.93 ± 1.47	98.43 ± 0.34
60	49.05 ± 5.13	63.04 ± 5.02	94.97 ± 0.54	99.13 ± 0.21

[a]Data are shown as Mean ± SD, n=3.

Table 4.13. Comparison of dissolution parameters

	Standard EFV	**PM**	**MF**	**LNS**
DE_5 %	2.36 ± 1.26	4.45 ± 1.04	9.77 ± 0.37*	45.13 ± 0.55*,#
DE_{60}%	29.38 ± 4.31	38.57 ± 3.76	62.39 ± 0.41*	92.46 ± 0.37*,#
DP_5%	4.72 ± 2.52	8.89 ± 2.08	19.54 ± 0.75*	90.25 ± 1.11*,#
DP_{60}%	49.05 ± 5.13	63.04 ± 5.02	94.97 ± 0.54*	99.13 ± 0.21*
$t_{50\%}$ (min)	>60	39.6 ± 7.77	16.2 ± 0.97*	2.80 ± 0.05*,#
MDT (min)	24.17 ± 1.63	23.32 ± 0.68	20.58 ± 0.08*	4.03 ± 0.18*,#
AUC	1762.7 ± 258.5	2314.4 ± 225.9	3743.4 ± 24.8*	5547.7 ± 22.0*,#

Data are shown as Mean ± SD, n=3.[a] DE: Dissolution efficiency; DP: Dissolution percentage; $t_{50\%}$: Time required for release 50% of drug; MDT: Mean dissolution time; AUC: Area under curve; *P<0.05 compared with standard EFV; #P<0.05 compared with marketed formulation.

4.7.5.6. Stability study

The physical and chemical stability of LNS formulations was evaluated at 4-8°C and 25°C for 6 months. It was found that there was no significant change in the MPS and

the PDI value when LNS was stored at 4-8°C and 25°C over 6 months. As reported in Table 4.14, after 6 months storage at 4-8°C and 25°C of LNSs, the MPS was 315.9 ± 2.01 nm and 320.4 ± 1.95 nm with a PDI of 0.217 ± 0.008 and 0.215 ± 0.005, respectively, which is in good agreement with zero time data. As seen from Table 4.14, the zeta-potential values did not change during the 6 months storage at 4-8°C and 25°C. Furthermore, the chemical stability of EFV was examined using an HPLC assay during this storage period. For instance, more than 97.5 % of EFV remained in the NS formulations for up to 6 months when stored at 4-8°C and 25°C as shown in Table 4.15. The results of DE and DP at 5 and 60 min of stability samples are represented in Table 4.15. At the end of 60 min LNS gave dissolution of 98.90% and 98.61% after 6 months of storage at 4-8°C and 25°C, respectively, which is comparable to the release of LNS at time zero. No significant difference in dissolution was observed for stability samples of LNSs compared to the dissolution of initial sample. The f_2 was found to be 98.52 and 98.48 at 4-8°C and 25°C of storage, respectively, indicating similar profiles. These results suggest that the lyophilized product can maintain the physical as well as chemical stability of the NS formulations during the shelf-life.

Table 4.14. Influence of time and temperature on the physical stability of EFV on LNS stored at different conditions and time intervals

Month	4-8°C			25°C		
	MPS (nm)	PDI	ZP (mV)	MPS (nm)	PDI	ZP (mV)
0	312.3 ± 0.93	0.210 ± 0.005	-32.8 ± 0.40	315.1 ± 1.21	0.212 ± 0.008	-32.3 ± 0.29
1	313.6 ± 1.12	0.215 ± 0.008	-31.9 ± 0.32	315.4 ± 1.32	0.211 ± 0.009	-32.7 ± 0.39
2	313.4 ± 0.82	0.212 ± 0.003	-33.1 ± 0.51	312.9 ± 1.05	0.211 ± 0.007	-32.4 ± 0.72
3	317. 2 ± 1.83	0.215 ± 0.009	-32.6 ± 0.74	318.3 ± 2.10	0.217 ± 0.004	-31.9 ± 0.41
6	315.9 ± 2.01	0.217 ± 0.008	-32. 3 ± 0.57	320.4 ± 1.95	0.215 ± 0.005	-32.2 ± 0.39

Data are shown as Mean ± SD, n=3.

Table 4.15. Influence of time and temperature on the chemical stability of EFV on LNS stored at different conditions and time intervals

Month	Drug assay	DE_5%	DE_{60}%	DP_5%	DP_{60}%
	4-8°C				
0	98.5 ± 1.43	44.98 ± 0.47	92.36 ± 0.29	89.95 ± 0.82	98.40 ± 1.07
1	98.2 ± 1.06	45.20 ± 0.38	93.27 ± 0.17	90.39 ± 1.03	99.04 ± 0.61
2	97.8 ± 0.82	45.09 ± 0.33	92.27 ± 0.30	90.18 ± 0.95	98.23 ± 0.70
3	98.9 ± 2.06	45.26 ± 0.51	91.67 ± 0.22	90.52 ± 0.69	97.90 ± 1.13
6	97.5 ± 1.58	45.19 ± 0.60	92.35 ± 0.41	90.38 ± 0.75	98.90 ± 0.54
	25°C				
0	97.9 ± 0.92	44.63 ± 0.53	92.37 ± 0.37	89.25 ± 1.11	99.03 ± 0.51
1	98.5 ± 1.81	45.30 ± 0.44	93.22 ± 0.44	90.59 ± 0.91	98.90 ± 0.79
2	98.1 ± 1.44	44.74 ± 0.31	91.74 ± 0.30	89.47 ± 0.57	98.40 ± 1.00
3	98.9 ± 1.28	45.04 ± 0.29	91.80 ± 0.40	90.08 ± 0.84	98.36 ± 0.72
6	98.3 ± 1.63	44.54 ± 0.35	92.31 ± 0.26	89.08 ± 1.02	98.61 ± 0.53

The values are shown as mean ± SD, n=3.

4.7.5.7. PAMPA study

Parallel artificial membrane permeability assay (PAMPA) was non-cell-based permeability model, developed as an alternative to the low throughput Caco-2 assay, used to estimate passive permeability because it lacks transporter- and pore-mediated permeability.[87-89] PAMPA assay is a robust and reproducible technique. It is relatively fast, inexpensive, and straightforward compared to Caco-2 assay.[27] Low solubility compounds have been a challenge for permeability measurements. Using a buffer containing organic solvents helps to increase the solubility of these compounds. In this study, buffer contains 20% methanol to increase solubility of EFV. The effective permeability (P_e) values for the standard EFV, MF and LNS are reported in Table 4.16. The LNS represents significant improvement in permeability than the MF in PAMPA model. Standard EFV demonstrated the lowest permeability (P_e value of 15.95×10^{-6} cm/s) whereas the LNS showed highest permeability (P_e value of 20.81×10^{-6} cm/s). The permeability ranking is as follows: LNS > MF > standard EFV. Thus, this is an indication that passive permeation of the drug has improved considerably on formulating it into NS. Since the permeation rate of Lucifer Yellow was negligible, we could conclude that the membrane was integral.

Table 4.16. Effective permeability value by PAMPA study (n=6)

	Effective permeability (P_e) ± S.D. (10^{-6} cm/s)
Standard EFV	15.95 ± 1.02
MF	16.84 ± 0.82
LNS	20.81 ± 1.10

4.7.6. Evaluation of EFV NS

4.7.6.1. *In situ* absorption property of EFV in rat intestine

In single pass intestinal perfusion model, drug is absorbed progressively from buffer as it passes through intestine during the permeation study. Therefore, decrease concentration of drug in perfusate was directly equivalent to amount of drug absorbed.[90] The intestinal absorption kinetics of LNS and MF of EFV was investigated. The absorption parameters such as K_a, $t_{1/2}$, $AUC_{0\text{-}6h\ in\ situ}$ and uptake percentage are reported in Table 4.17.

The K_a of LNS was 0.6266 ± 0.10 h^{-1} which was 2.47-fold higher as compared with that of MF (K_a = 0.2537 ± 0.01 h^{-1}). The $t_{1/2}$ of LNS and MF was found to be 1.12 ± 0.17 h and 2.73 ± 0.11 h, respectively. Significant difference was observed in percentage uptake between LNS (98.13 ± 0.78 %) and MF (80.97 ± 0.64 %). The $AUC_{0\text{-}6h\ in\ situ}$ of LNS was 155.72 ± 4.68 mg·h which was 1.62-fold higher as compared with that of MF (96.37 ± 4.50 mg·h). Absorption curve of LNS and MF in the rat small intestine was shown in Figure 4.12. Absorption curve of LNS represented significant improvement in drug absorption than the MF. The results indicate that intestinal permeability of EFV was increased in LNS form. This enhancement may be attributed to effect of the surfactants, nano-range particle size and adhesion property of NS. Igor Legen et al has been investigated the use of surfactants to increase the intestinal absorption of drugs.[91]

Table 4.17. Absorption parameters of LNS and MF.

Absorption parameter	LNS	MF
K_a (h^{-1})	0.6266 ± 0.10	0.2537 ± 0.01
$t_{1/2}$ (h)	1.12 ± 0.17	2.73 ± 0.11
Uptake percentage (%)	98.13 ± 0.78	80.97 ± 0.64
$AUC_{0\text{-}6h\ in\ situ}$ (mg·h)	155.72 ± 4.68	96.37 ± 4.50

Data are shown as Mean ± SD, n=3.

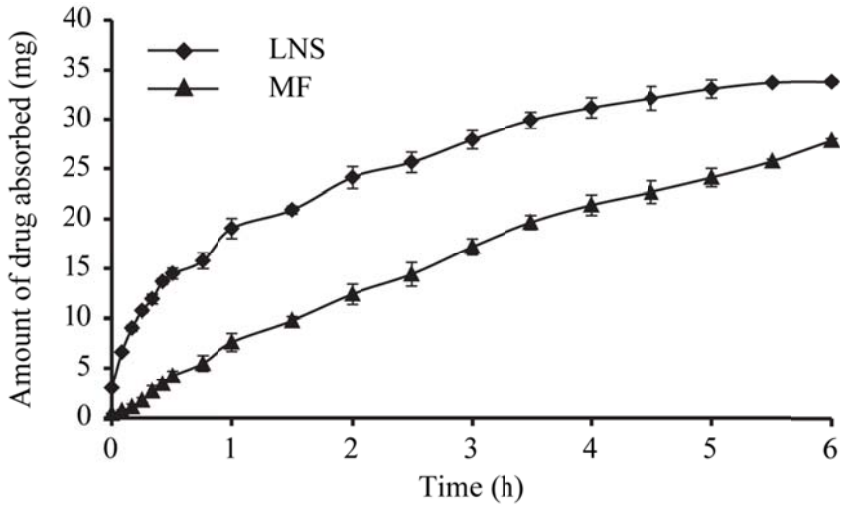

Figure 4.12. Amount of EFV absorbed from LNS (♦) and MF (▲) during *in situ* single pass intestinal perfusion studies showing higher absorption rate of EFV in NS compared to MF. Data are represented as Mean ± SD; n=3 for each group.

After incubation with the harvest blank perfusion solution for 6 h at 37°C, the EFV concentration was found to be 99.07 % ± 0.61 and 98.88 % ± 0.82 for LNS and MF, respectively, of the original concentration at 0 h. Results indicated that EFV was stable in blank intestinal perfusion solution.

4.7.6.2. *In vivo* pharmacokinetic study

Pharmacokinetic studies in rabbits were performed to investigate the improvement in oral bioavailability of EFV in LNS. Plasma drug concentration–time profiles and

pharmacokinetic parameters of standard EFV, MF and LNS resulted from the oral administration in rabbits are illustrated in Figure 4.13 and Table 4.18, respectively. Plasma drug concentration profile of LNS represented significant improvement in drug absorption compared with the MF. Area under the concentration–time curve (AUC_{0-t}) of EFV was 31589.00 ± 2448.55 ng·h/ml for LNS which was 2.19- and 3.77-fold higher as compared with that of MF (14408.93 ± 2538.73 ng·h/ml) and standard EFV (8379.59 ± 1476.33 ng·h/ml), respectively. Plasma peak concentration (C_{max}) of LNS was approximately 1.90-fold and 5.73-fold greater than that of MF and standard EFV, respectively. Time to reach maximum plasma concentration (t_{max}) of LNS, MF and standard EFV was found to be 2.5, 3.0 and 3.0 h, respectively. Mean residence time (MRT) of the LNS was decreased 1.05-fold and 1.23-fold compared to the MF and standard EFV, respectively.

The plasma clearance values of standard EFV, MF and LNS were found to be 2.06 ± 0.37, 1.29 ± 0.22 and 0.59 ± 0.05 $ml \cdot h^{-1}$, respectively. The volume of distribution of standard EFV, MF and LNS were found to be 48.03 ± 6.85, 23.34 ± 3.64 and 9.20 ± 0.78 L, respectively. LNS was absorbed easily which led to increased AUC_{0-t}, C_{max} and decreased t_{max}, MRT.

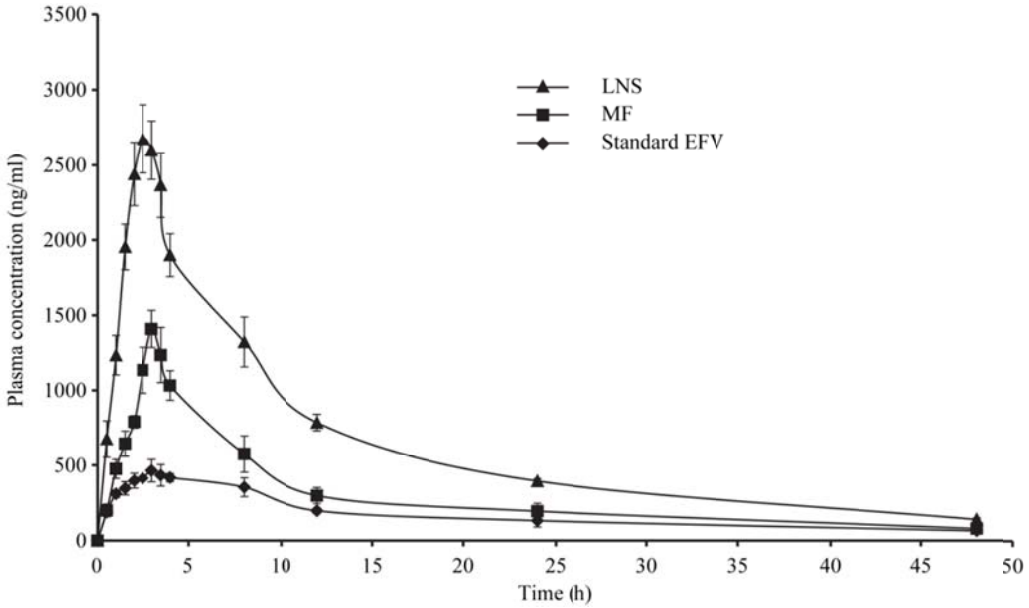

Figure 4.13. Plasma concentration-time curves for standard EFV (♦), MF (■) and LNS (▲) after oral administration in rabbits at a dose of 10 mg/kg of EFV showing higher

absorption rate and enhanced bioavailability of EFV in LNS.Data are represented as Mean ± SD; n=3 for each group.

These results indicated that the bioavailability of EFV in LNS was found to be better as compared to MF attributed to its greater dissolution rate, increased wettability and reduced particle size with increased surface area and reduced diffusion layer thickness.[76] This was in agreement with the in-vitro dissolution studies. In addition, nanoparticles could stay a longer time in the gastrointestinal tract due to the adhesive property.[92,93] The reduction of drug dose is not only favourable economically but also is desirable in decreasing its side effects especially when administered in multiple dosage regiments.

Table 4.18. Pharmacokinetic parameters after oral administration of standard EFV, MF and LNS in rabbits at a dose of 10 mg/kg of EFV

Pharmacokinetic parameters	standard EFV	MF	LNS
C_{max} (ng/ml)	466.92 ± 70.16	1409.1 ± 123.0*	2674.30 ± 226.0*,#
t_{max} (h)	3.00	3.00	2.50
k_a (h^{-1})	0.91 ± 0.055	0.44 ± 0.071*	0.74 ± 0.011*,#
k_{el} (h^{-1})	0.04 ± 0.0012	0.06 ± 0.0001*	0.06 ± 0.0006*
$t_{1/2}\alpha$ (h)	0.76 ± 0.046	1.60 ± 0.24*	0.94 ± 0.015*,#
$t_{1/2}\beta$ (h)	16.19 ± 0.47	12.02 ± 0.03*	10.93 ± 0.10*,#
V_d (L)	48.03 ± 6.85	23.34 ± 3.64*	9.20 ± 0.78*,#
V_{ss} (L)	37.96 ± 5.42	18.92 ± 2.90*	8.10 ± 0.74*,#
TCR (L/h)	2.06 ± 0.35	1.35 ± 0.21*	0.58 ± 0.04*,#
$AUC_{0\rightarrow t}$ (ng·h/ml)	8379.6 ± 1476.3	14408.9 ± 2538.7*	31589.0 ± 2448.6*,#
$AUC_{t\rightarrow\infty}$ (ng·h/ml)	1521.5 ± 253.51	1378.0 ± 152.9*	2204.8 ± 137.01*,#
$AUC_{0\rightarrow\infty}$ (ng·h/ml)	9901.1 ± 1729.8	15787.0 ± 2691.7*	33793.8 ± 2585.6*,#
$AUMC_{0\rightarrow t}$ (ng·h^2/ml)	131575.4 ± 27681.2	193481.24 ± 38776.73*	401887.4 ± 25630.9*,#
MRT (h)	15.64 ± 0.56	13.39 ± 0.34*	12.73 ± 0.18*
Cl (ml/h)	2.06 ± 0.37	1.29 ± 0.22*	0.59 ± 0.05*,#

Data are shown as mean ± SD, n=3. C_{max} - Plasma peak concentration; t_{max} - The time to reach maximum plasma concentration; k_a – Absorption rate constant; k_{el} - Elimination rate constant; $t_{1/2}\alpha$ - Distribution half-life; $t_{1/2}\beta$ - Elimination half-life; V_d - Volume of distribution; V_{ss} - Volume of distribution at steady state; TCR – Total clearance rate; AUC - Area under the plasma-concentration–time curve; $AUMC_{0\rightarrow t}$ - Total area under the first moment curve; MRT - Mean residence time; Cl - Total body clearance; *P<0.05 compared with standard EFV; #P<0.05 compared with marketed formulation.

4.8. Conclusion

The purpose of this study was to enhance the bioavailability by developing an oral administrable NS of the poorly water soluble drug, EFV. A media milling method using zirconium oxide beads was successfully employed to produce stable EFV NS. The results obtained in this study demonstrate that the particle size can be influenced by parameters, such as drug concentration, type and concentration of stabilizers. Efficient particle size reduction by nanogrinding was achieved by using excipients that provide proper wetting and physical stabilization (steric and electrostatic) of the practically water-insoluble drug, EFV. The combination of PVP K30–SLS stabilizer system was most suitable and optimized by the use of the Box-Behnken design to produce NSs with maximal particle size reduction. Lyophilization of the NSs with trehalose yielded nanopowders that were re-dispersed completely in the water. XRD and DSC data revealed that the crystalline state of EFV was not altered through operations, and shall be of great importance when considering long-term stability of EFV formulation. SEM images exhibited distinct differences in the morphological structure of nanoparticles influenced by the stabilizers. The NS was physically and chemically stable over 6 months. The PM of the drug and stabilizer did not significantly improve the dissolution of the drug suggests that the increased dissolution rate for the NS is primarily due to the reduction of the particle size. Significant enhancement in the saturation solubility of EFV in NS form was observed as compared to standard EFV. The *in vitro* transport study in PAMPA model demonstrated that NS was successful in enhancing the permeation of EFV. The results of *in situ* absorption of EFV in rat intestine suggested that NS played an important role in absorption enhancing effect. Pharmacokinetic evaluation clearly showed that the EFV NS exhibited improved pharmacokinetic properties compared to the MF. Oral bioavailability of EFV in rabbits resulted from NS was increased by 2.19-fold compared with the MF. The media milling method is easy to apply and needs only simple equipment and, thus, is a promising method for preparing drug NSs. Results of this study lead to the conclusion that NS approach is effective in preparing EFV formulations with enhanced dissolution velocity and oral bioavailability attributed to better wettability, increased saturation solubility and surface area, reduced particle size and decreased diffusion layer thickness. Moreover, NS may give added value by allowing a reduction in either the dose or its frequency of administration.

REFERENCES

1 Jia, L., Wong, H., Cerna, C. & Weitman, S. D. Effect of nanonization on absorption of 301029: ex vivo and in vivo pharmacokinetic correlations determined by liquid chromatography/mass spectrometry. *Pharmaceutical research* **19**, 1091-1096 (2002).

2 Liversidge, G. G. & Cundy, K. C. Particle-Size Reduction for Improvement of Oral Bioavailability of Hydrophobic Drugs .1. Absolute Oral Bioavailability of Nanocrystalline Danazol in Beagle Dogs. *Int J Pharm* **125**, 91-97 (1995).

3 Trotta, M., Gallarate, M., Pattarino, F. & Morel, S. Emulsions containing partially water-miscible solvents for the preparation of drug nanosuspensions. *J Control Release* **76**, 119-128 (2001).

4 Liversidge, G. G. & Conzentino, P. Drug Particle-Size Reduction for Decreasing Gastric Irritancy and Enhancing Absorption of Naproxen in Rats. *Int J Pharm* **125**, 309-313 (1995).

5 Niwa, T., Miura, S. & Danjo, K. Design of Dry Nanosuspension with Highly Spontaneous Dispersible Characteristics to Develop Solubilized Formulation for Poorly Water-Soluble Drugs. *Pharmaceutical research* **28**, 2339-2349, doi:DOI 10.1007/s11095-011-0465-y (2011).

6 Teeranachaideekul, V., Junyaprasert, V. B., Souto, E. B. & Muller, R. H. Development of ascorbyl palmitate nanocrystals applying the nanosuspension technology. *Int J Pharm* **354**, 227-234, doi:10.1016/j.ijpharm.2007.11.062 (2008).

7 Muller RH, J. C., Kayser O. *Nanosuspensions for the formulation of poorly soluble drugs. Pharmaceutical Emulsions and Suspensions.*, Vol. 105 (Marcel Dekker Inc, 2000).

8 Detroja, C., Chavhan, S. & Sawant, K. Enhanced antihypertensive activity of candesartan cilexetil nanosuspension: formulation, characterization and pharmacodynamic study. *Scientia pharmaceutica* **79**, 635-651, doi:10.3797/scipharm.1103-17 (2011).

9 Van Eerdenbrugh, B. *et al.* Microcrystalline cellulose, a useful alternative for sucrose as a matrix former during freeze-drying of drug nanosuspensions - A case study with itraconazole. *Eur J Pharm Biopharm* **70**, 590-596, doi:DOI 10.1016/j.ejpb.2008.06.007 (2008).

10 Singh, S. K. *et al.* Investigation of preparation parameters of nanosuspension by top-down media milling to improve the dissolution of poorly water-soluble glyburide. *Eur J Pharm Biopharm* **78**, 441-446, doi:DOI 10.1016/j.ejpb.2011.03.014 (2011).

11 Cerdeira, A. M., Mazzotti, M. & Gander, B. Miconazole nanosuspensions: Influence of formulation variables on particle size reduction and physical stability. *Int J Pharm* **396**, 210-218, doi:10.1016/j.ijpharm.2010.06.020 (2010).

12 Van Eerdenbrugh, B. *et al.* Drying of crystalline drug nanosuspensions-the importance of surface hydrophobicity on dissolution behavior upon

redispersion. *European journal of pharmaceutical sciences : official journal of the European Federation for Pharmaceutical Sciences* **35**, 127-135, doi:10.1016/j.ejps.2008.06.009 (2008).

13 Gao, L. *et al.* Studies on pharmacokinetics and tissue distribution of oridonin nanosuspensions. *Int J Pharm* **355**, 321-327, doi:10.1016/j.ijpharm.2007.12.016 (2008).

14 Kayser, O. A new approach for targeting to Cryptosporidium parvum using mucoadhesive nanosuspensions: research and applications. *Int J Pharm* **214**, 83-85 (2001).

15 Muller, R. H. & Peters, K. Nanosuspensions for the formulation of poorly soluble drugs - I. Preparation by a size-reduction technique. *Int J Pharm* **160**, 229-237 (1998).

16 Hanafy, A. *et al.* Pharmacokinetic evaluation of oral fenofibrate nanosuspensions and SLN in comparison to conventional suspensions of micronized drug. *Adv Drug Deliver Rev* **59**, 419-426, doi:DOI 10.1016/j.addr.2007.04.005 (2007).

17 Box GEP, B. D. Some new three level designs for the study of quantitative variables. *Technometrics* **2**, 455-475 (1960).

18 Bhavsar, M. D., Tiwari, S. B. & Amiji, M. M. Formulation optimization for the nanoparticles-in-microsphere hybrid oral delivery system using factorial design. *J Control Release* **110**, 422-430, doi:DOI 10.1016/j.jconrel.2005.11.001 (2006).

19 Ragonese, R., Macka, M., Hughes, J. & Petocz, P. The use of the Box-Behnken experimental design in the optimisation and robustness testing of a capillary electrophoresis method for the analysis of ethambutol hydrochloride in a pharmaceutical formulation. *Journal of pharmaceutical and biomedical analysis* **27**, 995-1007 (2002).

20 Massart D.L., V. B. G. M., Buydens L.M.C., De Jong S., Lewi P.J., Smeyers-Verbeke J. in *Data Handling in Science and Technology 20A: Handbook of Chemometrics and Qualimetrics. Part A* (Elsevier, 2001).

21 Montgomery, D. C. *Design and Analysis of Experiments*. Third edn, (Wiley, 1991).

22 Kincl, M., Turk, S. & Vrecer, F. Application of experimental design methodology in development and optimization of drug release method. *Int J Pharm* **291**, 39-49, doi:10.1016/j.ijpharm.2004.07.041 (2005).

23 Moschwitzer, J. & Muller, R. H. Spray coated pellets as carrier system for mucoadhesive drug nanocrystals. *Eur J Pharm Biopharm* **62**, 282-287, doi:DOI 10.1016/j.ejpb.2005.09.005 (2006).

24 Wang, Y. *et al.* Development and in vitro evaluation of deacety mycoepoxydiene nanosuspension. *Colloids and surfaces. B, Biointerfaces* **83**, 189-197, doi:10.1016/j.colsurfb.2010.10.029 (2011).

25 *http://www.usp.org/pdf/EN/pendingStandards/m4047.pdf*.

26 Zhang, Y. *et al.* DDSolver: an add-in program for modeling and comparison of drug dissolution profiles. *Aaps J* **12**, 263-271, doi:10.1208/s12248-010-9185-1 (2010).

27 Hiremath, P. S., Soppimath, K. S. & Betageri, G. V. Proliposomes of exemestane for improved oral delivery: Formulation and in vitro evaluation using PAMPA, Caco-2 and rat intestine. *Int J Pharm* **380**, 96-104, doi:DOI 10.1016/j.ijpharm.2009.07.008 (2009).

28 Singh, S. P., Wahajuddin, Tewari, D., Pradhan, T. & Jain, G. K. PAMPA permeability, plasma protein binding, blood partition, pharmacokinetics and metabolism of formononetin, a methoxylated isoflavone. *Food Chem Toxicol* **49**, 1056-1062, doi:DOI 10.1016/j.fct.2011.01.012 (2011).

29 *http://www.bdbiosciences.com/external_files/dl/doc/manuals/live/web-enabled/353015_pug.pdf*.

30 Stewart, W. W. Functional Connections between Cells as Revealed by Dye-Coupling with a Highly Fluorescent Naphthalimide Tracer. *Cell* **14**, 741-759 (1978).

31 Liu, H. L. *et al.* In vitro permeability of poorly aqueous soluble compounds using different solubilizers in the PAMPA assay with liquid chromatography/mass spectrometry detection. *Pharmaceutical research* **20**, 1820-1826 (2003).

32 Cirri, M., Mura, P. & Mora, P. C. Liquid spray formulations of xibornol by using self-microemulsifying drug delivery systems. *Int J Pharm* **340**, 84-91, doi:DOI 10.1016/j.ijpharm.2007.03.021 (2007).

33 Zhou, P., Li, L. P., Luo, S. Q., Jiang, H. D. & Zeng, S. Intestinal absorption of luteolin from peanut hull extract is more efficient than that from individual pure luteolin. *Journal of agricultural and food chemistry* **56**, 296-300, doi:10.1021/jf072612+ (2008).

34 Song, N. N., Li, Q. S. & Liu, C. X. Intestinal permeability of metformin using single-pass intestinal perfusion in rats. *World J Gastroentero* **12**, 4064-4070 (2006).

35 Zakeri-Milani, P. *et al.* Predicting human intestinal permeability using single-pass intestinal perfusion in rat. *J Pharm Pharm Sci* **10**, 368-379 (2007).

36 Stewart, B. H., Chan, O. H., Jezyk, N. & Fleisher, D. Discrimination between drug candidates using models for evaluation of intestinal absorption. *Adv Drug Deliver Rev* **23**, 27-45 (1997).

37 Cui, J. *et al.* Enhancement of oral absorption of curcumin by self-microemulsifying drug delivery systems. *Int J Pharm* **371**, 148-155, doi:DOI 10.1016/j.ijpharm.2008.12.009 (2009).

38 Li, H. L. *et al.* Enhancement of gastrointestinal absorption of quercetin by solid lipid nanoparticles. *J Control Release* **133**, 238-244, doi:DOI 10.1016/j.jconrel.2008.10.002 (2009).

39 Gao, Y. *et al.* Formulation optimization and in situ absorption in rat intestinal tract of quercetin-loaded microemulsion. *Colloid Surface B* **71**, 306-314, doi:DOI 10.1016/j.colsurfb.2009.03.005 (2009).

40 Chen, Y. *et al.* Self-microemulsifying drug delivery system (SMEDDS) of vinpocetine: Formulation development and in vivo assessment. *Biol Pharm Bull* **31**, 118-125 (2008).

41 Shin, S. C., Bum, J. P. & Choi, J. S. Enhanced bioavailability by buccal administration of triamcinolone acetonide from the bioadhesive gels in rabbits. *Int J Pharm* **209**, 37-43 (2000).

42 Muller, R. H., Jacobs, C. & Kayser, O. Nanosuspensions as particulate drug formulations in therapy. Rationale for development and what we can expect for the future. *Adv Drug Deliv Rev* **47**, 3-19 (2001).

43 Kesisoglou, F., Panmai, S. & Wu, Y. H. Nanosizing - Oral formulation development and biopharmaceutical evaluation. *Adv Drug Deliver Rev* **59**, 631-644, doi:DOI 10.1016/j.addr.2007.05.003 (2007).

44 Ain-Ai, A. & Gupta, P. K. Effect of arginine hydrochloride and hydroxypropyl cellulose as stabilizers on the physical stability of high drug loading nanosuspensions of a poorly Soluble compound. *Int J Pharm* **351**, 282-288, doi:DOI 10.1016/j.ijpharm.2007.09.029 (2008).

45 Lee, J. Drug nano- and microparticles processed into solid dosage forms: Physical properties. *J Pharm Sci* **92**, 2057-2068, doi:Doi 10.1002/Jps.10471 (2003).

46 Ghosh, I., Bose, S., Vippagunta, R. & Harmon, F. Nanosuspension for improving the bioavailability of a poorly soluble drug and screening of stabilizing agents to inhibit crystal growth. *Int J Pharm* **409**, 260-268, doi:10.1016/j.ijpharm.2011.02.051 (2011).

47 Ploehn H.J. , R. W. B. Interactions Between Colloidal Particles and Soluble Polymers. *Advances in Chemical Engineering* **15**, 137-228 doi:10.1016/S0065-2377(08)60194-5 (1990, Pages).

48 Muller, R. H. & Jacobs, C. Buparvaquone mucoadhesive nanosuspension: preparation, optimisation and long-term stability. *Int J Pharm* **237**, 151-161 (2002).

49 Xia, D. *et al.* Preparation of stable nitrendipine nanosuspensions using the precipitation-ultrasonication method for enhancement of dissolution and oral bioavailability. *European journal of pharmaceutical sciences : official journal of the European Federation for Pharmaceutical Sciences* **40**, 325-334, doi:10.1016/j.ejps.2010.04.006 (2010).

50 Muller, R. H. & Keck, C. M. Challenges and solutions for the delivery of biotech drugs--a review of drug nanocrystal technology and lipid nanoparticles. *Journal of biotechnology* **113**, 151-170, doi:10.1016/j.jbiotec.2004.06.007 (2004).

51 Ali, H. S., York, P. & Blagden, N. Preparation of hydrocortisone nanosuspension through a bottom-up nanoprecipitation technique using microfluidic reactors. *Int J Pharm* **375**, 107-113, doi:10.1016/j.ijpharm.2009.03.029 (2009).

52 Patravale, V. B., Date, A. A. & Kulkarni, R. M. Nanosuspensions: a promising drug delivery strategy. *The Journal of pharmacy and pharmacology* **56**, 827-840, doi:10.1211/0022357023691 (2004).

53 Merisko-Liversidge, E., Liversidge, G. G. & Cooper, E. R. Nanosizing: a formulation approach for poorly-water-soluble compounds. *European Journal of Pharmaceutical Sciences* **18**, 113-120, doi:Doi 10.1016/S0928-0987(02)00251-8 (2003).

54 Rabinow, B. E. Nanosuspensions in drug delivery. *Nature reviews. Drug discovery* **3**, 785-796, doi:10.1038/nrd1494 (2004).

55 Pongpeerapat, A. *et al.* Formation and stability of drug nanoparticles obtained from drug/PVP/SDS ternary ground mixture. *J Drug Deliv Sci Tec* **14**, 441-447 (2004).

56 Palla, B. J. & Shah, D. O. Stabilization of high ionic strength slurries using surfactant mixtures: Molecular factors that determine optimal stability. *J Colloid Interf Sci* **256**, 143-152, doi:DOI 10.1006/jcis.2002.8648 (2002).

57 Singh, S. K., Dodge, J., Durrani, M. J. & Khan, M. A. Optimization and Characterization of Controlled-Release Pellets Coated with an Experimental Latex .1. Anionic Drug. *Int J Pharm* **125**, 243-255 (1995).

58 Karnachi, A. A. & Khan, M. A. Box-Behnken design for the optimization of formulation variables of indomethacin coprecipitates with polymer mixtures. *Int J Pharm* **131**, 9-17 (1996).

59 Evertsson, H. & Nilsson, S. Microviscosity in clusters of ethyl hydroxyethyl cellulose and sodium dodecyl sulfate formed in dilute aqueous solutions as determined with fluorescence probe techniques. *Macromolecules* **30**, 2377-2385 (1997).

60 Berglund, K. D., Przybycien, T. M. & Tilton, R. D. Coadsorption of sodium dodecyl sulfate with hydrophobically modified nonionic cellulose polymers. 1. Role of polymer hydrophobic modification. *Langmuir* **19**, 2705-2713, doi:Doi 10.1021/La026429g (2003).

61 Lee, J., Choi, J. Y. & Park, C. H. Characteristics of polymers enabling nano-comminution of water-insoluble drugs. *Int J Pharm* **355**, 328-336, doi:DOI 10.1016/j.ijpharm.2007.12.032 (2008).

62 Van Eerdenbrugh, B. *et al.* A screening study of surface stabilization during the production of drug nanocrystals. *J Pharm Sci* **98**, 2091-2103, doi:10.1002/jps.21563 (2009).

63 Singare, D. S. *et al.* Optimization of formulation and process variable of nanosuspension: An industrial perspective. *Int J Pharm* **402**, 213-220, doi:10.1016/j.ijpharm.2010.09.041 (2010).

64 Tanaka, Y. *et al.* Nanoparticulation of Poorly Water Soluble Drugs Using a Wet-Mill Process and Physicochemical Properties of the Nanopowders. *Chem Pharm Bull* **57**, 1050-1057 (2009).

65 Kawabata, Y., Yamamoto, K., Debari, K., Onoue, S. & Yamada, S. Novel crystalline solid dispersion of tranilast with high photostability and improved oral bioavailability. *European journal of pharmaceutical sciences : official*

journal of the European Federation for Pharmaceutical Sciences **39**, 256-262, doi:10.1016/j.ejps.2009.12.009 (2010).

66 Gulsun, T., Gursoy, R. N. & Oner, L. Design and characterization of nanocrystal formulations containing ezetimibe. *Chem Pharm Bull (Tokyo)* **59**, 41-45 (2011).

67 Jacobs, C., Kayser, O. & Muller, R. H. Production and characterisation of mucoadhesive nanosuspensions for the formulation of bupravaquone. *Int J Pharm* **214**, 3-7 (2001).

68 Zingel, C., Sachse, A., Rossling, G. L. & Muller, R. H. Lyophilization and rehydration of iopromide-carrying liposomes. *Int J Pharm* **140**, 13-24 (1996).

69 Peters, K. *et al.* Preparation of a clofazimine nanosuspension for intravenous use and evaluation of its therapeutic efficacy in murine Mycobacterium avium infection. *J Antimicrob Chemoth* **45**, 77-83 (2000).

70 Jackson, C. L. & Mckenna, G. B. The Melting Behavior of Organic Materials Confined in Porous Solids. *J Chem Phys* **93**, 9002-9011 (1990).

71 Dodiya, S. S., Chavhan, S. S., Sawant, K. K. & Korde, A. G. Solid lipid nanoparticles and nanosuspension formulation of Saquinavir: preparation, characterization, pharmacokinetics and biodistribution studies. *J Microencapsul* **28**, 515-527, doi:Doi 10.3109/02652048.2011.590612 (2011).

72 Sun, W., Mao, S. R., Shi, Y., Li, L. C. & Fang, L. Nanonization of Itraconazole by High Pressure Homogenization: Stabilizer Optimization and Effect of Particle Size on Oral Absorption. *J Pharm Sci* **100**, 3365-3373, doi:Doi 10.1002/Jps.22587 (2011).

73 Van Eerdenbrugh, B. *et al.* Characterization of physico-chemical properties and pharmaceutical performance of sucrose co-freeze-dried solid nanoparticulate powders of the anti-HIV agent loviride prepared by media milling. *Int J Pharm* **338**, 198-206, doi:10.1016/j.ijpharm.2007.02.005 (2007).

74 Pardeike, J. *et al.* Nanosuspensions as advanced printing ink for accurate dosing of poorly soluble drugs in personalized medicines. *Int J Pharm* **420**, 93-100, doi:DOI 10.1016/j.ijpharm.2011.08.033 (2011).

75 Kocbek, P., Baumgartner, S. & Kristl, J. Preparation and evaluation of nanosuspensions for enhancing the dissolution of poorly soluble drugs. *Int J Pharm* **312**, 179-186, doi:10.1016/j.ijpharm.2006.01.008 (2006).

76 Hintz, R. J. & Johnson, K. C. The Effect of Particle-Size Distribution on Dissolution Rate and Oral Absorption. *Int J Pharm* **51**, 9-17 (1989).

77 Khan, K. A. The concept of dissolution efficiency. *The Journal of pharmacy and pharmacology* **27**, 48-49 (1975).

78 Khan, K. A. & Rhodes, C. T. Effect of compaction pressure on the dissolution efficiency of some direct compression systems. *Pharmaceutica acta Helvetiae* **47**, 594-607 (1972).

79 Barzegar-Jalali, M. *et al.* Enhancement of dissolution rate and anti-inflammatory effects of piroxicam using solvent deposition technique. *Drug development and industrial pharmacy* **28**, 681-686 (2002).

80 Mosharraf, M. & Nystrom, C. The Effect of Particle-Size and Shape on the Surface Specific Dissolution Rate of Microsized Practically Insoluble Drugs. *Int J Pharm* **122**, 35-47 (1995).

81 Anderberg, E. K., Bisrat, M. & Nystrom, C. Physicochemical Aspects of Drug Release .7. The Effect of Surfactant Concentration and Drug Particle-Size on Solubility and Dissolution Rate of Felodipine, a Sparingly Soluble Drug. *Int J Pharm* **47**, 67-77 (1988).

82 Bisrat, M. & Nystrom, C. Physicochemical Aspects of Drug Release .8. The Relation between Particle-Size and Surface Specific Dissolution Rate in Agitated Suspensions. *Int J Pharm* **47**, 223-231 (1988).

83 Dressman, J. B., Amidon, G. L., Reppas, C. & Shah, V. P. Dissolution testing as a prognostic tool for oral drug absorption: Immediate release dosage forms. *Pharmaceutical research* **15**, 11-22 (1998).

84 Horter, D. & Dressman, J. B. Influence of physicochemical properties on dissolution of drugs in the gastrointestinal tract. *Adv Drug Deliver Rev* **46**, 75-87 (2001).

85 Costa, P., Manuel, J. & Lobo, S. Modeling and comparison of dissolution profiles. *European Journal of Pharmaceutical Sciences* **13**, 123-133 (2001).

86 Breier, A. R., Paim, C. S., Steppe, M. & Schapoval, E. E. S. Development and validation of dissolution tests for fexofenadine hydrochloride capsules and coated tablets. *J Pharm Pharm Sci* **8**, 289-298 (2005).

87 Avdeef, A. *et al.* Drug absorption in vitro model: filter-immobilized artificial membranes. 2. Studies of the permeability properties of lactones in Piper methysticum Forst. *European journal of pharmaceutical sciences : official journal of the European Federation for Pharmaceutical Sciences* **14**, 271-280 (2001).

88 Kansy, M., Senner, F. & Gubernator, K. Physicochemical high throughput screening: Parallel artificial membrane permeation assay in the description of passive absorption processes. *J Med Chem* **41**, 1007-1010 (1998).

89 Wohnsland, F. & Faller, B. High-throughput permeability pH profile and high-throughput alkane/water log P with artificial membranes. *J Med Chem* **44**, 923-930 (2001).

90 Sharma, P., Varma, M. V., Chawla, H. P. & Panchagnula, R. In situ and in vivo efficacy of peroral absorption enhancers in rats and correlation to in vitro mechanistic studies. *Farmaco* **60**, 874-883, doi:10.1016/j.farmac.2005.08.007 (2005).

91 Legen, I., Kracun, M., Salobir, M. & Kerc, J. The evaluation of some pharmaceutically acceptable excipients as permeation enhancers for amoxicillin. *Int J Pharm* **308**, 84-89, doi:DOI 10.1016/j.ijpharm.2005.10.036 (2006).

92 Jinno, J. *et al.* Effect of particle size reduction on dissolution and oral absorption of a poorly water-soluble drug, cilostazol, in beagle dogs. *J Control Release* **111**, 56-64, doi:DOI 10.1016/j.jconrel.2005.11.013 (2006).

93 Shegokar, R. & Muller, R. H. Nanocrystals: Industrially feasible multifunctional formulation technology for poorly soluble actives. *Int J Pharm* **399**, 129-139, doi:DOI 10.1016/j.ijpharm.2010.07.044 (2010).

CHAPTER 5:

DEVELOPMENT OF EFAVIRENZ SMEDDS

5.1. Introduction

Most of the new drug candidates in development today are sparingly soluble and associated with poor bioavailability.[1] In recent years, much attention has been focused on lipid-microemulsion formulations with particular emphasis on self-microemulsifying or self-emulsifying drug delivery systems (SMEDDS and SEDDS) to improve oral bioavailability of poorly water-soluble drugs.[2,3] SEDDS and SMEDDS are isotropic mixtures of oil, surfactants, and cosurfactants that form fine oil-in-water emulsions (i.e., SEDDS) or microemulsions (i.e., SMEDDS) when introduced into an aqueous phase under gentle agitation.[4] Researchers have explored different novel approaches such as micronization, complexation with cyclodextrin[5,6], solid dispersions[7], nanosuspensions[8], liposomes[9] and polymeric nanoparticles [10,11] with the objective to improve the bioavailability of poorly water soluble drug. Majority of these approaches have resulted in limited success because of the need for specialized equipments, complicated manufacturing process, longer processing time, high cost in manufacturing and regulatory complexity. Although these approaches have shown some success to improve bioavailability, since last decade, microemulsions have gained a great interest as a commercially feasible novel lipid-based delivery system.[12]

At present, there are four drug products, Sandimmune® and Sandimmun Neoral® (cyclosporin A), Norvir® (ritonavir), and Fortovase® (saquinavir) on the pharmaceutical market, the active compounds of which have been formulated into specific self-emulsifying formulations, triggers much more attention on SMEDDS.[13] The various attractive advantages of SMEDDS such as nanosize (<100 nm), ease of scale-up and manufacturing, long shelf life, ability to improve dissolution rate and lymphatic transport of hydrophobic drugs give them an edge over other novel delivery systems such as liposomes, dendrimers and polymeric nanoparticles.[12] Studies of lipid based system reveals that spontaneous formation of microemulsion advantageously presents the drug in a dissolved form, and the resultant small droplet size provides a large interfacial surface area for drug release and absorption. Moreover, the oil used promotes the intestinal lymphatic transport of drugs.[4] SMEDDS formulations are normally prepared as liquids and dispensed in form of soft or hard gelatin capsule filled which give rise to some drawbacks such as interaction of the fill with the

capsule shell, risks of leakage when they are filled into hard gelatin capsules, limited shelf-life.[14,15] In recent years, there is a growing trend to formulate solid SMEDDS (S-SMEDDS) by adsorbing liquid SMEDDS (L-SMEDDS) onto suitable solid carriers.[16] Such S-SMEDDS can be easily filled in capsules and overcome the disadvantages of liquid formulations described above and on oral administration, they readily form microemulsion *in vivo*; presenting the drug in nano-sized and 'ready to absorb' form.[12] There are a limited number of publications reporting the oral bioavailability of solid SEDDS or SMEDDS.[12,14,17-20]

The objectives of our present study were to prepare and characterize S-SMEDDS formulation of efavirenz (EFV), and the physicochemical characteristics were evaluated *in vitro*, *in situ* and *in vivo*. Molecular structure of EFV is [(S)-6-chloro-4-(cyclopropylethynyl)-1,4-dihydro-4-(trifluoromethyl)-2H-3,1-benzoxazin-2-one].

According to the biopharmaceutical classification system guidance by Food and Drug Administration (FDA), EFV comes under a class II category drug, means it has low solubility and high intestinal permeability [21,22]. It is a crystalline lipophilic solid with an aqueous solubility of 3-9 μg/ml and with a low intrinsic dissolution rate of 0.037 mg/cm^2/min. Hence, it has very low bioavailability [23]. To achieve effective therapy against viral diseases for orally administered drugs, it is essential that the drug should be adequately and consistently absorbed. Frequent administration of EFV in relatively high doses, because of its low solubility hindering its absorption and biodistribution, is a main cause of patient incompliance.[24] Thus, there is a need of some innovative formulation approach to enhance the oral bioavailability. However, this problem can be overcome by increasing the solubility of the drug.

Formulation of L-SMEDDS requires a careful selection of oil, surfactant and cosurfactant. Selection of excipient was optimized using solubility, phase diagram and self-emulsification property. The application of a mixture experimental design has been demonstrated to be an efficient and satisfactory method for optimization of the formulation and to acquire the necessary information to understand the relationship between independent variables and dependent variables in a formulation.[25] Experimental mixture design using Design-Expert® software was applied to optimize L-SMEDDS that contain a minimum amount of surfactant, a maximum amount of lipid, and possess minimum droplet size and maximum % transmittance (% T). The

optimized L-SMEDDS formulation was converted into free flowing powder by adsorbing onto Aerosil 200 used as a solid carrier. Optimized SMEDDS formulation was characterized for various physicochemical parameters (like droplets size and size distribution, zeta potential (ZP), dilution studies, thermodynamic stability studies, morphology and stability studies). The morphology of S-SMEDDS and droplet size/distribution of EFV microemulsion were observed by scanning electron microscope (SEM) and transmittance electron microscope (TEM), respectively. Solid state characterization of S-SMEDDS performed by differential scanning calorimetry (DSC) and X-ray diffraction (XRD). The release profile of L- and S-SMEDDS from capsules were evaluated using paddle dissolution apparatus in water containing 1.0% w/v sodium lauryl sulfate (SLS) and compared the release of EFV from a MF. *In situ* absorption property in rat intestine and *in vivo* oral absorption in rabbit was performed with L- and S-SMEDDS and compared with a marketed formulation (MF) of EFV. S-SMEDDS show good potential to improve oral bioavailability for the delivery of EFV.

5.2. Materials and instruments

EFV was kindly gifted by Merck Ltd. (Mumbai, India). Capsules (Efavir 200, Cipla Ltd.) were purchased from local pharmacy. Excipients used for formulation development are shown in Table 5.1 and were used as received. Chemicals and reagents used for the preparation of buffers, analytical solutions, and other general experimental purposes are shown in Table 5.2. Equipments used at various stages are listed in Table 5.3. Purified HPLC grade water was obtained by filtering double distilled water through nylon filter paper 0.45 μm pore size and 47 mm diameter (Pall Life sciences, Mumbai, India).

Table 5.1. List of excipients

Excipients	**Manufacturer/Supplier**
Capmul MCM	Abitech Corporation, USA
Capmul MCM C8	Abitech Corporation, USA
Captex 200	Abitech Corporation, USA
Captex 200 P	Abitech Corporation, USA
Captex 355	Abitech Corporation, USA
Captex 500	Abitech Corporation, USA
Capryol 90	Gattefosse, France
Ethyl oleate	S.D. Fine Chemicals, Mumbai, India
Labrafac PG	Gattefosse, France
Labrafaclipophil WL 1349	Gattefosse, France
Labrafil M 2125 CS	Gattefosse, France
Oleic acid	Sigma Aldrich, India
Sesame oil	S.D. Fine Chemicals, Mumbai, India
Arachis oil	S.D. Fine Chemicals, Mumbai, India
olive oil	S.D. Fine Chemicals, Mumbai, India
castor oil	S.D. Fine Chemicals, Mumbai, India
Acconon MC8-2	Abitech Corporation, USA
Acconon CC 6	Abitech Corporation, USA
Tween 20	S.D. Fine Chemicals, Mumbai, India
Tween 80	S.D. Fine Chemicals, Mumbai, India
Cremophor EL	Sigma Aldrich, India
Cremophor RH 40	Sigma Aldrich, India
Lauroglycol 90	Gattefosse, France
PEG 200	S.D. Fine Chemicals, Mumbai, India
PEG 400	S.D. Fine Chemicals, Mumbai, India
Transcutol HP	Gattefosse, France

Table 5.2. List of chemicals and reagents

Chemicals/Reagents	**Manufacturer/Supplier**
Acetonitrile, HPLC grade	Spectrochem Labs Ltd, Vadodara, India
Ammonium acetate buffer, AR grade	S.D. Fine Chemicals, Mumbai, India
Disodium hydrogen phosphate, AR grade	S.D. Fine Chemicals, Mumbai, India
Glacial Acetic acid, HPLC grade	Spectrochem Labs Ltd, Vadodara, India
Glucose, AR grade	S.D. Fine Chemicals, Mumbai, India
Hydrochloric acid, AR grade	Spectrochem Labs Ltd, Vadodara, India
Lucifer Yellow	Sigma Aldrich, India
Magnesium chloride, AR grade	S.D. Fine Chemicals, Mumbai, India
Methanol, HPLC grade	Spectrochem Labs Ltd, Vadodara, India
Orthophosphoric acid, HPLC grade	Spectrochem Labs Ltd, Vadodara, India
Potassium chloride, AR grade	S.D. Fine Chemicals, Mumbai, India
Potassium dihydrogen phosphate, AR grade	S.D. Fine Chemicals, Mumbai, India
Sodium acetate, AR grade	Spectrochem Labs Ltd, Vadodara, India
Sodium bicarbonate, AR grade	S.D. Fine Chemicals, Mumbai, India
Sodium chloride, AR grade	S.D. Fine Chemicals, Mumbai, India
Sodium dihydrogen phosphate, AR grade	S.D. Fine Chemicals, Mumbai, India
Sodium hydroxide, AR grade	Spectrochem Labs Ltd, Vadodara, India
Tert- butyl methyl ether, HPLC grade	Spectrochem Labs Ltd, Vadodara, India

Table 5.3. List of instruments

Equipment	Manufacturer/Supplier
Bath sonicator	B. N. Scientific Enterprise, India
Centrifuge	Remi Instrument
Column oven	PCI Analytics, India
Differential scanning calorimeter (DSC 60)	Shimadzu, Japan
Dissolution apparatus	Veevo, India
High performance liquid chromatography	Shimadzu, Japan
Magnetic stirrer	Remi equipments Pvt Ltd., India
Particle size analyzer (Malvern Zetasizer Nano ZS)	Malvern Instrument, UK
Peristaltic pump	Electrolab, Mumbai, India
pH meter	LabIndia, India
Scanning electron microscopy	JSM 6380 LV, JEOL, Japan
Transmission electron microscopy	Tecnai 20 Philips
UV-visible spectrophotometer (UV-1700)	Shimadzu, Japan
Ventilator	Ugo-Basile, Germany
Vortex mixer	Spinix, Japan
Weighing Balance	Shimadzu, Japan
X-ray diffractometer	Bruker AXS D8, Germany

5.3. Development of EFV L-SMEDDS

SMEDDS is isotropic mixtures of an oil, surfactant, cosurfactant and drug. The basic principle of this system is its ability to form fine oil-in-water (o/w) microemulsions under gentle agitation following dilution by aqueous phases. Depending on solubility of drug, oil, surfactant and cosurfactant were selected.

The oil represents one of the most important excipients in the SMEDDS formulation not only because it can solubilize marked amounts of the lipophilic drug or facilitate self-emulsification but also and mainly because it can increase the fraction of lipophilic drug transported via the intestinal lymphatic system, thereby increasing absorption from the GI tract depending on the molecular nature of the triglyceride.

Several compounds exhibiting surfactant properties may be employed for the design of self-emulsifying systems, the most widely recommended ones being the non-ionic surfactants with a relatively high hydrophilic−lipophilic balance (HLB).

5.3.1. Screening of excipients

5.3.1.1. Solubility study

To find out appropriate oils and surfactants as compositions of SMEDDS, the solubility of drug in various oils and surfactants was determined. An excess amount of drug was added to 1 ml of oil or surfactant. The resultant mixtures were shaken at 37°C for 72 h, followed by centrifugation at 8000 rpm for 10 min. The supernatant was diluted with methanol; the drug concentration was quantified by HPLC.

5.3.1.2. Pseudoternary phase diagram

The first step towards the formulation development was to determine the feasibility of the microemulsion formation. The boundaries of the microemulsion domains were determined by plotting pseudoternary phase diagrams for the components short listed from solubility studies. The pseudoternary phase diagram of oil, surfactant − cosurfactant mixture and doubled distilled water was plotted using water titration method.[4] Pseudoternary phase diagrams were constructed in order to obtain the concentration range of components for the existing region of microemulsions. The weight ratio of surfactant to cosurfactant was varied as 1:1, 2:1 and 3:1. For each pseudoternary phase diagram at a specific surfactant/cosurfactant weight ratio, the mixtures of oil, surfactant and cosurfactant were prepared with the weight ratio of oil to the mixture of surfactant and cosurfactant at 10:0, 9:1, 8:2, 7:3, 6:4, 5:5, 4:6, 3:7, 2:8, and 1:9,respectively. To the resultant mixtures, water was added drop wise till the first sign of turbidity in order to identify the end point and after equilibrium; if the system became clear then the water addition was continued. The concentrations of the components were recorded in order to complete the pseudoternary phase diagrams, and then the contents of oil, surfactant, cosurfactant and water an appropriate weight

ratios were selected based on these results. In order to prepare SMEDDS, selection of microemulsion region from phase diagram was based on the fact that solution remains clear even on infinite dilution.

5.3.1.3. Self-emulsification and dispersilbility test

Ternary mixtures with varying compositions of oil, surfactant and cosurfactant were prepared. For any mixture, the total percent of oil, surfactant and cosurfactant concentrations was always kept at 100%. Ternary phase diagrams of oil, surfactant and cosurfactant were plotted: each of them representing an apex of the triangle. The mixture was introduced into 250 ml of water in a glass beaker at 37°C and the contents were mixed gently with a magnetic stir bar. After being equilibrated, the efficiency of self-emulsification, dispersibility, and appearance was observed visually according to the grading systems shown in Table 5.4.[26,27] Grade A region was SMEDDS region that formed clear microemulsions after infinite dilution. Phase diagrams were constructed identifying the good self-emulsifying region. All studies were repeated thrice, with similar observations being made between repeats.

Table 5.4. Classification of the SMEDDS formulation in accordance to comparative grades

Grade	Dispersibility and appearance
A	Rapid forming emulsion, which is clear and transparent in appearance
B	Rapid forming, slight less clear emulsion, which has a bluish white appearance
C	Bright white emulsion or grayish white emulsion with a slight oily appearance that is slow to emulsify
D	Exhibit poor or minimal emulsification with large oils droplets present on the surface

5.3.2. Optimization of EFV loaded L-SMEDDS by factorial design

In SMEDDS, amount of oil, surfactant and cosurfactant depends on each other. If percentage of one component is increased, then percentage of one or more of the other components must be decreased. The total concentration of the three components summed to 100%. Based on this information, mixture experimental design was generated by Design-Expert® 8.0 software for three component system to conduct the study. SMEDDS components were selected based on the results of phase diagram and self-emulsification test. A total of 25 experiments were designed by the software with 6 vertices, 6 centres of edges, 6 axial check blends, 6 interior check blends and 1 overall centroid points. Dependent variables were mean droplet size (MDS) (Y_1) and % T (Y_2). After generating the polynomial equations relating the dependent and independent variables, the process was optimized for the responses Y_1 and Y_2 values. Optimization was performed to obtain the levels of independent variables, which minimize Y_1 while maximizing Y_2.

5.3.3. Preparation of L-SMEDDS

After careful evaluation, captex 500 as oil, tween 20 as surfactant and transcutol HP as cosurfactant were selected as a SME mixture for drug delivery. L-SMEDDS formulation was prepared by dissolving 50 mg of EFV in the optimized SME mixture consisting of captex 500 (25%w/w), tween 20 (50%w/w) and transcutol HP (25%w/w). Briefly, oil, surfactant, and cosurfactant were accurately weighed into glass vials according to their ratios. Then, the components were mixed by gentle stirring and vortex mixing at 37°C until EFV was completely dissolved. The mixture was observed for any signs of turbidity or phase separation for a period of 48 hours.

5.3.4. Preparation of S-SMEDDS

For the preparation of S-SMEDDS, L-SMEDDS (equivalent to 50 mg of EFV) was mixed with various solid carriers namely dibasic calcium phosphate, anhydrous lactose, microcrystalline cellulose, calcium carbonate, magnesium carbonate, Aerosil 200 and aluminium magnesium silicate, in various ratios (2:1, 1:1, 1:2 and 1:4).

Briefly the, L-SMEDDS was added drop wise over the solid adsorbent contained in a broad bottom beaker. After each addition, the mixture was homogenized using glass rod to ensure uniform distribution of the droplet.[12] The adsorbent that was required in a small amount to give a free flowing S-SMEDDS was chosen for the further studies.

5.4. Characterization of EFV loaded SMEDDS formulations

5.4.1. Droplet size measurement

The droplet size and polydispersity Index (PDI) of L-SMEDDS and S-SMEDDS, 100 times diluted with double distilled water, were determined using a Malvern Zeta Sizer Nano ZS 90 (Malvern Instruments, Malvern, UK). The PDI indicates the width of a particle distribution (e.g. 0.0 for a narrow, 0.5 for a very broad distribution). Prior to the measurement, the samples were diluted with double distilled filtered water to a suitable scattering intensity. All measurements were performed in triplicate. The results are expressed as mean size ± SD.

5.4.2. ZP measurement

The ZP is a measure of the electric charge at the surface of the particles indicating the physical stability of colloidal systems.[28] ZP was measured using a Zeta Sizer Nano ZS 90 (Malvern Instruments, Malvern, UK). Each sample was suitably diluted with double distilled filtered water and placed in a disposable zeta cell. The ZP values were assessed by determining the particle electrophoretic mobility. The electrophoretic mobility was converted to the ZP via the Helmholtz–Smoluchowski equation. All measurements were performed in triplicate. The results are expressed as mean ± SD.

5.4.3. % T Measurement

A total of 1 ml of SMEDDS formulation was diluted 100 times with double distilled water. The % T of diluted SMEDDS was measured at 650 nm using UV

spectrophotometer (UV 1700, Shimadzu, Japan) keeping double distilled water as a blank.

5.4.4. Conductance

Type of microemulsion (o/w or w/o) can be determined by measure of conductance. It was measured by conductivity meter. The electroconductivity of the resultant system was measured by an electroconductometer (CM 180 conductivity meter, Elico, Mumbai, India). For the conductivity measurements, the tested microemulsions were prepared with a 0.01N aqueous solution of sodium chloride instead of distilled water.

5.4.5. Cloud point measurement

EFV SMEDDS was diluted with water in the ratio of 1:100, and the sample was placed in a water bath with the temperature increasing gradually, spectrophotometric analysis was carried out to measure % T of the sample.[29]

5.4.6. pH

pH of SMEDDS diluted with double distilled water were measured using pH meter (Electro lab).

5.4.7. Solid state characterization of S-SMEDDS

5.4.7.1. DSC analysis

The physical state of EFV in S-SMEDDS was characterized by DSC (Shimadz, Japan). Thermograms of standard EFV powder, Aerosil 200, their physical mixture (PM) and S-SMEDDS were recorded in order to characterize the physical state of EFV. A heating rate of 10°C/min was employed in the range of 25-300°C with

nitrogen atmosphere supplied at 40 ml/min. Each sample was taken (~4-8 mg) in an aluminium pan, crimped and sealed. An empty aluminum pan was used as reference.

5.4.7.2. XRD analysis

XRD diffractograms of standard EFV powder, Aerosil 200, their PM and S-SMEDDS were obtained using Bruker AXS D8 Advance X-ray diffractometer. Scans were performed between $5^{o} < 2\theta < 80^{o}$.

5.4.8. Morphology of L-SMEDDS and S-SMEDDS

The microstructure of microemulsions from L-SMEDDS and from S-SMEDDS was investigated by TEM (Tecnai 20 Philips). For TEM analysis, L-SMEDDS and S-SMEDDS was diluted with double distilled water and a drop of it was placed on a carbon-coated copper grid (300 mesh, 3mm) and air dried. Morphological evaluation of S-SMEDDS was conducted through SEM (JSM 6380 LV, JEOL, Japan). For SEM analysis, the S-SMEDDS, Aerosil 200 and standard EFV were fixed on a brass stub using carbon double sided tape. The samples were then subjected to conductive coating with Au-Pd (80% - 20%). The SEM was operated at an acceleration voltage of 20 kV.

5.4.9. Dissolution study

In vitro dissolution studies of L-SMEDDS, S-SMEDDS and MF containing 50 mg of EFV and 50 mg of standard EFV were performed in 1% SLS in water according to the United States Pharmacopeia (USP) using dissolution apparatus II (paddle method).[30] The dissolution medium used in this work was reported in the "Dissolution Methods for Drug Products" guide of Food and Drug Administration. The experiments were performed on 900 ml media (1% SLS in water) at 37 ± 0.5 °C at a rotation speed of 50 rpm. At preselected time intervals, 5 ml samples were withdrawn and replaced with 5 ml of pre-thermostated fresh dissolution medium. Samples were filtered through 0.1 µm syringe filter, the resulting filtrate was diluted with mobile phase and 20 µl was

injected into the HPLC for analysis. Dissolution tests were performed in triplicate. Graph of percent cumulative drug release *vs.* time was plotted. Dissolution profiles were evaluated on the basis of dissolution efficiency (DE) and percentage of drug dissolved (DP) at 5 min and 60 min, time needed to dissolve 50% of drug ($t_{50\%}$), area under the curve (AUC) and mean dissolution time (MDT). An add-in program (DD solver) for comparison of drug dissolution profiles was used to calculate different dissolution parameters.[31]

5.4.10. Assay

Optimized SMEDDS were analyzed to determine the content of EFV in SMEDDS. Systems were diluted as per method and amount of drug was determined by validated HPLC method. (Described in Chapter 3)

5.4.11. Stability studies

5.4.11.1. Robustness to dilution

Robustness of SMEDDS to dilution was studied as per Date et al., method with slight modification.[32] SMEDDS were diluted to 10, 100 and 1000 times with various media viz. water, 0.1N HCl and pH 7.4 phosphate buffers. The diluted microemulsions were stored for 12 hours and observed for any signs of phase separation or drug precipitation.

5.4.11.2. Thermodynamic stability studies

The objective of thermodynamic stability is to evaluate the phase separation and effect of temperature variation on SMEDDS formulations. EFV SMEDDS were diluted to 100 times with double distilled water and centrifuged at 10,000 rpm for 20 minutes and formulations were observed visually for phase separation. To evaluate the effect of temperature, the formulations were subjected to freeze–thaw cycles (-20°C for 2 days followed by +25°C for 2 days).[33] At the end of the cycle, the

formulations were diluted and centrifuged as described above and phase separation and the change in droplet size were determined.

5.4.11.3. Physical and chemical stability

Physical and chemical stability was evaluated by storing the L- and S-SMEDDS samples at 4-8°C (refrigerator) and 25°C for up to 6 months. Samples were withdrawn at predetermined time intervals after 1, 2, 3 and 6 months. The clarity, phase separation, particle size and ZP after dilution with double distilled water at 1:100 were measured for physical stability of EFV in SMEDDS. In addition, chemical stability of EFV in SMEDDS was determined by HPLC assay and dissolution method.

5.4.12. PAMPA study

The BD Gentest™ pre-coated PAMPA plates were used to perform permeability assays for standard EFV, MF, L- and S-SMEDDS. The permeability assay was carried out as per protocol described in references.[34-36] The 96-well filter plate, pre-coated with lipids, was used as the permeation acceptor and a matching 96-well receiver plate was used as the permeation donor. Sample solutions were prepared by diluting 10 mM stock solutions in 20% methanolic PBS pH 7.4 (final concentration of 200 µM). The sample solutions were added to the wells (300 µl/well) of the receiver plate and 20% methanolic PBS pH 7.4 was added to the wells (200 µl/well) of the pre-coated filter plate. The filter plate was then coupled with the receiver plate and the plate assembly was incubated at room temperature without agitation for six hours. The assembled plate was placed into a sealed container with wet paper towels to avoid evaporation. At the end of the incubation, samples from the donor and receiver plate were analyzed for EFV concentration by HPLC method described in chapter 3.

Permeability of the EFV was calculated using the following formula:

$$\text{Permeability } (P_e)\ (\text{cm/s}) = \{-\ln[1-C_A(t)/C_{equilibrium}]\}/\ [A*(1/V_D + 1/V_A)*t] \quad (1)$$

A = filter area (0.3 cm^2), V_D = donor well volume (0.3 ml), V_A = acceptor well volume (0.2 ml), t = incubation time (seconds), $C_A(t)$ = compound concentration in

acceptor well at time t (mM), $C_D(t)$ = compound concentration in donor well at time t (mM), and $C_{eq} = [C_D(t)*V_D+C_A(t)*V_A]/(V_D+V_A)$.

5.4.12.1. Membrane integrity test

Lucifer yellow, a fluorescence dye was selected to study membrane integrity in PAMPA with and without the addition of placebo which contains excipients of same concentrations used to prepare nanosuspension. Studies in the literature have shown that lucifer yellow CH does not cross the cell membrane as long as the cell lipid membrane remains intact.[37] Thus, in order to measure the stability of the lipid bilayer, the amount of lucifer yellow found in the acceptor well was measured. Three hundred microliters of lucifer yellow solution (concentration range- 0.03-1.0 µM) was added to selected wells in a donor plate. Three hundred microliters of lucifer yellow solution (concentration - 0.3 µM) contain placebo (Mixture of oil, surfactant and cosurfactant without drug used to prepare optimized SMEDDS) was added to another selected wells in a donor plate. 20% methanolic PBS pH 7.4 was added to the wells (200 µl/well) of acceptor plate. The donor plate was then coupled with the acceptor plate and the plate assembly was incubated at room temperature without agitation for five hours. The assembled plate was placed into a sealed container with wet paper towels to avoid evaporation. At the end of the incubation, fluorescence intensity of lucifer yellow in the wells of acceptor plate was measured by HPLC consisted fluorescence detector. The wavelength of the excitation filter was 430 nm. The wavelength of the emission filter was 530 nm.[38]

5.5. Evaluation of EFV SMEDDS

5.5.1. Animals

The male Albino rats (weighing approximately 200 ± 15 g) and New Zealand white male rabbits (weighing approximately 2.0 ± 0.2 kg) were used for the in situ intestinal absorption study and in vivo pharmacokinetic study, respectively. At first, the animals were acclimatized at a temperature of 25±2°C and a relative humidity of 70±5% under natural light/dark conditions and were fed with food and water *ad libitum*. Prior

to experiment the animals were kept under fasting overnight. The animal requirement was approved by the Institute Animal Ethics Committee (Protocol No. FTE/PHR/CPCSEA/2007/04), and all experiments were conducted as per the norms of the Committee for the Purpose of Supervision of Experiments on Animals, India.

5.5.2. *In situ* rat intestinal perfusion study

The absorption property of EFV in MF, L- and S-SMEDDS was investigated with the established *in situ* intestinal perfusion methods in rats.[39-46] Briefly, rats were anaesthetized with an intraperitoneal injection of ketamine at a dose of 100 mg/kg and were placed on a warming pad in a supine position under a surgical lamp to maintain body temperature at 37±1°C. The abdomen was opened with a midline longitudinal incision of 3–4 cm. The small intestine segment approximately 10-12 cm was exposed. A semi-circular incision was made at both sides of the segment. The selected intestinal segment was gently rinsed with pre-warmed normal saline (37±1°C) so as to eliminate any residual fecal matter and debris. The remaining saline was expelled with air. Both ends were cannulated with silicon tubing (diameter 0.4 cm) and ligated using silk suture, then attached to the perfusion assembly which consisted of a peristaltic pump (Electrolab, Mumbai, India) and a 100 ml volumetric cylinder as reservoir. The small intestine was returned to the abdominal cavity to maintain its viability without disrupting blood vessels. The exposed area was covered with sterilized absorbent gauze and saline (37°C) was applied to keep it warm and moist during the experiment. The L-SMEDDS equivalent to 35 mg EFV was dispersed in perfusion solution (Krebs- Ringer's solution; 7.8 g NaCl, 0.35 g KCl, 1.37 g NaHCO3, 0.02 g MgCl2, 0.22 g NaH2PO4 and 1.48 g glucose in 1000 mL purified water), maintained at 37°C, taken in to 100 ml volumetric cylinder. The perfusion was started by recirculation through the cannulated intestine segment at a flow rate of 5ml/min for 10 min to achieve steady state. Then, the flow rate of perfusion was adjusted to 2.5 ml/min and the volume of perfusion solution in the circulation system as the 0 min volume was recorded. The perfusion experiment lasted for 6 h and samples were collected at predetermined time intervals (5, 10, 15, 20, 25, 30, 45, 60, 90, 120, 150, 180, 210, 240, 270, 300, 330 and 360 min). 1ml of sample solution was taken out at each time interval, the volume of solution in the circulation system was

recorded, and then 2ml Krebs-Rings solution was added in. Samples were frozen immediately and stored at -20 ◦C until analysis. Before analysis, samples were thawed at room temperature and diluted to 5 ml with mobile phase and the resulting solution was centrifuged at 6000 rpm for 10min. A 20 μL of supernatant was injected into HPLC for determination of EFV using the HPLC method as described in section 4. S-SMEDDS and MF was dispersed in perfusion solution and processed with the above experimental method for comparison.

The absorption constant (K_a) is calculated using Fick's equation:

$$K_a = [-\ln(X/X_0)]/t \quad (2)$$

where X_0 is the amount of drug before absorption, X is the residue amount of drug after absorption. K_a can be obtained as the slope from the regression curve of $-\ln(X/X_0)$ *versus* time, and $t_{1/2}$ can be obtained when X is equal to $X_0/2$.[47]

Subsequently, the amount of drug absorbed into systemic circulation (mg) versus time (h) curve was constructed and AUC_{0-6h} *in situ* was calculated, in order to assess extent of drug absorption.

5.5.2.1. Stability of EFV in blank intestinal circulating solution

According to the rat's intestinal perfusion experiment *in situ* above, the blank intestinal circulating solution can be obtained after 6 h circulation. MF, L- and S-SMEDDS were diluted to 100 ml by blank perfusion solution, and then the resulting solution was treated with a water bath at 37°C for 6 h. The concentrations at 0 h and 6 h were determined and compared with each other.

5.5.3. *In vivo* pharmacokinetic study

Bioavailability of SMEDDS was compared with MF and standard EFV. Three rabbits were allocated at random to three treatment groups and administered standard EFV, MF, L- and S-SMEDDS in a crossover design. A washout period of 7 days was kept between consecutive dosing. The standard EFV, MF, L- and S-SMEDDS equivalent

to 10 mg/kg dose of EFV were filled in mini hard capsules and administrated orally. Blood samples (1.5 ml) were collected through the marginal ear vein into heparinized tubes at 0, 0.5, 1, 1.5, 2, 2.5, 3, 3.5, 4, 8, 12, 24 and 48 hr. Blood samples were centrifuged at 3000 rpm for 10 min using a high speed centrifuge machine and plasma samples were withdrawn and stored at -20°C until analysis.

5.5.3.1. Pharmacokinetic analysis

Plasma samples collected from the rabbits were analyzed using developed reverse phase HPLC method described in chapter 3. The drug plasma concentration values were determined from the calibration curve. Non-compartmental pharmacokinetic analysis was performed (Shin et al., 2000).[48] Trapezoidal method was employed to calculate the area under the curve (AUC) of plasma concentration as a function of time (t). Mean residence time (MRT) was calculated as area under the first moment curve (AUMC) divided by AUC. AUMC was determined from the plot of plasma concentration multiplied by time (C X t) versus time. All the pharmacokinetic parameters were calculated using MS-Excel software. The maximum plasma concentration (C_{max}) and the time to reach maximum plasma concentration (t_{max}) were determined by the plasma concentration curve using MS-Excel software. The elimination rate constant (K_{el}) was calculated by the regression analysis from the slope of the line and the half-life ($t_{1/2}$) of the drug was obtained by $0.693/K_{el}$. Other parameters, clearance (Cl) and volume of distribution at steady state (V_{ss}) were calculated using the following equations: Cl = Dose/AUC and V_{ss} = Dose X AUMC/$(AUC)^2$.

5.6. Statistical analysis

All data are reported as mean ± SD. The statistical significance of the differences between the groups was tested by one-way ANOVA followed by Bonferroni multiple comparison test using computer based program (Graphpad Prism 5.0).

5.7. Results and discussion

5.7.1. Screening of excipients

5.7.1.1. Solubility study

Solubility of EFV in different oils, surfactants and cosurfactants is given in Figure 5.1. SMEDDS consists of oil, surfactant and cosurfactant as constructing component of the system. Drug should be completely soluble in all three components and their mixture. Therefore solubility of drug should be one of the main criteria for selection of oil, surfactant and cosurfactant. Moreover solubility of drug is also important to decide the dose of drug. Hence SMEDDS should consist of such oil, surfactant and cosurfactant that accommodate dose of drug. Another factor which can be affected by solubility is partitioning effect. If drug is not soluble and stable in mixture it will be diffused towards water at the time of formation of microemulsion and as drug is water insoluble, it will precipitate out in the formulation. Considering both these facts, selection of excipients is crucial factor for successful formulation.

The choice of selecting excipients for developing SMEDDS is based on following criteria

1. The SMEDDS mixture should instantly self-microemulsify forming a fine oil-in-water nanoemulsion upon aqueous dilution in the GIT.

2. The SMEDDS mixture should be capable of solubilizing the entire drug dose in a volume that is acceptable for unit oral administration.

3. The drug should remain physically and chemically stable in the SMEDDS mixture.

4. The excipients should not produce any systemic toxicity.

The higher solubility of the drug in the oil phase is important for the SMEDDS to maintain the drug in solubilized form. If the surfactant or cosurfactant is contributing to drug solubilisation, there could be a risk of precipitation, as dilution of SMEDDS in GIT will lead to lowering of solvent capacity of surfactant or cosurfactant.[49] Medium chain triglycerides (MCT) are commonly used in the SMEDDS formulation.[50-52] MCT are medium-chain (6–12 carbons) fatty acid esters of glycerol. MCT passively diffuse from the GIT to the portal system (longer fatty acids are absorbed into the lymphatic

system) without requirement for modification like long chain fatty acids or very long chain fatty acids do. In addition, MCT do not require bile salts for digestion. MCT possess higher ester content per gram than long chain triglycerides (LCT) so drugs have higher solubility in MCT than LCT.[53-55] Figure 5.1 shows that EFV has good solubility in synthetic oils in comparison to vegetable oils. So, captex 500 (MCT) and capryol 90 (MCT) were selected as oil phase.

Safety is a major determining factor in choosing a surfactant as large amounts of surfactants may cause GI irritation. Nonionic surfactants are less toxic than ionic surfactants. O/W nanoemulsion dosage forms for oral or parenteral use based on non-ionic surfactants are likely to offer in vivo stability.[56] An important criterion for selection of the surfactants is that the required HLB value to form o/w nanoemulsion is greater than 10.[57] The right blend of low and high HLB surfactants leads to the formation of a stable nanoemulsion upon dilution with water.[27,57] In the present study, two surfactants namely tween 20 and acconon MC8-2 which can act as surfactant due to its high HLB values and showed good solubility of EFV were selected.

A lipophilic, non-volatile cosurfactant is less likely to migrate to the capsule shell than solvent such as ethanol and also more likely to be retained by the oil phase upon dilution with aqueous media, thus avoiding precipitation.[51,58] The third component of SMEDDS i.e cosurfactant which helps surfactant to stabilize the system is PEG 400 and transcutol HP. EFV showed significant solubility in theses cosurfactants.

5.7.1.2. Construction of pseudoternary phase diagram

Based on the results of solubility studies, eight potential different combinations of surfactant, cosurfactant, and oil (Table 5.5) were used for the phase diagram study for EFV SMEDDS. Corresponding pseudoternary phase diagram of each combination are presented in Figure 5.2A–D and Figure 5.3A–D.

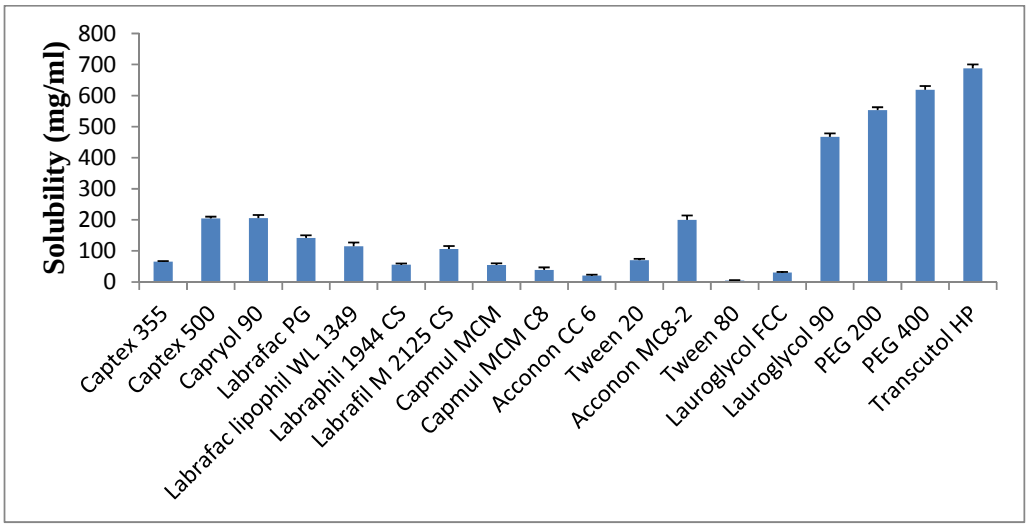

Figure 5.1. Solubility of EFV in various excipients. Data are expressed as mean ± SD (n = 3).

To determine optimum concentration of oil, surfactant and cosurfactant, pseudoternary phase diagram were constructed. SMEDDS forms microemulsion when titrated with water under agitation condition. The particle size of microemulsion is less than 100 nm and as the energy required to form microemulsion is very low, it is a thermodynamically spontaneous process.[51] This process is facilitated by presence of surfactant. The surfactant forms a layer around oil globule in such a way that polar head lies towards aqueous and non-polar tail pull out oil and thereby reduces surface tension between oil phase and aqueous phase.[49] Another factor affecting formation of microemulsion is the ratio of surfactant and cosurfactant. The lipid mixtures with different surfactant, cosurfactant and oil ratios lead to the formation of SMEDDS with different properties.[59] Since surfactant and cosurfactant adsorb at interface and providing mechanical barrier to coalescence, selection of oil, surfactant, cosurfactant and mixing ratio of surfactant to cosurfactant [S/CoS (k_m)], play important role in microemulsion formation.[60] The psuedoternary phase diagrams were constructed at the ratios of S/CoS (k_m) 1:1, 2:1 and 3:1. Initially, the concentration of oil taken was maximum, i.e. 90%, and amount of S/CoS was kept to minimum, i.e., 10%. Gradually, oil concentration was decreased and that of S/CoS was increased. It was observed during these experiments that high concentration of oil forms poor emulsion with entrapment of very less amount of water upon dilution. Another observation was that as concentration of S/CoS increases, the time estimated to form microemulsion

decreases. A series of microemulsions were prepared at different concentrations of oil and S/CoS, but concentration of oil was found to be a rate-limiting factor and in all cases, high oil concentration resulted in poor emulsion region. The black boundary covers microemulsion region. At any point beyond this boundary, microemulsion if formed initially, become turbid on further dilution of solution. This indicates formation of emulsion with higher particle size (<100 nm). Based on pseudoternary phase diagram, combination of captex 500, tween 20 and transcutol HP shows better microemulsion region then all other combinations (Figure 5.2 – 5.3).

5.7.1.3. Self-emulsification and dispersibility test

Self-emulsifying performance of oil, surfactant and cosurfactant mixture was assessed from their ternary phase diagrams. Only certain combinations of oil, surfactant and a cosurfactant in a certain composition range will produce a clear and transparent emulsion upon aqueous dilution. To check emulsification efficiency of mixtures, test for self-emulsification was performed on all eight combinations and the resultant dispersions were visually assessed by grading system. The area with light colour in the phase diagram displays the concentration range of mixture components that resulted in a clear and transparent emulsion out of all the trial concentrations. All the combinations under test formed a clear and transparent emulsion in certain concentrations, but the combination with wider self-emulsification region is considered to be a better combination in terms of self-emulsification efficiency.

Grade A, B, C and D represented by gainsboro, lightgray, darkgray and dimgray colour in phase diagram, respectively. (Figure 5.4) Combination of oil, surfactant and cosurfactant which contains highest grade A region was selected. In the current investigation, it could be seen that group I, containing transcutol HP, yielded SMEDDS containing as high as 40% oily phase composition. (Figure 5.4A) On the other hand, group II, containing PEG 400, produced SMEDDS till a maximum oil concentration of 20% only. (Figure 5.4B) A very small grade A region was observed with group III when oil concentration was less than 15% and surfactant concentration was more than 75% of SMEDDS formulation. (Figure 5.4C) This much large amount of surfactant may cause GI irritation. Hence, it is important to determine the minimum

surfactant concentration required to produce SMEDDS. Phase diagram of group V and VI shows that grade A region was observed when oil concentration was less than 15% of SMEDDS formulation. (Figure 5.4E and 5.4F) Group IV, VII and VIII does not contain grade A region in phase digram. (Figure 5.4D, 5.4G and 5.4H) Group IV, VII and VIII was not able to form clear and transparent emulsion in tested concentrations. In all groups, surfactant concentration less than 30% and oil concentration greater than 40% resulted in turbid and crude emulsions.

The captex 500, tween 20 and transcutol HP mixture possessed the largest grade A region in the phase diagrams and took the least time to self-emulsification. They were completely emulsified within a minute and the dispersion was clear and transparent. self-emulsification mixtures that passed the dispersibility test as grades A were taken for further study, because these formulations will remain as nanosized emulsions, once dispersed in GI fluid. Formulations that were falling under grades B, C, and D were not selected for further studies.

It has been reported that drug incorporation into SMEDDS can affect the self-emulsification performance.[51] This can be due to the drug interacting with the liquid crystalline phase of the self-emulsification mixtures causing blockage of drug charge movement in the system[61] or due to drug penetration into the surfactant monolayer producing perturbations at the interface.[51,62] To verify this, EFV loaded self-emulsification mixtures were subjected to the test for emulsification. No differences in self-emulsification region in the phase diagram and time taken for complete emulsifications were observed between the drug loaded and blank mixtures. This suggests that the presence of EFV does not affect self-emulsification property of the mixture.

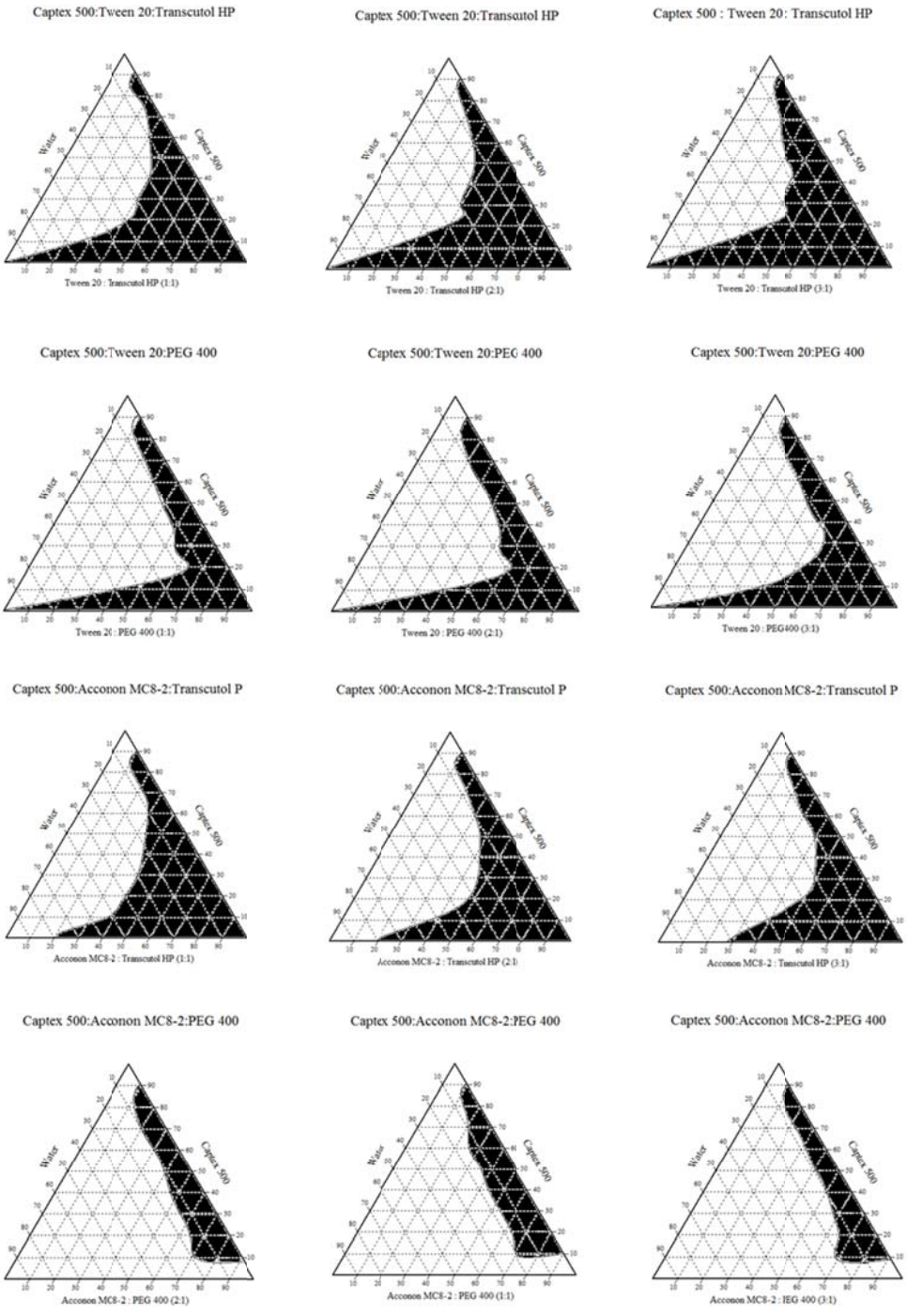

Figure 5.2. Pseudoternary phase diagram prepared with the following components: (A) oil-captex 500, surfactant-tween 20, cosurfactant-transcutol HP, (B) oil-captex 500, surfactant-tween 20, cosurfactant-PEG 400, (C) oil-captex 500, surfactant-acconon MC8-2, cosurfactant-transcutol HP, (D) oil-captex 500, surfactant-acconon MC8-2, cosurfactant- PEG 400. S/CoS ratio is 1:1, 2:1 and 3:1.

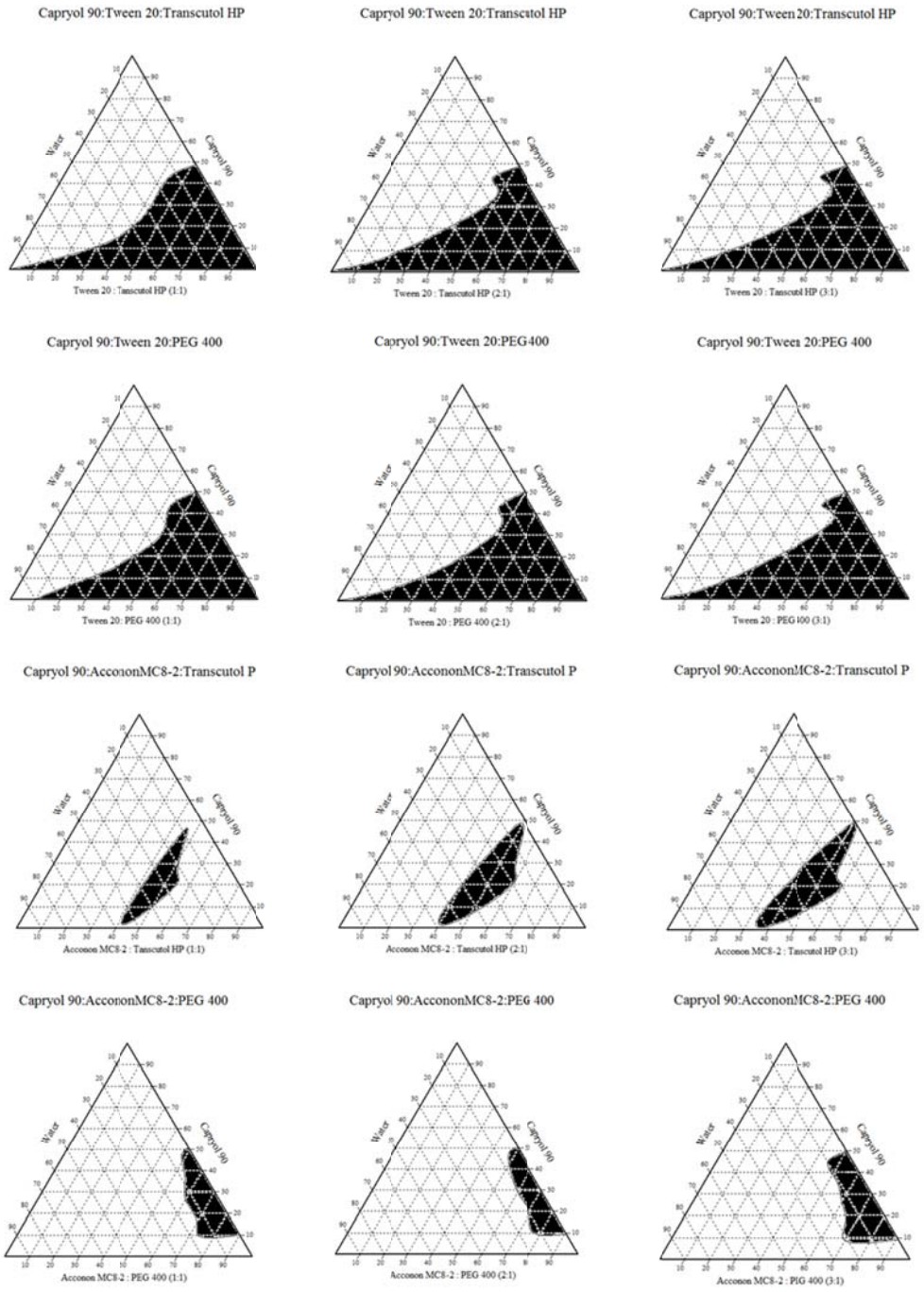

Figure 5.3. Pseudoternary phase diagram prepared with the following components: (A) oil-capryol 90, surfactant-tween 20, cosurfactant-transcutol HP, (B) oil- capryol 90, surfactant-tween 20, cosurfactant-PEG 400, (C) oil- capryol 90, surfactant-acconon MC8-2, cosurfactant-transcutol HP, (D) oil- capryol 90, surfactant-acconon MC8-2, cosurfactant- PEG 400. S/CoS ratio is 1:1, 2:1 and 3:1.

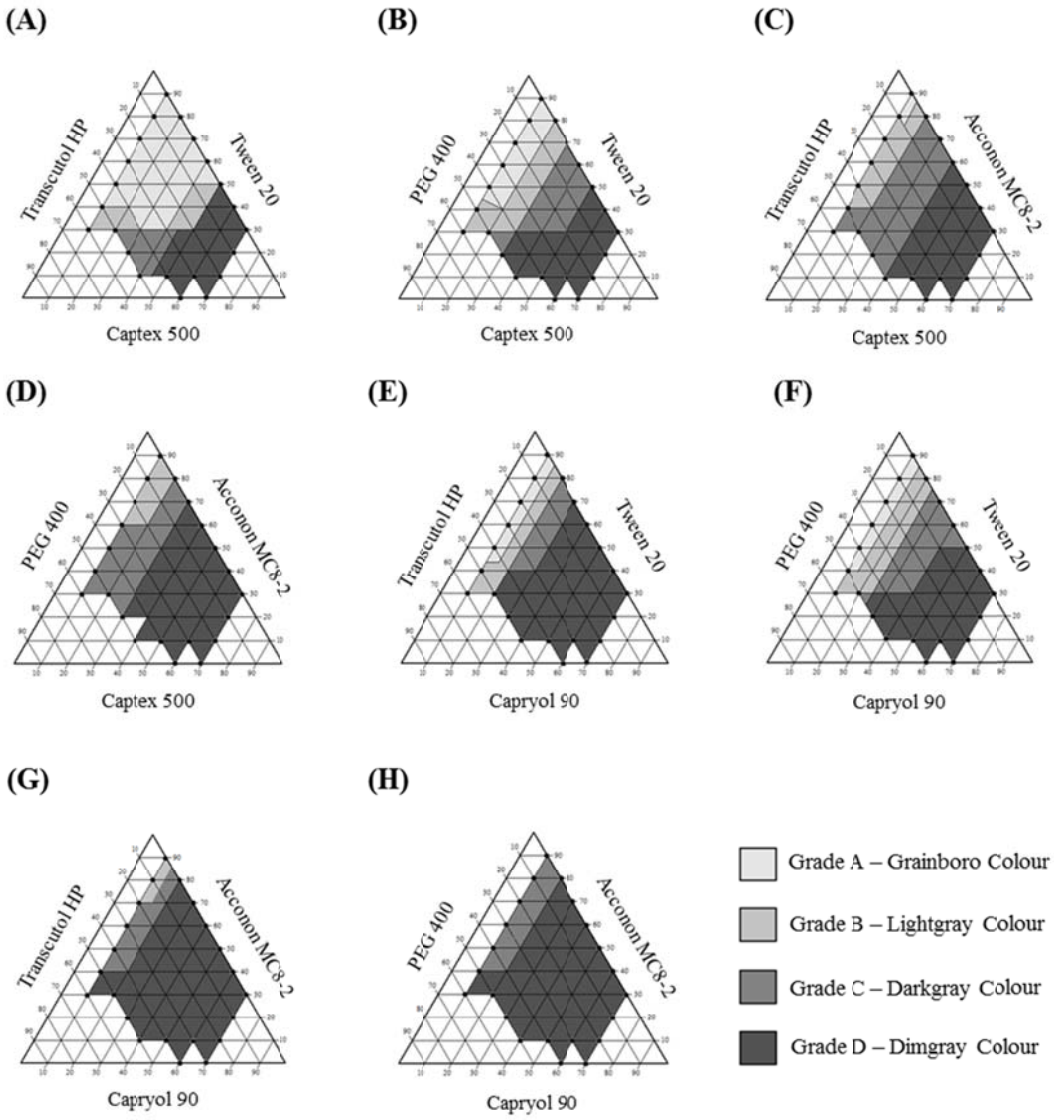

Figure 5.4. Phase diagram of group I-VIII mentioned in Table 5.5. The grainboro colour area represents SMEDDS region.

5.7.2. Optimization of SMEDDS

Based on the results of ternary phase diagrams and self-emulsification studies, captex 500 as oil (X_1), tween 20 as surfactant (X_2) and transcutol HP as cosurfactant (X_3) was selected for components of SMEDDS. In order to perform the mixture design, it was necessary to identify the self-emulsification region from phase diagrams of systems containing oil-surfactant-cosurfactant. As seen in Figure 5.4A, the gainsboro

colour region of the diagram represented the efficient self-emulsification region. Based on this diagram, the range of each component was selected as follows: 10% ≤ X_1 ≤ 40%, 30% ≤ X_2 ≤ 60%, 20% ≤ X_3 ≤ 50%. The drug content is kept constant 50 mg/g of the prepared SMEDDS. Mixture design was applied to selected optimum composition of SMEDDS. MDS (Y_1) and % T (Y_2) were selected as dependent variables.

Table 5.5. Oil, surfactants and cosurfactants grouped in different combinations

Group	Oil	Surfactant	Cosurfactant
I	Captex 500	Tween 20	Transcutol HP
II	Captex 500	Tween 20	PEG 400
III	Captex 500	Acconon MC8-2	Transcutol HP
IV	Captex 500	Acconon MC8-2	PEG 400
V	Capryol 90	Tween 20	Transcutol HP
VI	Capryol 90	Tween 20	PEG 400
VII	Capryol 90	Acconon MC8-2	Transcutol HP
VIII	Capryol 90	Acconon MC8-2	PEG 400

The experimental runs and the observed and predicted responses for the 25 formulations are reported in Table 5.6. The values of response Y_1 and Y_2 were ranged from 8.297 to 149.2 nm and 86 to 99.5 %, respectively.

The selection of model for analyzing the response was done based on the comparisons of several statistical parameters including standard deviation (SD), R-squared values and predicted residual sum of square (PRESS). The chosen model should have low SD, high R-squared value and lower PRESS value. The details of which are mentioned in Table 5.7, which suggests special cubic and quadratic model for analyzing Y_1 and Y_2 responses, respectively. The predicted R-Squared of 0.9654 and 0.8598 is in reasonable agreement with the adjusted R-Squared of 0.9711 and 0.8796 for Y_1 and Y_2, respectively. Adequate precision is measures the signal to noise ratio. A ratio greater than 4 is desirable. Ratio was found to be 37.166 and 18.395 for Y_1 and Y_2 responses, respectively, indicates an adequate signal.

For estimation of significance of the model, the analysis of variance (ANOVA) was applied. The ANOVA for Y_1 and Y_2 was summarized in Table 5.8. Using 5% significance level, a model is considered significant if the *p*-value (significance probability value) is less than 0.05. From the *p*-values presented in Table 5.8, it can be concluded that for responses Y_1 and Y_2, special cubic and quadratic model was significant, respectively. As shown in Table 5.8, the Model F-values of 135.44 and 36.06 for Y_1 and Y_2, respectively, implies the model is significant. Values of "Prob > F" less than 0.05 indicate model terms are significant. Therefore, interaction terms X_1X_2 and $X_1X_2X_3$ are significant terms for MDS; X_1X_2 and X_1X_3 are significant model terms for % T.

Table 5.6. Mixture experimental design: Independent (X) and dependent variables (Y), observed, predicted and residuals values for the responses Y_1 and Y_2.

	Independent Variables			Observed Values		Predicted Values		Residuals		ZP (mV)
Standard order	**X_1**	**X_2**	**X_3**	**Y_1**	**Y_2**	**Y_1**	**Y_2**	**Y_1**	**Y_2**	
1	40	30	30	149.2	86.0	149.48	86.0	-0.28	0.03	-19.3
2	10	60	30	9.022	98.9	7.34	99.3	1.68	-0.4	-9.33
3	40	40	20	122	87.3	128.21	87.4	-6.21	-0.1	-16.1
4	20	60	20	18.608	99.0	21.77	98.8	-3.16	0.19	-12.5
5	20	30	50	48.97	98.0	46.38	97.6	2.59	0.44	-17.3
6	10	40	50	8.585	99.0	10.67	99.5	-2.09	-0.5	-5.51
7	40	35	25	131.2	89.5	132.63	86.7	-1.43	2.78	-20.6
8	30	30	40	90.6	92.0	93.19	93.2	-2.59	-1.2	-21.2
9	15	60	25	8.297	99.5	6.88	99.4	1.42	0.08	-5.13
10	10	50	40	11.3	99.3	10.11	99.6	1.20	-0.3	-24.3
11	30	50	20	69.7	94.5	63.71	95.0	5.99	-0.5	-16.2
12	15	35	50	21.36	98.5	19.21	99.0	2.15	-0.5	-15.3
13	31	37	32	75.42	91.2	73.27	93.4	2.15	-2.2	-19.7
14	17	52	31	9.128	98.6	8.45	99.3	0.68	-0.7	-10.9
15	31	42	27	70.1	91.1	65.57	93.9	4.53	-2.8	-11.8
16	21	52	27	19.422	99.0	18.18	98.5	1.25	0.49	-15.7
17	21	37	42	33.42	99.4	31.46	97.8	1.96	1.59	-14.1
18	18	41	41	18.71	98.8	17.11	98.8	1.60	0.00	-20.2
19	32	39	29	96.2	90.3	74.71	93.0	21.49	-2.7	-19.2
20	27	37	36	40.42	97.4	53.96	95.5	-13.5	1.90	-18.0
21	19	52	29	10.12	99.4	12.36	99.0	-2.24	0.45	-12.7
22	17	47	36	9.859	99.4	10.08	99.2	-0.22	0.20	-15.2
23	27	47	26	31.09	98.1	42.54	96.3	-11.5	1.85	-19.9
24	20	39	41	21.04	98.5	24.71	98.2	-3.67	0.27	-15.5
25	24	43	33	29.483	98.8	31.28	97.2	-1.80	1.59	-15.8

X_1: Oil concentration (% w/w), X_2: Surfactant concentration (% w/w), X_3: Cosurfactant concentration (%w/w), Y_1: Mean droplet size (nm), Y_2: Transmittance (%)

Table 5.7. Results of regression analysis for responses Y_1 and Y_2

Source	SD		R-Squared		Adjusted R-Squared		Predicted R-Squared		PRESS	
	Y_1	Y_2	Y_1	Y_2	Y_1	Y_2	Y_1	Y_2	Y_1	Y_2
Linear	15.53	2.04	0.8785	0.7993	0.8675	0.7810	0.8403	0.7405	6975.37	117.88
Quadratic	7.98	1.51	0.9723	0.9047	0.9650	0.8796	0.9548	0.8598	1973.08	63.69
Special Cubic	7.25	1.51	0.9783	0.9096	0.9711	0.8795	0.9654	0.8597	1510.2	63.71
Cubic	7.59	1.48	0.9802	0.9279	0.9683	0.8847	0.9534	0.8327	2034.85	76
Special Quartic	7.48	1.54	0.9795	0.9166	0.9693	0.8748	0.9572	0.8296	1868.66	77.39

Table 5.8. ANOVA for responses Y_1 and Y_2

Source	Sum of Squares		df		Mean Square		F Value		p-value Prob > F	
	Y_1	Y_2	Y_1	Y_2	Y_1	Y_2	Y_1	Y_2	Y_1	Y_2
Model	42726.56	410.88	6	5	7121.09	82.18	135.44	36.06	< 0.0001	< 0.0001
Linear Mixture	38366.57	363	2	2	19183.29	181.5	364.85	79.65	< 0.0001	< 0.0001
X_1X_2	374.28	35.93	1	1	374.28	35.93	7.12	15.77	0.0157	0.0008
X_1X_3	65.6	19.41	1	1	65.6	19.41	1.25	8.52	0.2787	0.0088
X_2X_3	3.5	0.23	1	1	3.5	0.23	0.067	0.1	0.7992	0.7532
$X_1X_2X_3$	264.74	43.3	1	-	264.74	-	5.04	-	0.0377	-
Residual	946.4	454.18	18	19	52.58	2.28				
Cor Total	43672.96		24	24						

The mathematical relationship in the form of a polynomial equation generated by Design-Expert® 8.0 software for the measured responses, Y_1 and Y_2, are listed below in equation 2 and 3, respectively.

$$Y_1 = 4.071X_1 - 1.212X_2 - 2.675X_3 + 0.060X_1X_2 + 0.212X_1X_3 + 0.098X_2X_3 - 0.009X_1X_2X_3 \quad (2)$$

$$Y_2 = -0.289X_1 + 0.915X_2 + 0.960X_3 + 0.019X_1X_2 + 0.014X_1X_3 + 0.002X_2X_3 \quad (3)$$

The above equations represent the quantitative effect of independent variables (X_1, X_2 and X_3) and their interactions on the responses (Y_1 and Y_2). A positive sign represents a synergistic effect, while a negative sign indicates an antagonistic effect. The

theoretical values of Y_1 and Y_2 were obtained by substituting the values of X_1-X_3 into the above equation, which were in reasonably good agreement with the observed values as seen in Table 5.6.

The relationship between the dependent and independent variables was further elucidated using 2D contour plots. Figure 5.5 and 5.6 represents the effect of variables X_1, X_2 and X_3 on the response Y_1 and Y_2, respectively. The MDS shows linear pattern with variables X_1, X_2 and X_3 illustrated in Figure 5.5, it increased as oil concentration increased whereas it decreased as surfactant concentration increased. As shown in Figure 5.6, the % T of diluted SMEDDS decreases at higher oil concentration. Oil provides the largest contribution to MDS and % T of the diluted SMEDDS. As oil concentration increased from 10 to 40 % in SMEDDS composition, MDS was increased from 8.297 to 149.2 nm and % T decreased from 99.5 to 86 %. Due to higher droplet size, oil globules may reduce the transparency of microemulsion and thereby values of % T. The two other formulation components have more limited effects on both responses. As expected, compositions with higher % T showed lowest droplet size since aqueous dispersions with higher % T are optically clear and oil droplets are thought to be in a state of finer dispersion.

5.7.3. Optimum Formula

After studying the effect of the independent variables on the responses, the levels of these variables that give the optimum response were determined. Optimization was performed to find out the level of independent variables (X_1, X_2 and X_3) that would yield a minimum value of MDS with maximum value of % T. It is evident from the polynomial equation and contour plots that higher oil concentration increases MDS of SMEDDS. The optimum formulation is one that gives a minimum droplet size and high % T value along with high amount of oil and low amount of surfactant in the resultant SMEDDS. Using a Design-Expert software optimization process, selected values of X_1, X_2 and X_3 were 25.0 % w/w, 50.0% w/w and 25.0 % w/w, respectively, which gives theoretical values of 33.62 nm and 97.53 % for MDS and % T, respectively. For confirmation, a fresh formulation in triplicate was prepared at the optimum levels of the independent variables, and the resultant SMEDDS formulations

were evaluated for the responses. The observed values of MDS and % T were found to be 30.4 ± 0.15 nm with PDI value of 0.126 and 98.72 ± 0.53 %, respectively, which were in close agreement with the theoretical values. ZP value of optimized SMEDDS was -19.9 ± 0.45 mV. Figure 5.7A and 5.7B shows droplet size and ZP distribution curve of reconstituted optimized EFV loaded L-SMEDDS formulation.

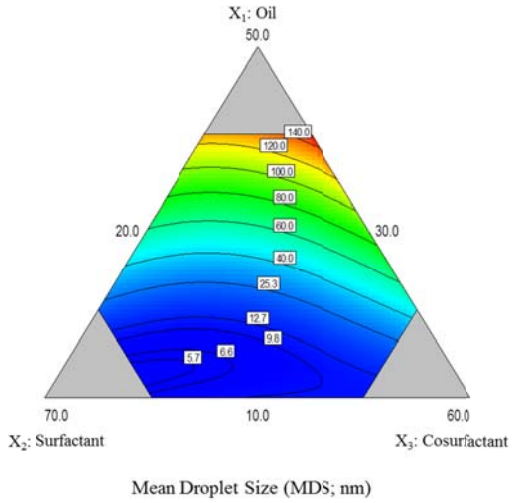

Figure 5.5. 2D contour plot for the effect of variables (X_1, X_2 and X_3) on the MDS (Y_1) of diluted EFV loaded L-SMEDDS.

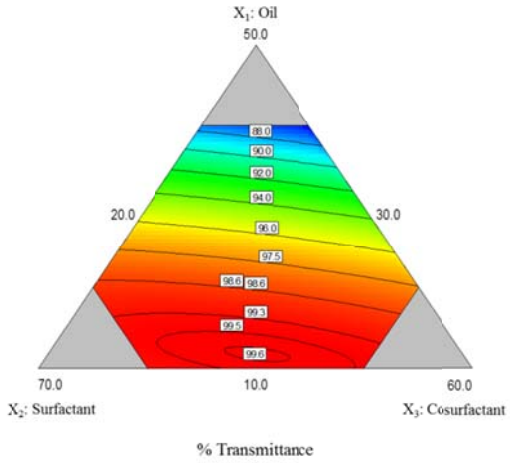

Figure 5.6. 2D contour plot for the effect of variables (X_1, X_2 and X_3) on the % T (Y_2) of diluted EFV loaded L-SMEDDS.

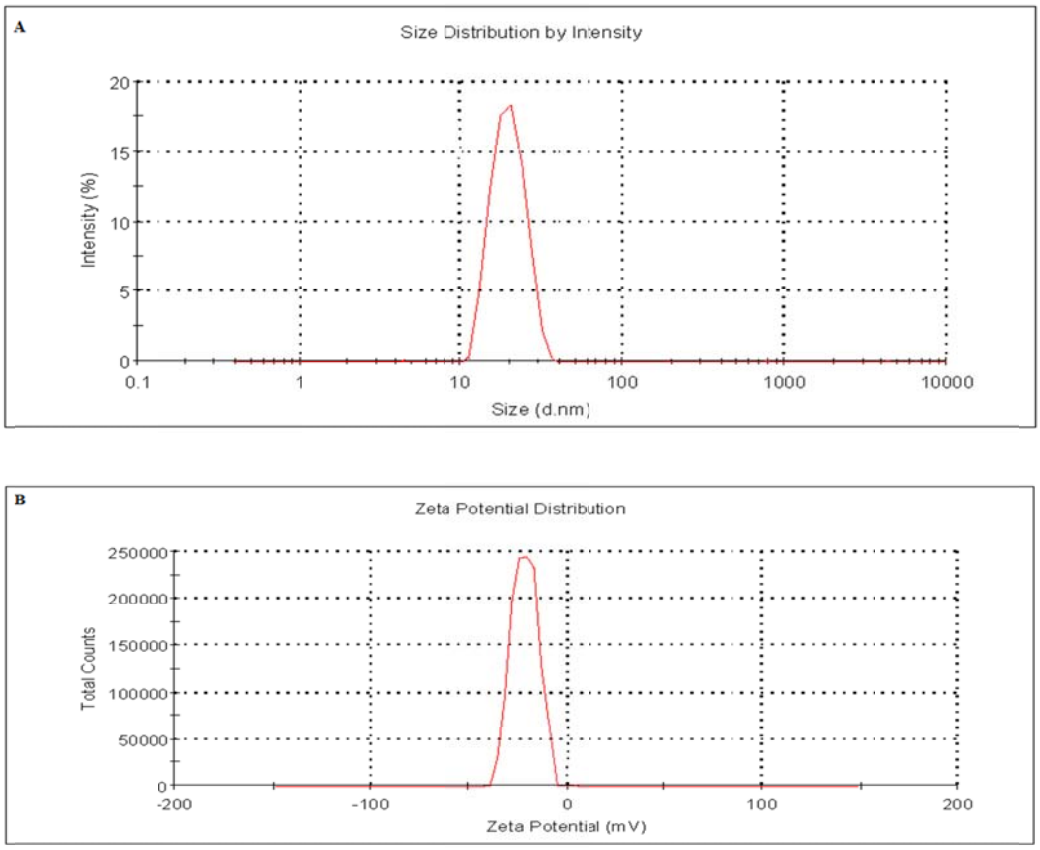

Figure 5.7. (A) Droplet size distribution curve and (B) ZP curve of optimized EFV L-SMEDDS after dilution with double distilled water.

5.7.4. Preparation of S-SMEDDS

It was observed that solid adsorbents such as dibasic calcium phosphate, anhydrous lactose, microcrystalline cellulose, calcium carbonate, magnesium carbonate and aluminum magnesium silicate did not have good adsorption capacity to yield a free flowing S-SMEDDS whereas Aerosil 200 exhibited good adsorption capacity to yield free flowing S-SMEDDS at the ratio of 4:1 (L-SMEDDS:Aerosil 200). Few researchers have reported conversion of L-SMEDDS to S-SMEDDS using Aerosil 200.[12,14,63]

S-SMEDDS was also tested for self-emulsification test and the result was similar to that obtained from L-SMEDDS. The MDS obtained from diluted L-SMEDDS was 30.4 ± 0.15 nm with PDI of 0.126, while MDS obtained from diluted S-SMEDDS was 32.8 ± 0.21 nm with PDI of 0.145. For S-SMEDDS samples, large Aerosil 200

particles were allowed to sediment and then the sample of microemulsion was tested for droplet size. Although the droplet size of the microemulsion increased after adsorption of EFV loaded L-SMEDDS on aerosol 200, the difference is not significant. S-SMEDDS showed a bimodal distribution due to the presence of Aerosil 200 particles in the sample. In their bi-modal distribution, more than 90% of the particles by volume constitute the microemulsion oil droplet, while the rest shows the size of the Aerosil 200 particles. These observations confirmed the presence of EFV in a solubilized form in the solid formulation. The physical state of EFV in the S-SMEDDS was further verified using DSC and XRD. Figure 5.8 shows droplet size distribution curve of optimized reconstituted EFV loaded S-SMEDDS formulation.

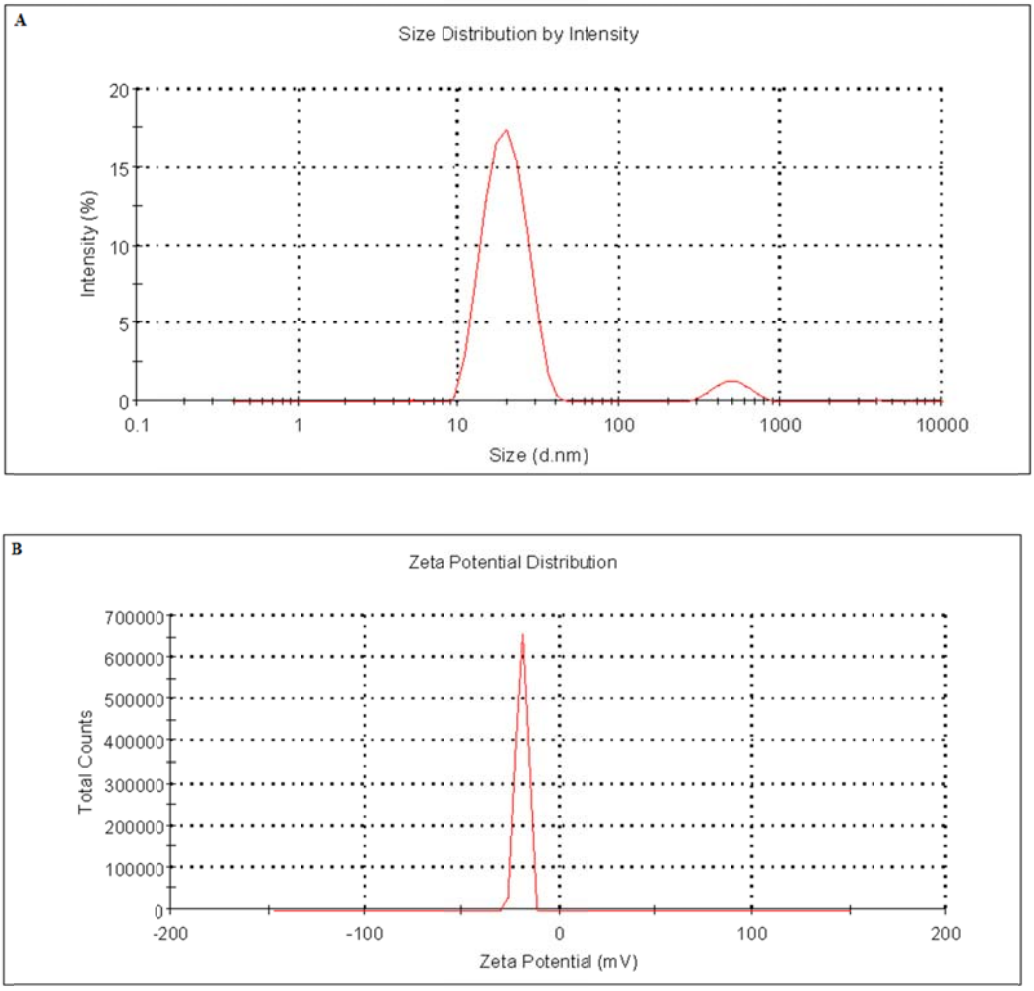

Figure 5.8. (A) Droplet size distribution curve and (B) ZP curve of optimized EFV S-SMEDDS after dilution with double distilled water.

5.7.5. Characterization of L- and S-SMEDDS

5.7.5.1. ZP measurement

ZP is related to surface charge of microemulsion droplet. It is highly dependent on surfactant used. The theory states that system remains stable due to deflocculation of microemulsion particles and for identical system ZP charge should be between ranges of -10 to -30 mV.[64] The charge of the oil droplets in conventional SMEDDS is negative due to the presence of free fatty acids. Non-ionic surfactants can be widely used and have minimal toxicity. Furthermore, the insensitivity of nonionic microemulsions to pH and electrolyte concentration relative to their ionic counterparts represents an added benefit.[65] The ZP results of diluted L-SMEDDS formulations are shown in Table 5.6. The values of ZP were ranged from -5.5 to -24.3 mV for tested EFV loaded SMEDDS formulations. The ZP obtained from reconstituted L-SMEDDS was -19.9 ± 0.45 mV, while ZP obtained from reconstituted S-SMEDDS was -19.2 ± 0.39 mV.

5.7.5.2. Conductivity

Conductivity measurements provide a means of determining whether a microemulsion is oil-continuous or water-continuous as well as providing a means of monitoring percolation or phase inversion phenomena.[66] Conductivity values of optimized L- and S-SMEDDS formulation were found to be 98.34 ± 0.14 µS and 98.12 ± 0.36 µS, respectively. Optimized SMEDDS formulations were water continuous and no phase inversion were observed.

5.7.5.3. Cloud point measurement

The cloud point is the temperature above which the formulation clarity turns into cloudiness. The cloud point is an essential factor in the SMEDDS consisting of non-ionic surfactants, and it is responsible for the successful formation of a stable microemulsion. When the temperature is higher than the cloud point, an irreversible phase separation will occur and the cloudiness of the preparation would have a bad

effect on drug absorption, because of the dehydration of the polyethylene oxide moiety.[29,67] Hence, the cloud point for SMEDDS should be above 37°C, which will avoid phase separation occurring in the gastrointestinal tract. The cloud point of optimized L- and S-SMEDDS formulation was found to be 83 ± 2.12 °C and 79 ± 2.39°C, respectively. Cloudiness was reversible after minutes. Therefore, it would suggest a stable microemulsion of EFV can be formed at physiological temperature *in vivo*.

5.7.5.4. pH

The excipients used in formulation decide the pH of the final preparation. Change in pH may change ZP of formulation which in turn can affect the stability of preparation. So pH is also responsible for stability of microemulsion. Optimized L- and S-SMEDDS formulations showed similar pH values in the range of 5.5 to 6.0. So here pH is not affecting stability. So it can be assumed that drug remains in oil phase only and since water is in external phase entire system showed pH of water.

Characterization of L-SMEDDS and S-SMEDDS are summarized in Table 5.9.

Table 5.9. Summary

	L-SMEDDS	**S-SMEDDS**
MDS	30.4 ± 0.15	32.8 ± 0.21
PDI	0.126	0.145
ZP	-19.9 ± 0.45	-19.2 ± 0.39
% T	98.72 ± 0.53	98.14 ± 0.11
Conductivity	98.34 ± 0.14	98.12 ± 0.36
Cloud point measurement	83 ± 2.12	79 ± 2.39
pH	5.7 ± 0.20	5.9 ± 0.10

Each value represents the mean ± SD (n = 3).

5.7.5.5. Solid state characterization of S-SMEDDS

DSC and XRD were performed to investigate the physical state of EFV in S-SMEDDS. DSC thermograms of EFV, Aerosil 200, their PM and S-SMEDDS are shown in Figure 5.9. The DSC curve of standard EFV exhibits a single endothermic peak at an onset temperature of 139.80°C, corresponding to its melting point. (Figure 5.9A) Aerosil 200 did not show any peak over the entire range of the tested temperatures (Figure 5.9B). The physical mixture was prepared by mixing well 250 mg of Aerosil 200 and 50 mg of EFV using mortar and pestle. Due to the dilution by Aerosil 200, the PM exhibited small endothermic peak for EFV. (Figure 5.9C) No obvious peak of the drug was found in the S-SMEDDS of EFV (Figure 5.9D), indicating that the drug must be present in molecularly dissolved state in S-SMEDDS.[14]

From X-ray diffractograms shown in Figure 5.10, the internal physical state of EFV in the S-SMEDDS was further verified. No obvious peaks representing crystals of EFV were seen for the S-SMEDDS.

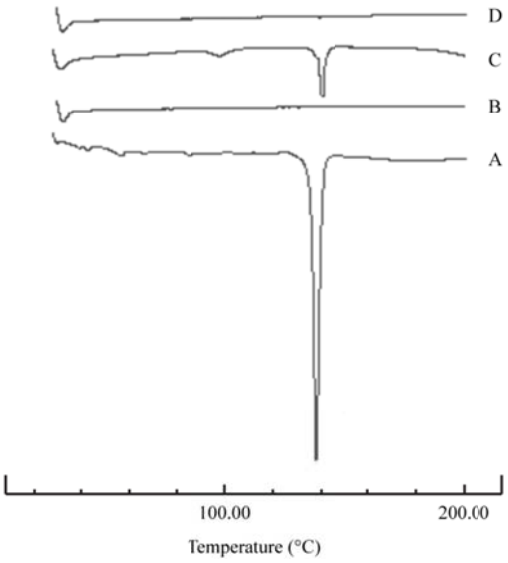

Figure 5.9. DSC thermograms of (A) standard EFV, (B) Aerosil 200, (C) PM, (D) S-SMEDDS.

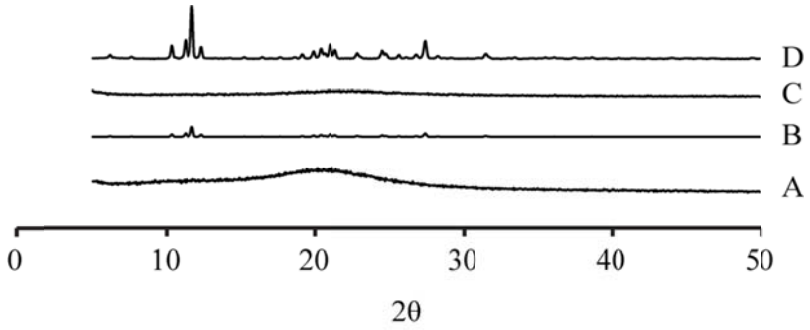

Figure 5.10. XRD spectra of (A) S-SMEDDS, (B) PM, (C) Aerosil 200, (D) standard EFV.

5.7.5.6. Morphology of L- and S-SMEDDS

For converting L-SMEDDS into the solid state, a highly porous powder with good oil adsorbing capacity is required. Such powders can adsorb oil components of the L-SMEDDS and convert them into a free flowing powder. SEM reveals the morphology of S-SMEDDS. As shown in Figure 5.11A, standard EFV appeared as crystalline nature. Aerosil 200 (Figure 5.11B) appeared with a rough surface with porous particles. Micrographs of S-SMEDDS shows L-SMEDDS is absorbed or coated inside the pores of Aerosil 200. (Figure 5.11C) Crystalline structures characteristic of EFV are not seen in S-SMEDDS micrographs suggesting that the drug is present in a completely dissolved state.

The morphology of diluted L-SMEDDS was examined with a TEM. (Figure 5.12) The microemulsion droplets appear dark with the bright surroundings. TEM image confirmed that the droplets of microemulsin are spherical in shape. Some droplet sizes are measured using TEM, as it is capable of point-to-point resolution. The droplet size is in agreement with the results obtained from droplet size analysis using zetasizer.

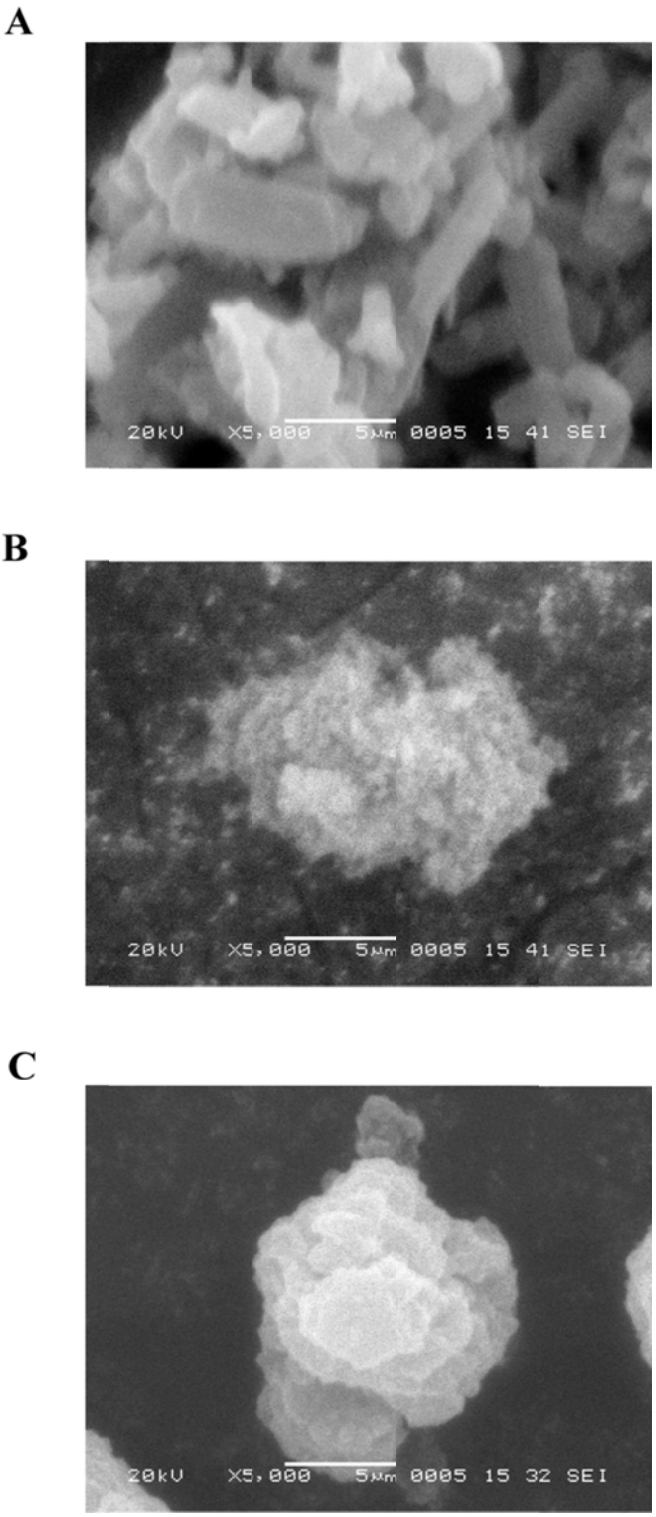

Figure 5.11. SEM images of (A) standard EFV (B) Aerosil 200 and (C) S-SMEDDS.

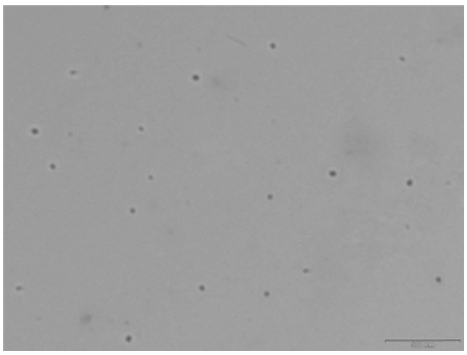

Figure 5.12. TEM image of diluted EFV loaded L-SMEDDS showing spherical shape of EFV particles in L-SMEDDS.

5.7.5.7. Dissolution study

The dissolution profiles of standard EFV, MF, L- and S-SMEDDS are illustrated in Figure 5.13 and Table 5.10. The dissolution rate was markedly enhanced in the L- and S-SMEDDS, as 92.45% ± 1.20 and 82.25% ± 1.06 of the drug dissolved in 5 min, as compared to only 4.72% ± 2.52 and 19.54% ± 0.75 from standard EFV and MF, respectively. The faster dissolution from SMEDDS may be attributed to the fact that in this formulation, the drug is in solubilized form and upon exposure to dissolution medium results in small droplets that can dissolve rapidly in the dissolution medium.[63] The standard EFV did not achieve complete dissolution during the 60 min test period and only 49.05% ± 5.13 of the drug dissolved over 60 min, owing to the large crystal size, while L- and S-SMEDDS showed a significantly enhanced dissolution rate with 99.78% ± 0.42 and 98.79% ± 0.44 of the drug dissolved over 60 min, respectively.

Different dissolution parameters are reported in Table 5.11. As can be seen, DE and DP values increased in the following order: standard EFV < MF < S-SMEDDS < L-SMEDDS; while the MDT and $t_{50\%}$ decreased in the same order. As the MDT and $t_{50\%}$ decreases, the drug release rate increases. The time to dissolve 50% of the drug was strongly reduced to 2.72 and 3.05 min for L- and S-SMEDDS, respectively, as compared to 16.2 min required for MF. The L- and S-SMEDDS showed a 1.49 and 1.45-fold higher AUC than MF, respectively. There was no significant difference observed between L- and S-SMEDDS.

Two dissolution profiles are declared similar if difference factor (f_1) is between 0 and 15 and if similarity factor (f_2) is between 50 and 100. The similarity factors f_2 were calculated between L- and S-SMEDDS. The value f_2 was 63.77 showed that the profiles are similar, ensuring that the S-SMEDDS preserved the improvement of *in vitro* dissolution of L-SMEDDS. The f_2 calculated on dissolution data of MF and S-SMEDDS formulation is 19.65 which indicate that MF is dissimilar to S-SMEDDS formulation.

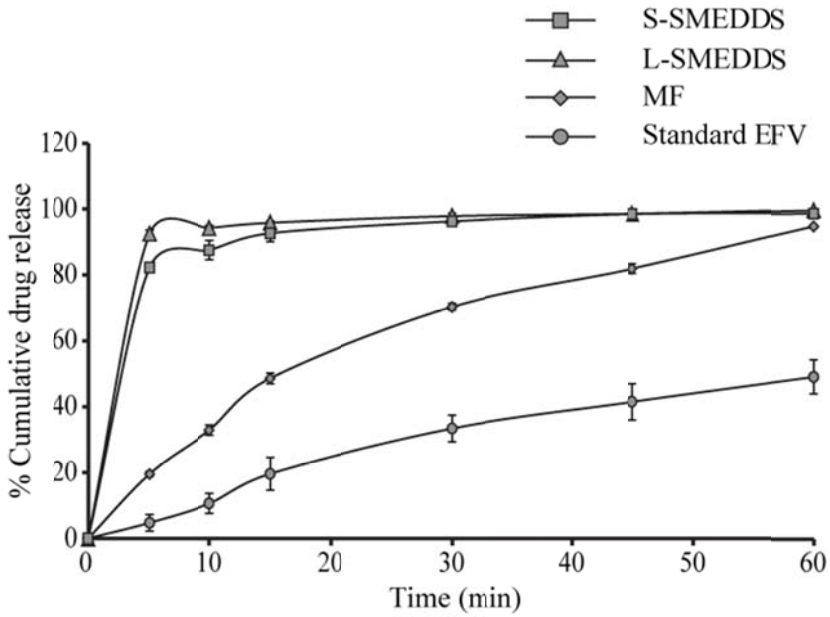

Figure 5.13. % Cumulative drug release of standard EFV (●), MF (♦), L-SMEDDS (▲), and S-SMEDDS (■)from capsule in 1% SLS in water dissolution media showing no significant difference between L- and S-SMEDDS whereas showing higher dissolution rate of SMEDDS compared to standard EFV and MF. Data are represented as Mean ± SD; n=3 for each group.

Table 5.10. Release profile of standard EFV, MF, L- and S-SMEDDS in dissolution media (1% SLS in water).

	% Cumulative Drug Release ± SD (n=3)			
Time (min)	**Standard EFV**	**MF**	**L-SMEDDS**	**S-SMEDDS**
5	4.72 ± 2.52	19.54 ± 0.75	92.45 ± 1.20	82.25 ± 1.06
10	10.59 ± 3.00	32.93 ± 1.51	94.22 ± 0.83	87.50 ± 2.88
15	19.58 ± 5.00	48.58 ± 1.60	95.79 ± 0.58	92.63 ± 2.48
30	33.36 ± 4.03	70.27 ± 1.08	97.81 ± 0.92	96.23 ± 0.72
45	41.47 ± 5.54	81.93 ± 1.47	98.55 ± 0.54	98.43 ± 0.34
60	49.05 ± 5.13	94.97 ± 0.54	99.78 ± 0.42	98.79 ± 0.44

Table 5.11. Comparison of dissolution parameters*

	Standard EFV	**MF**	**L-SMEDDS**	**S-SMEDDS**
DE_5%	2.36 ± 1.26	9.77 ± 0.37	46.23 ± 0.60	41.13 ± 0.53
DE_{60}%	29.38 ± 4.31	62.39 ± 0.41	93.08 ± 0.58	90.60 ± 0.97
DP_5%	4.72 ± 2.52	19.54 ± 0.75	92.45 ± 1.20	82.25 ± 1.06
DP_{60}%	49.05 ± 5.13	94.97 ± 0.54	99.78 ± 0.42	98.79 ± 0.44
$t_{50\%}$	>60	16.2 ± 0.97	2.72 ± 0.04	3.05 ± 0.07
MDT (min)	24.17 ± 1.63	20.58 ± 0.08	4.02 ± 0.29	4.98 ± 0.44
AUC	1762.7 ± 258.5	3743.4 ± 24.8	5585.05 ± 34.75	5435.96 ± 58.36

*Mean ± S.D. (n=3), DE: dissolution efficiency, DP: Dissolution percentage, $t_{50\%}$: time required for release 50% of drug, $t_{50\%}$: time required for release 50% of drug, MDT: mean dissolution time, AUC: Area under curve

5.7.5.8. Stability study

Dilution may better mimic conditions in the stomach following oral administration of SMEDDS pre-concentrate. Dilution study was done to access the effect of dilution on SMEDDS pre-concentrates. Diluted SMEDDS did not show any precipitation or phase separation on storage in various media. This suggests that all media were robust to dilution.

Microemulsions are thermodynamically stable systems and are formed at a particular concentration of oil, surfactant and water, with no phase separation, creaming or cracking. In thermodynamic stability studies, formulations selected were subjected to

different stress tests like centrifugation and freeze-thaw test. If the SMEDDS formulations are stable in this condition, metastable formulations thus avoided and frequent tests need not to be performed during storage. No phase separation and no change in droplet size of the optimized EFV SMEDDS formulations were observed on centrifugation and freeze-thaw test. Optimized SMEDDS formulation was found to be thermodynamically stable.

SMEDDS has a very limited shelf life owing to its liquid characteristics and the possibility of precipitation of the drug from the system. Thus, the developed optimized formulation was subjected to stability studies to evaluate its stability and the integrity of the dosage form. The physical and chemical stability of L- and S-SMEDDS formulations were evaluated at 4-8°C and 25°C for 6 months. It was found that there was no significant change in the MDS and PDI value when SMEDDS was stored at 4-8°C and 25°C over 6 months. As reported in Table 5.12, after 6 months storage at 4-8°C and 25°C of SMEDDS, the MDS of L-SMEDDS was 32.1 ± 1.17 nm and 31.9 ± 1.92 nm, for S-SMEDDS, MDS was 31.9 ± 1.03 nm and 33.9 ± 1.11 nm, respectively, which is in good agreement with zero time data. As seen from Table 5.12, the zeta-potential values did not change during the 6 months storage at 4-8°C and 25°C. Furthermore, the chemical stability of EFV was examined using an HPLC assay during this storage period. For instance, more than 97.6 % of EFV remained in the L- and S-SMEDDS formulations for up to 6 months when stored at 4-8°C and 25°C as shown in Table 5.13-5.14. The results of DE and DP at 5 and 60 min of stability samples are represented in Table 5.13-5.14. At the end of 60 min L- and S-SMEDDS gave dissolution of 99.14 ± 0.34 % and 98.19 ± 0.53 % after 6 months of storage at 4-8°C; 99.23 ± 0.48 % and 98.11 ± 0.70 % after 6 months of storage at 25°C, respectively, which is comparable to the release at time zero. No significant difference in dissolution was observed for stability samples of L- and S-SMEDDS compared to the dissolution of initial sample. These results suggest that the L- and S-SMEDDS can maintain the physical as well as chemical stability of the EFV during the shelf-life.

Table 5.12. Influence of time and temperature on the physical stability of EFV loaded L- and S-SMEDDS stored at different conditions and time intervals

Month	4-8°C			25°C		
	MPS (nm)	ZP (mV)	Drug content	MPS (nm)	ZP (mV)	Drug content
	L-SMEDDS					
0	31.6 ± 0.71	-20.3 ± 0.29	98.64 ± 0.44	31.6 ± 0.71	-20.3 ± 0.29	98.64 ± 0.44
1	31.2 ± 0.84	-19.8 ± 0.19	97.91 ± 0.25	29.2 ± 0.88	-21.4 ± 0.27	98.02 ± 0.48
2	30.8 ± 0.79	-18.5 ± 0.11	98.14 ± 0.54	30.4 ± 1.28	-19.4 ± 0.20	98.23 ± 0.36
3	31.4 ± 1.69	-19.9 ± 0.22	98.48 ± 0.33	30.1 ± 1.90	-20.5 ± 0.31	98.15 ± 0.62
6	32.1 ± 1.17	-19.5 ± 0.30	98.27 ± 0.41	31.9 ± 1.92	-20.1 ± 0.34	98.59 ± 0.53
	S-SMEDDS					
0	32.2 ± 0.94	-19.5 ± 0.19	97.84 ± 0.15	32.2 ± 0.94	-19.5 ± 0.19	97.84 ± 0.15
1	32.9 ± 1.10	-18.9 ± 0.17	97.68 ± 0.29	30.4 ± 0.87	-18.9 ± 0.31	98.12 ± 0.29
2	33.7 ± 0.63	-20.3 ± 0.28	97.89 ± 0.41	32.8 ± 0.72	-18.4 ± 0.29	98.28 ± 0.31
3	31.3 ± 0.82	-19.8 ± 0.18	98.12 ± 0.37	33.2 ± 1.01	-20.4 ± 0.33	98.11 ± 0.49
6	31.9 ± 1.03	-20.1 ± 0.10	98.03 ± 0.35	33.9 ± 1.11	-21.2 ± 0.30	98.37 ± 0.27

The values are shown as mean ± SD, n=3

5.7.5.9. PAMPA study

The effective permeability (P_e) values for the standard EFV, MF L- and S-SMEDDS are reported in Table 5.15. The L- and S-SMEDDS represents significant improvement in permeability than the MF in PAMPA model. Standard EFV demonstrated the lowest permeability (P_e value of 15.95×10^{-6} cm/s) whereas L- and S-SMEDDS showed P_e value of 21.27×10^{-6} and 19.96×10^{-6} cm/s, respectively. There was no significant difference observed between L- and S-SMEDDS. Thus, this is an indication that passive permeation of the drug has improved considerably on

formulating it into SMEDDS. Since the permeation rate of lucifer yellow was negligible, we could conclude that the membrane was integral.

Table 5.13. Influence of time and temperature on the chemical stability of EFV on L-SMEDDS stored at different conditions and time intervals

Month	Drug assay	DE_5%	DE_{60}%	DP_5%	DP_{60}%
	4-8°C				
0	99.5 ± 1.23	46.56 ± 0.32	93.08 ± 0.33	93.12 ± 0.63	99.16 ± 0.97
1	98.4 ± 0.59	46.12 ± 0.21	92.60 ± 0.30	92.24 ± 0.42	98.89 ± 1.30
2	97.6 ± 1.65	45.69 ± 0.17	92.43 ± 0.28	91.38 ± 0.34	98.90 ± 0.71
3	98.5 ± 0.89	46.10 ± 0.19	92.70 ± 0.18	92.19 ± 0.38	99.61 ± 0.73
6	98.8 ± 1.22	46.29 ± 0.15	92.73 ± 0.21	92.58 ± 0.29	99.14 ± 0.34
	25°C				
0	99.5 ± 1.23	46.45 ± 0.38	93.13 ± 0.29	92.89 ± 0.76	99.46 ± 1.02
1	98.5 ± 1.11	45.74 ± 0.22	92.56 ± 0.32	91.48 ± 0.45	99.09 ± 0.51
2	99.1 ± 0.74	46.28 ± 0.21	92.27 ± 0.11	92.55 ± 0.43	98.83 ± 0.66
3	98.9 ± 0.88	46.80 ± 0.19	93.10 ± 0.15	93.59 ± 0.38	99.52 ± 0.59
6	98.2 ± 1.03	46.29 ± 0.29	92.76 ± 0.21	92.58 ± 0.57	99.23 ± 0.48

The values are shown as mean ± SD, n=3

Table 5.14. Influence of time and temperature on the chemical stability of EFV on S-SMEDDS stored at different conditions and time intervals

Month	Drug assay	DE_5%	DE_{60}%	DP_5%	DP_{60}%
	4-8°C				
0	98.3 ± 0.43	41.13 ± 0.56	90.60 ± 0.22	82.25 ± 1.12	98.79 ± 0.39
1	97.8 ± 0.82	40.19 ± 0.66	89.76 ± 0.30	80.38 ± 1.31	98.13 ± 0.23
2	98.9 ± 1.06	40.64 ± 0.59	89.16 ± 0.19	81.28 ±1.18	97.72 ± 0.28
3	97.5 ± 0.58	39.62 ± 0.49	88.40 ± 0.16	79.23 ± 0.99	98.10 ± 0.29
6	98.2 ± 0.91	40.39 ± 0.37	89.48 ± 0.18	80.79 ± 0.75	98.19 ± 0.53
	25°C				
0	98.3 ± 0.43	40.91 ± 0.43	90.48 ± 0.14	81.82 ± 0.86	98.16 ± 0.51
1	98.5 ± 0.81	39.96 ± 0.94	88.61 ± 0.20	79.91 ± 1.88	98.24 ± 0.44
2	98.8 ± 1.04	40.19 ± 1.01	88.90 ± 0.34	80.37 ± 2.01	98.32 ± 0.63
3	98.8 ± 1.18	39.79 ± 0.48	88.13 ± 0.29	79.58 ± 0.96	97.73 ± 0.28
6	98.9 ± 1.01	40.21 ± 0.37	89.03 ± 0.24	80.42 ± 0.75	98.11 ± 0.70

The values are shown as mean ± SD, n=3

Table 5.15. Effective permeability value by PAMPA study (n=6)

	Effective permeability (P_e) ± S.D. (10^{-6} cm/s)
Standard EFV	15.95 ± 1.02
MF	16.84 ± 0.82
L-SMEDDS	21.27 ± 0.95
S-SMEDDS	19.96 ± 1.21

5.7.6. Evaluation of EFV loaded L- and S-SMEDDS

5.7.6.1. *In situ* absorption property of EFV in rat intestine

Among all absorption screening methods, *in situ* intestinal perfusion study in rats was considered as a simple and relevant method of absorption assessment and the absorption properties were most similar to human beings. The intestinal absorption kinetics of MF, L- and S-SMEDDS of EFV was investigated. The absorption parameters such as K_a, $t_{1/2}$, $AUC_{0\text{-}6h\ in\ situ}$ and uptake percentage are reported in Table 5.16. The K_a value of L- and S-SMEDDS were 0.6630 ± 0.13 h^{-1} and 0.5701 ± 0.10 h^{-1}, which was 2.62- and 2.25-fold higher as compared with that of MF (K_a = 0.2537 ± 0.01 h^{-1}), respectively. The $t_{1/2}$ of MF, L- and S-SMEDDS was found to be 2.73 ± 0.11, 1.07 ± 0.20 h and 1.24 ± 0.21 h, respectively. Significant difference was observed in percentage uptake between MF and SMEDDS. The $AUC_{0\text{-}6h\ in\ situ}$ of L- and S-SMEDDS were 164.68 ± 5.03 and 151.03 ± 5.38 mg·h which was 1.71- and 1.57-fold higher as compared with that of MF (96.37 ± 4.50 mg·h), respectively. There was no significant difference observed in absorption parameters of L- and S-SMEDDS. The absorption curve of MF, L- and S-SMEDDS in the rat small intestine was shown in Figure 5.14. The absorption curve of SMEDDS represents significant improvement in drug absorption than the MF. The results indicate that intestinal permeability of EFV was increased in SMEDDS form. This enhancement may be attributed to lipid composition of SMEDDS. Lipids, as compositions of intestine mucous membrane, have an important effect on absorption enhancement via the lymphatic route.[68]

After incubation with the harvest blank perfusion solution for 6 h at 37°C, the EFV concentration was found to be 98.97 % ± 0.56 and 99.07 % ± 0.93 for L- and S-

SMEDDS, respectively, of the original concentration at 0 h. Results indicated that EFV was stable in blank intestinal perfusion solution.

Table 5.16. Absorption parameters of LNS and MF.

Absorption parameter	L-SMEDDS	S-SMEDDS	MF
K_a (h^{-1})	0.6630 ± 0.13	0.5701 ± 0.10	0.2537 ± 0.01
$t_{1/2}$ (h)	1.07 ± 0.20	1.24 ± 0.21	2.73 ± 0.11
Uptake percentage (%)	98.89 ± 0.66	98.09 ± 1.26	80.97 ± 0.64
$AUC_{0\text{-}6h\ in\ situ}$ (mg·h)	164.68 ± 5.03	151.03 ± 5.38	96.37 ± 4.50

The values are shown as mean ± SD, n=3

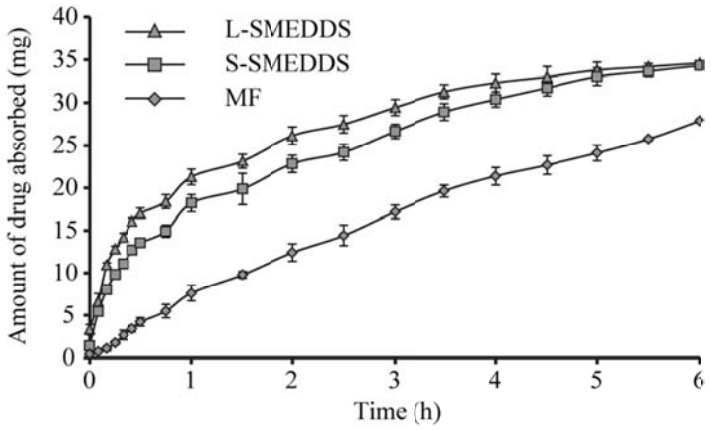

Figure 5.14. Amount of EFV absorbed from MF (♦), L-SMEDDS (▲) and S-SMEDDS (■) during *in situ* single pass intestinal perfusion studies showing higher absorption rate of EFV in SMEDDS compared to MF. Data are represented as Mean ± SD; n=3 for each group.

5.7.6.2. *In vivo* pharmacokinetic study

Pharmacokinetic studies were performed in rabbits to investigate the improvement in oral bioavailability of EFV in L- and S-SMEDDS. The plasma drug concentration–time profiles and pharmacokinetic parameters of standard EFV, MF L- and S-SMEDDS resulted from the oral administration in rabbits are illustrated in Figure 5.15 and Table 5.17, respectively. The plasma drug concentration profile of SMEDDS

represents significant improvement in drug absorption than the MF. The L- and S-SMEDDS gave significantly higher AUC_{0-t} and C_{max} of EFV than did MF. The AUC_{0-t} of EFV was 30724.51 ± 511.24 and 31157.05 ± 1751.39 ng·h/ml for L- and S-SMEDDS, which was 2.13- and 2.16-fold higher as compared with MF (14408.93 ± 2538.73 ng·h/ml), respectively. The C_{max} of L- and S-SMEDDS were approximately 2.10- and 1.97-fold greater than that of MF, respectively. Additionally, t_{max} of L- and S-SMEDDS formulations was all shorter than that of the MF, suggesting that SMEDDS could improve drug release and absorption in GIT. However, t_{max} of S-SMEDDS was relatively delayed compared to L-SMEDDS (2.5 h vs. 2.0 h), consistent with the dissolution performances.

Mean residence time (MRT) of the L- and S-SMEDDS was decreased 2.47- and 2.32-fold compared to the MF, respectively. The plasma clearance values of standard EFV, MF, L- and S-SMEDDS were found to be 2.06 ± 0.37, 1.29 ± 0.22, 0.60 ± 0.02 and 0.60 ± 0.03 ml/h, respectively. The volume of distribution of standard EFV, MF, L- and S-SMEDDS were found to be 48.03 ± 6.85, 23.34 ± 3.64, 11.47 ± 0.84 and 11.00 ± 0.03 L, respectively. EFV loaded L- and S-SMEDDS were absorbed easily which led to increased AUC_{0-t}, C_{max} and decreased t_{max}, MRT.

Increased bioavailability of SMEDDS may due to its lymphatic transport through transcellular pathway.[69] It is also reported that the long-chain oils promote lipoprotein synthesis and subsequent lymphatic absorption.[70] The main rate-limiting barrier for drug absorption/diffusion is the single layer of intestinal epithelial cell. High content of surfactants in SMEDDS could increase the permeability by disturbing the cell membrane.[4] It should be noted that the surfactant with best enhancement ability requires both hydrophilic and lipophilic domains reaching a balance with intermediate values of HLB such as Tween 20 used in our study, having a polyoxyethylene and intermediate hydrocarbon chain. Its structural characteristics impart both lipophilic and hydrophilic properties to the surfactant, allowing it to partition between lipid and protein domains. Surfactant also demonstrated a reversible effect on the opening of tight junction; it may interact with the polar head groups of the lipid bilayers, modifying hydrogen bonding and ionic forces between these groups. It may also insert itself between the lipophilic tails of the bilayers, resulting in a disruption of the

lipid-packing arrangement.[4,71] Surfactants can reduce the interfacial surface tension and enhance penetration of EFV to the epithelial cells.

These results indicated that the bioavailability of EFV in SMEDDS was found to be better as compared to MF attributed to spontaneous formation of a microemulsion in GIT, when EFV loaded SMEDDS administered orally, presenting EFV in a dissolved form will be beneficial to enhance its absorption. The initial rate of absorption from S-SMEDDS tended to be slightly lower than from L-SMEDDS. However, there was no significantly statistical difference between L- and S-SMEDDS. Our results showed that it is possible to improve the bioavailability of EFV if given in the S-SMEDDS and suggested that the S-SMEDDS was kept well as a solid form of L-SMEDDS.

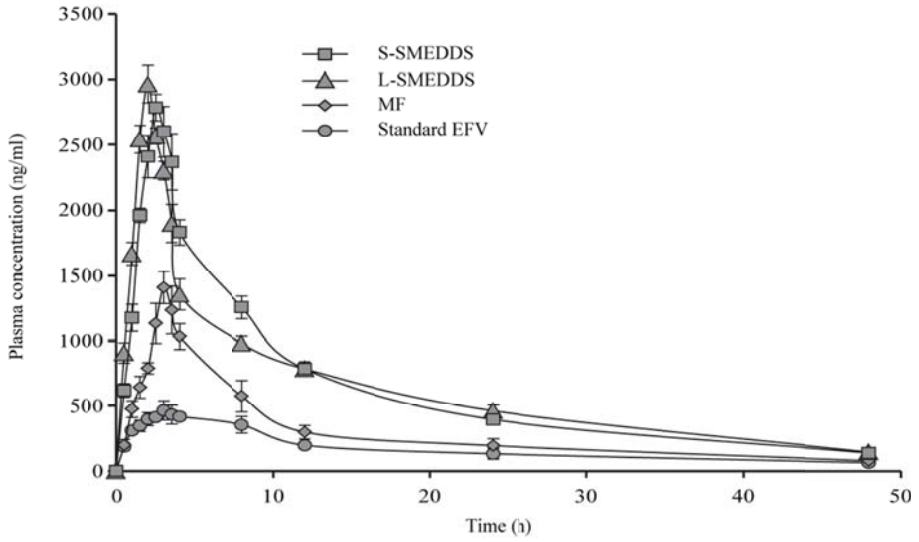

Figure 5.15. Plasma concentration-time curves for standard EFV (●), MF (♦), L-SMEDDS (▲) and S-SMEDDS(■) after oral administration in rabbits at a dose of 10 mg/kg of EFV showing higher absorption rate and enhanced bioavailability of EFV in SMEDDS.Data are represented as Mean ± SD; n=3 for each group.

Table 5.17. Pharmacokinetic parameters after oral administration of standard EFV, MF and LNS in rabbits at a dose of 10 mg/kg of EFV

Pharmacokinetic parameters	Standard EFV	MF	L-SMEDDS	S-SMEDDS
C_{max} (ng/ml)	466.9 ± 70.2	1409.1 ± 123.0	2963.9 ± 143.4	2782.8 ± 101.5
t_{max} (h)	3.00	3.00	2.00	2.50
k_a (h^{-1})	0.91 ± 0.055	0.44 ± 0.071	0.37 ± 0.08	0.69 ± 0.004
k_{el} (h^{-1})	0.04 ± 0.0012	0.06 ± 0.0001	0.06 ± 0.002	0.06 ± 0.0002
$t_{1/2}\alpha$ (h)	0.76 ± 0.046	1.60 ± 0.24	1.92 ± 0.44	1.00 ± 0.01
$t_{1/2}\beta$ (h)	16.19 ± 0.47	12.02 ± 0.03	11.87 ± 0.46	11.00 ± 0.03
V_d (L)	48.03 ± 6.85	23.34 ± 3.64	11.47 ± 0.84	9.41 ± 0.63
V_{ss} (L)	37.96 ± 5.42	18.92 ± 2.90	8.87 ± 0.35	8.24 ± 0.48
TCR (L/h)	2.06 ± 0.35	1.35 ± 0.21	0.67 ± 0.06	0.59 ± 0.57
$AUC_{0\rightarrow t}$ (ng·h/ml)	8379.6 ± 1476.3	14408.9 ± 2538.7	30724.5 ± 511.2	31157.1 ± 1751.4
$AUC_{t\rightarrow\infty}$ (ng·h/ml)	1521.51 ± 253.51	1378.02 ± 152.92	2514.17 ± 341.20	2220.34 ± 154.10
$AUC_{0\rightarrow\infty}$ (ng·h/ml)	9901.10 ± 1729.84	15786.95 ± 2691.65	33238.68 ± 825.30	33377.40 ± 1904.69
$AUMC_{0\rightarrow t}$ (ng·h^2/ml)	131575.42 ± 27681.23	193481.24 ± 38776.73	418484.76 ± 17164.98	399219.47 ± 21721.56
MRT (h)	15.64 ± 0.56	13.39 ± 0.34	13.62 ± 0.50	12.81 ± 0.03
Cl (ml/h)	2.06 ± 0.37	1.29 ± 0.22	0.60 ± 0.02	0.60 ± 0.03

Data are shown as mean ± SD, n=3. C_{max} - Plasma peak concentration; t_{max} - The time to reach maximum plasma concentration; k_a – Absorption rate constant; k_{el} - Elimination rate constant; $t_{1/2}\alpha$ - Distribution half-life; $t_{1/2}\beta$ - Elimination half-life; V_d - Volume of distribution; V_{ss} - Volume of distribution at steady state; TCR – Total clearance rate; AUC - Area under the plasma-concentration–time curve; $AUMC_{0\rightarrow t}$ - Total area under the first moment curve; MRT - Mean residence time; Cl - Total body clearance.

5.8. Conclusion

The purpose of this study was to develop an oral administrable SMEDDS of the poorly water soluble drug, EFV. Solubility evaluation, pseudoternary phase diagram and self-emulsification test were carried out to select excipients of SMEDDS. Composition of EFV loaded SMEDDS was optimized using factorial design. Optimal SMEDDS contains captex 500 as oil phase, tween 20 as a surfactant and transcutol

HP as cosurfactant, in the ratio of 25:50:25 %w/w, formulates SMEDDS with lower droplet size (30.4 nm), PDI (0.126), and ZP (-19.9 mV) values. The L-SMEDDS converted into S-SMEDDS using Aerosil 200 as a solid carrier. Both DSC measurements and X-ray diffraction analysis suggested that EFV in the S-SMEDDS may be in the molecular dispersion state. Following self-emulsification in water the droplet size distribution of the S-SMEDDS was nearly same to the L-SMEDDS, and the in vitro dissolution performance was similar for L- and S-SMEDDS both significantly higher than the MF. The L- and S-SMEDDS were physically and chemically stable over 6 months. The *in vitro* transport study in PAMPA model demonstrated that L- and S-SMEDDS was successful in enhancing the permeation of EFV. The results of *in situ* absorption of EFV in rat intestine suggested that SMEDDS played an important role in absorption enhancing effect. Pharmacokinetic evaluation clearly showed that the EFV loaded L- and S-SMEDDS exhibited improved pharmacokinetic properties compared to the MF. The oral bioavailability of EFV from S-SMEDDS was 2.16-fold higher than the MF and no significant difference compared with the L-SMEDDS. Our results illustrated the potential use of S-SMEDDS to dispense poorly water soluble drug by oral route.

REFERENCES

1 Stegemann, S., Leveiller, F., Franchi, D., de Jong, H. & Linden, H. When poor solubility becomes an issue: From early stage to proof of concept. *European Journal of Pharmaceutical Sciences* **31**, 249-261, (2007).

2 Pouton, C. W. Lipid formulations for oral administration of drugs: non-emulsifying, self-emulsifying and 'self-microemulsifying' drug delivery systems. *Eur J Pharm Sci* **11**, S93-S98, (2000).

3 Kang, B. K. *et al.* Development of self-microemulsifying drug delivery systems (SMEDDS) for oral bioavailability enhancement of simvastatin in beagle dogs. *International journal of pharmaceutics* **274**, 65-73, (2004).

4 Dixit, A. R., Rajput, S. J. & Patel, S. G. Preparation and bioavailability assessment of SMEDDS containing valsartan. *Aaps Pharmscitech* **11**, 314-321, (2010).

5 Shown, I., Banerjee, S., Ramchandran, A. V., Geckeler, K. E. & Murthy, C. N. Synthesis of Cyclodextrin and Sugar-Based Oligomers for the Efavirenz Drug Delivery. *Macromol Symp* **287**, 51-59, (2010).

6 Sathigari, S. *et al.* Physicochemical Characterization of Efavirenz-Cyclodextrin Inclusion Complexes. *Aaps Pharmscitech* **10**, 81-87, (2009).

7 Serajuddin, A. T. M. Solid dispersion of poorly water-soluble drugs: Early promises, subsequent problems, and recent breakthroughs. *Journal of pharmaceutical sciences* **88**, 1058-1066, (1999).

8 Patravale, V. B., Date, A. A. & Kulkarni, R. M. Nanosuspensions: a promising drug delivery strategy. *Journal of Pharmacy and Pharmacology* **56**, 827-840, (2004).

9 Pollock, S., Dwek, R. A., Burton, D. R. & Zitzmann, N. N-Butyldeoxynojirimycin is a broadly effective anti-HIV therapy significantly enhanced by targeted liposome delivery. *AIDS* **22**, 1961-1969, (2008).

10 Chiappetta, D. A., Hocht, C., Taira, C. & Sosnik, A. Oral pharmacokinetics of the anti-HIV efavirenz encapsulated within polymeric micelles. *Biomaterials* **32**, 2379-2387, (2011).

11 Chiappetta, D. A., Hocht, C. & Sosnik, A. A Highly Concentrated and Taste-Improved Aqueous Formulation of Efavirenz for a More Appropriate Pediatric Management of the Anti-HIV Therapy. *Curr Hiv Res* **8**, 223-231, (2010).

12 Joshi, M., Pathak, S., Sharma, S. & Patravale, V. Solid microemulsion preconcentrate (NanOsorb) of artemether for effective treatment of malaria. *International journal of pharmaceutics* **362**, 172-178, (2008).

13 Elnaggar, Y. S. R., El-Massik, M. A. & Abdallah, O. Y. Self-nanoemulsifying drug delivery systems of tamoxifen citrate: Design and optimization. *International journal of pharmaceutics* **380**, 133-141, (2009).

14 Balakrishnan, P. *et al.* Enhanced oral bioavailability of dexibuprofen by a novel solid self-emulsifying drug delivery system (SEDDS). *Eur J Pharm Biopharm* **72**, 539-545, (2009).

15 Mura, P., Valleri, M., Cirri, M. & Mennini, N. New solid self-microemulsifying systems to enhance dissolution rate of poorly water soluble drugs. *Pharmaceutical development and technology*, (2010).

16 Ito, Y. *et al.* Oral solid gentamicin preparation using emulsifier and adsorbent. *Journal of Controlled Release* **105**, 23-31, (2005).

17 Yi, T., Wan, J. L., Xu, H. B. & Yang, X. L. A new solid self-microemulsifying formulation prepared by spray-drying to improve the oral bioavailability of poorly water soluble drugs. *Eur J Pharm Biopharm* **70**, 439-444, (2008).

18 Yan, Y. D. *et al.* Enhanced Oral Bioavailability of Curcumin via a Solid Lipid-Based Self-Emulsifying Drug Delivery System Using a Spray-Drying Technique. *Biol Pharm Bull* **34**, 1179-1186, (2011).

19 Chen, Y. *et al.* Development of a Solid Supersaturatable Self-Emulsifying Drug Delivery System of Docetaxel with Improved Dissolution and Bioavailability. *Biol Pharm Bull* **34**, 278-286, (2011).

20 Wang, Z. Y. *et al.* Solid self-emulsifying nitrendipine pellets: Preparation and in vitro/in vivo evaluation. *International journal of pharmaceutics* **383**, 1-6, (2010).

21 Kasim, N. A. *et al.* Molecular properties of WHO essential drugs and provisional biopharmaceutical classification. *Mol Pharmaceut* **1**, 85-96, (2004).

22 Takano, R. *et al.* Oral absorption of poorly water-soluble drugs: Computer simulation of fraction absorbed in humans from a miniscale dissolution test. *Pharmaceutical research* **23**, 1144-1156, (2006).

23 Bindu Madhavi B, K. B., Krishna Chatanya CH, Naga Madhu M, Sri Harsha V , David Banji. Dissolution enhancement of efavirenz by solid dispersion and PEGylation techniques. *International journal of pharmaceutical investigation* **1**, 29-34, (2011).

24 Baert, L. *et al.* Development of an implantable infusion pump for sustained anti-HIV drug administration. *Int J Pharm* **355**, 38-44, (2008).

25 Basalious, E. B., Shawky, N. & Badr-Eldin, S. M. SNEDDS containing bioenhancers for improvement of dissolution and oral absorption of lacidipine. I: Development and optimization. *International journal of pharmaceutics* **391**, 203-211, (2010).

26 Cui, S. X. *et al.* Preparation and evaluation of self-microemulsifying drug delivery system containing vinpocetine. *Drug Dev Ind Pharm* **35**, 603-611, (2009).

27 Shafiq, S. *et al.* Development and bioavailability assessment of ramipril nanoemulsion formulation. *Eur J Pharm Biopharm* **66**, 227-243, (2007).

28 Teeranachaideekul, V., Junyaprasert, V. B., Souto, E. B. & Muller, R. H. Development of ascorbyl palmitate nanocrystals applying the nanosuspension technology. *Int J Pharm* **354**, 227-234, (2008).

29 Zhang, P., Liu, Y., Feng, N. & Xu, J. Preparation and evaluation of self-microemulsifying drug delivery system of oridonin. *International journal of pharmaceutics* **355**, 269-276, (2008).

30 *http://www.usp.org/sites/default/files/usp_pdf/EN/USPNF/pendingStandards-/m4047.pdf*.

31 Zhang, Y. *et al.* DDSolver: an add-in program for modeling and comparison of drug dissolution profiles. *Aaps J* **12**, 263-271, (2010).

32 Date, A. A. & Nagarsenker, M. S. Design and evaluation of self-nanoemulsifying drug delivery systems (SNEDDS) for cefpodoxime proxetil. *International journal of pharmaceutics* **329**, 166-172, (2007).

33 Singh, A. K. *et al.* Exemestane loaded self-microemulsifying drug delivery system (SMEDDS): development and optimization. *Aaps Pharmscitech* **9**, 628-634, (2008).

34 Hiremath, P. S., Soppimath, K. S. & Betageri, G. V. Proliposomes of exemestane for improved oral delivery: Formulation and in vitro evaluation using PAMPA, Caco-2 and rat intestine. *Int J Pharm* **380**, 96-104, (2009).

35 Singh, S. P., Wahajuddin, Tewari, D., Pradhan, T. & Jain, G. K. PAMPA permeability, plasma protein binding, blood partition, pharmacokinetics and metabolism of formononetin, a methoxylated isoflavone. *Food Chem Toxicol* **49**, 1056-1062, (2011).

36 *http://www.bdbiosciences.com/external_files/dl/doc/manuals/live/web_enabled/353015_pug.pdf*.

37 Stewart, W. W. Functional Connections between Cells as Revealed by Dye-Coupling with a Highly Fluorescent Naphthalimide Tracer. *Cell* **14**, 741-759, (1978).

38 Liu, H. L. *et al.* In vitro permeability of poorly aqueous soluble compounds using different solubilizers in the PAMPA assay with liquid chromatography/mass spectrometry detection. *Pharmaceutical research* **20**, 1820-1826, (2003).

39 Cirri, M., Mura, P. & Mora, P. C. Liquid spray formulations of xibornol by using self-microemulsifying drug delivery systems. *Int J Pharm* **340**, 84-91, (2007).

40 Zhou, P., Li, L. P., Luo, S. Q., Jiang, H. D. & Zeng, S. Intestinal absorption of luteolin from peanut hull extract is more efficient than that from individual pure luteolin. *Journal of agricultural and food chemistry* **56**, 296-300, (2008).

41 Song, N. N., Li, Q. S. & Liu, C. X. Intestinal permeability of metformin using single-pass intestinal perfusion in rats. *World J Gastroentero* **12**, 4064-4070, (2006).

42 Zakeri-Milani, P. *et al.* Predicting human intestinal permeability using single-pass intestinal perfusion in rat. *J Pharm Pharm Sci* **10**, 368-379, (2007).

43 Stewart, B. H., Chan, O. H., Jezyk, N. & Fleisher, D. Discrimination between drug candidates using models for evaluation of intestinal absorption. *Adv Drug Deliver Rev* **23**, 27-45, (1997).

44 Cui, J. *et al.* Enhancement of oral absorption of curcumin by self-microemulsifying drug delivery systems. *Int J Pharm* **371**, 148-155, (2009).

45 Li, H. L. *et al.* Enhancement of gastrointestinal absorption of quercetin by solid lipid nanoparticles. *J Control Release* **133**, 238-244, (2009).

46 Gao, Y. *et al.* Formulation optimization and in situ absorption in rat intestinal tract of quercetin-loaded microemulsion. *Colloid Surface B* **71**, 306-314, (2009).

47 Chen, Y. *et al.* Self-microemulsifying drug delivery system (SMEDDS) of vinpocetine: Formulation development and in vivo assessment. *Biol Pharm Bull* **31**, 118-125, (2008).

48 Shin, S. C., Bum, J. P. & Choi, J. S. Enhanced bioavailability by buccal administration of triamcinolone acetonide from the bioadhesive gels in rabbits. *Int J Pharm* **209**, 37-43, (2000).

49 Lawrence, M. J. & Rees, G. D. Microemulsion-based media as novel drug delivery systems. *Advanced drug delivery reviews* **45**, 89-121, (2000).

50 Charman, S. A. *et al.* Self-Emulsifying Drug Delivery Systems - Formulation and Biopharmaceutic Evaluation of an Investigational Lipophilic Compound. *Pharmaceutical research* **9**, 87-93, (1992).

51 Constantinides, P. P. Lipid microemulsions for improving drug dissolution and oral absorption: physical and biopharmaceutical aspects. *Pharmaceutical research* **12**, 1561-1572, (1995).

52 Shah, N. H., Carvajal, M. T., Patel, C. I., Infeld, M. H. & Malick, A. W. Self-Emulsifying Drug-Delivery Systems (Sedds) with Polyglycolyzed Glycerides for Improving in-Vitro Dissolution and Oral Absorption of Lipophilic Drugs. *International journal of pharmaceutics* **106**, 15-23, (1994).

53 Singh, A. K. *et al.* Oral Bioavailability Enhancement of Exemestane from Self-Microemulsifying Drug Delivery System (SMEDDS). *Aaps Pharmscitech* **10**, 906-916, (2009).

54 Khoo, S. M., Humberstone, A. J., Porter, C. J. H., Edwards, G. A. & Charman, W. N. Formulation design and bioavailability assessment of lipidic self-emulsifying formulations of halofantrine. *International journal of pharmaceutics* **167**, 155-164, (1998).

55 Marten, B., Pfeuffer, M. & Schrezenmeir, J. Medium-chain triglycerides. *Int Dairy J* **16**, 1374-1382, (2006).

56 Kawakami, K., Yoshikawa, T., Hayashi, T., Nishihara, Y. & Masuda, K. Microemulsion formulation for enhanced absorption of poorly soluble drugs - II. In vivo study. *Journal of Controlled Release* **81**, 75-82, (2002).

57 Kommuru, T. R., Gurley, B., Khan, M. A. & Reddy, I. K. Self-emulsifying drug delivery systems (SEDDS) of coenzyme Q10: formulation development and bioavailability assessment. *International journal of pharmaceutics* **212**, 233-246, (2001).

58 Pouton, C. W. Lipid formulations for oral administration of drugs: non-emulsifying, self-emulsifying and 'self-microemulsifying' drug delivery systems. *European journal of pharmaceutical sciences : official journal of the European Federation for Pharmaceutical Sciences* **11 Suppl 2**, S93-98, (2000).

59 Gursoy, R. N. & Benita, S. Self-emulsifying drug delivery systems (SEDDS) for improved oral delivery of lipophilic drugs. *Biomedicine & pharmacotherapy = Biomedecine & pharmacotherapie* **58**, 173-182, (2004).

60 Patel, A. R. & Vavia, P. R. Preparation and in vivo evaluation of SMEDDS (self-microemulsifying drug delivery system) containing fenofibrate. *The AAPS journal* **9**, E344-352, (2007).

61 Craig, D. Q. M., Lievens, H. S. R., Pitt, K. G. & Storey, D. E. An Investigation into the Physicochemical Properties of Self-Emulsifying Systems Using Low-Frequency Dielectric-Spectroscopy, Surface-Tension Measurements and Particle-Size Analysis. *International journal of pharmaceutics* **96**, 147-155, (1993).

62 Malcolmson, C. & Lawrence, M. J. A Comparison of the Incorporation of Model Steroids into Nonionic Micellar and Microemulsion Systems. *Journal of Pharmacy and Pharmacology* **45**, 141-143, (1993).

63 Nekkanti, V., Karatgi, P., Prabhu, R. & Pillai, R. Solid self-microemulsifying formulation for candesartan cilexetil. *Aaps Pharmscitech* **11**, 9-17, (2010).

64 Liu, R. *Water-insoluble drug formulation*. 2nd edn, 203 (CRC Press, 2008).

65 Attwood, D., Mallon, C., Ktistis, G. & Taylor, C. J. A study on factors influencing the droplet size in nonionic oil-in-water microemulsions. *International journal of pharmaceutics* **88**, 417-422, (1992).

66 Kizilbash, N. A., Asif, S., Nazar, M. F., Shah, S. S. & Alenizi, D. Design of a Microemulsion-Based Drug Delivery System for Diclofenac Sodium. *J Chem Soc Pakistan* **33**, 1-6, (2011).

67 Itoh, K., Tozuka, Y., Oguchi, T. & Yamamoto, K. Improvement of physicochemical properties of N-4472 part I formulation design by using self-microemulsifying system. *International journal of pharmaceutics* **238**, 153-160, (2002).

68 Khoo, S. M., Shackleford, D. M., Porter, C. J. H., Edwards, G. A. & Charman, W. N. Intestinal lymphatic transport of halofantrine occurs after oral administration of a unit-dose lipid-based formulation to fasted dogs. *Pharmaceutical research* **20**, 1460-1465, (2003).

69 Baboota, S., Shakeel, F., Ahuja, A., Ali, J. & Shafiq, S. Design, development and evaluation of novel nanoemulsion formulations for transdermal potential of celecoxib. *Acta Pharm* **57**, 315-332, (2007).

70 Charman, W. N. & Stella, V. J. Transport of Lipophilic Molecules by the Intestinal Lymphatic-System. *Advanced drug delivery reviews* **7**, 1-14, (1991).

71 Wu, W., Wang, Y. & Que, L. Enhanced bioavailability of silymarin by self-microemulsifying drug delivery system. *Eur J Pharm Biopharm* **63**, 288-294, (2006).

CHAPTER 6:

DEVELOPMENT OF EFAVIRENZ PLGA NANOPARTICLES

6.1. Introduction

An estimated 60 million people are infected with human immunodeficiency type-1 (HIV-1) worldwide.[1] The majority of infected people live in the developing world with limited treatment resources. Antiretroviral (ARV) therapy has significantly reduced HIV-1 disease morbidity and improved life expectancy. However, the economics of drug treatment, treatment failures due to the development of resistance, and limited global access has prevented world-wide utility of ARV therapy.[2,3] Dosing regimens that require multiple daily dosing with diet considerations and ARV side effects have compromised the achievement of long-term HIV-1 suppression in infected patients.[4] Additionally, the use of ARV requires a concerted level of commitment from the patient to prevent treatment failure due to resistance.

The CD4+ T lymphocyte is the major target for infection by HIV-1. Cells of the mononuclear phagocyte system also serve as a reservoir for HIV. Macrophages are mature, non-proliferating and immunologically active cells that can be productively infected with HIV-1 and HIV-2.[5-7] Altered cellular functions in the macrophage population may contribute to the development and clinical progression of AIDS. Evidence has accumulated that cells of the macrophage lineage are vectors for the transmission of HIV-1. The placental macrophage is likely to be the primary cell type responsible for vertical transmission of HIV-1.[8] An important property of HIV-1 for mucosal transmission is the ability to infect macrophages.[9] Because of the important role of cells of the monocytes/macrophage lineage in the pathogenesis of HIV-1, fully effective AR must react with monocytes/macrophage in addition to other targets.

Many promising compounds suffer from poor physiochemical properties leading to poor solubility and biodistribution. Such properties limit drug-receptor interactions to cause desired effects. Nanoparticles are stable, solid colloidal particles consisting of macromolecular material ranging in size from 10 to 1,000 nm. Drugs can be adsorbed on the particle surface, entrapped within the particle, or dissolved in the particle matrix.[10] Nanoparticles represent an interesting carrier system for the transport of antiviral drugs to monocytes/macrophage in an attempt to reduce the required dose, minimize toxicity and side effects, and improve the delivery of substances, which have insufficient intracellular uptake.

Biodegradable NP can be successfully used for modulating the drug release profile by controlling the polymer degradation. One of the best known biodegradable carriers for controlled and sustained release is poly lactide-co-glycolide (PLGA).[11] Features such as biocompatibility, prediction of biodegradation kinetics, ease of fabrication and regulatory approval has attracted its attention for a variety of biomedical applications.[12,13] Moreover, both hydrophilic and lipophilic drugs can be successfully encapsulated in the PLGA matrix.[14] PLGA has been used for delivery of drugs for both oral[15,16] and parenteral[17,18] routes. FDA has already approved some of the formulations using PLGA which are currently being marketed and others are at various stages of clinical trials.[19]

Efavirenz (EFV) is a crystalline lipophilic solid with an aqueous solubility of 3-9 μg/ml and with a low intrinsic dissolution rate of 0.037 mg/cm^2/min. Hence, it has very low bioavailability.[20,21] To achieve effective therapy against viral diseases for orally administered drugs, it is essential that the drug should be adequately and consistently absorbed. The frequent administration of several drugs in relatively high doses is a main cause of patient incompliance.[22] The reason for this is very low solubility of EFV hinders its administration, absorption and biodistribution. These problems can be overcome by designing target-specific drug delivery systems. Macrophages possess various receptors such as fucose receptors, mannosyl, galactosyl, and many others.[23] Mannose receptors are present at the surface of monocyte macrophages, alveolar macrophages, astrocytes in brain, hepatocytes in liver and so on.[24-27] Therefore, targeting of ARV drugs to HIV infected macrophages could be a positive approach in improving the therapeutic efficacy and reducing the toxicity of ARV drugs.

In the present study, EFV loaded PLGA NPs were prepared and their formulation parameters were statistically optimized using 3^2 factorial designs. Incorporation of mannose (MN) in PLGA was carried out and EFV loaded PLGA-MN NPs were prepared. The optimized formulations were characterized for particle size, entrapment efficiency, differential scanning calorimetry (DSC) and transmission electron microscopy (TEM). The formulations were evaluated for *in vitro* drug release, *in vitro* drug uptake in peritoneal macrophages and *in vivo* biodistribution study.

6.2. Materials and instruments

EFV was kindly gifted by Merck Ltd. (Mumbai, India). PLGA was obtained as a gift sample from Boehringer Ingelheim, Germany. Excipients used for formulation development are shown in Table 6.1 and were used as received. Chemicals and reagents used for the preparation of buffers, analytical solutions, and other general experimental purposes are shown in Table 6.2. Equipments used at various stages are listed in Table 6.3. Purified HPLC grade water was obtained by filtering double distilled water through nylon filter paper 0.45 μm pore size and 47 mm diameter (Pall Life sciences, Mumbai, India). RPMI, fetal bovine serum (FBS), fetal calf serum (FCS), phosphate buffered saline (PBS), thioglycollate medium, penicillin, streptomycin were purchased from Himedia, India.

Table 6.1. List of excipients

Excipients	**Manufacturer/Supplier**
6-Coumarin	Sigma, India
Mannitol	S.D. Fine Chemicals, Mumbai, India
Mannose	Sigma, India
Polaxamer 188	BASF, Germany
Poloxamer 407	BASF, Germany
Poly vinyl alcohol	S.D. Fine Chemicals, Mumbai, India
Trehalose	S.D. Fine Chemicals, Mumbai, India

Table 6.2. List of chemicals and reagents

Chemicals/Reagents	**Manufacturer/Supplier**
3-(4,5-dimethylthiazole-2-yl)-2,5-diphenyltetrazoliumbromide (MTT)	Himedia, India
Acetone, HPLC grade	Spectrochem Labs Ltd, Vadodara, India
Acetonitrile, HPLC grade	Spectrochem Labs Ltd, Vadodara, India
Ammonium acetate buffer, AR grade	S.D. Fine Chemicals, Mumbai, India
Dimethylformamide	Sigma, India
Dimethyl sulphoxide	S.D. Fine Chemicals, Mumbai, India
Hydrochloric acid, AR grade	Spectrochem Labs Ltd, Vadodara, India
Isopropyl alcohol	Spectrochem Labs Ltd, Vadodara, India
Methanol, HPLC grade	Spectrochem Labs Ltd, Vadodara, India
1-ethyl-3-C3-dimethyl aminopropyl carbodiimide (EDC HCl)	Sigma, India
Orthophosphoric acid, HPLC grade	Spectrochem Labs Ltd, Vadodara, India
Phenol	S.D. Fine Chemicals, Mumbai, India
Sodium Hydroxide	S.D. Fine Chemicals, Mumbai, India
Sulphuric acid	S.D. Fine Chemicals, Mumbai, India
Tetrahydrofuran	S.D. Fine Chemicals, Mumbai, India
Tris buffer	Sigma, India
Triton X-100	S.D. Fine Chemicals, Mumbai, India
Tert- butyl methyl ether, HPLC grade	Spectrochem Labs Ltd, Vadodara, India

Table 6.3. List of instruments

Equipment	**Manufacturer/Supplier**
Bath sonicator	B. N. Scientific Enterprise, India
Centrifuge	Remi Instrument
Column oven	PCI Analytics, India
Differential scanning calorimeter (DSC 60)	Shimadzu, Japan
High performance liquid chromatography	Shimadzu, Japan
Magnetic stirrer	Remi equipments Pvt Ltd., India
Particle size analyzer (Malvern Zetasizer Nano ZS)	Malvern Instrument, UK
pH meter	LabIndia, India
Transmission electron microscopy	Tecnai 20 Philips
UV-visible spectrophotometer (UV-1700)	Shimadzu, Japan
Vortex mixer	Spinix, Japan
Weighing Balance	Shimadzu, Japan
X-ray diffractometer	Bruker AXS D8, Germany

6.3. Development of PLGA nanoparticles

PLGA nanoparticles were prepared using nanoprecipitation method.[28] The formulation was prepared by dissolving PLGA and EFV in organic solvent. This organic phase was added into aqueous phase contains surfactant with continuous stirring on magnetic stirrer at room temperature. Stirring was continued for 3-4 h to allow complete evaporation of organic solvent. Finally, traces of organic solvent were eliminated under reduced pressure in rotary flask evaporator at 40°C for 30 min. The formulation optimizations in the development of nanoparticles are discussed in the following sections.

6.3.1. Formulation optimization

The optimized formulation was selected on the basis of particle size, PDI and % entrapment efficiency (% EE).

6.3.1.1. Preliminary experiments for PLGA nanoparticles

Preliminary experiments were carried out by varying one parameter at a time, while keeping other constant, so that effect of various parameters could be evaluated. For Preliminary experiments, various parameters like type of organic phase (Acetone, Acetonitrile (ACN) and Tetrahydrofuran (THF)), type of surfactant (Poloxamer 188, Poloxamer 407 and poly vinyl alcohol (PVA)), ratio of organic phase to aqueous phase (3:10, 4:10 and 5:10) and concentration of PLGA (1.0, 1.25 and 1.5 % w/v) were varied and the effect on particle size of PLGA nanoparticles was studied. The parameters were optimized to obtain nano-ranged particles with narrow size distribution.

6.3.1.2. Optimization of EFV loaded PLGA nanoparticles using factorial design

Studies based on factorial designs allow all the factors to be varied simultaneously, thus enabling evaluation of the effects of each variable at each level and showing interrelationship among them. Most important variables which affect the system function are selected and systematic experiments are then performed to the specified factorial design. The number of independent variables selected decides the number of experiments that are to be performed. A prior knowledge and understanding of the process and the process variables under investigation is necessary for achieving a more realistic model.

Two independent factors selected for this study included drug: polymer ratio and surfactant concentration. These factors were operated at three levels i.e., +1, 0 and −1. Type of surfactant (Poloxamer 188), type of solvent (Acetone), ratio of organic phase:aqueous phase (5:10) and rate of addition of organic phase to aqueous phase (0.5 ml/min) were kept same for all the experiments.

A two-factor, three-level factorial design was generated by Design-Expert® 8.0 software to conduct the study. A total of 9 experiments were designed by the software. Table 6.4 shows the independent factors and their design levels used in this study. Dependent variables were MPS (Y_1) and % EE (Y_2). After generating the polynomial equations relating dependent and independent variables, the process was

optimized for responses Y_1 and Y_2 values. Optimization was performed to obtain the levels of independent variables, which minimize Y_1 while maximizing Y_2.

Table 6.4. Variables for 3^2 factorial design.

Independent variables		Design level		
Uncoded	**Coded**	**Low (-1)**	**Middle (0)**	**High (+1)**
Drug : Polymer ratio	X_1	5:50	7.5:50	10:50
Concentration of surfactant (%w/v)	X_2	0.50	0.75	1.00

6.3.1.3. Mannose (MN) incorporation in PLGA (PLGA-MN)

Incorporation of MN to COOH terminated PLGA was achieved by using EDC as an activator.[29] Carboxylic group of PLGA (1 gm) was activated by addition of EDC (100 mg) in distilled DMF (free from moisture) and stirred for 1 h in ice-cold condition to form PLGA-EDC. After 45 min, MN (2 gm) was added in to it and was allowed to stir at room temperature overnight. PLGA-MN was then precipitated with addition of ice-cold water. Reaction mixture was centrifuged to collect precipitates. The excess reagents and soluble by-products in precipitate were then washed three times using cold water and centrifuged at 10000 RPM for 15 min to collect precipitate. Precipitate was dispersed in water and lyophilized (HetoDry, Germany). Lyophilised product was stored under refrigeration till further use.

6.3.1.3.1. Level of MN incorporation

The ester bonds between MN and PLGA molecules were dissociated before analysis of MN. In this method, 2 ml NaOH (1N) solution was added to a dispersion of MN-PLGA (10 mg) in 200 µl water and stirred overnight. The pH was adjusted to neutral with HCl, followed by centrifugation at 10000 rpm for 15 min and MN in supernatant was then analyzed. MN quantification was accomplished by colorimetric assay using phenol-sulfuric acid method.[30] In this method, 1.50 mL of concentrated sulfuric acid (96%) was added rapidly to 50 µL of supernatant in ria vials. This was followed by the addition of 300 µL of 5% (w/v) phenol and mixing. The vials were then placed in a heated water bath for 5 min at 90 °C to allow for color development followed by

cooling down to room temperature to stop the reaction. The absorbance was read at 490 nm.

6.3.1.4. Preparation of PLGA NPs

EFV loaded PLGA NPs were prepared by solvent diffusion (nanoprecipitation) technique as described by Fessi *et al*.[28] The organic phase (acetone) containing EFV (7.5 mg) and PLGA (50 mg) were slowly injected (0.5 mL/min) into 10 ml of aqueous phase containing Poloxamer 188 (0.5% w/v) as stabilizer on a magnetic stirrer (Remi Equipments, Mumbai). With the diffusion of solvent in to the aqueous phase, the polymer precipitates with entrapped EFV in polymer matrix, leading to formation of EFV loaded PLGA NPs. The resulting nanoparticle dispersion was further stirred to evaporate the organic phase under vacuum on rotary flask evaporator (Superfit Equipments, India). NPs were recovered by centrifugation for 30 min at 25,000 rpm at 4°C (Sigma 3K30, Germany) washed three times with distilled water to remove excess surfactant, resuspended with double distilled water. EFV loaded PLGA-MN NPs were prepared in same way by replacing PLGA with PLGA-MN. 6-coumarin loaded nanoparticles were prepared in similar way with addition of 6-coumarin (2 mg) in place of EFV.

6.3.1.5. Lyophilization of EFV loaded NPs

The major limitation of colloidal carriers is their instability i.e. they tend to agglomerate during storage. In liquid formulations the agglomeration may be caused due to a greater surface area of the system and the resulting thermodynamic instability that favors aggregation of colloidal particles. The freeze drying of the liquid NPs formulations therefore is necessary as it is one of the well-established methods of preservation of unstable molecules over a long period of time. To the suspension of the optimized batch from the above studies, different cryoprotectants like mannitol and trehalose were added in different concentrations before freeze-drying. The effect of these cryoprotectants at different cryoprotectant to nanoparticle ratios (1:1, 3:1 and 5:1) on the re-dispersibility of the freeze-dried formulations and the size of the

nanoparticles before and after freeze-drying was investigated. Briefly, EFV NPs were cooled down to −70°C for 12 h followed by freeze-dried in a freeze-drier (Heto DryWinner, Denmark) under vacuum for 24 h. The lyophilized product was re-dispersed with the double distilled filtered water.

6.4. Characterization of EFV loaded NPs formulations

6.4.1. Particle size measurement

The particle size analysis and PDI of EFV NPs were determined using a Malvern Zeta Sizer Nano ZS 90 (Malvern Instruments, Malvern, UK). The PDI indicates the width of particle distribution (e.g. 0.0 for a narrow, 0.5 for a very broad distribution in the sample matrix). Prior to the measurement, the samples were diluted with double distilled filtered water to a suitable scattering intensity and re-dispersed by handshaking before the measurement. All measurements were performed in triplicate. The results are expressed as mean ± standard deviation (SD).

6.4.2. ZP measurement

The ZP is a measure of the electric charge at the surface of the particles indicating the physical stability of colloidal systems. ZP was measured using a Zeta Sizer Nano ZS 90 (Malvern Instruments, Malvern, UK). Each sample was suitably diluted with double distilled filtered water and placed in a disposable zeta cell. The ZP values were assessed by determining the particle electrophoretic mobility. The electrophoretic mobility was converted to the ZP via the Helmholtz–Smoluchowski equation. All measurements were performed in triplicate. The results are expressed as mean ± SD.

6.4.3. Entrapment efficiency

Lyophilized NPs were dissolved in acetonitrile. The content of EFV is estimated using HPLC (Shimadzu Corporation, Kyoto, Japan) method after suitable dilution with acetonitrile. Chromatographic separation was performed using a Phenomenex

Hypersil C4 (100 mm × 4.6 mm i.d., 5 µm particle size) column. Separation was achieved using a mobile phase consisting of acetonitrile and 100 mM ammonium acetate buffer pH 7.0 in the ratio of 45:55 (v/v), pumped at a flow rate of 1 ml/min. The eluent was monitored using UV detector at a wavelength of 247 nm. Column was maintained at 40°C and an injection volume of 20 µl was used. The % EE was calculated as a ratio of the total entrapped EFV to the total amount of EFV used as below equation:

$$\% \text{ EE} = \frac{\text{Amount of Entrapped drug X 100}}{\text{Total added drug}}$$

6.4.4. DSC analysis

Thermal properties of the lyophilized NPs samples were investigated with a Shimadzu differential scanning calorimeter (Shimadz, Japan). Thermograms of standard EFV, PLGA, PLGA-MN, and lyophilized EFV loaded NPs were recorded in order to characterize the physical state of EFV in the NPs. A heating rate of 10°C/min was employed in the range of 25-300°C with nitrogen atmosphere supplied at 40 ml/min. Each sample was taken (~4-8 mg) in an aluminium pan, crimped and sealed. An empty aluminum pan was used as reference.

6.4.5. Morphology of NPs by TEM

Morphological evaluation of EFV loaded PLGA and PLGA-MN NPs was conducted through TEM (Tecnai 20 Philips). For TEM analysis, NPs was diluted with double distilled water and a drop of it was placed on a carbon-coated copper grid (300 mesh, 3mm) and air dried.

6.4.6. *In-vitro* drug release study

In vitro diffusion study of EFV loaded PLGA and PLGA-MN NPs were performed in 1% SLS in water, selected as the drug release medium. Nanoparticle suspension (3 ml corresponding to 1.5 mg of EFV) transferred into a dialysis membrane (MW cut-off:

12000 Da, Himedia India). The dialysis bag was placed in 25 mL release medium. The release study was performed at 37℃ on magnetic stirrer. At preselected time intervals, 1 ml samples were withdrawn and replaced with 1 ml of pre-thermostated fresh dissolution medium. Samples were filtered through 0.1 µm syringe filter; filtrate was diluted with acetonitrile and 20 µl was injected into HPLC for analysis. Dissolution tests were performed in triplicate. Graph of percent cumulative drug release *vs.* time was plotted.

6.4.7. Stability studies

Stability is defined as the capacity of a drug substance or drug product to remain within established specifications to maintain its identity, strength, quality, and purity throughout the retest or expiration periods. Nanoparticles have been extensively used to deliver a wide range of drugs as they can protect the drug from metabolizing enzymes, acidic degradation and also from oxidative degradation as the drug remains in encapsulated or entrapped form which prevent exposure of drug. During preparation, particulate delivery systems are lyophilized and, although compactly arranged, can be readily suspended in aqueous media after being stored at 4°C. However, storage temperature is important in maintaining the integrity of these delivery systems.

The stability studies were performed for the lyophilized NPs. The samples were kept in transparent glass vials and stored at 4-8°C (refrigerator) and at 25°C for up to 3 months. At different time points the samples were withdrawn and were subjected to reconstitution properties, particle size, zeta potential and drug content studies. During sampling, the vials were visually examined for the evidence of any change in cake morphology and discoloration.

6.5. Evaluation of EFV NPs formulation

6.5.1. Animals

Male Albino rats (200 ± 15 g) were used for *in vitro* and *in vivo* study. Animals were maintained at a temperature of 25 ± 2°C and a relative humidity of 70 ± 5% under natural light/dark conditions and were fed with food and water *ad libitum*. Prior to experiment the animals were kept under overnight fasting. Animal experiments were approved by the Institute Animal Ethics Committee of Pharmacy Department (Protocol No. FTE/PHR/CPCSEA/2007/04) and were conducted as per the guidelines of the Committee for the Purpose of Control and Supervision of Experiments on Animals, India.

6.5.2. Isolation of rat peritoneal macrophages

The two most convenient sources of primary macrophages are the bone marrow and the peritoneal cavity.[31,32] Resident peritoneal macrophages can readily be harvested from mice and purified by adherence to tissue culture plastic. The injection of thioglycollate broth into the peritoneal cavity produces an inflammatory response allowing the purification of large numbers of elicited macrophages. The macrophages obtained by the following protocol are normally 90% pure and can be used further for assay like drug uptake, phagocytosis etc.

Rats were injected with 5 ml thioglycollate medium (3% w/v Brewer's complete thioglycollate broth) in peritoneal cavity using a syringe with 27 G needle. After 72 h, rats were anaesthetized and macrophages were harvested. All external areas of the rat were disinfected with 70% IPA. Small incision in the abdominal region was made and the skin was gently ripped downward to expose the intra-peritoneal cavity. Sterile PBS (10 ml) was injected into the intra-peritoneal cavity using a syringe with a 23 G needle and the abdomen was massaged gently for 2 minutes. The injected PBS was retracted using syringe with 18 G needle. Care was taken not to injure the internal organs during this process. The microphage suspension was centrifuged at 1300 rpm for 10 min at 4°C. Supernatant was discarded and 1 ml of Gey's balancing salt solution (Sigma-aldrich, USA) was added. The solutions were mixed properly with

micropipette slowly and incubated on ice for 2-5 minutes. 1 ml of FBS was added to this suspension and centrifuged at 1300 rpm for 10 min at 4°C. Washed with PBS containing 5% FBS and then suspended in 1ml of RPMI supplemented with FCS and antibiotics. The cells were counted using hemocytometer. Peritoneal cells were seeded in different well plates and incubated for 60 minutes at 37°C. The nonadherent cells were removed by washing 3 times in 0.5 ml warm PBS, using a gentle swirling action. The adherent cells normally contain >90% macrophages.

6.5.3. Cell viability by MTT assay

The 3-(4,5-dimethylthiazole-2-yl)-2,5-diphenyltetrazoliumbromide (MTT) assay is widespread method to assess cell viability.[33,34] MTT is colorimetric assay that measures the reduction of yellow MTT by mitochondrial succinate dehydrogenase. The MTT enters the cells and passes into the mitochondria where it is reduced to an insoluble, coloured (dark purple) formazan product. The cells are then solubilized with organic solvent and the released, solubilized formazan reagent is measured spectrophotometrically. Since reduction of MTT only occurs in metabolically active cells, the level of activity is measure of the viability of the cells.

The effect of EFV, EFV loaded PLGA NPs and PLGA-MN NPs on cell proliferation was determined by MTT based colorimetric assay. Isolated macrophage cells were plated onto 96-well, flat-bottomed plates at 5-10 × 10^3 cells per well. 200 µl of growth medium was added to each well. After incubation of 24 h at 37˚C in CO_2 incubator, medium was removed and treated with 200 µl medium containing varying concentrations of EFV, EFV loaded PLGA NPs and PLGA-MN NPs ranging from 0.1, 1, 10 and 100 µg/ml. Again plate was incubated at 37°C in CO_2 incubator for 48 h. After 48 h, medium was removed, replaced with medium containing 100 µl MTT (500 µg/ml) and incubated for 4 h. The medium containing MTT was removed from wells and remaining MTT-formazan crystals were dissolved by adding 100 µl of DMSO was added to all the wells and incubated for 30 min at room temperature with constant shaking. Absorbance was read at 570 nm using ELX800 Universal Microplate Reader (Bio-Tek instruments, Inc, Winooski, VT) and subsequently % cell viability was calculated. The amount of MTT that is converted to formazan indicates the number of viable cells.

6.5.4. *In vitro* drug uptake study

Isolated rat peritoneal macrophages are used for *in vitro* uptake study of EFV loaded PLGA and PLGA-MN NPs. Peritoneal macrophage cells were seeded in 24 well plates at the density of 3×10^5 cells per well. 500 µl RPMI medium containing EFV, EFV loaded PLGA NPs and PLGA-MN NPs, at concentration of 100 µg/ml, were added to six wells of I, II and III rows. The amount of EFV was kept same in all the wells. The plates were incubated in a controlled environment at a temperature of 37° ± 1°C for a period of 48 hours. During incubation of the plates, at appropriate time points of 0, 1, 4, 8, 24 and 48 hours, the medium from each well was removed and cells were harvested mechanically from each well using fresh RPMI media. The cells were separated from the medium in the form of a pellet by centrifuging at 4000 rpm for 15 minutes. About 0.5 ml of Triton X-100 was added to the pellet to rupture the cells and the mixture incubated at 25°C for 5-6 hours and then centrifuged at 4000 rpm for 15 minutes. Supernatants were analysed by HPLC after suitable dilution with acetonitrile to determine dug uptake.

6.5.5. Fluorescence microscopy

Fluorescence microscopy was performed to study the qualitative uptake of prepared NPs by macrophage cells. The 6-coumarin was used as a fluorescent marker and loaded into PLGA-NPs and PLGA-MN NPs instead of EFV. 6-coumarin is a lipophilic fluorescent dye. The major advantage is its high fluorescence even at low dye loading in NPs. Isolated peritoneal macrophage cells were seeded in 6 well plates at the density of 1×10^5 cells per well and incubated for 60 min to allow cell attachment. After 60 min, cells were treated with 6-coumarin loaded PLGA NPs and PLGA-MN NPs followed by incubated for 60 min for phagocytosis. After treatment all well plates were washed with PBS buffer for 3 times. 500 µl of PBS was added in to each well and visualized under fluorescence microscope.

6.5.6. *In Vivo* biodistribution study

Rats were allocated to three treatment groups. The lyophilized EFV loaded PLGA NPs and PLGA-MN NPs powder was weighed and the equivalent of 20 mg/kg was dissolved in PBS and injected intraperitoneal to first and second group of rats, respectively.[35] EFV was dissolved in ethyl alcohol and then further dissolved in PBS and injected intraperitoneal to third group. The three animals of each group were sacrificed at time point 1, 3, 6, 12, and 24 hours. Tissues of interest (Brain, Kidney, Liver, Lung and Spleen) were collected immediately after, lightly rinsed with normal saline and dried with tissue paper. Plasma and tissue samples were frozen at -20°C until analysed by HPLC.

6.6. Results and discussion

6.6.1. Preliminary study

Nano-precipitation technique involves a spontaneous gradient-driven diffusion of water miscible organic solvents into the continuous aqueous phase. This process may apparently appear simple, but it may involve complex interfacial hydrodynamic phenomenon. Here the addition of organic solution of polymer and drug resulted in spontaneous emulsification of the oily solution in the form of nano-droplets. This occurs as a result of some kind of interface instability arising from rapid diffusion of the acetone across the interface and marked decrease in the interfacial tension. The origin of the mechanism of nanosphere formation could be explained in terms of interfacial turbulence between two unequilibrated liquid phases, involving flow, diffusion and surface processes (Marangoni effect). The interfacial turbulence is caused by localized lowering of the interfacial tension where the oil phase undergoes rapid and erratic pulsations each of which is quickly damped out by a viscous drag.

The molecular mechanism of interfacial turbulence could be explained by the continuous formation of eddies of solvent (e.g. acetone) at the interface. Such eddies originate either during drop formation or in thermal inequality in the system. Thus, once the process has started, movements associated with previous kicks change the pressure inside the solvent by increasing the surface pressure inside the solvent or decreasing the interfacial tension. Thus, if the solvent droplets formed contain

polymer, these will tend to aggregate and form nanoparticles because of continuous diffusion of solvents and because of the presence of a non-solvent medium.[36] Among various factors, solute transfer out of the phase of higher viscosity, concentration gradients near the interface and interfacial tension sensitive to solute concentration are the most important factors. The presence of surfactant may markedly complicate the situation since they act to suppress interfacial flow and the rapid diffusion of acetone to the aqueous phase. The main advantage of surfactants in process is the instantaneous and reproducible formation of nanometric, monodispersed nanospheres exhibiting a high drug loading capacity.[28,37]

Type of organic phase, type of surfactant and ratio of organic phase to aqueous phase have marked effect on particle size and PDI value of the PLGA NPs. Concentration of surfactant (0.5% w/v), PLGA (50 mg), EFV (5 mg) and rate of addition of organic phase into aqueous phase (0.5 ml/min) were kept same for all the experiments.

6.6.1.1. Selection of organic solvent

Three different organic solvents namely acetone, ACN and THF were used for preparation of PLGA NPs. Results are presented in Table 6.5. Better organic solvent was selected based on size of nanoparticles formed. The MPS of NPs, prepared with acetone is significantly lower than that with acetonitrile and THF.

Table 6.5. Selection of organic phase

Formulation Parameters				
Organic phase	**Surfactant**	**Ratio of organic phase:aqueous phase**	**MPS ± SD (n=3)**	**PDI ± SD (n=3)**
Acetone	Poloxamer 188	5:10	175.29 ± 3.27	0.110 ± 0.008
Acetonitrile	Poloxamer 188	5:10	288.13 ± 4.91	0.214 ± 0.027
Tetrahydrofuran	Poloxamer 188	5:10	341.96 ± 3.12	0.308 ± 0.015

6.6.1.2. Selection of surfactant

Three different surfactants were initially used for formulation development namely poloxamer 188, poloxamer 407 and PVA. From these better one is selected based on resultant particle size. Results are presented in Table 6.6. Smallest particle size was observed with poloxamer 188 as compared to poloxamer 407 and PVA. So poloxamer 188 was used as stabilizer for further development of formulation. For selection of stabilizer it was necessary to investigate reconstitution property and solid state stability. Non-ionic surfactants (poloxamer 188 and 407) provide steric repulsion between the particles causing a reduction in surface tension of the particles resulting in lower particle size.[38,39] After reconstitution study it was found that poloxamer 188 readily reconstituted while poloxamer 407 and PVA show lump formation. Size increase on storage also found significantly high with poloxamer 407.

Table 6.6. Selection of surfactant

Formulation Parameters					
Organic phase	**Surfactant**	**Ratio of organic phase:aqueous phase**	**MPS ± SD (n=3)**	**MPS ± SD (n=3) (After reconstitution)**	**PDI ± SD (n=3) (After reconstitution)**
Acetone	Poloxamer 188	5:10	175.29 ± 3.27	187.14 ± 4.22	0.123 ± 0.005
Acetone	Poloxamer 407	5:10	238.12 ± 4.36	275.27 ± 5.31[a]	0.413 ± 0.014
Acetone	PVA	5:10	267.23 ± 4.28	NA[b]	NA

[a] Few aggregates were observed. Sonication required for reconstitution.
[b]Lump formation was observed.

6.6.1.3. Effect of organic: aqueous phase volume ratio on particle size and entrapment efficiency

Organic to Aqueous phase volume ratio was found to have a profound effect on particle size and % EE. As the ratio increased, the MPS decreased and % EE increased (Table 6.7). This can be attributed to lower volume of organic phase rapidly mixes with the aqueous phase, causing faster precipitation and therefore giving larger particles in comparison to higher volume of organic phase.[40] As the ratio decreases

the % EE decreases because the evaporation rate of solvent is less and the drug diffuses into the aqueous phase and also the viscosity of the organic phase is less at lower ratios. Hence the droplet size formed before precipitation is smaller resulting lower % EE. [41,42]

Table 6.7. Effect of organic: aqueous phase volume ratio

Formulation Parameters					
Organic phase	**Surfactant**	**Ratio of organic:aqueous phase**	**MPS ± SD (n=3)**	**PDI ± SD (n=3)**	**% EE ± SD (n=3)**
Acetone	Poloxamer 188	3:10	189.22 ± 3.15	0.129 ± 0.009	62.70 ± 3.81
Acetone	Poloxamer 188	4:10	183.30 ± 2.88	0.136 ± 0.010	64.29 ± 2.13
Acetone	Poloxamer 188	5:10	175.29 ± 3.27	0.110 ± 0.008	77.28 ± 3.12

6.6.1.4. Effect of polymer concentration on particle size and % EE

The polymer concentration is varied from 1.0 to 1.5 %w/v while keeping other processing parameters at standard conditions. Increasing the polymer concentration leads to a gradual increase in particle size was observed that can be attributed to increase in viscosity of the organic phase which led to a reduction in net shear stress and promoting the formation of droplets with larger size (Table 6.8). Also the increased viscosity of the organic phase would hinder rapid dispersion of PLGA solution into the aqueous phase resulting in larger droplets. These large droplets would form larger NPs as the solvent evaporates.[41,43] In addition, as the polymer concentration increases the amount needed of poloxamer 188 (stabilizer) that is insufficient to cover the surface of droplets completely resulting in coalescence of droplets during solvent evaporation and hence aggregation of NPs occurs which lead to higher particle size.

The increase in polymer concentration increases the organic phase viscosity, which increases the diffusional resistance to drug molecules from organic phase to the aqueous phase, thereby enhancing the % EE of drug in NPs.[42,44] Additionally, the

increase of particle size may be relevant to the increase of drug % EE.[44] The increase of nanoparticles size with the increasing PLGA concentration can increase the length of diffusional pathways of drug from the organic phase to the aqueous phase, thereby reducing the drug loss through diffusion and increasing the drug % EE.[45] As the polymer concentration increases there is an increase in the ZP towards the negative side because of the improperly shielded functional groups on the surface.

Table 6.8. Effect of PLGA concentration on particle size and % entrapment efficiency

	PLGA concentration (%w/v)		
	1.0	**1.25**	**1.5**
MPS ± SD (n=3)	175.29 ± 3.27	237.00 ± 4.37	298.61 ± 5.24
PDI ± SD (n=3)	0.110 ± 0.008	0.134 ± 0.012	0.141 ± 0.010
% EE ± SD (n=3)	77.28 ± 3.12	81.14 ± 3.43	85.36 ± 4.01

Organic Phase: Acetone
EFV: 5 mg
Surfactant: Poloxamer 188 (0.5 %w/v)
Ratio of organic:aqueous phase: 5:10

6.6.2. Optimization of EFV loaded PLGA nanoparticles using factorial design

The effect of drug : polymer ratio and surfactant (Poloxamer 188) concentration on particle size was assessed by using Design-Expert® 8.0 software. The factor levels are evenly spaced and coded for low, medium and high settings, as −1, 0 and +1. The experimental runs and the observed and predicted responses for the 9 formulations are reported in Table 6.9. The values of response Y_1 (MPS) and Y_2 (% EE) ranges from 146.23 to 294.33 nm and 72.67 to 91.23 %, respectively. The ratio of maximum to minimum for both the responses Y_1 and Y_2 is 2.01 and 1.26, respectively; therefore power transformation was not applied to the obtained values.

The selection of model for analyzing the response was done based on the comparisons of several statistical parameters including SD, R-squared values and predicted residual sum of square (PRESS). The chosen model should have low SD, high R-squared value and lower PRESS value. The details of which are mentioned in Table 6.10 and 6.11, which suggests quadratic model for analyzing the both the responses. The predicted R-Squared of 0.9987 and 0.9867 is in reasonable agreement with the

adjusted R-Squared of 0.9997 and 0.9971 for MPS and % EE, respectively. The higher value of correlation coefficients signifies an excellent correlation between the independent variables. All the above considerations indicate an excellent adequacy of the regression model.

For estimation of significance of the model, the analysis of variance (ANOVA) was applied. The ANOVA for Y_1 and Y_2 was summarized in Table 6.12. Using 5% significance level, a model is considered significant if the *p*-value (significance probability value) is less than 0.05. From the *p*-values presented in Table 6.12, it can be concluded that for responses Y_1 and Y_2, linear model was significant. As shown in Table 6.12, the Model F-values of 4851.97 and 549.46 for MPS and % EE, respectively, implies the model is significant. Values of "Prob > F" less than 0.05 indicate model terms are significant. Therefore, X_1, X_2 and X_2X_2 are significant model terms for MPS and X_1, X_2 and X_1X_1 are significant model terms for % EE.

The mathematical relationship in the form of a polynomial equation generated by Design-Expert® 8.0 software for the measured responses, Y_1 and Y_2, are listed below in equation 3 and 4, respectively.

$$Y_1 = 260.054 + 16.922X_1 + 57.678X_2 + 0.432X_1X_2 - 0.712X_1X_1 - 39.682X_2X_2 \quad (3)$$

$$Y_2 = 83.84 + 4.96X_1 - 4.415X_2 + 0.252X_1X_2 - 1.54X_1X_1 - 0.095X_2X_2 \quad (4)$$

The above equations represent the quantitative effect of independent variables (X_1 and X_2) and their interactions on the responses (Y_1 and Y_2). A positive sign represents a synergistic effect, while a negative sign indicates an antagonistic effect. The theoretical values of Y_1 and Y_2 were obtained by substituting the values of X_1 and X_2 into the above equation, which were in reasonably good agreement with the observed values as seen in Table 6.9.

The relationship between the dependent and independent variables was further elucidated using perturbation and response surface plots. A perturbation graph was plotted to find those factors that most affects the response. A steep slope or curvature in a factor shows that the response is sensitive to that factor. A relatively flat line shows insensitivity to change in that particular factor. In case of response Y_1, factor X_2 shows a steep slope and factor X_1 exhibits a slight slope. Whereas, in case of

response Y_2, factors X_1 and X_2 shows a steep slope. Figure 6.1 represent perturbation plots for response Y_1 and Y_2.

Three-dimensional (3D) response surface plots for the measured responses were formed, based on the model polynomial functions to assess the change of the response surface. Also the relationship between the dependent and independent variables can be further understood by these plots. Figure 6.2 represents the effect of factors X_1 and X_2 on the responses Y_1 and Y_2. When drug:polymer ratio increased, MPS and % EE were increased.

The presence of surfactant molecules stabilizes the nanodroplets and prevents them from coalescing with each other. For effective stabilization, the surfactant molecules must cover the organic/aqueous interfacial area of all the droplets. Therefore a minimum number of surfactant molecules are required to achieve small particle size and narrow size distribution. With increase in surfactant concentrations the MPS of PLGA NPs was found to increases up to certain limit which may be attributed to the increased viscosity of the external phase that caused a decrease in net shear stress resulting in increased particle size.[44] The miscibility of acetone with aq. poloxamer 188 solution results in partitioning of poloxamer 188 into the polymeric part of the organic phase. More molecules of poloxamer 188 can be physically incorporated onto the NP surface.[46] Hence a large number of hydroxyl groups extending into the medium could be hydrated forming a hydrated layer at the surface of NPs surface to hinder nanoparticle aggregation. As the poloxamer 188 concentration is increased further, the size of particles produced by method plateaus. As the poloxamer 188 concentration is increased, the % EE decreases possibly due to increase in solubility of drug in aqueous medium.[47] (Figure 6.2B). If the concentration of stabilizer is too low, aggregation of the polymer will take place, whereas, if too much stabilizer is used, drug incorporation could be reduced as a result of the interaction between the drug and stabilizer.

Table 6.9. 3^2 Factorial design: Independent (X) and dependent variables (Y), Observed and predicted and residuals values for the responses Y_1 (MPS) and Y_2 (% EE).

	Independent Variables		Observed Values		Predicted Values		Residuals		ZP (mV)
Std order	X_1	X_2	Y_1	Y_2	Y_1	Y_2	Y_1	Y_2	
1	-1.0	-1.0	146.23	82.11	145.49	81.91	0.74	0.20	- 13.3 ± 0.70
2	0.0	0.0	260.8	83.83	260.05	83.84	0.75	-0.01	- 6.74 ± 0.06
3	-1.0	1.0	260.2	72.67	259.99	72.58	0.21	0.09	-7.11 ± 0.07
4	1.0	1.0	294.33	82.8	294.69	83.00	-0.36	-0.20	-4.71 ± 0.11
5	1.0	-1.0	178.63	91.23	178.47	91.33	0.16	-0.10	- 10.29 ± 3.7
6	0.0	-1.0	161.8	88.06	162.69	88.16	-0.89	-0.10	-11.83 ± 1.4
7	0.0	1.0	278.2	79.44	278.05	79.33	0.15	0.11	-7.21 ± 0.35
8	1.0	0.0	276.47	87.56	276.26	87.26	0.21	0.30	-7.045 ± 0.02
9	-1.0	0.0	241.47	77.05	242.42	77.34	-0.95	-0.29	-7.64 ± 0.19

X_1: Drug : Polymer ratio; X_2: Surfactant concentration (% w/v); Y_1: Mean particle size (nm); Y_2: % Entrapment Efficiency.

Table 6.10. Fit summaries for responses Y_1 and Y_2

Source	Sum of Squares		Df		Mean Square		F Value		p-value Prob > F	
	Y_1	Y_2	Y_1	Y_2	Y_1	Y_2	Y_1	Y_2	Y_1	Y_2
Mean	489127.7	61628.06	1	1	489127.7	61628.06				
Linear	21678.8	264.563	2	2	10839.4	132.28	20.619	149.45	0.0020	< 0.0001
2FI	0.748225	0.255025	1	1	0.748225	0.2550	0.00118	0.2522	0.9739	0.6368
Quadratic	3150.282	4.76125	2	2	1575.141	2.3806	1538.98	24.261	< 0.0001	0.0141
Cubic	1.819817	0.29415	2	2	0.909908	0.1470	0.7275	653.66	0.6382	0.0276
Residual	1.250669	0.000225	1	1	1.250669	0.00022				
Total	513960.6	61897.94	9	9	57106.74	6877.54				

Table 6.11. Regression analysis for responses Y_1 and Y_2

Source	SD		R-Squared		Adjusted R-Squared		Predicted R-Squared		PRESS	
	Y_1	Y_2	Y_1	Y_2	Y_1	Y_2	Y_1	Y_2	Y_1	Y_2
Linear	22.93	0.94	0.8730	0.9803	0.8306	0.9738	0.7390	0.9575	6482.62	11.47
2FI	25.11	1.01	0.8730	0.9813	0.7968	0.9700	0.5267	0.9246	11753.29	20.34
Quadratic	1.01	0.31	0.9999	0.9989	0.9997	0.9971	0.9987	0.9867	31.49	3.59

Table 6.12. ANOVA for responses Y_1 and Y_2

Source	Sum of Squares		Df		Mean Square		F Value		p-value Prob > F	
	Y_1	Y_2	Y_1	Y_2	Y_1	Y_2	Y_1	Y_2	Y_1	Y_2
Model	24829.83	269.58	5	5	4965.97	53.92	4851.97	549.46	< 0.0001	0.0001
X_1	1718.06	147.61	1	1	1718.06	147.61	1678.62	1504.30	< 0.0001	< 0.0001
X_2	19960.74	116.95	1	1	19960.74	116.95	19502.52	1191.88	< 0.0001	< 0.0001
$X_1 X_2$	0.75	0.26	1	1	0.75	0.26	0.73	2.60	0.4554	0.2053
$X_1 X_1$	1.01	4.74	1	1	1.01	4.74	0.99	48.34	0.3931	0.0061
$X_2 X_2$	3149.27	0.02	1	1	3149.27	0.02	3076.97	0.18	< 0.0001	0.6969
Residual	3.07	0.29	3	3	1.02	0.10				
Cor Total	24832.90	269.87	8	8						

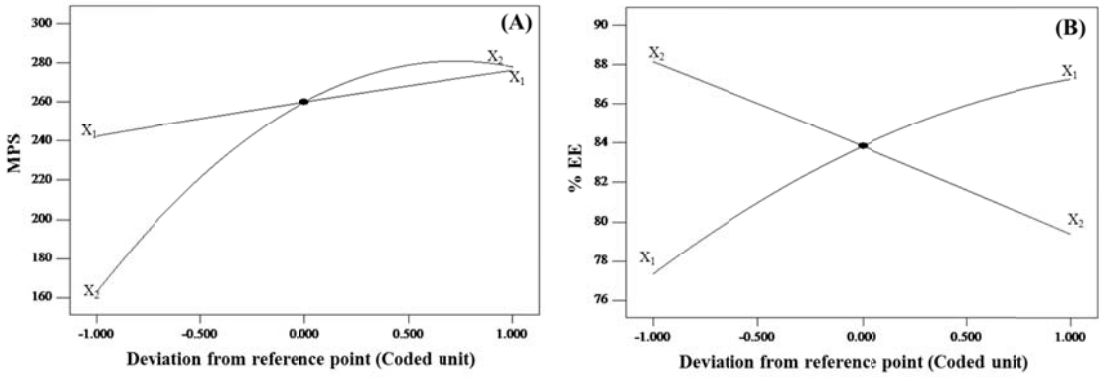

Figure 6.1. Perturbation graph for effect of individual factor on response (A) Y_1 (MPS) and (B) Y_2 (% EE)

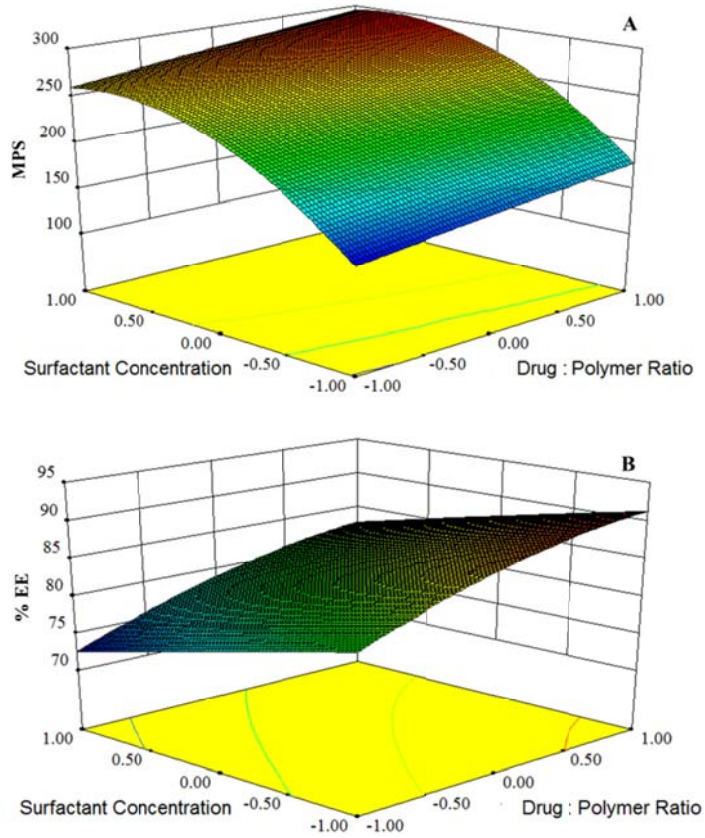

Figure 6.2. 3D Response surface plots: Effect of drug:polymer ratio (X_1) and surfactant concentration on the response (A) Y_1 (MPS) and (B) Y_2 (% EE).

6.6.2.1. Optimum formula

After studying the effect of the independent variables on the responses, the levels of these variables that give the optimum response were determined. Optimization was performed to find out the level of independent variables (X_1 and X_2) that would yield a minimum value of MPS with maximum value of % EE. Using a Design-Expert® 8.0 software optimization process, selected values of X_1 and X_2 were 7.5:50 ratio and 0.5 %w/v, respectively, which gives theoretical values of 162.69 nm and 88.16 % for MPS and % EE, respectively. For confirmation, a fresh formulation in triplicate was prepared at the optimum levels of the independent variables, and the resultant NPs formulations were evaluated for the responses. The observed values of MPS and % EE were found to be 160.9 ± 3.42 nm and 88.73 ± 1.04 %, respectively, which were in close agreement with the theoretical values. PDI and ZP of optimized NPs formulation were found to be 0.142 ± 0.010, which shows narrow size distribution, and -11.83 ± 1.4 mV, respectively. Figure 6.3 shows particle size distribution and ZP curve of optimized EFV loaded PLGA NPs formulation.

6.6.3. Level of MN incorporation in PLGA-MN

Accurately 50 mg of MN was weighed in to 25 mL volumetric flask. Approximately 20 mL of double distilled water was added and vortexed to dissolve the MN. The final volume was adjusted up to the mark with double distilled water to prepare stock solution of concentration 2 mg/ml. Aliquots ranging from 1 ml to 7 ml were taken, from stock solution, in 10 ml volumetric flask and diluted to 10 ml with double distilled water to give final concentration of 0.2, 0.4, 0.6, 1.0, 1.4 mg/ml. From each concentration, 50 µl was taken in ria vials, separately. 1.50 mL of concentrated sulphuric acid (96%) was added rapidly in ria vials. This was followed by the addition of 300 µL of 5% (w/v) phenol and mixing. The vials were then placed in a heated water bath for 5 min at 90 °C to allow for color development followed by cooling down to room temperature to stop the reaction. The absorbance was read at 490 nm. Graph of absorbance *Vs* concentration of MN was plotted and linear regression analysis was performed on the resultant curves. The calibration curves (n=3) constructed for MN were linear over the concentration range of 0.2-2 mg/ml with r^2 of

0.9988. Typically, the regression equation for the calibration curve was found to be y = 0.5085x + 0.0063, where x is the concentration in mg/ml (Figure 6.4). Incorporation of MN in PLGA was found to be 272 ± 42.5 µg of MN/mg of PLGA-MN.

EFV loaded PLGA-MN NPs was prepared as per optimum formula (50 mg of PLGA-MN was used instead of PLGA). All other parameters were same. EFV loaded PLGA-MN NPs was also tested for MPS, % EE and ZP and found to be 167.3 ± 2.61 nm with PDI of 0.173 ± 0.008, 87.91 ± 1.26 % and -14.26 ± 1.1 mV, respectively. The MPS of EFV loaded PLGA-MN NPs was slight higher than PLGA NPs. ZP of EFV loaded PLGA-MN NPs was slightly more negative than PLGA NPs. There is no significant difference in % EE between PLGA-MN NPs and PLGA NPs. Figure 6.5 shows particle size distribution and ZP curve of optimized EFV loaded PLGA-MN NPs formulation.

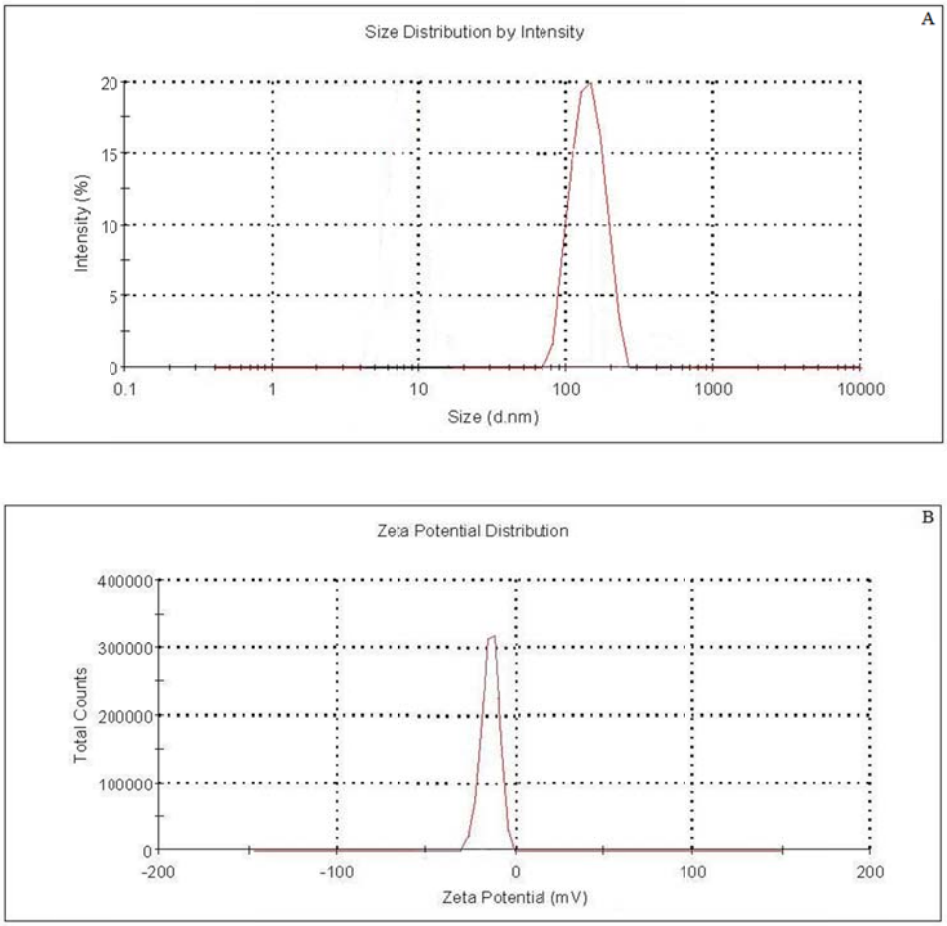

Figure 6.3. (A) Particle size distribution curve and (B) ZP curve of optimized EFV loaded PLGA NPs

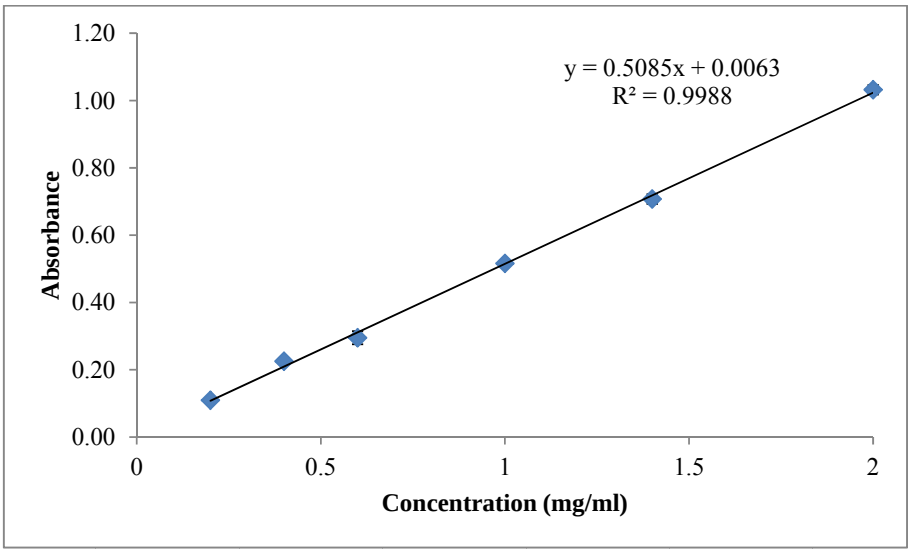

Figure 6.4. Calibration curve of MN.

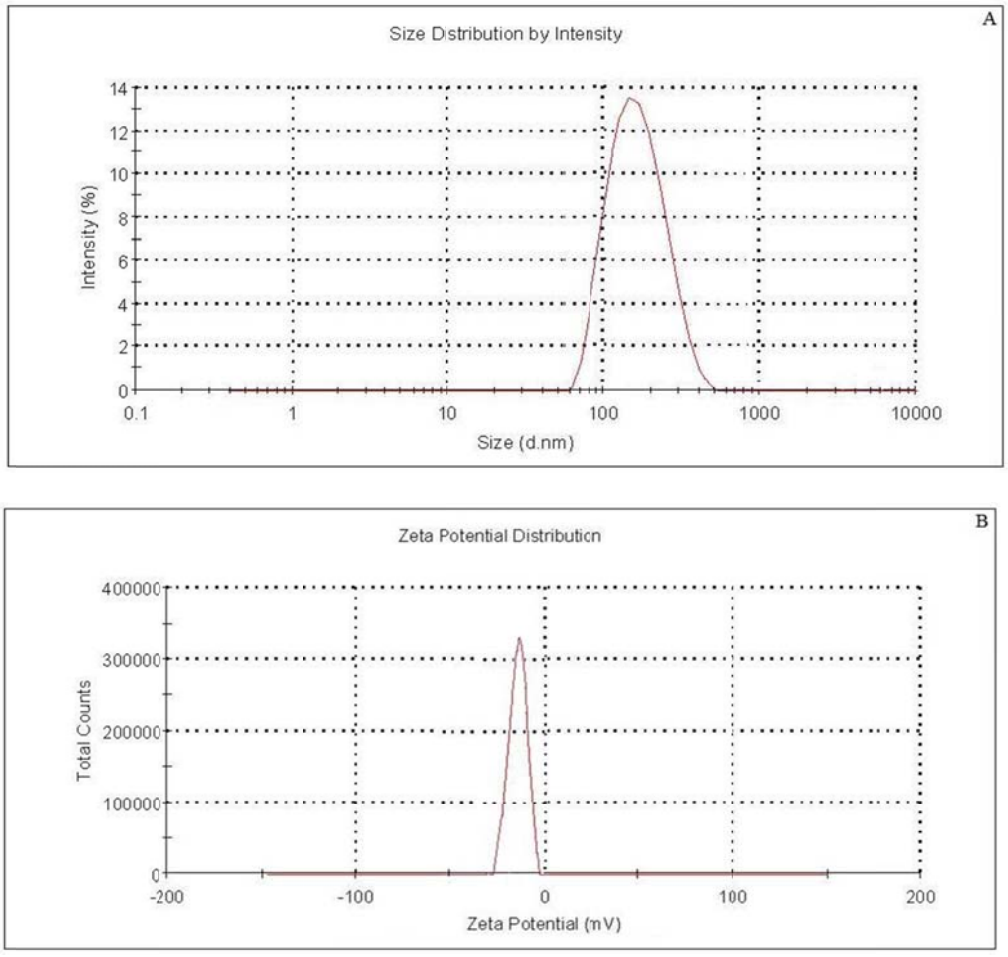

Figure 6.5. (A) Particle size distribution curve and (B) ZP curve of optimized EFV loaded PLGA-MN NPs

6.6.4. Selection of cryoprotectant for lyophilization

Freeze-drying has been the most utilized drying method of nanoparticle suspensions. It is a promising way to increase chemical and physical stability of NPs over extended period of time. Transformation of the NPs suspension into a solid form will prevent Ostwlad ripening and avoid hydrolysis reaction. It is expected that lyophilize state would have a better chemical and physical stability than aqueous dispersions. Two important transformations occur during the process. The 1st is from aqueous dispersion to powder which involves freezing of the sample and evaporation of water under vacuum. Freezing of the sample might cause instability due to the freezing out effects which results in changes of osmolarity and pH. The second transformation is re-dispersion of the powder. Here at least in initial stages, situations arise which favor particle aggregation (low water and high particle content, high osmotic pressure). The protective effect of the surfactant can be compromised by lyophilization. After freeze drying, easy and rapid reconstitution and unchanged particle size of the product are important features. In order to decrease NPs aggregation and to obtain a dry product addition of cryoprotectors will be necessary. For nanoparticles carbohydrates have been perceived to be suitable cryoprotectants since they are chemically innocuous and can be easily vitrified during freezing. There are considerable differences in the cryoprotective abilities of different carbohydrates.

Cryoprotectants decrease the osmotic activity of water and crystallization and favor the glassy state of the frozen samples. They are space holders which prevent the contact between the discrete NPs. Furthermore, they interact with the polar head groups of the surfactants and serve as a kind of “pseudo hydration shell”. It could be expected that particle size would increase after lyophilization, because nanoparticles tend to aggregate during this process. If the aggregated particles do not separate during re-dispersion, then larger particle sizes will be measured. Cryoprotectant, present at the nanoparticle surface, protects the particles from aggregation and make sure the re-dispersion requires a minimum of energy, being attributed to the formation of a steric barrier between the particles during lyophilization or to a stabilization of the particle dispersion due to electrostatic repulsions.[36,48]

The optimized batches of nanoparticles were lyophilized using different concentrations of mannitol and trehalose. Table 6.13 depicts the effect of mannitol

and trehalose concentrations on the MPS of EFV loaded NPs after reconstituting the lyophilized powder with double distilled water. The results showed that trehalose was effective cryoprotectant than mannitol in preventing nanoparticles from aggregation during lyophilization process. At lower concentration of mannitol, NPs formulations were not re-dispersing with water after lyophilization. At higher concentration of mannitol (NPs:Cryoprotectant- 1:3 and 1:5), sonication required for re-dispersion of NPs formulations with water after lyophilization and also shown higher MPS after lyophilization (Table 6.13).

NPs formulations with trehalose as cryoprotectant could completely re-disperse by manual shaking for 1 min. Trehalose at 3 times w.r.t the total solid content was found to be optimum to be added during freeze drying for preserving the particle size of the NPs (Table 6.13). The NPs formulation stabilized with trehalose had similar particle size as before lyophilization. In addition, trehalose did not reveal any significant effect on the recorded ZP values.

Table 6.13. Particle size of NPs formulations before and after lyophilization

EFV loaded NPs Formulation	Cryoprotectant	Ratio of NPs : Cryoprotectant	MPS (nm)	
			Before lyophilization	After lyophilization
PLGA NPs	-	1:0	160.9 ± 3.42	Lump formation
	Mannitol	1:1		Not re-dispersed
		1:3		285.2 ± 4.82
		1:5		263.5 ± 5.91
	Trehalose	1:1		175.4 ± 3.05
		1:3		167.2 ± 4.02
		1:5		165.8 ± 3.85
PLGA-MN NPs	-	1:0	167.3 ± 2.61	Lump formation
	Mannitol	1:1		Not re-dispersed
		1:3		278.1 ± 5.41
		1:5		269.7 ± 4.68
	Trehalose	1:1		181.7 ± 4.11
		1:3		173.3 ± 3.95
		1:5		174.1 ± 3.82

6.6.5. DSC analysis

DSC was performed to investigate the effect of excipients on the inner structure of EFV in NPs. DSC curve of pure EFV exhibited a single endothermic peak at an onset temperature of 139.80°C, corresponding to its melting point, indicating a crystalline nature (Figure 6.6A). The comparison between DSC thermograms of standard EFV with loaded NPs formulated with PLGA and PLGA-MN showed similar behaviors. The DSC thermograms revealed that EFV melting peak totally disappeared in loaded PLGA and PLGA-MN NPs, thus evidencing the absence of crystalline drug in the samples (Figure 6.6D and 6.6E). These results suggested that the nano-encapsulation inhibited the crystallization of EFV during NPs formation. Thus, it can be assumed that EFV was present in the NPs either in an amorphous or disordered crystalline phase or in the solid solution state.[49,50] The loaded NPs exhibited the same endothermic peak for PLGA as shown in PLGA and PLGA-MN, suggesting that the nano-encapsulation procedure did not affect the polymer structure.

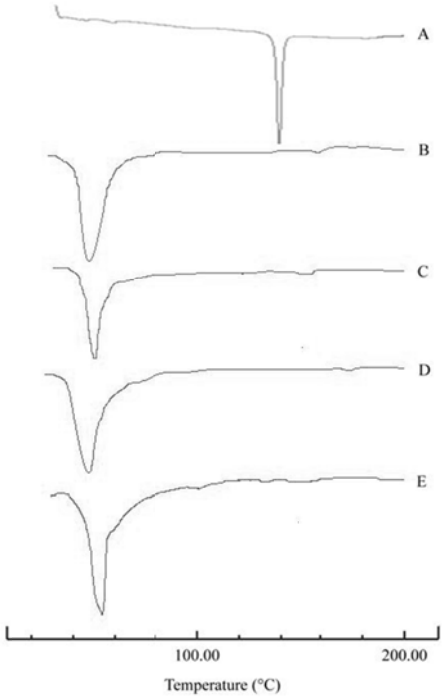

Figure 6.6. DSC thermograms of (A) standard EFV, (B) PLGA, (C) PLGA-MN, (D) EFV loaded PLGA NPs (E) EFV loaded PLGA-MN NPs

6.6.6. Morphology of NPs by TEM

TEM images of EFV loaded PLGA and PLGA-MN NPs reveal the spherical shape and smooth surface of the NPs (Figure 6.7). It confirms the particle size in the nanometric range. The spherical nature of the NPs was not altered after mannose incorporation. The particle size measured in TEM is very similar to particle size from zetasizer instrument.

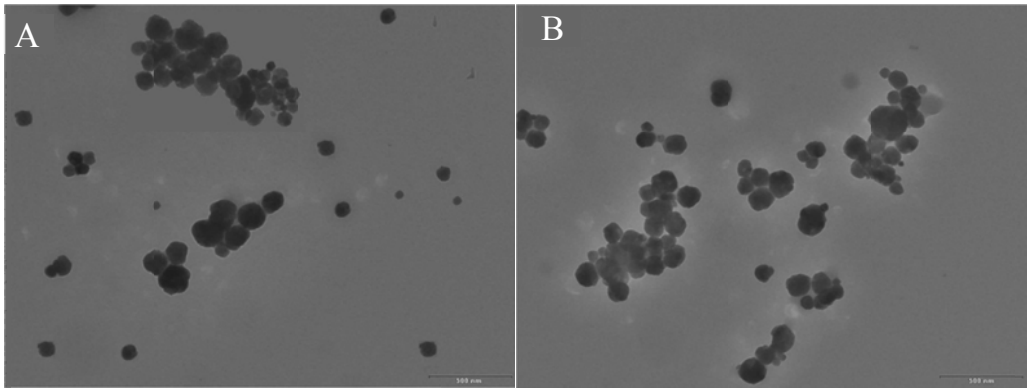

Figure 6.7 TEM images of EFV loaded PLGA NPs (A) and PLGA-MN NPs (B)

6.6.7. *In-vitro* drug release

PLGA degrades by hydrolysis of its ester linkages in the presence of water. In general the mechanism by which active agent is released from a delivery vehicle is a combination of diffusion of the active agent from the polymer matrices, bulk erosion of the polymer, swelling and degradation of the polymer. The degradation of PLGA is slow, therefore the release of EFV from NPs may depend on drug diffusion and PLGA surface and bulk erosion or swelling.[51] The release profile of the EFV-loaded PLGA NPs and PLGA-MN NPs is shown in Figure 6.8. *In-vitro* drug release studies of EFV-loaded PLGA and PLGA-MN NPs showed biphasic release profile that is characterized by an initial burst, followed by a slower sustained release. An initial-burst drug release for PLGA NPs (28.32 ± 1.51 %) and PLGA-MN NPs (23.17 ± 1.63 %) was observed until 8 hours, then a constant slow drug release until day 5. The

PLGA NPs formulation showed 50.31 ± 1.39 % drug release in 120 h, whereas the PLGA-MN NPs formulation showed 45.49 ± 1.56 % drug release at the end of 120 h. A high initial burst was observed which can be attributed to the immediate dissolution and release of EFV adhered on the surface and located near the surface of the NPs.[52] Then release is mainly due to the diffusion of drug molecules through the polymeric matrix of the NPs afterwards, the matrix material would require time to erode in the aqueous environment, and then the release mechanisms of surface release and polymer erosion might be the main causes of the release behavior.[53] PLGA NPs, the release rate is dependent upon the molecular weight and lactide content of the polymer. The release rate reduces as the molecular weight and lactide content of the polymer increase. Slow release in the case of the PLGA-MN NPs formulation may be attributed to the presence of the protective coat of mannose on the nanoparticle surface, which interferes with the drug release.[54]

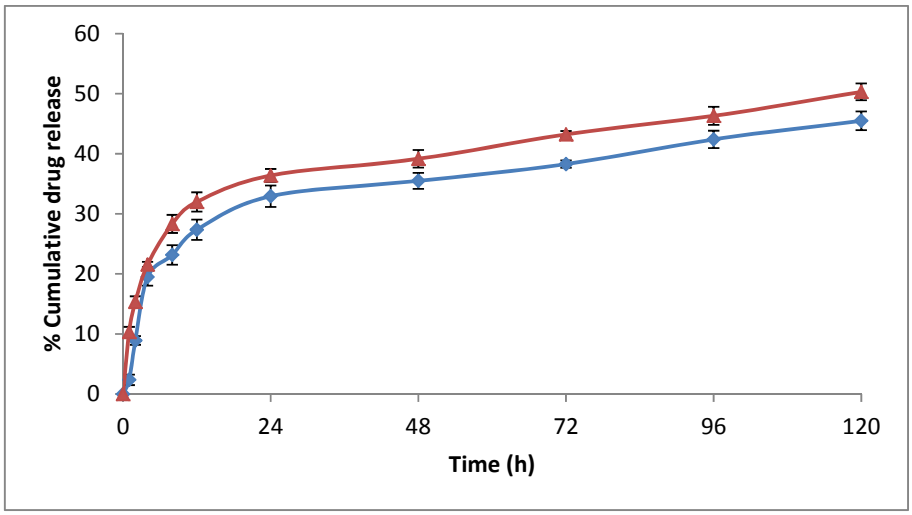

Figure 6.8. % Cumulative drug release of EFV loaded PLGA (▲) and PLGA-MN NPs (♦) in 1 % SLS in water dissolution media. Data are represented as Mean ± SD; n=3 for each group.

6.6.8. Stability studies

The physical and chemical stability of lyophilized PLGA NPs and PLGA-MN NPs formulations were evaluated at 4-8°C and 25°C for 3 months. It was found that there was no significant change in the MPS, ZP and drug content when NPs were stored at 4-8°C and 25°C over 3 months. As reported in Table 6.14, after 3 months storage at 4-8°C and 25°C of NPs, the MPS of PLGA NPs was 162.6 ± 3.31 nm and 162.3 ± 4.03 nm, for PLGA-MN NPs, MPS was 169.5 ± 2.89 nm and 170.2 ± 3.05 nm, respectively, which is in good agreement with zero time data. As seen from Table 6.14, the zeta-potential values did not change during the 3 months storage at 4-8°C and 25°C. Furthermore, the chemical stability of EFV was examined using an HPLC assay during this storage period. For instance, more than 97.7 % of EFV remained in the NPs formulations for up to 3 months when stored at 4-8°C and 25°C as shown in Table 6.14. All the samples stored at 4-8°C and 25°C were re-dispersed easily in double distilled water within 2 minutes. These results suggest that the lyophilized product can maintain the physical as well as chemical stability of the NPs formulations during the shelf-life. A long term stability study is necessary for determining the optimum storage conditions for the lyophilized NPs.

6.6.9. MTT assay

To address whether the uptake of NPs by macrophages affected cell viability, MTT assays were performed (Figure 6.9). MTT assays measure the viability of cells by assessing the presence of active mitochondrial dehydrogenases that convert MTT into water-insoluble, purple formazan crystals. MTT assay confirmed that the dose selected for the study was nontoxic to the cells. EFV loaded PLGA and PLGA-MN NPs do not interfere with macrophage viability.

Table 6.14. Influence of time and temperature on the physical stability of EFV loaded PLGA and PLGA-MN NPs stored at different conditions and time intervals

Month	4-8°C			25°C		
	MPS (nm)	ZP (mV)	Drug content	MPS (nm)	ZP (mV)	Drug content
	PLGA NPs					
0	157.4 ± 2.95	-11.62 ± 1.07	98.3 ± 1.05	157.4 ± 2.95	-11.62 ± 1.07	98.3 ± 1.05
1	160.8 ± 3.08	-11.87 ± 0.94	97.8 ± 1.14	158.0 ± 3.72	-11.52 ± 1.22	98.8 ± 0.73
2	159.9 ± 3.16	-12.10 ± 1.17	96.9 ± 0.87	160.5 ± 4.11	-11.94 ± 1.16	97.7 ± 0.91
3	162.6 ± 3.31	-11.90 ± 1.30	97.7 ± 1.07	162.3 ± 4.03	-11.80 ± 1.42	96.8 ± 1.16
	PLGA-MN NPs					
0	165.4 ± 3.71	-13.93 ± 1.12	98.9 ± 2.06	165.4 ± 3.71	-13.93 ± 1.12	98.9 ± 2.06
1	167.2 ± 2.93	-14.18 ± 1.02	97.9 ± 0.99	166.9 ± 2.94	-14.58 ± 0.80	98.5 ± 1.33
2	166.9 ± 4.02	-14.23 ± 0.85	98.1 ± 1.28	168.3 ± 3.11	-13.86 ± 1.28	97.8 ± 0.72
3	169.5 ± 2.89	-14.64 ± 0.77	98.3 ± 1.53	170.2 ± 3.05	-14.27 ± 1.41	98.2 ± 1.16

The values are shown as mean ± SD, n=3

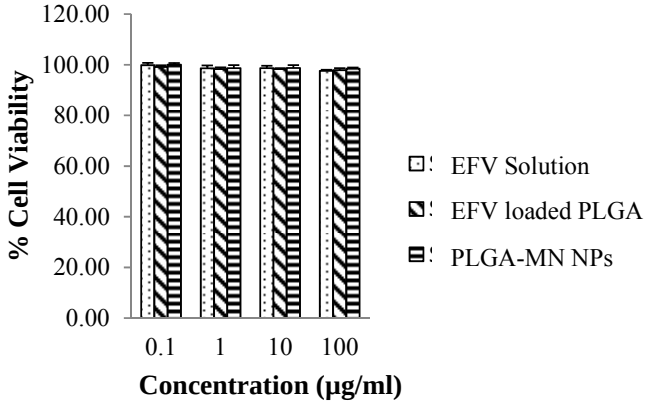

Figure 6.9. Cell viability determinations for EFV solution, EFV loaded PLGA and PLGA-MN NPs after 48 h using MTT assay. Data presented as Mean ± SD, n = 8.

6.6.10. *In vitro* drug uptake study

Macrophage uptake of EFV from NPs formulations is shown in Figure 6.10. A significant increase in macrophage uptake of EFV was observed when PLGA-MN NPs (90.61 ± 3.01 %) were used, which was 37.0 and 1.7 times higher than that of free EFV (2.45 ± 1.10 %) and PLGA NPs (52.84 ± 3.11 %) at 48 hours, respectively. In the case of PLGA NPs, drug uptake was 21.6 times that of free drug at 48 h. Higher uptake was observed with PLGA-MN NPs than PLGA NPs. This may be because

mannose receptors are present on macrophages. They recognize the PLGA-MN NPs, which are taken up by receptor mediated endocytosis mechanism, thus resulting in higher uptake and localization of the NPs.

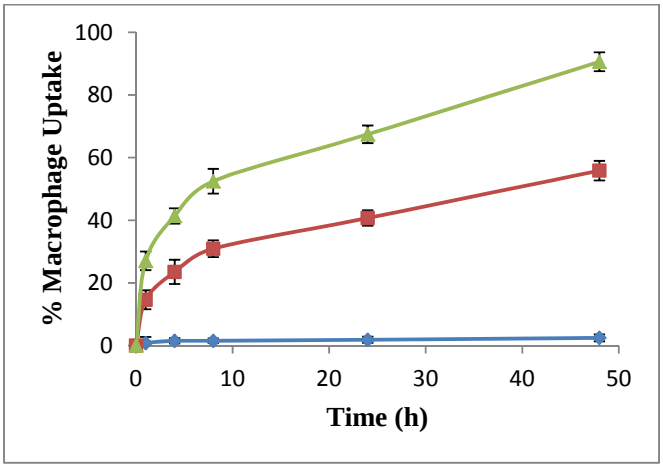

Figure 6.10. Drug uptake by macrophages for EFV solution (▲), EFV loaded PLGA (■) and PLGA-MN NPs (♦) at different time points at 37 ± 2°C. Data presented as Mean ± SD, n = 3.

6.6.11. Fluorescence microscopy

6-Coumarin was used to prepare fluorescent PLGA and PLGA-MN NPs. Fluorescent macrophages were observed by fluorescence microscopy. Direct fluorescence showed the presence and relative localization of nanoparticles in macrophages following incubation and uptake. The fluorescence microscopic study revealed that uptake in macrophages was higher in the case of PLGA-MN NPs in comparison to PLGA NPs, and fluorescence was not observed in control cells (Figure 6.11). The results were in accordance with drug uptake studies, which also indicated higher uptake in macrophages, occurred with PLGA-MN NPs in comparison to PLGA NPs.

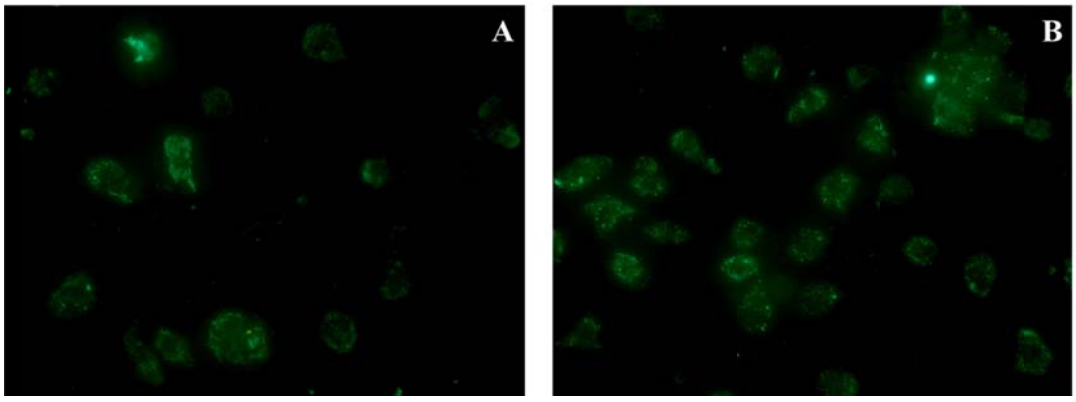

Figure 6.11. Fluorescent NPs uptake by macrophages following 60 min incubation with 6-Coumarin loaded PLGA (A) and PLGA-MN NPs (B), Macrophages fluoresce due to NPs uptake.

6.6.12. *In Vivo* biodistribution study

Biodistribution of EFV in organs was evaluated in albino rats until 24 hours after injection. Free drug and different formulations were given to rats through intraperitoneal injection at a dose of 20 mg/kg body weight. The amount of EFV present in liver, spleen, lung, kidney and brain at different time intervals after intraperitoneal injection of EFV loaded PLGA and PLGA-MN NPs revealed that maximum accumulation of the drug in these organs was achieved within 3 hours. The accumulation in different organs was 15.47 ± 1.1 % in liver, 14.29 ± 0.7 % in spleen, 10.73 ± 0.6 % in lung, 5.28 ± 0.5 % in kidney, and 3.28 ± 0.3% in brain after 3 hour with the PLGA NPs formulation and 20.38 ± 0.7 % in liver, 20.82 ± 1.0 % in spleen, 14.34 ± 0.9 % in lung, 6.28 ± 0.3 % in kidney, and 5.74 ± 0.3% in brain after 3 hour in the case of PLGA-MN NPs formulation. However, the maximum amounts of drug accumulated in liver, spleen, lung, kidney and brain are considerably lower on administration of free drug in comparison to PLGA and PLGA-MN NPs. (Figure 6.12).

The biodistribution data suggested that the PLGA-MN NPs exhibit the best targeting potential, evidenced by recovery of higher and prolonged concentration of administered dose by macrophage rich tissues. PLGA-MN NPs showed significant increase in the uptake by these macrophage-rich organs due to receptor-mediated

endocytosis.[55] A mannose-conjugated drug delivery system with site specificity could help to reduce the toxicity of the available anti-HIV dosage forms.

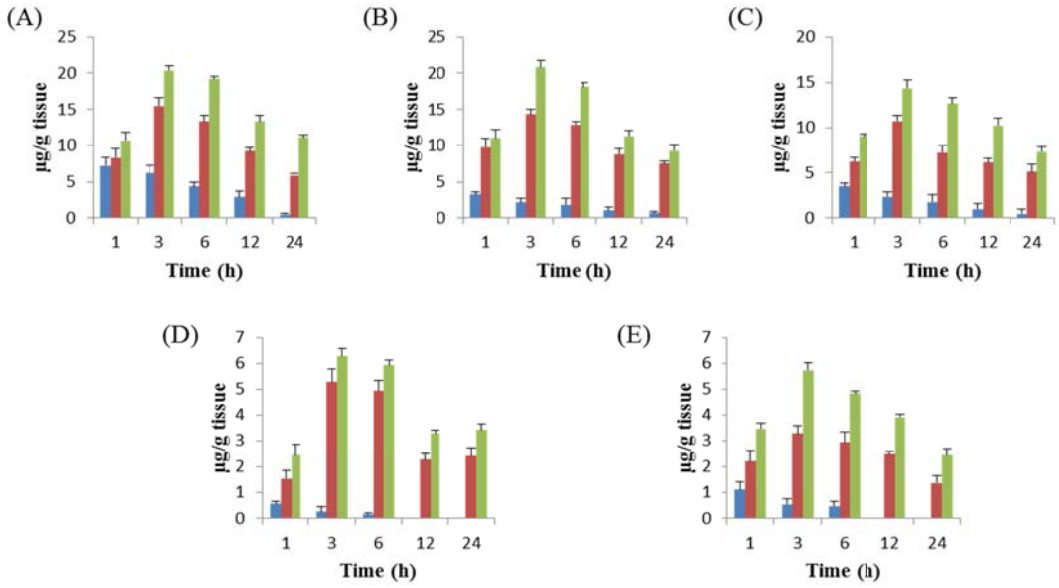

Figure 6.12. Biodistribution pattern of EFV solution (■), EFV loaded PLGA (■) and PLGA-MN NPs (■) in various organs; (A) liver, (B) spleen, (C) lung, (D) kidney, (E) brain. Data presented as Mean ± SD, n = 3.

6.7. Conclusion

EFV loaded PLGA NPs prepared by the nanoprecipitation method had high % EE, spherical shape, regular surface and particle size less than 200 nm. The application of a 3^2 factorial design proved to be a useful tool for the optimization of EFV loaded PLGA-NPs. The analysis of the obtained results led to the polynomial equations obtained by multiple regression described adequately the influence of the selected variables (drug:polymer ratio and surfactant concentration) at three levels on the responses. According to the studied factors, the selected optimum formulation was that prepared with 7.5:50 drug:polymer ratio and 0.5 %w/v surfactant concentration. Incorporation of MN in PLGA can be used as a successful strategy to enhance the uptake of PLGA-MN NPs by macrophages. *In vitro* drug release study showed 50.31 ± 1.39 % EFV release from PLGA NPs and 45.49 ± 1.56 % EFV release from PLGA-MN NPs in 5 days. The NPs formulations were stable over 3 months. DSC

thermograms indicated that EFV was dispersed as amorphous state in the NPs. The NPs penetrate macrophages and do not cause toxicity to these cells by MTT assay. Higher uptake in peritoneal macrophages was observed with PLGA-MN NPs than PLGA NPs. Administration of PLGA-MN NPs resulted in a significantly higher concentration of EFV in liver, lung, spleen, kidney and brain as compared to PLGA NPs as well as free drug administration. These nanoparticles sustained the release of EFV and may be used to reduce the frequency of administration and dose-dependent side-effects, reducing the chances of dose dumping and increasing the patient compliance.

REFERENCES

1 Piot, P., Bartos, M., Ghys, P. D., Walker, N. & Schwartlander, B. The global impact of HIV/AIDS. *Nature* **410**, 968-973, doi:10.1038/35073639 (2001).

2 Chen, R. Y. *et al.* Immunologic and virologic consequences of temporary antiretroviral treatment interruption in clinical practice. *AIDS research and human retroviruses* **18**, 909-916, doi:10.1089/088922202760265588 (2002).

3 Chulamokha, L., DeSimone, J. A. & Pomerantz, R. J. Antiretroviral therapy in the developing world. *Journal of neurovirology* **11 Suppl 1**, 76-80 (2005).

4 Fellay, J. *et al.* Prevalence of adverse events associated with potent antiretroviral treatment: Swiss HIV Cohort Study. *Lancet* **358**, 1322-1327 (2001).

5 Gartner, S. *et al.* The role of mononuclear phagocytes in HTLV-III/LAV infection. *Science* **233**, 215-219 (1986).

6 Nicholson, J. K., Cross, G. D., Callaway, C. S. & McDougal, J. S. In vitro infection of human monocytes with human T lymphotropic virus type III/lymphadenopathy-associated virus (HTLV-III/LAV). *J Immunol* **137**, 323-329 (1986).

7 von Briesen, H. *et al.* Infection of monocytes/macrophages by HIV in vitro. *Research in virology* **141**, 225-231 (1990).

8 McGann, K. A. *et al.* Human immunodeficiency virus type 1 causes productive infection of macrophages in primary placental cell cultures. *The Journal of infectious diseases* **169**, 746-753 (1994).

9 Milman, G. & Sharma, O. Mechanisms of HIV/SIV mucosal transmission. *AIDS research and human retroviruses* **10**, 1305-1312 (1994).

10 Beck, P. H., Kreuter, J., Muller, W. E. G. & Schatton, W. Improved peroral delivery of avoral with polybutylcyanoacrylate nanoparticles. *European journal of pharmaceutics and biopharmaceutics : official journal of Arbeitsgemeinschaft fur Pharmazeutische Verfahrenstechnik e.V* **40**, 134-137 (1994).

11 Panyam, J. *et al.* Polymer degradation and in vitro release of a model protein from poly(D,L-lactide-co-glycolide) nano- and microparticles. *Journal of controlled release : official journal of the Controlled Release Society* **92**, 173-187 (2003).

12 Shive, M. S. & Anderson, J. M. Biodegradation and biocompatibility of PLA and PLGA microspheres. *Advanced drug delivery reviews* **28**, 5-24 (1997).

13 Sehra, S. & Dhake, A. S. Formulation and evaluation of sustained release microspheres of poly-lactide-co-glycolide containing tamoxifen citrate. *Journal of microencapsulation* **22**, 521-528, doi:10.1080/02652040500162170 (2005).

14 Barichello, J. M., Morishita, M., Takayama, K. & Nagai, T. Encapsulation of hydrophilic and lipophilic drugs in PLGA nanoparticles by the nanoprecipitation method. *Drug development and industrial pharmacy* **25**, 471-476, doi:10.1081/DDC-100102197 (1999).

15 Avgoustakis, K. Pegylated poly(lactide) and poly(lactide-co-glycolide) nanoparticles: preparation, properties and possible applications in drug delivery. *Current drug delivery* **1**, 321-333 (2004).

16 Jiao, Y. *et al.* In vitro and in vivo evaluation of oral heparin-loaded polymeric nanoparticles in rabbits. *Circulation* **105**, 230-235 (2002).

17 Fonseca, C., Simoes, S. & Gaspar, R. Paclitaxel-loaded PLGA nanoparticles: preparation, physicochemical characterization and in vitro anti-tumoral activity. *Journal of controlled release : official journal of the Controlled Release Society* **83**, 273-286 (2002).

18 Panagi, Z. *et al.* Effect of dose on the biodistribution and pharmacokinetics of PLGA and PLGA-mPEG nanoparticles. *International journal of pharmaceutics* **221**, 143-152 (2001).

19 Bala, I., Hariharan, S. & Kumar, M. N. PLGA nanoparticles in drug delivery: the state of the art. *Critical reviews in therapeutic drug carrier systems* **21**, 387-422 (2004).

20 Zakeri-Milani, P., Barzegar-Jalali, M., Azimi, M. & Valizadeh, H. Biopharmaceutical classification of drugs using intrinsic dissolution rate (IDR) and rat intestinal permeability. *European journal of pharmaceutics and biopharmaceutics : official journal of Arbeitsgemeinschaft fur Pharmazeutische Verfahrenstechnik e.V* **73**, 102-106, doi:10.1016/j.ejpb.2009.04.015 (2009).

21 Madhavi, B. B. *et al.* Dissolution enhancement of efavirenz by solid dispersion and PEGylation techniques. *International journal of pharmaceutical investigation* **1**, 29-34, doi:10.4103/2230-973X.76726 (2011).

22 Baert, L. *et al.* Development of an implantable infusion pump for sustained anti-HIV drug administration. *International journal of pharmaceutics* **355**, 38-44, doi:10.1016/j.ijpharm.2008.01.029 (2008).

23 Auger, M. J. & Ross, J. A. *The biology of the macrophage in the natural immune system: the macrophage.*, (1992).

24 Levy, J. A. Pathogenesis of human immunodeficiency virus infection. *Microbiological reviews* **57**, 183-289 (1993).

25 Weiss, R. A. How does HIV cause AIDS? *Science* **260**, 1273-1279 (1993).

26 Largent, B. L., Walton, K. M., Hoppe, C. A., Lee, Y. C. & Schnaar, R. L. Carbohydrate-specific adhesion of alveolar macrophages to mannose-derivatized surfaces. *The Journal of biological chemistry* **259**, 1764-1769 (1984).

27 Haltiwanger, R. S. & Hill, R. L. The ligand binding specificity and tissue localization of a rat alveolar macrophage lectin. *The Journal of biological chemistry* **261**, 15696-15702 (1986).

28 Fessi, H., Puisieux, F., Devissaguet, J. P., Ammoury, N. & Benita, S. Nanocapsule formation by interfacial polymer deposition following solvent displacement. *International journal of pharmaceutics* **55**, R1-R4 (1989).

29 Ghotbi, Z. *et al.* Active targeting of dendritic cells with mannan-decorated PLGA nanoparticles. *Journal of drug targeting* **19**, 281-292, doi:10.3109/1061186X.2010.499463 (2011).

30 Masuko, T. *et al.* Carbohydrate analysis by a phenol-sulfuric acid method in microplate format. *Analytical biochemistry* **339**, 69-72, doi:10.1016/j.ab.2004.12.001 (2005).

31 Ray, A. & Dittel, B. N. Isolation of mouse peritoneal cavity cells. *Journal of visualized experiments : JoVE*, doi:10.3791/1488 (2010).

32 Weischenfeldt, J. & Porse, B. Bone Marrow-Derived Macrophages (BMM): Isolation and Applications. *CSH protocols* **2008**, pdb prot5080, doi:10.1101/pdb.prot5080 (2008).

33 Mosmann, T. Rapid colorimetric assay for cellular growth and survival: application to proliferation and cytotoxicity assays. *Journal of immunological methods* **65**, 55-63 (1983).

34 Ramanlal Chaudhari, K. *et al.* Bone metastasis targeting: a novel approach to reach bone using Zoledronate anchored PLGA nanoparticle as carrier system loaded with Docetaxel. *Journal of controlled release : official journal of the Controlled Release Society* **158**, 470-478, doi:10.1016/j.jconrel.2011.11.020 (2012).

35 Destache, C. J., Belgum, T., Goede, M., Shibata, A. & Belshan, M. A. Antiretroviral release from poly(DL-lactide-co-glycolide) nanoparticles in mice. *The Journal of antimicrobial chemotherapy* **65**, 2183-2187, doi:10.1093/jac/dkq318 (2010).

36 Quintanar-Guerrero, D., Allemann, E., Fessi, H. & Doelker, E. Preparation techniques and mechanisms of formation of biodegradable nanoparticles from preformed polymers. *Drug development and industrial pharmacy* **24**, 1113-1128, doi:10.3109/03639049809108571 (1998).

37 Derakhshandeh, K., Erfan, M. & Dadashzadeh, S. Encapsulation of 9-nitrocamptothecin, a novel anticancer drug, in biodegradable nanoparticles: factorial design, characterization and release kinetics. *European journal of pharmaceutics and biopharmaceutics : official journal of Arbeitsgemeinschaft fur Pharmazeutische Verfahrenstechnik e.V* **66**, 34-41, doi:10.1016/j.ejpb.2006.09.004 (2007).

38 Behan, N., Birkinshaw, C. & Clarke, N. Poly n-butyl cyanoacrylate nanoparticles: a mechanistic study of polymerisation and particle formation. *Biomaterials* **22**, 1335-1344 (2001).

39 Huang, C. Y., Chen, C. M. & Lee, Y. D. Synthesis of high loading and encapsulation efficient paclitaxel-loaded poly(n-butyl cyanoacrylate) nanoparticles via miniemulsion. *International journal of pharmaceutics* **338**, 267-275, doi:10.1016/j.ijpharm.2007.01.052 (2007).

40 Muthu, M. S., Rawat, M. K., Mishra, A. & Singh, S. PLGA nanoparticle formulations of risperidone: preparation and neuropharmacological evaluation. *Nanomedicine : nanotechnology, biology, and medicine* **5**, 323-333, doi:10.1016/j.nano.2008.12.003 (2009).

41 Chorny, M., Fishbein, I., Danenberg, H. D. & Golomb, G. Lipophilic drug loaded nanospheres prepared by nanoprecipitation: effect of formulation variables on size, drug recovery and release kinetics. *Journal of controlled release : official journal of the Controlled Release Society* **83**, 389-400 (2002).

42 Song, X. *et al.* Dual agents loaded PLGA nanoparticles: systematic study of particle size and drug entrapment efficiency. *European journal of pharmaceutics and biopharmaceutics : official journal of Arbeitsgemeinschaft fur Pharmazeutische Verfahrenstechnik e.V* **69**, 445-453, doi:10.1016/j.ejpb.2008.01.013 (2008).

43 Govender, T. *et al.* Defining the drug incorporation properties of PLA-PEG nanoparticles. *International journal of pharmaceutics* **199**, 95-110 (2000).

44 Budhian, A., Siegel, S. J. & Winey, K. I. Haloperidol-loaded PLGA nanoparticles: systematic study of particle size and drug content. *International journal of pharmaceutics* **336**, 367-375, doi:10.1016/j.ijpharm.2006.11.061 (2007).

45 Song, X. *et al.* PLGA nanoparticles simultaneously loaded with vincristine sulfate and verapamil hydrochloride: systematic study of particle size and drug entrapment efficiency. *International journal of pharmaceutics* **350**, 320-329, doi:10.1016/j.ijpharm.2007.08.034 (2008).

46 Galindo-Rodriguez, S., Allemann, E., Fessi, H. & Doelker, E. Physicochemical parameters associated with nanoparticle formation in the salting-out, emulsification-diffusion, and nanoprecipitation methods. *Pharmaceutical research* **21**, 1428-1439 (2004).

47 Joshi, S. A., Chavhan, S. S. & Sawant, K. K. Rivastigmine-loaded PLGA and PBCA nanoparticles: preparation, optimization, characterization, in vitro and pharmacodynamic studies. *European journal of pharmaceutics and biopharmaceutics : official journal of Arbeitsgemeinschaft fur Pharmazeutische Verfahrenstechnik e.V* **76**, 189-199, doi:10.1016/j.ejpb.2010.07.007 (2010).

48 Vandervoort, J. & Ludwig, A. Biocompatible stabilizers in the preparation of PLGA nanoparticles: a factorial design study. *International journal of pharmaceutics* **238**, 77-92 (2002).

49 Musumeci, T. *et al.* PLA/PLGA nanoparticles for sustained release of docetaxel. *International journal of pharmaceutics* **325**, 172-179, doi:10.1016/j.ijpharm.2006.06.023 (2006).

50 Sanna, V. *et al.* Novel docetaxel-loaded nanoparticles based on poly(lactide-co-caprolactone) and poly(lactide-co-glycolide-co-caprolactone) for prostate cancer treatment: formulation, characterization, and cytotoxicity studies. *Nanoscale research letters* **6**, 260, doi:10.1186/1556-276X-6-260 (2011).

51 Mu, L. & Feng, S. S. PLGA/TPGS nanoparticles for controlled release of paclitaxel: effects of the emulsifier and drug loading ratio. *Pharmaceutical research* **20**, 1864-1872 (2003).

52 Magenheim, B., Levy, M. Y. & Benita, S. A new in vitro technique for the evaluation of drug release profile from colloidal carriers - ultrafiltration

technique at low pressure. *International journal of pharmaceutics* **94**, 115-123 (1993).

53 Esmaeili, F. *et al.* PLGA nanoparticles of different surface properties: preparation and evaluation of their body distribution. *International journal of pharmaceutics* **349**, 249-255, doi:10.1016/j.ijpharm.2007.07.038 (2008).

54 Jain, S. K., Gupta, Y., Jain, A., Saxena, A. R. & Khare, P. Mannosylated gelatin nanoparticles bearing an anti-HIV drug didanosine for site-specific delivery. *Nanomedicine : nanotechnology, biology, and medicine* **4**, 41-48, doi:10.1016/j.nano.2007.11.004 (2008).

55 Nahar, M. & Jain, N. K. Preparation, characterization and evaluation of targeting potential of amphotericin B-loaded engineered PLGA nanoparticles. *Pharmaceutical research* **26**, 2588-2598, doi:10.1007/s11095-009-9973-4 (2009).

CHAPTER 7:

SUMMARY & CONCLUSION

7.1. Summary

An estimated 60 million people are infected with human immunodeficiency type-1 (HIV-1) worldwide. The majority of infected people live in the developing world with limited treatment resources. Antiretroviral (ARV) therapy has significantly reduced HIV-1 disease morbidity and improved life expectancy. However, the economics of drug treatment, treatment failures due to the development of resistance, and limited global access has prevented world-wide utility of ARV therapy. Dosing regimens that require multiple daily dosing with diet considerations and ARV side effects have compromised the achievement of long-term HIV-1 suppression in infected patients.[4] Additionally, the use of ARV requires a concerted level of commitment from the patient to prevent treatment failure due to resistance.

ARV drug therapy has contributed significantly to improved patient/disease management, its current use is associated with several disadvantages and inconveniences to the HIV/AIDS patient. Many ARV drugs undergo extensive first pass metabolism and gastrointestinal degradation leading to low and erratic bioavailability. The half-life for several ARV drugs is short, which then requires frequent administration of doses leading to decreased patient compliance. A major limitation is that HIV is localised in certain inaccessible compartments of the body such as the CNS, the lymphatic system and within the macrophages. The severe side effects associated with ARV therapy can therefore be attributed to the subsequent large doses essential for achieving a therapeutic effect, due to the inadequate drug concentrations at the site of action, and/or the poor bioavailability of several ARV drugs. These drugs also suffer from physico-chemical problems such as poor solubility that may lead to formulation difficulties.

According to the biopharmaceutical classification system guidance by FDA, efavirenz (EFV) comes under a class II category drug, i.e. it has low solubility and high intestinal permeability. It is a crystalline lipophilic solid with an aqueous solubility of 3-9 μg/ml and with a low intrinsic dissolution rate of 0.037 mg/cm^2/min. Hence, it has very low bioavailability. To achieve effective therapy against viral diseases for orally administered drugs, it is essential that the drug should be adequately and consistently absorbed. Therefore, the recommended dose of EFV in adults is 600 mg q.d. The

frequent administration of several drugs in relatively high doses is a main cause of patient incompliance. The reason for this is very low solubility of EFV hinders its administration, absorption and biodistribution. Thus, there is need to have some innovative formulation approach to enhance the bioavailability and for site-specific drug delivery. The objective of studies was to develop stable nanosuspension (NS) and self- microemulsifying drug delivery system (SMEDDS) of EFV for improvement of oral bioavailability by improving its solubility, dissolution and absorption properties. Another objective was to develop EFV loaded mannose (MN) incorporated PLGA nanoparticles (MN-PLGA NPs) for site-specific delivery to macrophages.

Present first study has been undertaken to develop NS of EFV, by media milling method, with improved oral bioavailability. Formulation of NS requires a careful selection of stabilizers. Steric and electrostatic stabilizers are needed to stabilize the nanoparticles against inter-particle forces and prevent them from aggregating. Steric stabilization is often combined with electrostatic stabilization for additional repulsive contribution. Different pharmaceutical excipients including povidone (PVP K30), and poloxamers (188 and 407) as steric stabilizer and sodium lauryl sulphate (SLS) as anionic electroststic stabilizer were used in an effort to develop stable EFV loaded NS. In order to obtain best formulation of NS, the relationship between dependent variable and independent variable must be understood. Design of experiment can serve as an efficient and economical method of obtaining the necessary information to understand relationship between variables. Box-Behnken design, one of response surface method (RSM) design, was applied to optimize the NS formulation. The independent variables for the present study were the following: concentration of drug (X_1), concentration of polymer (X_2), concentration of surfactant (X_3) and milling time (X_4). The dependent variables included mean particle size (MPS) and zeta potential (ZP). NSs were subsequently transformed to dry powder by lyophilization, to enhance the stability of EFV. The physicochemical properties of NSs in terms of MPS, polydispersity index (PDI), and ZP before and after lyophilisation were investigated. Dissolution velocity and saturation solubility are generally performed using official pharmacopoeia methods. Corresponding physical properties of the prepared EFV NS were characterized by differential scanning calorimetry (DSC), X-ray diffraction (XRD), scanning electronic microscopy (SEM) and transmission

electron microscopy (TEM). The chemical stability of NS was assessed by determining percentage of EFV present in the formulations stored at different temperatures (4-8°C and 25°C) during a period of 6 months. *In situ* intestinal permeability and *in vitro* parallel artificial membrane permeability assay (PAMPA) study were carried out to assess permeability of EFV in NS. Finally, oral bioavailability of NS was evaluated in rabbits and compared with standard EFV and marketed EFV formulation (MF). We hypothesized that NS formulation of EFV might lead to improved oral bioavailability due to enhanced solubility, dissolution and, thus absorption.

Present second study has been undertaken to develop and characterize S-SMEDDS formulation of EFV, and the physicochemical characteristics were evaluated *in vitro*, *in situ* and *in vivo*. Formulation of L-SMEDDS requires a careful selection of oil, surfactant and cosurfactant. Selection of excipient was optimized using solubility, phase diagram and self-emulsification property. The application of a mixture experimental design has been demonstrated to be an efficient and satisfactory method for optimization of the formulation and to acquire the necessary information to understand the relationship between independent variables and dependent variables in a formulation. Experimental mixture design using Design-Expert® software was applied to optimize L-SMEDDS that contain a minimum amount of surfactant, a maximum amount of lipid, and possess minimum droplet size (MDS) and maximum % transmittance (% T). Based on the results of ternary phase diagrams and self-emulsification studies, captex 500 as oil (X_1), tween 20 as surfactant (X_2) and transcutol HP as cosurfactant (X_3) was selected for components of SMEDDS. The range of each component was selected as follows: $10\% \leq X_1 \leq 40\%$, $30\% \leq X_2 \leq 60\%$, $20\% \leq X_3 \leq 50\%$. The optimized L-SMEDDS formulation was converted into free flowing powder by adsorbing onto Aerosil 200 used as a solid carrier. Optimized SMEDDS formulation was characterized for various physicochemical parameters (like droplets size and size distribution, ZP, dilution studies, thermodynamic stability studies, morphology and stability studies). The morphology of solid SMEDDS (S-SMEDDS) and droplet size/distribution of EFV microemulsion were observed by SEM and TEM, respectively. Solid state characterization of S-SMEDDS performed by DSC and XRD. The release profile of L- and S-SMEDDS from capsules were evaluated using paddle dissolution apparatus in water containing 1.0% w/v SLS and

compared the release of EFV from a MF. *In situ* absorption property in rat intestine and *in vivo* oral absorption in rabbit was performed with L- and S-SMEDDS and compared with a marketed formulation (MF) of EFV. S-SMEDDS show good potential to improve oral bioavailability for the delivery of EFV.

Present third study has been undertaken to develop EFV loaded PLGA nanoparticles (NPs) and their formulation parameters were statistically optimized using 3^2 factorial designs. PLGA NPs were prepared using nanoprecipitation method. The formulation was prepared by dissolving PLGA and EFV in organic solvent. This organic phase was added into aqueous phase contains surfactant with continuous stirring on magnetic stirrer at room temperature. Stirring was continued for 3-4 h to allow complete evaporation of organic solvent. Finally, traces of organic solvent were eliminated under reduced pressure in rotary flask evaporator at 40°C for 30 min. Preliminary experiments were carried out by varying one parameter at a time, while keeping other constant, so that effect of various parameters could be evaluated. For Preliminary experiments, various parameters like type of organic phase, type of surfactant, ratio of organic phase to aqueous phase and concentration of PLGA were varied and the effect on particle size of PLGA nanoparticles was studied. The parameters were optimized to obtain nano-ranged particles with narrow size distribution. The effect of drug : polymer ratio and surfactant (Poloxamer 188) concentration on particle size was assessed by using Design-Expert® software. The factor levels are evenly spaced and coded for low, medium and high settings, as −1, 0 and +1. Dependent variables were MPS (Y_1) and % entrapment efficiency (% EE) (Y_2). Incorporation of mannose (MN) in PLGA was carried out and EFV loaded PLGA-MN NPs was prepared. NPs were subsequently transformed to dry powder by lyophilization, to enhance the stability of EFV. The optimized formulations were characterized for particle size, % EE, DSC and TEM. In vitro diffusion study of EFV loaded PLGA and PLGA-MN NPs were performed in 1% SLS in water, selected as the drug release medium. The chemical stability of NPs were assessed by determining percentage of EFV present in the formulations stored at different temperatures (4-8°C and 25°C) during a period of 3 months. Isolated rat peritoneal macrophages are used for *in vitro* uptake study of EFV loaded PLGA and PLGA-MN NPs. The effect of EFV, EFV loaded PLGA NPs and PLGA-MN NPs on cell proliferation was determined by MTT based colorimetric assay. Fluorescence microscopy was

performed to study the qualitative uptake of prepared NPs by macrophage cells. The 6-coumarin was used as a fluorescent marker and loaded into PLGA-NPs and PLGA-MN NPs instead of EFV. Biodistribution of EFV loaded PLGA and PLGA-MN NPs in organs was evaluated in albino rats until 24 hours after intraperitoneal injection and amount of EFV present in liver, spleen, lung, kidney and brain at different time intervals were determined.

HPLC analytical method were developed and validated to estimate EFV in various developed formulations (NS, SMEDDS, PLGA NPs), *in vitro* and *in vivo* studies. The chromatographic separation was performed using a Phenomenex Hypersil C4 (100 mm × 4.6 mm i.d., 5 µm particle size) column. Separation was achieved using a mobile phase consisting of acetonitrile and 100 mM ammonium acetate buffer pH 7.0 in the ratio of 45:55 (v/v), pumped at a flow rate of 1 ml/min. The eluent was monitored using UV detector at a wavelength of 247 nm. The column was maintained at 40°C and an injection volume of 20 µL was used. Method was validated for system suitability, accuracy, precision, robustness. All validation parameters meet the acceptance criteria as per ICH guideline. Extraction of EFV from plasma and tissue homogenates was carried out using Tert- butyl methyl ether and analyzed using validated HPLC method.

7.2. Conclusion

A media milling method using zirconium oxide beads was successfully employed to produce stable EFV NS. The results obtained in this study demonstrate that the particle size can be influenced by parameters, such as drug concentration, type and concentration of stabilizers. Efficient particle size reduction by nanogrinding was achieved by using excipients that provide proper wetting and physical stabilization (steric and electrostatic) of the practically water-insoluble drug, EFV. The combination of PVP K30–SLS stabilizer system was most suitable and optimized by the use of the Box-Behnken design to produce NSs with maximal particle size reduction. Lyophilization of the NSs with trehalose yielded nanopowders that were re-dispersed completely in the water. XRD and DSC data revealed that the crystalline state of EFV was not altered through operations, and shall be of great importance when considering long-term stability of EFV formulation. SEM images exhibited

distinct differences in the morphological structure of nanoparticles influenced by the stabilizers. The NS was physically and chemically stable over 6 months. The physical mixture of the drug and stabilizer did not significantly improve the dissolution of the drug suggests that the increased dissolution rate for the NS is primarily due to the reduction of the particle size. Significant enhancement in the saturation solubility of EFV in NS form was observed as compared to standard EFV. The *in vitro* transport study in PAMPA model demonstrated that NS was successful in enhancing the permeation of EFV. The results of *in situ* absorption of EFV in rat intestine suggested that NS played an important role in absorption enhancing effect. Pharmacokinetic evaluation clearly showed that the EFV NS exhibited improved pharmacokinetic properties compared to the MF. Oral bioavailability of EFV in rabbits resulted from NS was increased by 2.19-fold compared with the MF. The media milling method is easy to apply and needs only simple equipment and, thus, is a promising method for preparing drug NSs. Results of this study lead to the conclusion that NS approach is effective in preparing EFV formulations with enhanced dissolution velocity and oral bioavailability attributed to better wettability, increased saturation solubility and surface area, reduced particle size and decreased diffusion layer thickness. Moreover, NS may give added value by allowing a reduction in either the dose or its frequency of administration.

Solubility evaluation, pseudoternary phase diagram and self-emulsification test were carried out to select excipients of SMEDDS. Composition of EFV loaded SMEDDS was optimized using factorial design. Optimal SMEDDS contains captex 500 as oil phase, tween 20 as a surfactant and transcutol HP as cosurfactant, in the ratio of 25:50:25 %w/w, formulates SMEDDS with lower droplet size (30.4 nm), PDI (0.126), and ZP (-19.9 mV) values. The L-SMEDDS converted into S-SMEDDS using Aerosil 200 as a solid carrier. Both DSC measurements and X-ray diffraction analysis suggested that EFV in the S-SMEDDS may be in the molecular dispersion state. Following self-emulsification in water the droplet size distribution of the S-SMEDDS was nearly same to the L-SMEDDS, and the in vitro dissolution performance was similar for L- and S-SMEDDS both significantly higher than the MF. The L- and S-SMEDDS were physically and chemically stable over 6 months. The *in vitro* transport study in PAMPA model demonstrated that L- and S-SMEDDS was successful in enhancing the permeation of EFV. The results of *in situ* absorption of EFV in rat

intestine suggested that SMEDDS played an important role in absorption enhancing effect. Pharmacokinetic evaluation clearly showed that the EFV loaded L- and S-SMEDDS exhibited improved pharmacokinetic properties compared to the MF. The oral bioavailability of EFV from S-SMEDDS was 2.16-fold higher than the MF and no significant difference compared with the L-SMEDDS. Our results illustrated the potential use of S-SMEDDS to dispense poorly water soluble drug by oral route.

EFV loaded PLGA NPs prepared by the nanoprecipitation method had high % EE, spherical shape, regular surface and particle size less than 200 nm. The application of a 3^2 factorial design proved to be a useful tool for the optimization of EFV loaded PLGA-NPs. The analysis of the obtained results led to the polynomial equations obtained by multiple regression described adequately the influence of the selected variables (drug:polymer ratio and surfactant concentration) at three levels on the responses. According to the studied factors, the selected optimum formulation was that prepared with 7.5:50, drug:polymer ratio and 0.5 %w/, surfactant concentration. Incorporation of MN in PLGA can be used as a successful strategy to enhance the uptake of PLGA-MN NPs by macrophages. *In vitro* drug release study showed 50.31 ± 1.39 % EFV release from PLGA NPs and 45.49 ± 1.56 % EFV release from PLGA-MN NPs in 5 days. The NPs formulations were stable over 3 months. DSC thermograms indicated that EFV was dispersed as amorphous state in the NPs. The NPs penetrate macrophages and do not cause toxicity to these cells by MTT assay. Higher uptake in peritoneal macrophages was observed with PLGA-MN NPs than PLGA NPs. Administration of PLGA-MN NPs resulted in a significantly higher concentration of EFV in liver, lung, spleen, kidney and brain as compared to PLGA NPs. These nanoparticles sustained the release of EFV and may be used to reduce the frequency of administration and dose-dependent side-effects, reducing the chances of dose dumping and increasing the patient compliance.